A METHOD OF MEASURING AIR MOVEMENTS IN COMPARTMENTALIZED BUILDINGS

A thesis presented to

The University of Manchester

for the degree of

Doctor of Philosophy

by

C. IRWIN

University of Manchester Institute of Science and Technology

Department of Building

JUNE , 1985

DECLARATION:-

The work in this thesis has never been submitted in full or in part to any University or Academic Institution in support of any other qualification.

Abstract

The aim of this study is the development of a method for measuring airflows between internal spaces of any compartmentalised building. Existing methods of measuring air movements are generally unable to cope with random measurement errors.

A general method is presented for measuring airflows in up to three spaces where air is passing in both directions. Tracer gases are injected and their growths and decays monitored in up to three different sections of a building.

The theory of the general solution is derived in full for two and three connected spaces, together with the most suitable method of data analysis. A method of estimating errors in calculated airflows caused by random measurement errors is presented.

Comparison is made with existing methods of data analysis and the effects of random measurement errors are shown using a worked example.

The experimental technique developed by the author, for measuring tracer gas concentrations uses parallel gas chromatographic separation columns and an electron capture detector. An examination of air movements between two and three connected spaces in dwellings, shows the application of the technique developed in determining multiple space air movements from site measurements of tracer gas concentration.

The conclusion of this study is that the multiple tracer gas technique is capable of determining inter-space airflows in a variety of buildings. The method of data analysis adopted can cope with random measurement errors on individual data points and their subsequent effect on inter-space airflows calculated from such data.

CONTENTS PAGE

CONTENTS

CONTENTS PAGE

CONTENTS PAGE

CONTENTS

CONTENTS

Chapter 1: EXISTING WORK ON AIR MOVEMENTS IN BUILDINGS.

1.1) Introduction

The advent of increased costs for primary fuels (oil, gas, coal) has resulted in a growing awareness by society of the need to conserve energy.

If one considers in the U.K., that 30% of the primary energy used is in the domestic sector [1], then a relatively modest reduction in energy consumption would create significant savings. Consequently, a great deal of research effort has occurred to achieve practicable energy conservation in dwellings.

These energy conservation techniques have one of two forms. Firstly, to increase the thermal resistance of the building fabric and secondly, to control the rate of natural ventilation inside the building envelope. Increasing the thermal resistance of the building envelope can be achieved by applying cavity wall insulation, loft insulation or insulated batts between the joists of suspended ground floors.

One is then faced with a more complex problem, namely the effect of natural ventilation of a dwelling and its contribution to total dwelling heat loss. For example an insulated dwelling, under winter conditions, with a whole house ventilation rate varying between 0.5-2 air changes per hour, the ventilation heat loss contributes between 25 - 60% of the total heat loss [2,3].

An uninsulated dwelling experiencing the same ventilation rates would have a ventilation heat loss 10-30% of the total heat loss. Thus, controlling the ventilation rates in insulated buildings also controls the degree of energy conservation in them.

A further effect of controlling the amount of natural ventilation is to increase the emphasis on controlling the levels of atmospheric pollutants (water vapour, body odour, carbon dioxide, carbon monoxide), that are generated in occupied buildings. Air quality is dependant upon the assumption that infiltrating fresh air dilutes any generated atmospheric pollutants and the exfiltrating room air removes these pollutants to the external environment. Where recirculation of air occurs between connected spaces in a building, pollutants generated internally can be dispersed to adjacent spaces. A detailed knowledge of air movement paths can only be deduced from multiple tracer gas measurements between connected spaces in buildings.

1.2) Previous work on natural ventilation in buildings.

The references to existing publications mentioned in the following discussion are not exhaustive. A selection of existing research into the causes and effects of natural ventilation is made. A detailed summary of available literature published in the field of ventilation and air movements in buildings is available from the data base provided by the Air Infiltration Centre.*

* A.I.C. Old Bracknell Lane, BRACKNELL, BERKSHIRE.

The two physical mechanisms which cause dwelling ventilation are the effects of wind and temperature differences. The driving force behind air leakage and hence ventilation of dwellings is the pressure difference caused by these two mechanisms across the building envelope.

Infiltration of cold air and exfiltration of warm house air occurs through openings in the building shell. Such openings are of two distinct types, adventitions or purpose provided. Adventitions openings generally occur in the form of cracks around doors and windows. Purpose provided openings are built into the building envelope by the designer. They are normally air bricks, window ventilators or chimneys.

The development of prediction techniques for calculating air infiltration from such openings has been widely reported [4,5,6] These techniques generally require a knowledge of the pressure distributions caused by wind effects around the building envelope to estimate air leakage rates.

A detailed knowledge of the pressure distributions caused by wind effects across the building envelope are achieved either by site testing [7] or studied using a variety of model shapes in a wind tunnel [8,9].

As an alternative to such prediction techniques for dwelling ventilation, is the correlation of wind and temperature effects on

existing dwellings and the ventilation rate induced. Much research effort has been reported, see for example refs [10,11,12]. These and other workers have all generally reported that there is no straightforward relationship between prevailing weather conditions and dwelling ventilation. Their work has shown that dwelling air leakage is a complex function of wind direction, velocity, temperature difference, building shape and local terrain effects, all of which can vary the local wind velocity profiles around dwellings [13,14].

1.3) Existing methods of measuring air movements.

For the ventilation of dwellings to occur, air infiltrates and exfiltrates across the building envelope. The airflows which result from such wind and temperature actions and their distribution between internal spaces of a dwelling are of great interest to the building designers. Such air motion can affect temperatures in living areas and cause condensation where warm moist air is carried to a cold surface. An illustrative example of this occurs when one examines the effects of airflows between the occupied dwelling space and the cold unheated roofspace above. Roof condensation can cause mould growth on roof timbers and rot in extreme cases, where water drips from the sarking felt onto the ceiling, unsightly staining occurs along with a general decrease in the thermal resistivity of any insulating material laid between ceiling joists [15,16].

instrumentation used by these workers is described in Chapter (6), Sections (6.1) and (6.2).

The method of data analysis developed by Perera [20], using numerical differentiation of tracer gas concentration, time curves is examined in Chapter (3), Section (3.4). The same method of analysis has been adopted by Prior et al [19].

The second data analysis method developed by I'Anson et al [21], using a general solution to the fundamental tracer gas equations is examined in Chapter (3), Section (3.6) .

A further method of analysis has been developed by Penman [27] this worker has developed a method of estimating the incoming air movements into a single space from adjacent, connected spaces by measuring carbon dioxide concentrations in occupied buildings. This analysis method can be adapted for use in multiple tracer gas measurements and is examined in Chapter (3), Section (3.5).

1.4) The present technique

Chapter (2) examines the strategies available when tracer gases are injected into a test space and used to determine air movements and air change rates.

Chapter (3) describes the different methods available for solution of the conservation of mass of tracer gas equations. Reference

Little information has been published on air movements inside dwellings [17,18]. Dick [17], carried out a series of tests using a single tracer gas to determine the proportions of outside air and recirculating house air ventilating internal rooms of dwellings. Sanders [18], more recently has carried out research in Scottish housing using a single tracer gas, to obtain estimates of one directional air movement between occupied dwelling spaces and the roofspace above. The single tracer gas technique used by Sanders has a major disadvantage when applied to air movements between two spaces. Estimating air flows between connected spaces requires the simultaneous measurement of the air change rates in all spaces under consideration. To overcome this problem, Sanders "characterized" the dwelling by measuring the influence of prevailing wind speed on air change rates. When roofspace air change rate measurements were taken, measurement of prevailing wind speeds during the test period enabled an estimate of dwelling air change rate to be made.

Air movement between two or more connected spaces in a building requires a measurement technique that can monitor tracer gas concentrations in all spaces under examination. Having obtained such data a method of analysis is then required to calculate inter-space air movements and air change rates.

There are currently three measurement techniques available which can monitor simultaneously the concentration of tracer gases in up to three connected spaces [19], [20], [21]. The measuring

is made to a worked example of known air flows and air change rates, three existing analysis methods are used to estimate air movements. Imposing random measurements errors of known size, the effects on calculated airflows found from such data are shown.

Chapters (4) and (5) describe a new method of solving the fundamental tracer gas equations. This alternative solution is applied to 2 cell air movements and air change rates in Chapter (4), and 3 cell air movements in Chapter (5). The validity of the analysis method is considered using the worked example for known airflows described in Chapter (3).

Chapter (6) describes the existing instrumentation used to measure multiple tracer gas concentrations. An improved instrument based on I'Anson's gas chromatograph is discussed, together with the experimental validation of the analysis methods of Chapters (4) and (5).

Chapter (7) presents the results of site measurements using the modified gas chromatograph in a variety of dwellings.

Chapter (8) considers further applications for multiple tracer gas measurements in any compartmentalized buildings, together with recommendations for further research.

Chapter 2: ANALYSIS OF VENTILATION RATES USING TRACER GASES.

2.1) General Requirements

The requirements for a suitable method of measuring air movements in compartmentalised buildings, is a compromise between portability, inexpensive equipment, simultaneous measurements of several different tracer gases, uses low concentrations of non-toxic tracer gases and airflows under examination should not be altered by the measuring method in use.

There are three tracer release strategies used widely [22], [23], to determine single volume ventilation rates in buildings: decay, constant concentration and constant flow methods. Any of these could theoretically be used to make airflow measurements. The following discussion suggests the decay of tracer gas concentration, as the best compromise between the conflicting requirements for airflow measurements.

2.2) Decay Technique

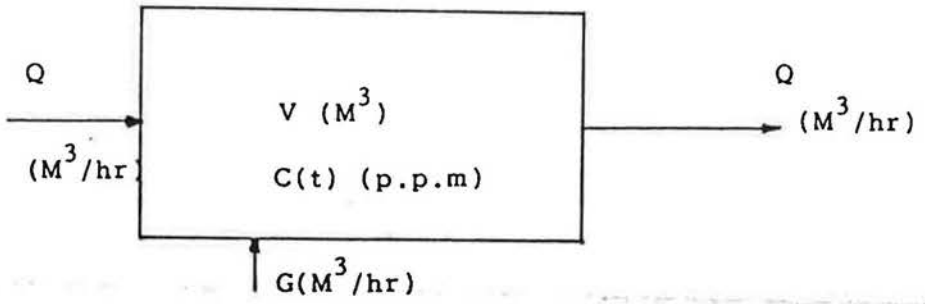

Consider a single cell of volume (V)M^3 containing a tracer gas concentration C(t). A pulse of tracer gas is released at time zero (G=0).

Assuming fresh air enters and leaves the cell at a rate (Q) M^3/hour, then the rate of change of tracer concentration if found from the continuity equation.

$$-\frac{dC}{dt} = \frac{Q.C_{(t)}}{V} \qquad (2.2.1)$$

Integrating between $C_{(t)} = Co$, t=0 and $C_{(t)} = C_{(t)}$, t = t

$$-\int_{Co}^{C(t)} \frac{dC}{C(t)} = \int_{t=o}^{t=t} \frac{Q}{V}\, dt \qquad (2.2.2)$$

$$-Ln\,(C_{(t)} - C_{(o)}) = \frac{Q.t}{V} \qquad (2.2.3)$$

Re-arranging and substituting for $\frac{Q}{V} = N$ we obtain

$$C_{(t)} = Co\ e^{-Nt} \qquad (2.2.4)$$

where N is the air change rate of the cell under consideration.

The value of N is obtained from plots of ln $C_{(t)}$ concentration varying with time, the gradient of the straight line obtained being the cell ventilation rate N.

The decay technique is widely used because it requires minimal measuring equipment and is generally well suited for making short term measurements. The major disadvantage occurs where the air/tracer gas mixture is not uniformly distributed, normally the problem is overcome using mechanical mixing fans. Additionally if poor mixing is suspected the test can be easily repeated.

2.3) Constant concentration

The concentration of tracer gas (C) is maintained at a constant value by controlling the rate (G) M^3/hr, at which tracer gas is released into the cell.

The continuity equation gives

$$Q = \frac{G}{C} \qquad (2.3.1)$$

This method gives a continuous measurement of ventilation rate. However, under non-steady conditions the required complexity of gas releasing equipment which is capable of the short response times needed, is expensive. To maintain a constant concentration under changing weather conditions demands a sophisticated control system to minimise system response time and is very difficult to achieve in practice.

2.4) Constant flow

Tracer gas (G) M^3/hr is released at a constant rate. When equilibrium concentration is reached, the rate of input of tracer (G) M^3/hr equals the rate of supply of ventilating air (Q) M^3/hr leaving the cell at a concentration (C).

The continuity equation is

$$\frac{Q}{G} = C \qquad (2.4.1)$$

This method requires less complex equipment than for the constant concentration method. Unfortunately the method consumes large quantities of tracer gas as equilibrium approaches. The major disadvantage is achieving equilibrium concentration under varying ventilation rates.

2.5) The problem of mixing

If a tracer gas is released in a space there are three types

of mixing that can occur. These are mixing with fresh air entering the space; mixing of air and tracer gas in the space and circulation of air within the space. Each of these mixing problems may affect the measured tracer concentration differently, (see Ref. [23]).

Firstly, fresh air entering a space may not be uniformly distributed, consequently the concentration of the air/ tracer gas mixture will vary for different locations.

Secondly, air infiltrating into a space and then exfiltrating out again without mixing, can occur. This does not effect tracer gas concentration and generally is not of interest.

The final mixing problem occurs if one considers that the physical volume of the space and the effective volume of the space may be different. Effective volume is defined as that volume of the space participating in the air exchange process. The presence of cupboards, furniture can lead to the effective volume being smaller than the physical volume. Conversely the presence of a suspended ceiling, attached to the space under consideration, having a significant air leakage will cause the effective volume of the space to be larger than the physical volume.

Chapter 3 : ANALYSIS OF AIRFLOWS FROM MULTIPLE TRACER GAS MEASUREMENTS.

3.1) General

The decay of the concentration of a tracer gas with time, in a single cell, is, under ideal conditions, exponential.

However, where tracer gas is also entering the test cell from a neighbouring connected cell, the resulting curve shape is not a simple exponential. In many cases, if a quantity of tracer gas is released in a cell (1), which is connected with an adjacent cell (2) then tracer gas will infiltrate into cell (2), after mixing with the air in cell (2) it may be returned to cell (1). This process is called recirculation of tracer gas. The origins of airflow measurements lie in a series of papers published by Dick in the late nineteen forties [10,11,17]. He derived equations that estimated one directional air movements between two connected rooms in dwellings.

In recent years the basic equations governing tracer gas concentrations in multi-cell structures have been examined by Sinden [24], Sherman [23], Perera [25], I'Anson [26], Penman [27] and Honma [28].

This chapter derives the multi-cell equations and examines the different methods of solution adopted.

3.2) Fundamental Tracer equations

The following analysis uses a similar approach to that adopted by Perera [25] and Sinden [24].

The following assumptions are made:

a) the structure under consideration is composed of N cells in which air and tracer gas are perfectly mixed.

b) Qij and Qji are the volume flow rates of air (M^3/hr) between cells i and j, Qij is not necessarily equal to Qji,

c) the volume of each cell is Vi (M^3),

d) $Ci_{(t)}$ is the time variation in the concentration of tracer gas in the i^{th} cell (P.P.M)

e) the rate of production of tracer in any cell i is $fi_{(t)}$ (M^3/hr)

f) the airspace surrounding the structure under consideration has Vo $\longrightarrow \infty$ therefore $Co_{(t)} \Rightarrow 0$

The conservation of mass of tracer gas gives

$$Vi \frac{dCi}{dt} = fi + \left[\sum_{j=1}^{N} Q_{ji} C_j(1-\delta ij)\right] - \left[Q_{io}Ci + \sum_{j=1}^{N} Q_{ij}(1-\delta ij)Ci\right] \qquad (3.2.1)$$

for i = 1, 2....N and j = 1,2 ....N

The Kronecker delta is defined as:

$$\delta ij = 0 \quad i \neq j$$

and

$$\delta ij = 1 \quad i = j$$

A second set of equations is obtained from the conservation of mass of air:

$$Qoi + \sum_{j=1}^{N} Q_{ji} \ (1-\delta ij) = Q_{io} + \sum_{j=1}^{N} Q_{ij} \ (1-\delta ij) \qquad (3.2.2)$$

if we define Si as the outflow of air from cell i to the outside, substituting for Si in equation (3.2.2.) we obtain

$$Si = Q_{io} + \sum_{j=1}^{N} Q_{ij} \ (1-\delta ij) \qquad (3.2.3)$$

Equations (3.2.1) and (3.2.3) can be solved for the Qij's from site measurements of $C_{i(t)}$. The quantities $\frac{dC_i}{dt}$, $Ci_{(t)}$, $fi_{(t)}$ and Vi are known or can be measured.

There are $(N^2 - N)$ unknown values of intercell airflows Q_{ij}, Q_{ji} plus 2N unknown values of Q_{io} and Q_{oi}. We have therefore $(N^2 + N)$ unknown values of airflows and only N equations from equation (3.2.1) plus N equations from equation (3.2.3) in which to solve them.

3.3) Methods of solving the fundamental tracer equations

Using the N equations of equation (3.2.3), we are left with N^2 unknown airflows and only N equations from equation (3.2.1). Therefore (N-1) independant sets similar to equation (3.2.1) have to be generated.

There are three methods of generating the required (N-1) independent sets of equations:

(1) Using continuous tracer gas injection, the injection rate being varied N times,

(2) Observing Ci(t), $\frac{dCi}{dt}$ at N different time points,

(3) Using N different tracer gases

Option (1) requires the use of sophisticated micro-processor controlled tracer injection, which creates problems of maintaining a constant trace concentration. Assuming these difficulties are overcome, N cell airflow measurements using a single tracer gas greatly increases the duration of a test run. The assumption of Qij's remaining constant over such long periods of time is dubious. The further difficulty of continuously mixing air/tracer gas mixtures without disturbing existing airflow patte has also to be considered. Grimsrud et al [12] has carried out site measurements using this technique.

Option (2) suggests the use of a single tracer gas released in one cell and monitored in all N cells. The variations in tracer concentrations with time C(i)t can then be subdivided into K time periods, if $K > N$ then the unknown Qij's can be solved by the methods of

least squares. There are however several disadvantages, if the K time periods are close together, the system of N^2 equations will be badly determined. Conversely if the time periods are widely spaced, then the assumption of steady Qij's will be uncertain.

The derivation of N^2 equations from a single tracer gas are discussed in great detail by Sinden [24] and Penman [27], the inherant uncertainties of the method of analysis are discussed in detail in section (3.5)

Option (3), using N tracer gases removes the difficulties associated with extended test periods encountered with single tracer gas techniques. The consequent increase in analysis equipment to accommodate multiple tracer gas monitoring can be greatly eased by using decay methods of multiple tracer gas injection.

Such methods have been used by Perera [25] and I'Anson et al [26].

3.4) Method 1 : The fundamental tracer equations as solved by Perera

The method of analysis of equations (3.2.1) and (3.2.3) adopted by Perera can be applied to any number of interconnected cells, the limiting factor being the number of suitable tracer gases available.

The corresponding sets of equations derived from equation (3.2.1) will get considerably larger and use of a micro-computer becomes ess-

ential for data manipulation. To enable comparison between other researchers we shall solve the "Perera" equations for N = 2 cells.

Equation (3.2.1), the conservation of mass of tracer gas gives for the two cell case:

$$Vi \frac{dCi}{dt} = fi + \left[\sum_{j=1}^{N=2} Q_{ji} Cj(1-\delta ij)\right] - \left[Q_{io} Ci + \sum_{j=1}^{N=2} Q_{ij}(1-\delta ij)Ci\right] \qquad (3.4.1)$$

The total outflow of air, equation (3.2.3) becomes:

$$Si = Q_{io} + \sum_{j=1}^{N=2} Q_{ij}(1 - \delta ij) \qquad (3.4.2)$$

Substituting for equation (3.4.2) in equation (3.4.1) we obtain

$$Vi \frac{dCi}{dt} = fi + \left[\sum_{j=1}^{N=2} Q_{ji} C_j (1-\delta ij)\right] - S_i C_i \qquad (3.4.3)$$

which is the fundamental tracer gas equation for the N = 2 cell case.

To solve equation (3.4.3) consider figure (1), two connected cells have different tracer gases released in each of the two cells. In cell (1), tracer gas (A) is released and in cell (2) tracer gas (B); by considering a single pulse of tracer gas injected into each cell f(i) in equation (3.4.3) = 0.

Considering Cell (1), equation (3.4.3) can be written:

For Gas (A)

$$V_1 \frac{dC_{A1}}{dt} = Q_{21} C_{A2} - S_1 C_{A1} \qquad (3.4.4)$$

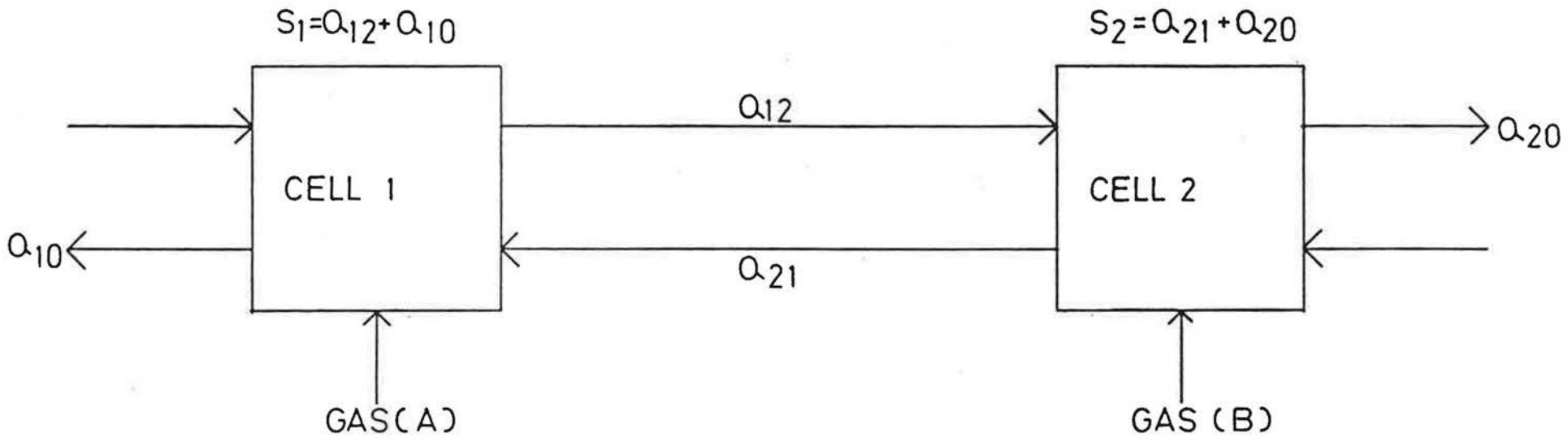

FIGURE 1 TWO CELL AIRFLOWS

For Gas (B)

$$V_1 \frac{dC_{B1}}{dt} = Q_{21}C_{B2} - S_1C_{B1} \qquad (3.4.5)$$

Considering Cell (2), equation (3.4.3) becomes

For Gas (A)

$$V_2\frac{dC_{A2}}{dt} = Q_{12}C_{A1} - S_2C_{A2} \qquad (3.4.6)$$

For Gas (B)

$$V_2\frac{dC_{B2}}{dt} = Q_{12}C_{B1} - S_2C_{B2} \qquad (3.4.7)$$

Equations (3.4.4) to (3.4.7) are solved by matrix methods as suggested by Sinden [24].

Expressing in matrix form equations (3.4.4) to (3.4.7) becomes

$$[Y] = [A].[X] \qquad (3.4.8)$$

where $[Y] = \begin{bmatrix} V_1 \frac{dC_{A1}}{dt} \\ V_1 \frac{dC_{B1}}{dt} \\ V_2 \frac{dC_{A2}}{dt} \\ V_2 \frac{dC_{B2}}{dt} \end{bmatrix}$

$$[A] = \begin{bmatrix} C_{A2} & C_{A1} & 0 & 0 \\ C_{B2} & C_{B1} & 0 & 0 \\ 0 & 0 & C_{A1} & C_{A2} \\ 0 & 0 & C_{B1} & C_{B2} \end{bmatrix}$$

$$[X] = \begin{bmatrix} Q_{21} \\ -S_1 \\ Q_{12} \\ -S_2 \end{bmatrix}$$

The airflow vector [X] is found by calculating the inverse tracer gas concentration matrix $[A]^{-1}$, equation (3.4.8) becomes:-

$$[A]^{-1} \cdot [Y] = [X] \qquad (3.4.9)$$

The curve shapes described by equations (3.4.4) and (3.4.6) are shown in figure (2).

3.4.1) Estimating S_1, S_2. Q_{12}, Q_{21} from site measurements.

The four first order differential equations described by equation (3.4.8), for the two cell case, have four unknown airflows S_1, S_2, Q_{12} and Q_{21}.

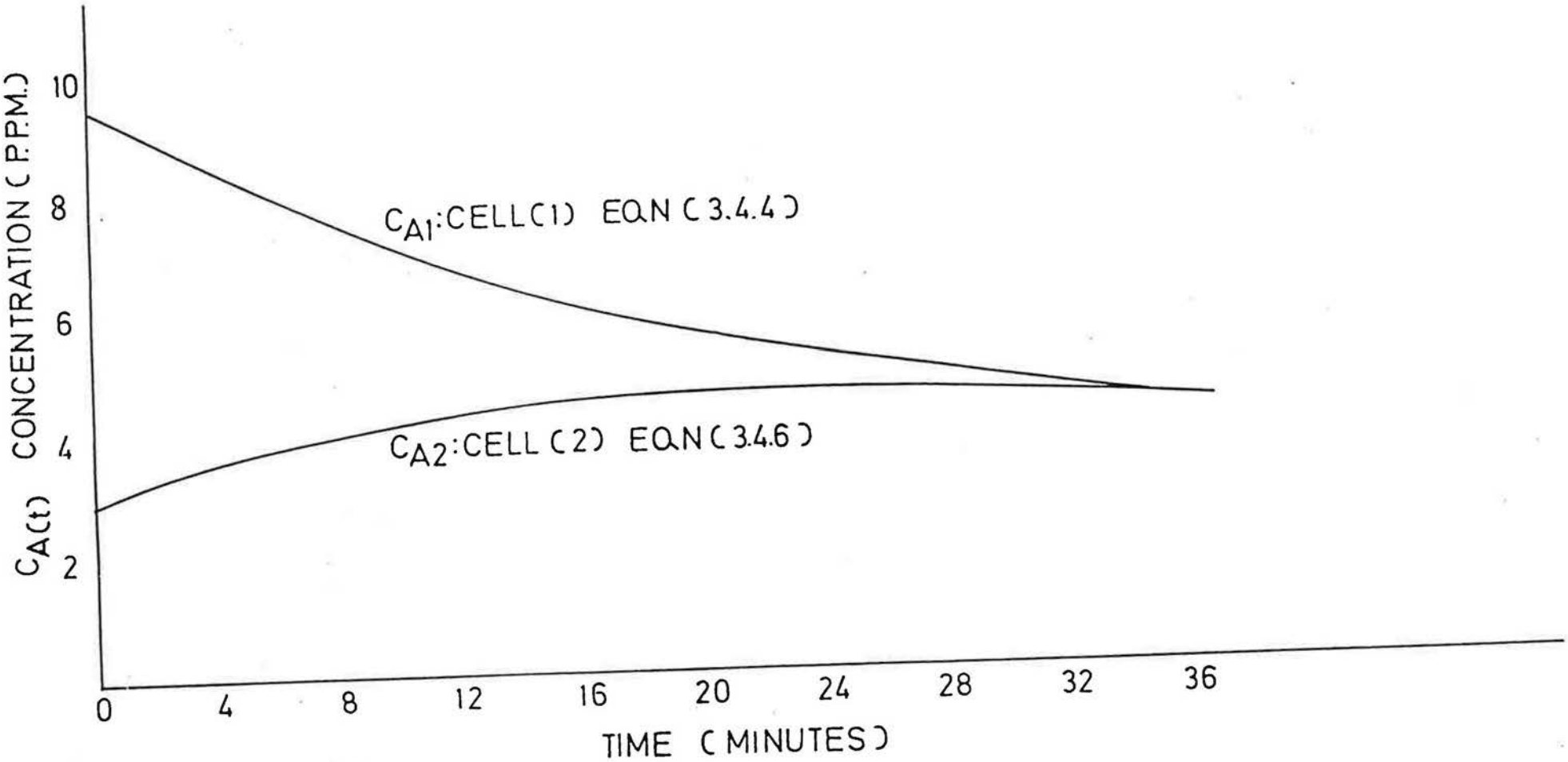

FIGURE 2 VARIATIONS IN $C_{A(t)}$ CONCENTRATION

The quantities C_{A1}, C_{A2}, C_{B1} and C_{B2} are obtained from site measurement of tracer gas concentrations varying with time. The physical volumes V_1 and V_2 of each cell are obtained by site inspection.

Therefore the remaining unknowns are the four tracer gas concentration gradients $\frac{dC}{dt}_{A1}$, $\frac{dC}{dt}_{A2}$, $\frac{dC}{dt}_{B1}$ and $\frac{dC}{dt}_{B2}$

Solution of Equation (3.4.8) for the unknown airflows requires either that numerical values of concentration gradients are estimated at a specific time(t) or equation (3.4.8) is integrated with respect to time. If these equations are integrated, the time dependancy of C_{A1}, C_{A2}, C_{B1} C_{B2} have to be known. Unfortunately only the time dependancy of the simplest multi-cell airflows are known(see for example refs 17,26).

Perera therefore uses numerical estimates of concentration gradients at a specific time (t). Such estimates are obtained by drawing a straight line between two points on the tracer concentration curves; the time interval between points being approximately 5 minutes. The absolute value of tracer concentration at the middle point is also taken and used in equation (3.4.8).

3.4.2) Discussion of Perera's Analysis Method

The difficulties encountered in estimating airflows using the preceeding method are best illustrated using a worked example. Referring to figures (3) & (4), the fundamental tracer equations described by equation (3.4.8) has been solved for known airflows S_1, S_2,

Q_{12}, Q_{21} and initial tracer gas concentrations. Thus the time variations of C_{A1}, C_{B1} in cell (1) and C_{A2}, C_{B2} in cell (2) are fully described from time (t) = 0 to (t) = 30 minutes.

When site measurements are made of tracer concentration in air, uncertainties in the measured values occurs. These uncertainties are caused by imperfect mixing of air/tracer gas, lack of repeatability in measuring equipment and other faults in the measurement method.

In the measurement of tracer gas concentrations such errors are seen as the spread of concentration points about the plotted curve giving the best fit. The magnitude of such errors will vary between different measurement methods, the following discussion assumes that the above mentioned errors are $\pm$5% of the absolute value of tracer concentration.

It must be stated that the effects of variations in prevailing weather conditions during site measurements will have a considerably larger effect on the tracer gas concentration measurements than the measurement errors previously mentioned.

To simulate the effects of errors of measurement, the theoretical tracer concentration histories given in Appendix (A) have a random $\pm$ 5% error imposed on each data point.

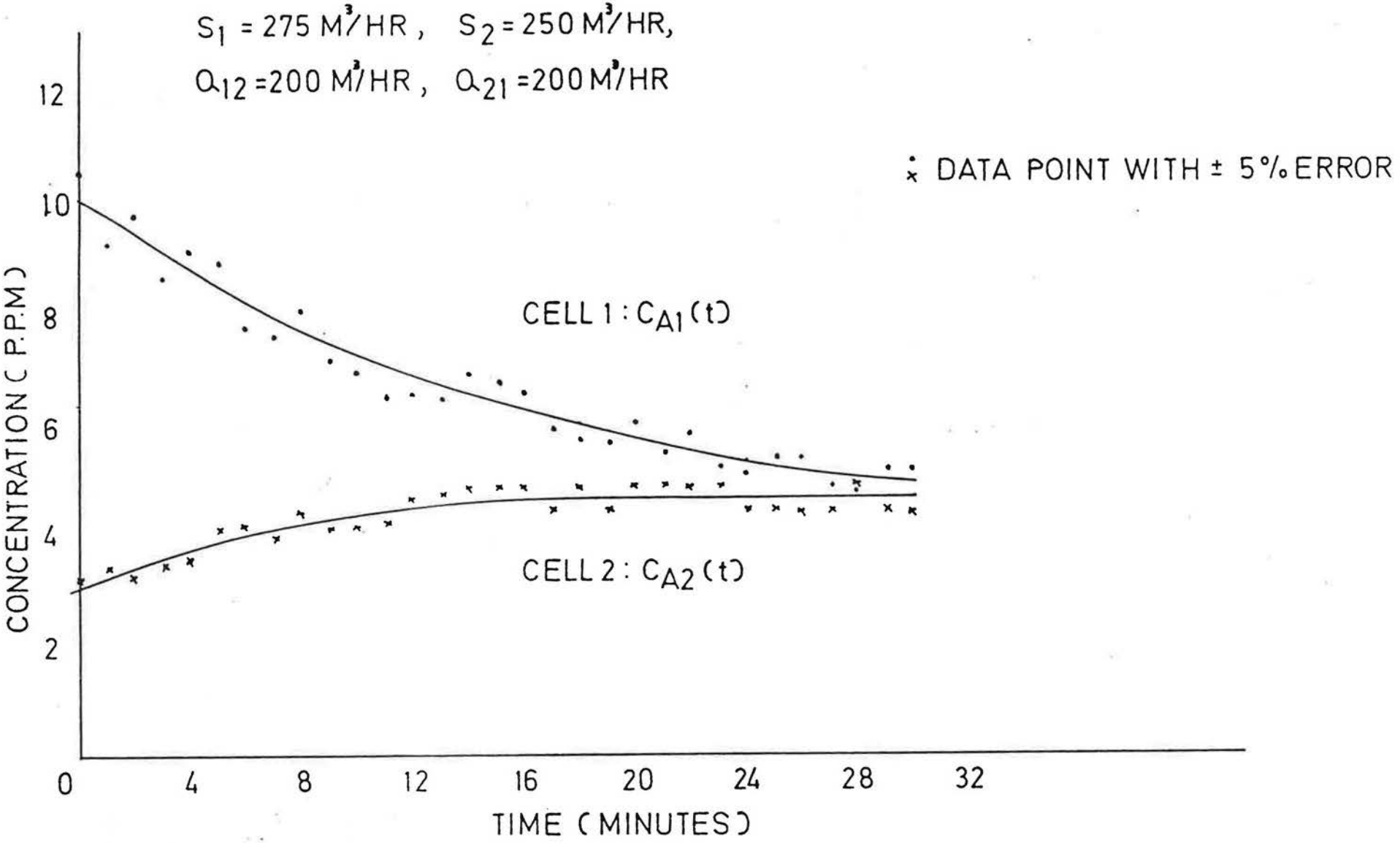

FIGURE 3 $C_A(t)$ VARYING WITH TIME FOR KNOWN AIRFLOWS

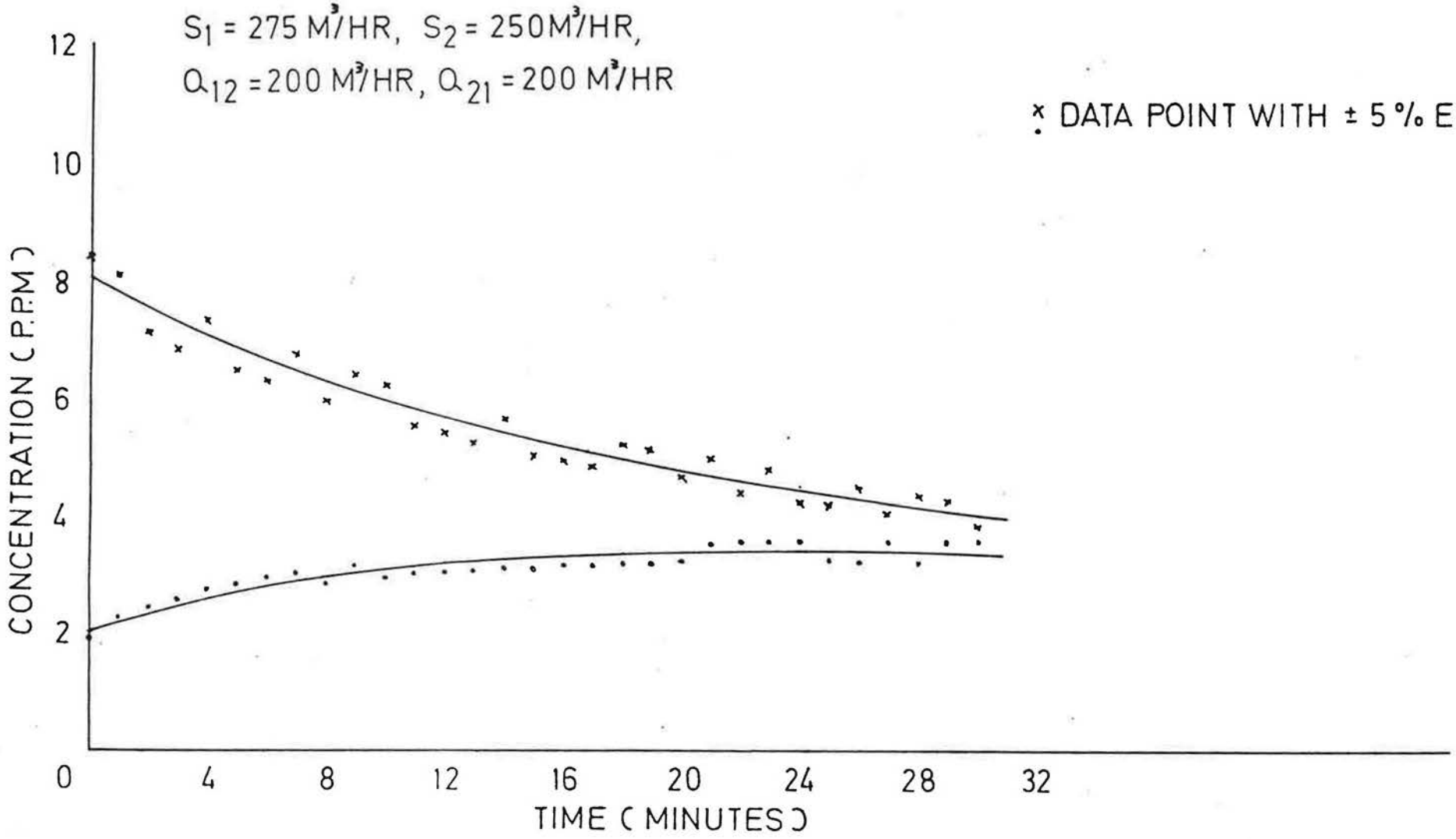

FIGURE 4 $C_B(t)$ VARYING WITH TIME FOR KNOWN AIRFLOWS

Comparison between the known values of S_1, S_2, Q_{12}, Q_{21} and the calculated values in Appendix (A) show calculation errors between 1.5% - 43.5%. The cause of such large errors is found by examining the method of estimating the concentration gradients

$$\frac{dC_{A1}}{dt}, \quad \frac{dC_{A2}}{dt}, \quad \frac{dC_{B1}}{dt}, \quad \frac{dC_{B2}}{dt}$$

Consider the concentration gradient $\frac{dC_{A1}}{dt}$ which is calculated from:

$$\frac{dC_{A1}}{dt} = \frac{C_{A1}(t_2) - C_{A1}(t_1)}{t_2 - t_1} \qquad (3.4.10)$$

If we assume that point $C_{A1}(t_1)$ has an error of $\pm E_1$ and $C_{A1}(t_2)$ has an error $\pm E_2$, then the most probable error in the calculated values of $\frac{dC_{A1}}{dt}$ is equal to:

$$E_{\dot{C}A1} = \left| \frac{\sqrt{E_1^2 + E_2^2}}{t_2 - t_1} \right| \qquad (3.4.11)$$

From the worked example shown in Appendix (A) this leads to a 22% uncertainty in the calculated value of concentration gradient $\frac{dCA_1}{dt}$. Similar difficulties occur when the remaining concentration gradients are estimated. A further complication arises in selecting which part of the tracer concentration curve to use for the concentration gradient calculations. The time interval has to be selected from the earliest possible part of the concentration

curve, Perera [20] suggests between t_1 = 5 minutes and t_2 = 10 minutes. The concentration gradient at this time is then hopefully discernable above the variations in tracer gas concentration caused by any experimental errors.

3.4.3) Suggested improvements to analysis method

As previously stated the major source of error in the analysis method is the method of calculating tracer concentration gradients, equation (3.4.11) shows the effects of increasing the time interval.

An arbitary doubling of the time interval will ideally, halve the error on $E_{C_{Al}^{\bullet}}$. There are two problems which then have to be overcome:(i) The estimate of C_{Al} concentration which is used to calculate airflows will be subject to increasing errors; C_{Al} concentration being taken by Perera as the value corresponding to the mid-point on the straight line joining $C_{Al}(t_1)$ and $C_{Al}(t_2)$.

(ii) when two connected cells have large interconnecting airflows, it is possible for the growth and decay of tracer gas concentrations to have reached equilibrium conditions 20 minutes after the start of a site test. Uncertainties in initial tracer gas concentrations at the beginning of site measurements is a common problem. Similarly discerning variations in tracer concentrations above experimental errors as equilibrium concentrations are reached is a further difficulty. Concentration gradient estimates will therefore be subject to potentially large errors.

The problem of estimating $C_{Al\ (t)}$ tracer gas concentration at the midpoint can be overcome by using numerical integration (for example Simpson's rule).

The second problem cannot be readily overcome, the time interval selected will vary to suit the particular site measurement under investigation.

Generally, numerical differention of tracer concentration data which is subject to possibly large measurement errors is not to be recommended.

3.5) Method 2: The fundamental tracer equation as solved by Penman.

The work of Penman is primarily concerned with deriving multi-component airflows and ventilation rates in occupied spaces using carbon dioxide concentration measurements. The method of solution of the fundamental tracer equations adopted by Penman is included here because the method can be adopted to the analysis of multi-cell airflows. Considering figure 5, the conservation of mass of tracer gas can be written:

$$Vi \frac{dC_i}{dt} = fi + \sum_{j=o}^{N} Q_{ji} (Cj - Ci) \qquad (3.5.1)$$

which is the form of equation suggested by Honma [28].

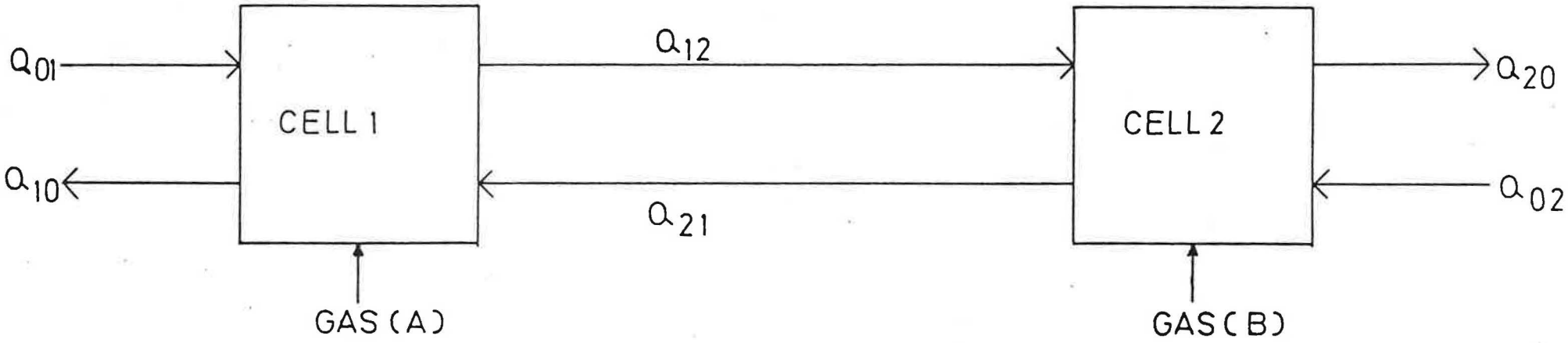

FIGURE 5 TWO CELL AIRFLOWS

The following assumptions are made:

(a) Qji are the volume flow rates of air (M^3/hr) between cells j and i,

(b) the volume of each cell is Vi $(M^3)_1$

(c) $Ci_{(t)}$, $Cj_{(t)}$ are the time variations in tracer gas concentrations in cells i and j respectively. (P.P.M),

(d) the rate of production of tracer in any cell i is $fi_{(t)}$ (M^3/hr),

(e) the airspace surrounding the structure under consideration has Vo $\Rightarrow \infty$ therefore $Co_{(t)} \Rightarrow 0$,

(f) the air/tracer gas are perfectly mixed.

Once again let us consider the N = 2 cell case, equation (3.5.1) can be integrated between a time step (t_1) - (t_2)

Equation (3.5.1) becomes:

$$Vi\ [Ci_{(t2)} - Ci_{(t1)}] = \sum_{j=0}^{N=2} \left[\int_{t1}^{t2} (Cj-Ci)dt \right] Qji \qquad (3.5.2)$$

fi = 0 when a single pulse of tracer gas is injected into each cell.

Considering Cell (1), equation (3.5.2) can be written:

For Gas (A)

$$Vi\left[C_{A1(t2)} - C_{A1(t1)}\right] = -\int_{t1}^{t2} C_{A1}dt\ Q_{o1} + \int_{t1}^{t2} (C_{A2}-C_{A1})dt\ Q_{21} \qquad (3.5.3)$$

For Gas (B)

$$Vi\left[C_{B1(t2)} - C_{B1(t1)}\right] = -\int_{t1}^{t2} C_{B1}dt\ Q_{o1} + \int_{t1}^{t2} (C_{B2}-C_{B1})dt\ Q_{21} \qquad (3.5.4)$$

Considering Cell (2), equation (3.5.2) becomes:

For Gas (A)

$$V_2\left[C_{A2(t2)} - C_{A2(t1)}\right] = -\int_{t1}^{t2} C_{A2}\,dt \;\; Q_{02} + \int_{t1}^{t2} (C_{A1}-C_{A2})\,dt \;\; Q_{12} \quad (3.5.5)$$

For Gas (B)

$$V_2\left[C_{B2(t2)} - C_{B2(t1)}\right] = -\int_{t1}^{t2} C_{B2}\,dt \; Q_{02} + \int_{t1}^{t2} (C_{B1}-C_{B2})\,dt \;\; Q_{12} \quad (3.5.6)$$

where the Qij's are assumed constant between time period $(t_1) - (t_2)$.

3.5.1) Estimating Q_{01}, Q_{02}, Q_{12}, Q_{21} from site measurement.

The integrals in equations (3.5.3) - (3.5.6) are evaluated approximately, using numerical integration of time variations in tracer concentration, obtained from site data for the period (t1) - (t2).

The tracer concentration curves can be divided into several time periods (tj = 1,2...K), the unknown airflows are found using a least squares approximation for $K \geq N+1$ time periods. Where multiple tracer gas measurements are being used, separate estimates of unknown airflows are possible for each tracer gas.

For the N = 2 cell case, tracers A and B enable two estimates of unknown airflows to be made. Appendix (B) illustrates the method of least squares approximation adopted by Penman, applied to a worked example. The fundamental tracer equation (3.5.1) has been solved for known airflows Q_{01}, Q_{02}, Q_{12}, Q_{21} and initial tracer gas

concentrations, the time variation in tracer concentration for t=0 to t=30 minutes are fully described. Experimental errors are assumed as $\pm$ 5%, and are imposed on each data point, see figures (3) and (4).

3.5.2) Discussion of Penman's analysis method

Comparison between the known values of Q_{01}, Q_{02}, Q_{12}, Q_{21} and the calculated values of Appendix (B) show errors between 10% - 81 %. The resulting error in cell air change rates are approximately 1 -42% for cell (1) and 37 - 57% for cell (2). The cause of such large errors induced from $\pm$ 5% random errors on the data is reflected in the concentration difference term.

$$\Delta Ci_{(t2)-(t1)} = Ci_{(t2)} - Ci_{(t1)} \qquad (3.5.7)$$

Assuming Ci(tl) is in error by $\pm E_1$ and Ci (t2) by $\pm E_2$

then the error in equation (3.5.7) is:

$$E_{\Delta Ci} = \sqrt{E_1^2 + E_2^2} \qquad (3.5.8)$$

From Appendix (B), the error in calculating C_{A1} from site data with a random $\pm$5% error suggests E_{CA_1} is approximately 50% of its "true" value. Similar errors will also occur for the other concentration difference terms.

The major disadvantage is therefore the reliance on pairs of site data points in constructing the K linear equations to be solved using a least square approximation for unknown airflows (Qij). In addition where the number of cells under consideration is $N \geq 4$, the amount of site data required to construct the K linear equations makes the assumption of unchanging intercell airflows over a long test period somewhat dubious.

Any analysis method used to solve intercell airflows must, if possible, use all site data points collected. The effects of random measurement errors will then most probably be minimised.

3.6) Method 3: The fundamental tracer equations as solved by I'Anson et al.

There are two researchers who have derived analytical solutions for the fundamental tracer gas equations, Sinden [24] and I'Anson [26]. The latter is the only one who has shown how such an analytical solution can be used to calculate airflows from site measurements of tracer gas concentration data. The analysis method adopted by I'Anson is applicable only when two connected cells are considered.

From section (3.4), the fundamental tracer gas equation is for the two cell case:

$$V_i \frac{dC_i}{dt} = f_i + \left[\sum_{j=1}^{2} Q_{ji} C_j (1-\delta ij) \right] - SiCi \qquad (3.6.1)$$

Once again consider two connected cells with tracer gas (A) released in cell (1) and tracer gas (B) released in cell (2). A single pulse of tracer gas is injected into each cell at time zero then $f_{(i)}$ in equation (3.6.1) equals zero.

Considering Cell (1), equation (3.6.1) can be written:

For gas (A)

$$V_1 \frac{dC_{A1}}{dt} = Q_{21} C_{A2} - S_1 C_{A1} \qquad (3.6.2)$$

For gas (B)

$$V_1 \frac{dC_{B1}}{dt} = Q_{21} C_{B2} - S_1 C_{B1} \qquad (3.6.3)$$

And for Cell (2) equation (3.6.1) becomes:

For gas (A)

$$V_2 \frac{dC_{A2}}{dt} = Q_{12} C_{A1} - S_2 C_{A2} \qquad (3.6.4)$$

For gas (B)

$$V_2 \frac{dC_{B2}}{dt} = Q_{12} C_{B1} - S_2 C_{B2} \qquad (3.6.5)$$

Let us consider for the moment tracer gas (A) only.

Define the air change rate in cell (1) as $N_1 = \frac{S1}{V1}$ and

for Cell (2) $N_2 = \frac{S2}{V2}$

Re-arranging equations (3.6.2) and (3.6.4) for C_{A2} and C_{A1} respectively and using N_1, N_2 defined above, equation (3.6.2) becomes:-

$$C_{A2} = \frac{V_1 N_1}{Q_{21}} C_{A1} + \frac{V_1}{Q_{21}} \frac{dC_{A1}}{dt} \qquad (3.6.6)$$

Equation (3.6.4) becomes:

$$C_{A1} = \frac{N_2 V_2}{Q_{12}} C_{A1} + \frac{V_2}{Q_{12}} \frac{dC_{A2}}{dt} \qquad (3.6.7)$$

Substituting for C_{A1} from equation (3.6.7) into equation (3.6.6) and substituting for C_{A2} from equation (3.6.6) into equation (3.6.7) two second order differential equations are obtained:

$$\frac{V_1 V_2}{Q_{12}} \frac{d^2 C_{A2}}{dt^2} + \frac{V_1 V_2}{Q_{12}} (N_1+N_2) \frac{dC_{A2}}{dt} + (\frac{N_1 V_1 N_2 V_2}{Q_{12}} - Q_{21}) C_{A2} = 0 \quad (3.6.8)$$

$$\frac{V_1 V_2}{Q_{21}} \frac{d^2 C_{A1}}{dt^2} + \frac{V_1 V_2}{Q_{21}} (N_1+N_2) \frac{dC_{A1}}{dt} + (\frac{N_1 V_1 N_2 V_2}{Q_{21}} - Q_{12}) C_{A1} = 0 \quad (3.6.9)$$

The above equations are both linear homogeneous differential equations with constant coefficients. For all practical cases they can be solved by application of an auxiliary equation.

For equation (3.6.8):

$$\frac{V_1V_2}{Q_{12}} M^2 + \frac{V_1V_2}{Q_{12}} (N_1+N_2)M + \left(\frac{N_1V_1N_2V_2}{Q_{12}} - Q_{21}\right) = 0 \qquad (3.6.10)$$

and for equation (3.6.9):

$$\frac{V_1V_2}{Q_{21}} n^2 + \left(\frac{V_1V_2}{Q_{21}} (N_1 + N_2)\right) n + \left(\frac{N_1V_1N_2V_2}{Q_{21}} - Q_{12}\right) = 0 \qquad (3.6.11)$$

These quadratic equations are solved to give expressions for M and n. The solutions for C_{A1} and C_{A2} are:-

$$C_{A1} = A \exp(M_1t) + B \exp(M_2t) \qquad (3.6.12)$$

$$C_{A2} = C \exp(n_1t) + D \exp(n_2t) \qquad (3.6.13)$$

The solution of equations (3.6.10) and (3.6.11) shows that $M_1 = n_1 = Y$, $M_2 = n_2 = Z$ where :

$$Y = \frac{-N_1-N_2 + \sqrt{(N_1+N_2)^2 - 4\left(N_1N_2 - \frac{Q_{12}Q_{21}}{V_1V_2}\right)}}{2} \qquad (3.6.14)$$

$$Z = \frac{-N_1-N_2 - \sqrt{(N_1+N_2)^2 - 4\left(N_1N_2 - \frac{Q_{12}Q_{21}}{V_1 V_2}\right)}}{2} \qquad (3.6.15)$$

Applying the following boundary conditions the constants A,B,C, D can be found.

1) At time zero, $C_{A1} = CO_{A1}$, $C_{A2} = CO_{A2}$

2) At time zero, Equations (3.6.6) and (3.6.7) are satisfied.

Therefore constants A,B,C,D are defined as:

$$A = \frac{\frac{Q_{21}CO_{A2}}{V_1} - (N_1 + Z)\, CO_{A1}}{Y - Z}$$

$$B = \frac{(Y+N_1)CO_{A1} - \frac{Q_{21}CO_{A2}}{V_1}}{Y - Z} \qquad (3.6.16)$$

$$C = \frac{\frac{Q_{12}CO_{A1}}{V_2} - (N_2+Z)\, CO_{A2}}{Y - Z}$$

$$D = \frac{(Y+N_2)\, CO_{A2} - \frac{Q_{12}}{V_2}\, CO_{A1}}{Y - Z}$$

The general equations defining the concentration of tracer gas (A) in two connected cells are given by:

$$C_{A1} = A \exp Yt + B \exp Zt \qquad (3.6.17)$$

$$C_{A2} = C \exp Yt + D \exp Zt \qquad (3.6.18)$$

The second tracer gas (B) can be used to derive a second set of equations for the two cell case and are given by:

$$C_{B1} = E \exp Yt + F \exp Zt \qquad (3.6.19)$$

$$C_{B2} = G \exp Yt + H \exp Zt \qquad (3.6.20)$$

where the coefficients E,F,G, H are defined as:

$$E = \frac{\frac{Q_{21}CO_{B2}}{V_1} - (N_1 + Z)\,CO_{B1}}{Y - Z}$$

$$F = \frac{(Y + N_1)CO_{B1} - \frac{Q_{21}CO_{B2}}{V_1}}{Y - Z}$$

$$G = \frac{\frac{Q_{12}CO_{B1}}{V_2} - (N_2 + Z)\,CO_{B2}}{Y - Z} \qquad (3.6.21)$$

$$H = \frac{(Y + N_2)CO_{B2} - \frac{Q_{12}}{V_2}\,CO_{B1}}{Y - Z}$$

Typical curve shapes for equations (3.6.17) and (3.6.18) are shown in figure (6) where comparison is made with the fundamental tracer equation (3.6.1) solved for known airflows and initial tracer gas concentrations.

3.6.1) Estimating N_1, N_2, Q_{12}, Q_{21} from site measurements.

In order to obtain estimates of airflows from the relationships described by equations (3.6.14) - (3.6.18), values of C_{A1}, C_{A2} must be manipulated to find the curve shapes given by these equations, which most closely fit the experimental data.

The method of data manipulation adopted by I'Anson is called Prony's method [29].

The approximation required is of the form:

$$C_{A1}(t) = A \exp Yt + B \exp Zt \qquad (3.6.22)$$

which can be rewritten

$$C_{A1(t)} = AU_1^{\,t} + BU_2^{\,t} \qquad (3.6.23)$$

where $U_1 = \exp Y$, $U_2 = \exp Z$

One of the requirements for this method is that the K experimental points are equally spaced and the variables are changed such that $t = 0,1,2....,K-1$.

From equation (3.6.23)

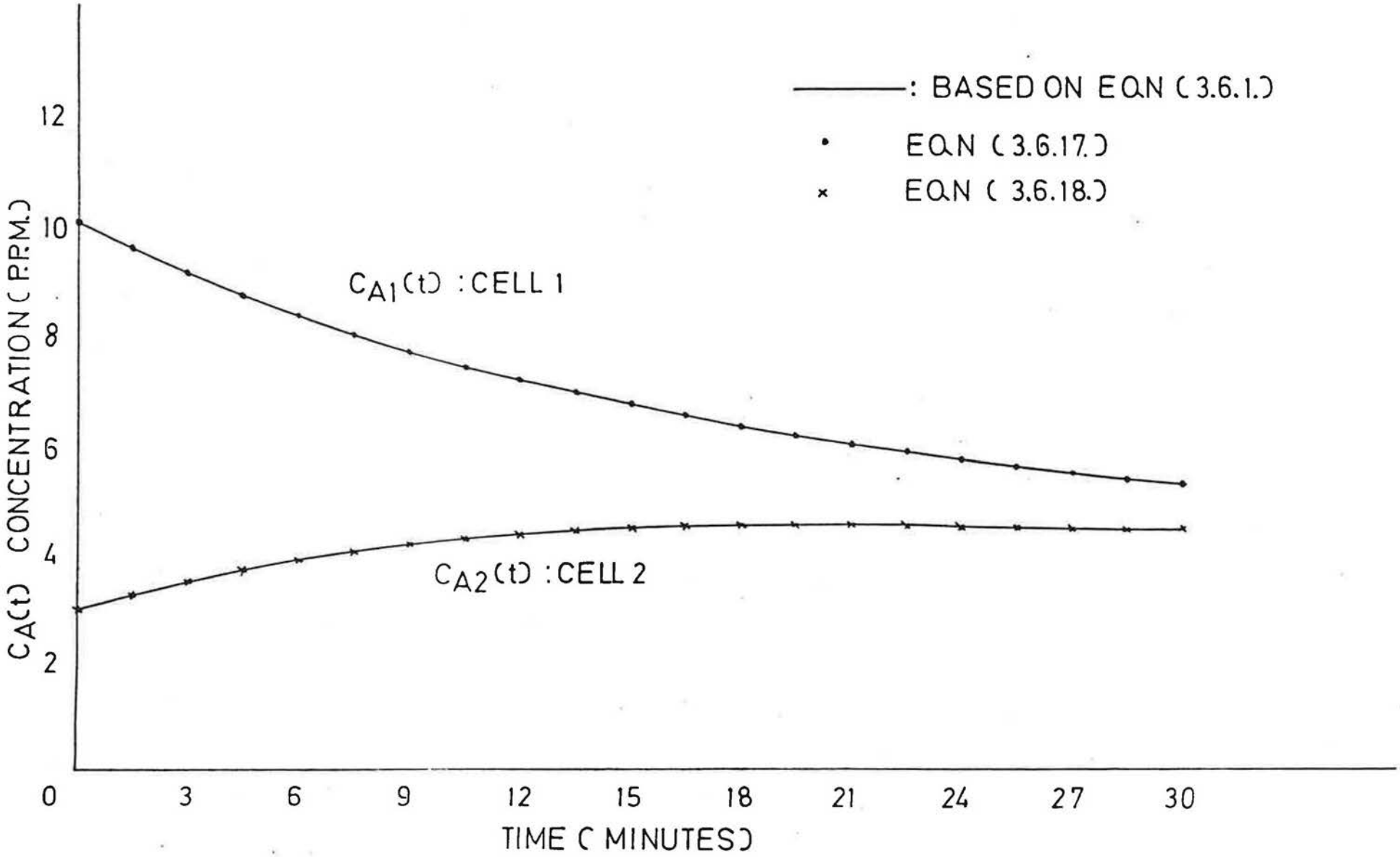

FIGURE 6 THEORETICAL VARIATIONS IN $C_A(t)$ FOR KNOWN AIRFLOWS

$$
\begin{aligned}
C(0) &= A + B \\
C(1) &= AU_1 + BU_2 \\
C(2) &= AU_1^2 + BU_2^2 \\
&\;\;\vdots \qquad\quad \vdots \qquad\quad \vdots \\
C(K-1) &= AU_1^{K-1} + BU_2^{K-1}
\end{aligned}
\tag{3.6.24}
$$

If the constants U_1 and U_2 were known, then this set would comprise K linear equations in the two unknowns A and B. If $K \geq 2$ these could then be solved for A and B. Unfortunately the U's are also unknown.

To find U_1 and U_2 they must be expressed as the roots of the algebraic equation:

$$U^2 - \alpha_1 U - \alpha_2 = 0 \tag{3.6.25}$$

so that the left hand side is identified with the product $(U-U_1).\ (U-U_2)$. In order to determine α_1 and α_2 we multiply the first equation of (3.6.24) by α_2, the second equation by α_1, and the third equation by - 1 and add the results.

The result becomes:

$$C(2) - \alpha_1 C(1) - \alpha_2 C(0) = 0 \tag{3.6.26}$$

A set of K - 3 additional equations of similar type is obtained in the same way by starting successive equations with the second, third....(K-2)th equations. In this way equations (3.6.24) and (3.6.25) imply the (K-2) linear equations:

$$C(1)\alpha_1 + C(0)\alpha_2 = C(2)$$

$$C(2)\alpha_1 + C(1)\alpha_2 = C(3)$$

$$C(3)\alpha_1 + C(2)\alpha_2 = C(4)$$

$$C(K-2)\alpha_1 + C(K-3)\alpha_2 = C(K-1) \qquad (3.6.27)$$

This set of equations can be solved exactly if K = 4, or as is more usual, approximately by the method of least squares as explained by Hildebrand [29]. The calculated values α_1, α_2 can then be used to find the roots U_1, U_2 of equation (3.6.25). These in turn are used to solve equation (3.6.24) for the unknown coefficients A and B.

The foregoing procedure is repeated for $C_{A2}(t)$ to find the unknown coefficients C and D.

When estimates have been obtained for A,B,Y and Z for Cell (1) and C,D,Y and Z for cell (2) the values of N_1,N_2,Q_{12} and Q_{21} are calculated from:

$$N_1 = \frac{ADY - BCZ}{BC - AD} \qquad (3.6.28)$$

$$N_2 = \frac{BCY - ADZ}{AD-BC} \qquad (3.6.29)$$

$$Q_{12} = \frac{V_2}{CO_{A1}} [CY + DZ + CO_{A2}N_2] \qquad (3.6.30)$$

$$Q_{21} = \frac{V_1}{CO_{A2}} [AY + BZ + CO_{A1}N_1] \qquad (3.6.31)$$

3.6.2) Discussion on I'Ansons analysis method

Appendix (C) illustrates the method of analysis adopted by I'Anson, applied to a worked example. The fundamental tracer equation (3.6.1) has been solved for known airflows N_1, N_2, Q_{12} Q_{21} and initial tracer gas concentrations, the time variations in tracer concentration to t = 0 to t = 30 minutes are fully described. Experimental errors are assumed as $\pm$ 5% and are imposed on each data point, see figure (3). Reference to Appendix (C) highlights the major disadvantage of the prony method. A random $\pm$ 5% error on concentration data causes equation (3.6.25) to have complex, negative roots (U_1,U_2) which means the data would be rejected as unsuitable for analysis.

Generally, small random errors commonly experienced during site tracer concentration measurements will ensure a significant failure rate (complex roots) if data analysis is carried out using the prony method.

When site data gives real, positive roots in equation (3.6.25) a small random error in concentration data leads to significant errors in the calculated coefficients A,B,C,D, Y and Z.

The airflows subsquently found from these coefficients will compound such errors.

Chapter 4: AN ALTERNATIVE ANALYSIS METHOD FOR CALCULATING AIRFLOWS: TWO CELL CASE

4.1) General

The existing methods of analysis as discussed in Chapter (3) have two basic disadvantages:

1) The numerical methods used either rely on pairs of site data points or apply numerical differentiation to concentration/time points which are subject to considerable random errors of measurement.

2) The analytical method concentrates random errors of measurment in the roots of a quadratic equation which leads to a high failure rate (complex, negative roots) when processing data.

To overcome the above mentioned difficulties the following analysis method has been developed by the author.

4.2) Analytical solution of the fundamental tracer gas equations

The following method of analysis can be used for $N>2$ cells if required. However for comparison purposes the $N=2$ cell case is considered first.

The fundamental tracer gas equation is for N=2 cells expressed as:

$$Vi \frac{dC_i}{dt} = fi + \left[\sum_{j=1}^{2} Q_{ji} C_j \ (1-\delta ij) \right] - SiCi \qquad (4.2.1)$$

If a pulse of tracer gas (A) is released in cell (1) at time zero and a pulse of tracer gas (B) is released in cell (2) at the same time, equation (4.2.1) becomes for cell (1):

Gas (A)

$$V_1 \frac{dC_{A1}}{dt} = Q_{21}C_{A2} - S_1C_{A1} \qquad (4.2.2)$$

Gas (B)

$$V_1 \frac{dC_{B1}}{dt} = Q_{21}C_{B2} - S_1C_{B1} \qquad (4.2.3)$$

and for cell (2)

Gas (A)

$$V_2 \frac{dC_{A2}}{dt} = Q_{12}C_{A1} - S_2C_{A2} \qquad (4.2.4)$$

Gas (B)

$$V_2 \frac{dC_{B2}}{dt} = Q_{12}C_{B1} - S_2C_{B2} \qquad (4.2.5)$$

Using the relationships $N_1 = \frac{S_1}{V_1}$ and $N_2 = \frac{S_2}{V_2}$ equations (4.2.2) to (4.2.5) can be re-arranged as follows:-

For Cell (1), tracer (A)

$$\frac{dC_{A1}}{dt} + N_1 C_{A1} = \frac{Q_{21}}{V_1} C_{A2} \qquad (4.2.6)$$

and for tracer (B)

$$\frac{dC_{B1}}{dt} + N_1 C_{B1} = \frac{Q_{21}}{V_1} C_{B2} \qquad (4.2.7)$$

For cell (2), tracer (A)

$$\frac{dC_{A2}}{dt} + N_2 C_{A2} = \frac{Q_{12}}{V_2} C_{A1} \qquad (4.2.8)$$

and for tracer (B)

$$\frac{dC_{B2}}{dt} + N_2 C_{B2} = \frac{Q_{12}}{V_2} C_{B1} \qquad (4.2.9)$$

Let us consider the solution of equation (4.2.6) for C_{A1}; Equation (4.2.6) is a first order differential equation which may be solved for C_{A1} using integrating factors. The integrating factor required for equation (4.2.6) is $e^{N_1 t}$

i.e. $\frac{d}{dt}(C_{A1} e^{N_1 t}) = \frac{dC_{A1}}{dt} e^{N_1 t} + N_1 C_{A1} e^{N_1 t}$, therefore

equation (4.2.6) may be expressed as:

$$C_{A1}e^{N_1 t} = \frac{Q_{21}}{V_1}\int C_{A2}e^{N_1 t}\,dt + A \qquad (4.2.10)$$

Similarly, equation (4.2.8) for C_{A2} may be solved using e^{N2t} as the integrating factor and becomes:

$$C_{A2}e^{N_2 t} = \frac{Q_{12}}{V_2}\int C_{A1}e^{N_2 t}dt + B \qquad (4.2.11)$$

where coefficients A and B are constants of integration.

To integrate equations(4.2.10) and(4.2.11) for C_{A2} and C_{A1} respectively their time variations must be either known or assumed. We shall initially <u>assume</u> that no recirculation of tracer gas occurs between the two cells ($Q_{21} = 0$) then, from Dick's equations [17] the time variation in C_{A2} concentration is given by:

$$C_{A2} = CO_{A2}e^{-N_2 t} + \frac{Q_{12}CO_{A1}}{V_2(N_2-N_1)}\left[e^{-N_1 t} - e^{-N_2 t}\right] \qquad (4.2.12)$$

Where CO_{A2} = initial concentration of tracer gas (A) in cell (2) at time zero

CO_{A1} = initial concentration of tracer gas (A) in cell (1) at time zero.

Substituting for C_{A2} from equation (4.2.12) into equation (4.2.10) we obtain:

$$C_{A1}e^{N_1 t} = \frac{Q_{21}}{V_1}\int\left(CO_{A2}e^{(N_1 - N_2)t} + \frac{Q_{12}CO_{A1}}{V_2(N_2-N_1)}\left(1 - e^{(N_1-N_2)t}\right)\right)dt + A \quad (4.2.13)$$

Integrating equation (4.2.13) gives:

$$C_{A1}e^{N_1 t} = \frac{Q_{21}CO_{A2}}{V_1(N_1-N_2)}e^{(N_1-N_2)t} + \frac{Q_{21}Q_{12}CO_{A1}}{V_1V_2(N_2-N_1)}\left[t - \frac{e^{(N_1-N_2)t}}{N_1-N_2}\right] + A \quad (4.2.14)$$

By applying the boundary condition that at time zero, $C_{A1} = CO_{A1}$

The constant of integration A is:

$$A = CO_{A1} - \frac{Q_{21}CO_{A2}}{V_1(N_1-N_2)} - \frac{Q_{21}Q_{12}CO_{A1}}{V_1V_2(N_2-N_1)} \quad (4.2.15)$$

Substituting for A in equation (4.2.14) and re-arranging

$$C_{A1} = CO_{A1}e^{-N_1 t} + \frac{Q_{21}CO_{A2}}{V_1(N_1-N_2)}\left[e^{-N_2 t - N_1 t} - e^{-N_1 t}\right] + \frac{Q_{21}Q_{12}CO_{A1}}{V_1V_2(N_2-N_1)}\left[te^{-N_1 t} + \frac{(e^{-N_2 t} - e^{-N_1 t})}{(N_2 - N_1)}\right] \quad (4.2.16)$$

Equation (4.2.11) can be solved for C_{A2} by substituting for C_{A1} from equation (4.2.16) and becomes:

$$C_{A2}e^{N_2 t} = \frac{Q_{12}}{V_2}\int CO_{A1}e^{(N_2-N_1)t} + \frac{Q_{21}CO_{A2}}{V_1(N_1-N_2)}(1-e^{(N_2-N_1)t}) +$$

$$\frac{Q_{21}Q_{12}CO_{A1}}{V_1V_2(N_2-N_1)}\left[te^{(N_2-N_1)t} + \frac{(1-e^{(N_2-N_1)t})}{N_2-N_1}\right]dt + B \qquad (4.2.17)$$

Integrating equation (4.2.17) gives:

$$C_{A2}e^{N_2 t} = \frac{Q_{12}CO_{A1}e^{(N_2-N_1)t}}{V_2(N_2-N_1)} + \frac{Q_{12}Q_{21}CO_{A1}}{V_1V_2(N_1-N_2)}\left(t - \frac{e^{(N_2-N_1)t}}{N_2-N_1}\right) +$$

$$\frac{Q_{21}Q_{12}^2CO_{A1}}{V_1V_2^2(N_2-N_1)}\left[\frac{t}{N_2-N_1} + \frac{te^{(N_2-N_1)t}}{N_2-N_1} - \frac{2e^{(N_2-N_1)t}}{(N_2-N_1)^2}\right] + B \qquad (4.2.18)$$

By applying the boundary condition that at time zero, $C_{A2}=CO_{A2}$ the constant of integration B is:

$$B = CO_{A2} - \frac{Q_{12}CO_{A1}}{V_2(N_2-N_1)} - \frac{Q_{12}Q_{21}CO_{A2}}{V_1V_2(N_1-N_2)} + \frac{2Q_{21}Q_{12}CO_{A1}}{V_1V_2^2(N_2-N_1)} \qquad (4.2.19)$$

Substituting for B in equation (4.2.18) and re-arranging

$$C_{A2}=CO_{A2}e^{-N_2 t} + \frac{Q_{12}CO_{A1}}{V_2(N_2-N_1)}\left[e^{-N_1 t}-e^{-N_2 t}\right] + \frac{Q_{12}Q_{21}CO_{A2}}{V_1V_2(N_1-N_2)}\left[te^{-N_2 t} + \frac{(e^{-N_2 t}-e^{N_1 t})}{(N_2-N_1)}\right]$$

$$+ \frac{Q_{21}Q_{12}^2CO_{A1}}{V_1V_2^2(N_2-N_1)}\left[\frac{(2e^{-N_2 t}-2e^{-N_1 t})}{(N_2-N_1)^2} + \frac{(te^{-N_2 t}+te^{-N_1 t})}{(N_2-N_1)}\right] \qquad (4.2.20)$$

The same derivation is applied to equations (4.2.7) and (4.2.9) for C_{B1} and C_{B2} respectively.

$$C_{B1} = CO_{B1}e^{-N_1 t} - \frac{Q_{21}CO_{B2}}{V_1(N_1-N_2)}\left[e^{-N_2 t - N_1 t}\right] + \frac{Q_{21}Q_{12}CO_{B1}}{V_1V_2(N_2-N_1)}\left[te^{-N_1 t} + \frac{(e^{-N_2 t - N_1 t})}{(N_2-N_1)}\right] \quad (4.2.21)$$

$$C_{B2} = CO_{B2}e^{-N_2 t} + \frac{Q_{12}CO_{B1}}{V_2(N_2-N_1)}\left[e^{-N_1 t - N_2 t}\right] + \frac{Q_{12}Q_{21}CO_{B2}}{V_1V_2(N_1-N_2)}\left[(te^{-N_2 t} + \frac{(e^{-N_2 t - N_1 t})}{(N_2-N_1)}\right] +$$

$$\frac{Q_{21}Q_{12}^2CO_{B1}}{V_1V_2^2(N_2-N_1)}\left[\frac{(2e^{-N_2 t} - 2e^{-N_1 t})}{(N_2-N_1)^2} + \frac{(te^{-N_2 t} + te^{-N_1 t})}{(N_2 - N_1)}\right] \quad (4.2.22)$$

Typical curves shapes for C_{A1}, equation (4.2.16) and C_{A2}, equation (4.2.20) are shown in figure (7) where comparison is made with the fundamental tracer equation (4.2.1) solved for known airflows and initial tracer gas concentrations.

4.3) Calculating N_1, N_2, Q_{12}, Q_{21} from site measurements

Considering two connected cells, if a quantity of tracer gas is released in Cell (1), then tracer gas will infiltrate into the second cell (2) and, after mixing with the air there, it may then be returned to cell (1). The following discussion assumes that the effects of recirculation of tracer gas are time dependant. Provided sufficient site data (minimum of 10 Ci(t) points) are collected before recirculation

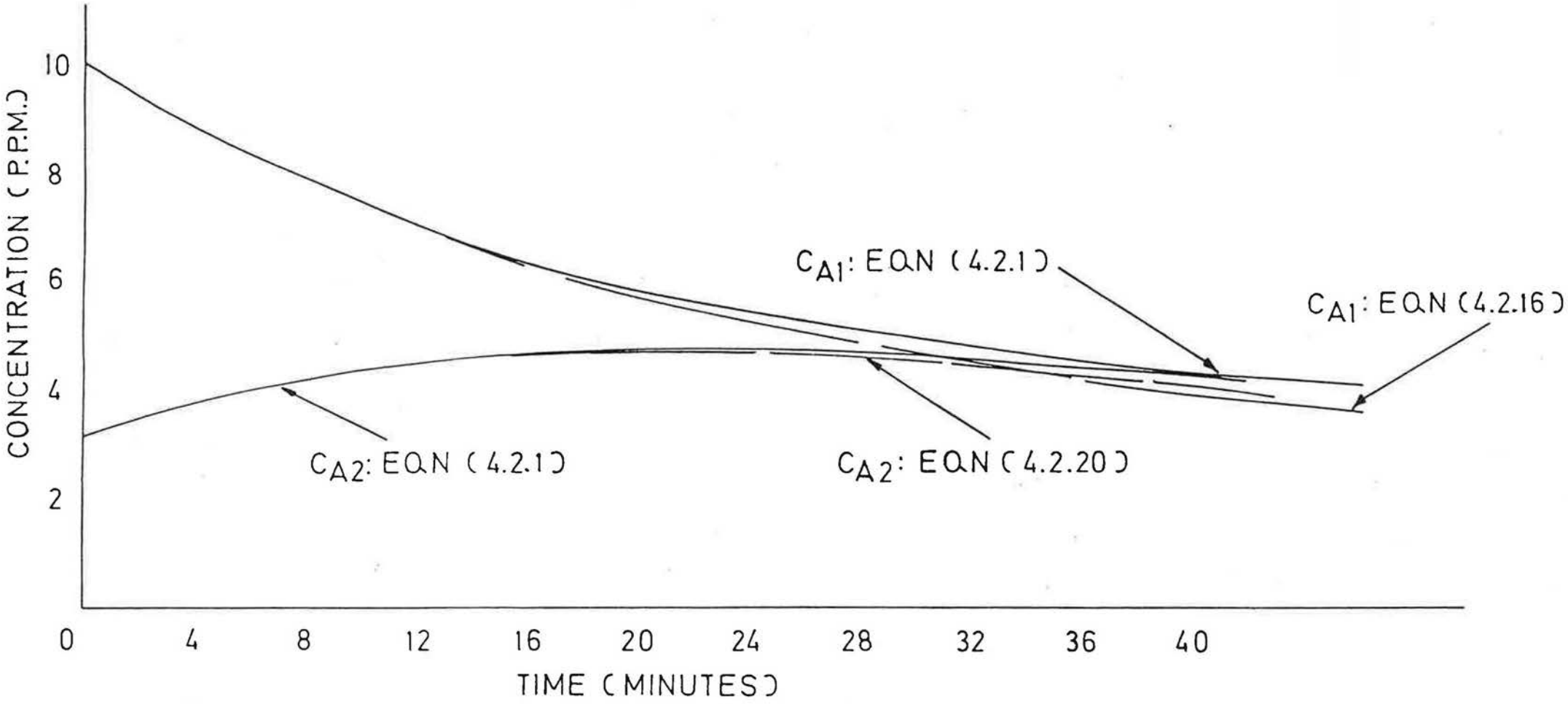

FIGURE 7 COMPARISON BETWEEN THEORETICAL VARIATIONS IN C_A (t)

of tracer gas is greater than 15% of Ci(t), then a simplified form of equations (4.2.16) and (4.2.20) may be used to calculate the unknown airflows N_1, N_2, Q_{12} and Q_{21}. Reference to figures (8) and (9) shows the relative contributions varying with time for each term in equations (4.2.16) and (4.2.20) for C_{A1} and C_{A2} respectively. For the example given, the effects of recirculation of tracer gas are less than 15% of $C_{A1}(t)$ and $C_{A2}(t)$ for time (t) $\leqslant$ 20 minutes. Therefore, if sufficient data points can be collected in this time, equations (4.2.16) and (4.2.20) can be simplified to:

$$C_{A1}=CO_{A1}e^{-N_1t}+\frac{Q_{21}CO_{A2}}{V_1(N_1-N_2)}\left(e^{N_2t-N_1t}\right) \qquad (4.3.1)$$

$$C_{A2}=CO_{A2}e^{-N_2t}+\frac{Q_{12}CO_{A1}}{V_2(N_2-N_1)}\left(e^{-N_1t-N_2t}\right) \qquad (4.3.2)$$

Similarly equations (4.2.21) and (4.2.22) for C_{B1} and C_{B2} respectively, can be simplified to:

$$C_{B1}=CO_{B1}e^{-N_1t}+\frac{Q_{21}CO_{B2}}{V_1(N_1-N_2)}\left(e^{-N_2t-N_1t}\right) \qquad (4.3.3.)$$

$$CB_2=CO_{B2}e^{-N_2t}+\frac{Q_{12}CO_{B1}}{V_2(N_1-N_2)}\left(e^{-N_2t-N_1t}\right) \qquad (4.3.4)$$

$$C_{A_1} = \underset{\text{(A)}}{C_{OA_1} e^{-N_1 t}} + \underset{\text{(B)}}{\frac{Q_{21} C_{OA_2}}{V_1 (N_1 - N_2)} \left[e^{-N_2 t} - e^{-N_1 t} \right]} + \underset{\text{(C)}}{\frac{Q_{21} Q_{12} C_{OA_1}}{V_1 V_2 (N_2 - N_1)} \left[te^{-N_1 t} + \frac{(e^{-N_2 t} - e^{-N_1 t})}{N_2 - N_1} \right]}$$

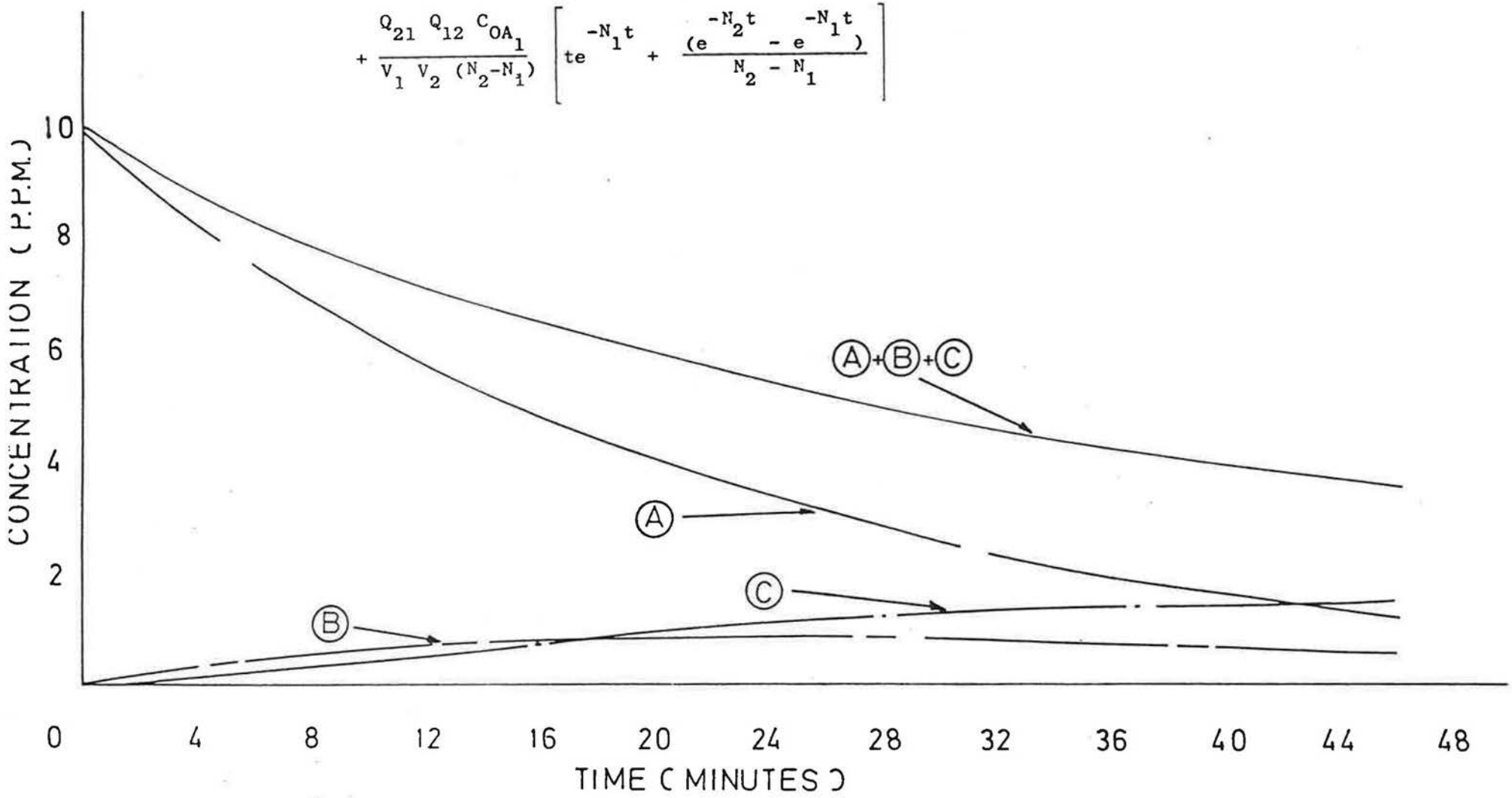

FIGURE 8 C_{A1} CONCENTRATION DESCRIBED BY EQUATION (4.2.16.)

$$C_{A_2} = \underset{\text{(A)}}{C_{OA_2} e^{-N_2 t}} + \underset{\text{(B)}}{\frac{Q_{12} C_{OA_1}}{V_2(N_2-N_1)} \left[e^{-N_1 t} - e^{-N_2 t} \right]}$$

$$+ \underset{\text{(C)}}{\frac{Q_{12} Q_{21} C_{OA_2}}{V_1 V_2 (N_1-N_2)} \left[te^{-N_2 t} + \frac{(e^{-N_2 t} - e^{-N_1 t})}{N_2 - N_1} \right]}$$

$$+ \underset{\text{(D)}}{\frac{Q_{21} Q_{12}^2 C_{OA_1}}{V_1 V_2^2 (N_2-N_1)} \left[\frac{2e^{-N_2 t} - 2e^{-N_1 t}}{(N_2 - N_1)^2} + \frac{(te^{-N_2 t} + te^{-N_1 t})}{(N_2 - N_1)} \right]}$$

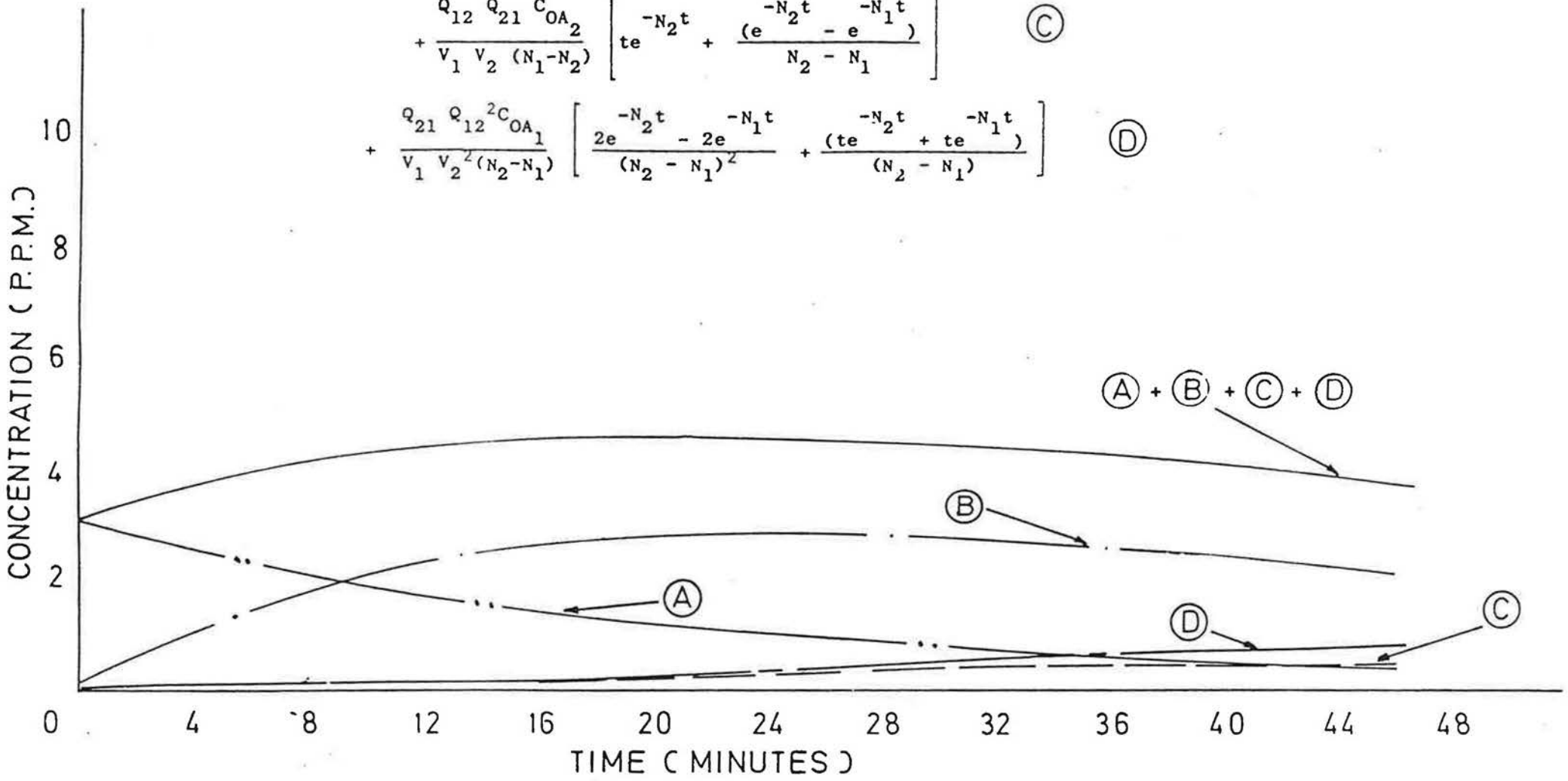

FIGURE 9 C_{A2} CONCENTRATION DESCRIBED BY EQUATION (4.2.20.)

The first exponential term in equations (4.3.1) to (4.3.4) can be expressed as a Maclaurin series expansion of the form:

$$e^{-N_1 t} = 1 - N_1 t + \frac{N_1(N_1 t^2)}{2!} - \frac{N_1(N_1^2 t^3)}{3!} + \frac{N_1(N_1^3 t^4)}{4!} - \frac{N_1(N_1^4 t^5)}{5!} \qquad (4.3.5)$$

$$e^{-N_2 t} = 1 - N_2 t + \frac{N_2(N_2 t^2)}{2!} - \frac{N_2(N_2^2 t^3)}{3!} + \frac{N_2(N_2^3 t^4)}{4!} - \frac{N_2(N_2^4 t^5)}{5!} \qquad (4.3.6)$$

Then equations (4.3.1) and (4.3.2) become for C_{A1} and C_{A2} respectively

$$C_{A1} = CO_{A1}\left[\left(1 - N_1 t + \frac{N_1(N_1 t^2)}{2!} - \frac{N_1(N_1^2 t^3)}{3!} + \frac{N_1(N_1^3 t^4)}{4!} - \frac{N_1(N_1^4 t^5)}{5!}\right)\right] + \frac{Q_{21} CO_{A2}}{V_1(N_1 - N_2)}\left[\exp(-N_2 t) - \exp(-N_1 t)\right] \qquad (4.3.7)$$

$$C_{A2} = CO_{A2}\left(1 - N_2 t + \frac{N_2(N_2 t^2)}{2!} - \frac{N_2(N_2^2 t^3)}{3!} + \frac{N_2(N_2^3 t^4)}{4!} - \frac{N_2(N_2^4 t^5)}{5!}\right) + \frac{Q_{12} CO_{A1}}{V_2(N_2 - N_1)}\left[\exp(-N_1 t) - \exp(-N_2 t)\right] \qquad (4.3.8)$$

Similarly for C_{B1} and C_{B2} equations (4.3.3) and (4.3.4) become:

$$C_{B1} = CO_{B1}(1-N_1t+N_1\frac{(N_1t^2)}{2!} - N_1\frac{(N_1^2t^3)}{3!}+N_1\frac{(N_1^3t^4)}{4!} - N_1\frac{(N_1^4t^5)}{5!}) +$$

$$\frac{Q_{21}CO_{B2}}{V_1(N_1-N_2)} [\exp(-N_2t)-\exp(-N_1t)] \qquad (4.3.9)$$

$$C_{B2}=CO_{B2}(1-N_2t+N_2\frac{(N_2t^2)}{2!}-N_2\frac{(N_2^2t^3)}{3!}+ N_2\frac{(N_2^3t^4)}{4!}-N_2\frac{(N_2^4t^5)}{5!}) +$$

$$\frac{Q_{12}CO_{B1}}{V_2(N_2-N_1)} [\exp(-N_1t) - \exp(-N_2t)] \qquad (4.3.10)$$

To calculate airflows N_1, N_2, Q_{12} and Q_{21} from equations (4.3.7) to (4.3.10) we require a first order estimate of N_1. This is achieved by taking the first six data points of C_{A1}, time in cell (1). Similarly an estimate of N_2 is obtained from C_{B2}, time data points in cell (2). The result of a least squares fit on such data points will provide an estimate of N_1 and N_2, let us indicate such an estimate as N_1' for cell (1) and N_2' for cell (2) air change rates. Substituting for N_1' and N_2' in equations (4.3.7) to (4.3.10) we obtain:

$$C_{A1} = CO_{A1}\left[(1-N_1t + \frac{N_1(N_1't^2)}{2!} - \frac{N_1(N_1'^2t^3)}{3!} + \frac{N_1(N_1'^3t^4)}{4!} - \frac{N_1(N_1'^4t^5)}{5!}\right] +$$

$$\frac{Q_{21}CO_{A2}}{V_1}\ \frac{[\exp(-N_2't) - \exp(-N_1't)]}{(N_1' - N_2')} \qquad (4.3.11)$$

$$C_{A2} = CO_{A2}\left[1-N_2t + \frac{N_2(N_2't^2)}{2!} - \frac{N_2(N_2'^2t^3)}{3!} + \frac{N_2(N_2'^3t^4)}{4!} - \frac{N_2(N_2'^4t^5)}{5!}\right]$$

$$\frac{Q_{12}CO_{A1}}{V_2}\ \frac{[\exp(-N_1't) - \exp(-N_2't)]}{(N_2' - N_1')} \qquad (4.3.12)$$

$$C_{B1} = CO_{B1}\left[1-N_1t+\frac{N_1(N_1't^2)}{2!} - \frac{N_1(N_1'^2t^3)}{3!} + \frac{N_1(N_1'^3t^4)}{4!} - \frac{N_1(N_1'^4t^5)}{5!}\right] +$$

$$\frac{Q_{21}CO_{B2}}{V_1}\ \frac{[\exp(-N_2't) - \exp(-N_1't)]}{(N_1' - N_2')} \qquad (4.3.13)$$

$$C_{B2} = CO_{B2}\left[1-N_2t+\frac{N_2(N_2't^2)}{2!} - \frac{N_2(N_2'^2t^3)}{3!} + \frac{N_2(N_2'^3t^4)}{4!} - \frac{N_2(N_2'^4t^5)}{5!}\right] +$$

$$\frac{Q_{12}CO_{B1}}{V_2}\ \frac{[\exp(-N_1't) - \exp(-N_2't)]}{(N_2' - N_1')} \qquad (4.3.14)$$

The initial tracer gas concentrations CO_{A1}, CO_{A2}, CO_{B1}, CO_{B2} are taken from site data. The mean concentrations of tracer gas $C_{A1}(t)$, $C_{A2}(t)$ and $C_{B1}(t)$, $C_{B2}(t)$ are found by numerical integration of all site data concentration points obtained during a test run (t = 0 , t = K). This mean concentration is expressed as:

$$\tilde{C}_i(t) = \frac{\int_{t=0}^{t=k} C_i(t)\,dt}{\Delta t \qquad 0 \quad K} \tag{4.3.15}$$

Substituting for $\tilde{C}_i(t)$ in equations (4.3.11) and (4.3.13) and re-arranging we obtain:

$$N_1 = \left[\frac{1}{A} - \frac{\tilde{C}_{A1}}{CO_{A1}A}\right] + \frac{Q_{21}CO_{A2}}{V_1 CO_{A1} A}\left[\frac{e^{-N_2' t} - e^{-N_1' t}}{N_1' - N_2'}\right] \tag{4.3.16}$$

$$Q_{21} = \frac{[\tilde{C}_{B1} + CO_{B1}(N_1 A - 1)][V_1(N_1' - N_2')]}{CO_{B2}[\exp(-N_2' t) - \exp(-N_1' t)]} \tag{4.3.17}$$

where $A = -t + \frac{N_1' t^2}{2!} - \frac{N_1'^2 t^3}{3!} + \frac{N_1'^3 t^4}{4!} - \frac{N_1'^4 t^5}{5!} \times (-1)$

Substituting for $\tilde{C}_i(t)$ in equations (4.3.14) and (4.3.12) and re-arranging we obtain:

$$N_2 = \left[\frac{1}{D} - \frac{\tilde{C}_{B2}}{CO_{B2}D}\right] + \frac{Q_{12}CO_{B1}}{V_2 CO_{B2} D}\left[\frac{\exp(-N_1' t) - \exp(N_2' t)}{N_2' - N_1'}\right] \tag{4.3.18}$$

$$Q_{12} = \frac{(\widetilde{C_{A2}} + CO_{A2}(DN_2 - 1))(V_2(N_2' - N_1'))}{CO_{A1}(\exp(-N_1't) - \exp(-N_2't))} \qquad (4.3.19)$$

where $$D = \left(-t + \frac{N_2't^2}{2!} - \frac{N_2'^2t^3}{3!} + \frac{N_2'^3t^4}{4!} - \frac{N_2'^4t^5}{5!}\right) \times (-1)$$

Values of N_1, Q_{21}, N_2 and Q_{12} are found using numerical iteration; the Gauss-Seidel method causes convergance after six steps. The airflow values calculated can be substituted into equations (4.3.16)-(4.3.20) and the calculation of N_1, N_2, Q_{12}, Q_{21} repeated.

When the solution of equations (4.3.16) - (4.3.20) converges for the calculated airflows, the theoretical time variations in tracer gas concentration can be found by substitution of such values into equations (4.2.2) and (4.2.4) for C_{A1} and C_{A2} respectively. C_{B1} and C_{B2} theoretical concentration variations are found from equations (4.2.3) - (4.2.5). The resulting curves can then be compared with site data points and direct comparison made.

4.4) Estimating errors in N1, N2, Q12, Q21

The following discussion assumes that all variables in equations (4.3.16) - (4.3.19) vary independantly of each other and there is no error in measured values of time.

Considering equation (4.3.16) for N_1:

$$N_1 = \left[\frac{1}{A} - \frac{\widetilde{C_{A1}}}{CO_{A1}A}\right] + \frac{Q_{21}CO_{A2}}{V_1CO_{A1}A}\left[\frac{\exp(-N_2't) - \exp(-N_1't)}{N_1' - N_2'}\right] \qquad (4.4.1)$$

The absolute standard error in N_1 can be estimated from

$$(\Delta N_1)^2 = \left|\frac{\partial N_1}{\partial N_1'}\Delta N_1'\right|^2 + \left|\frac{\partial N_1}{\partial N_2'}\Delta N_2\right|^2 + \left|\frac{\partial N_1}{\partial CO_{A1}}\Delta CO_{A1}\right|^2 + \left|\frac{\partial N_1}{\partial CO_{A2}}\Delta CO_{A2}\right|^2$$
$$+ \left|\frac{\partial N_1}{\partial C_{A1}}\Delta C_{A1}\right|^2 + \left|\frac{\partial N_1}{\partial V_1}\Delta V_1\right|^2 + \left|\frac{\partial N_1}{\partial Q_{21}}\Delta Q_{21}\right|^2 + \left|\frac{\partial N_1}{\partial A}\Delta A\right|^2 \qquad (4.4.2)$$

where $$\frac{\partial N_1}{\partial N_1'} = \frac{(CO_{A1}AV_1)(N_1'-N_2')(Q_{21}CO_{A2}te^{-N_1't}) - (Q_{21}CO_{A2}(e^{-N_2't} - e^{-N_1't})CO_{A1}AV_1)}{[CO_{A1}AV_1\ (N_1' - N_2')]^2} \qquad (4.4.3)$$

$$\frac{\partial N_1}{\partial N_2'} = \frac{(CO_{A1}AV_1(N_1'-N_2')(-te^{-N_2't}Q_{21}CO_{A2}) - (Q_{21}CO_{A2}(e^{-N_2't} - e^{-N_1't})(-CO_{A1}AV_1)}{[CO_{A1}AV_1(N_1' - N_2')]^2} \qquad (4.4.4)$$

$$\frac{\partial N_1}{\partial CO_{A1}} = \left[\frac{C_{A1}}{CO_{A1}^2 A}\right]\frac{Q_{21}CO_{A2}[e^{-N_2't} - e^{-N_1't}]}{CO_{A1}^2\ AV_1\ [N_1' - N_2']} \qquad (4.4.5)$$

$$\frac{\partial N_1}{\partial CO_{A2}} = \frac{Q_{21}}{CO_{A1}AV_1}\left[\frac{e^{-N_2't} - e^{-N_1't}}{(N_1' - N_2')}\right] \qquad (4.4.6)$$

$$\frac{\partial N_1}{\partial \tilde{C}_{A1}} = -\frac{1}{CO_{A1}\ A} \qquad (4.4.7)$$

$$\frac{\partial N_1}{\partial V_1} = -\frac{Q_{21}CO_{A2}}{V_1^2 CO_{A1} A}\left[\frac{e^{-N_2' t} - e^{-N_1' t}}{N_1' - N_2'}\right] \qquad (4.4.8)$$

$$\frac{\partial N_1}{\partial Q_{21}} = \frac{CO_{A2}}{V_1 CO_{A1} A}\left[\frac{e^{-N_2' t} - e^{-N_1' t}}{N_1' - N_2'}\right] \qquad (4..4.9)$$

$$\frac{\partial N_1}{\partial A} = \left|\frac{-1}{A^2} + \frac{\tilde{C}_{A1}}{CO_{A1} A^2}\right| - \frac{Q_{21}CO_{A2}}{V_1 CO_{A1} A^2}\left[\frac{e^{-N_2' t} - e^{-N_1' t}}{N_1' - N_2'}\right] \qquad (4.4.10)$$

The absolute error for Q_{21} is found by considering equation (4.3.17)

$$Q_{21} = \frac{(\tilde{C}_{B1} + CO_{B1}(N_1 A - 1))(V_1(N_1' - N_2'))}{CO_{B2}[e^{-N_2' t} - e^{-N_1' t}]} \qquad (4.4.11)$$

and

$$(\Delta Q_{21})^2 = \left|\frac{\partial Q_{21}}{\partial N_1'}\Delta N_1'\right|^2 + \left|\frac{\partial Q_{21}}{\partial N_2'}\Delta N_2'\right|^2 + \left|\frac{\partial Q_{21}}{\partial CO_{B1}}\Delta CO_{B1}\right|^2 + \left|\frac{\partial Q_{21}}{\partial CO_{B2}}\Delta CO_{B2}\right|^2 + \left|\frac{\partial Q_{21}}{\partial C_{B1}}\Delta C_{B1}\right|^2 +$$

$$\left|\frac{\partial Q_{21}}{\partial N_1}\Delta N_1\right|^2 + \left|\frac{\partial Q_{21}}{\partial V_1}\Delta V_1\right|^2 + \left|\frac{\partial Q_{21}}{\partial A}\Delta A\right|^2 \qquad (4.4.12)$$

$$\frac{\partial Q_{21}}{\partial N_1'} = \frac{V_1(\tilde{C}_{B1}+CO_{B1}(N_1A-1)(CO_{B2}(e^{-N_2't-N_1't} - e^{-N_1't})) - (CO_{B2}te^{-N_1't})(\tilde{C}_{B1}+CO_{B1}(N_1A-1)(V_1(N_1'-N_2'))}{[CO_{B2}(e^{-N_2't} - e^{-N_1't})]^2} \quad (4.4.13)$$

$$\frac{\partial Q_{21}}{\partial N_2'} = \frac{-V_1(\tilde{C}_{B1}+CO_{B1}(N_1A-1))(CO_{B2}(e^{-N_2't} - e^{-N_1't})) - (-CO_{B2}te^{-N_2't})(\tilde{C}_{B1}+CO_{B1}(N_1A-1))(N_1'-N_2')V_1}{[CO_{B2}(e^{-N_2't} - e^{-N_1't})]^2} \quad (4.4.14)$$

$$\frac{\partial Q_{21}}{\partial CO_{B1}} = \frac{(N_1A-1)V_1(N_1'-N_2')}{CO_{B2}(e^{-N_2't} - e^{-N_1't})} \quad (4.4.15)$$

$$\frac{\partial Q_{21}}{\partial CO_{B2}} = \frac{-(\tilde{C}_{B1} + CO_{B1}(N_1A-1))(V_1(N_1'-N_2'))}{CO_{B2}^2(e^{-N_2't} - e^{-N_1't})} \quad (4.4.16)$$

$$\frac{\partial Q_{21}}{\partial \tilde{C}_{B1}} = \frac{V_1(N_1' - N_2')}{CO_{B2}(e^{-N_2't} - e^{-N_1't})} \quad (4.4.17)$$

$$\frac{\partial Q_{21}}{\partial N_1} = \frac{CO_{B1}AV_1(N_1' - N_2')}{CO_{B2}(e^{-N_2't} - e^{-N_1't})} \quad (4.4.18)$$

$$\frac{\partial Q_{21}}{\partial V_1} = \frac{(\tilde{C}_{B1} + CO_{B1}(N_1A-1)(N_1' - N_2')}{CO_{B2}[e^{-N_2't} - e^{-N_1't}]} \quad (4.4.19)$$

$$\frac{\partial Q_{21}}{\partial A} = \frac{CO_{B1}N_1V_1(N_1'-N_2')}{CO_{B2}(e^{-N_2't} - e^{-N_1't})} \quad (4.4.20)$$

Equation (4.3.18) gives for N_2:

$$N_2 = \left[\frac{1}{D} - \frac{\tilde{C}_{B2}}{CO_{B2}D}\right] + \frac{Q_{12}CO_{B1}}{V_2CO_{B2}D}\left[\frac{e^{-N_1't} - e^{-N_2't}}{N_2' - N_1'}\right] \qquad (4.4.21)$$

The absolute error in N_2 is estimated from

$$(\Delta N_2)^2 = \left|\frac{\partial N_2}{\partial N_1'}\Delta N_1\right|^2 + \left|\frac{\partial N_2}{\partial N_2'}\Delta N_2\right|^2 + \left|\frac{\partial N_2}{\partial CO_{B1}}\Delta CO_{B1}\right|^2 + \left|\frac{\partial N_2}{\partial CO_{B2}}\Delta CO_{B2}\right|^2 + \left|\frac{\partial N_2}{\partial C_{B2}}\Delta C_{B2}\right|^2 + \left|\frac{\partial N_2}{\partial V_2}\Delta V_2\right|^2 +$$

$$\left|\frac{\partial N_2}{\partial Q_{12}}\Delta Q_{12}\right|^2 + \left|\frac{\partial N_2}{\partial D}\Delta D\right|^2 \qquad (4.4.22)$$

where

$$\frac{\partial N_2}{\partial N_1'} = \frac{Q_{12}CO_{B1}(-te^{-N_1't})(V_2CO_{B2}D(N_2'-N_1')) - (-V_2CO_{B2}D(Q_{12}CO_{B1}(e^{-N_1't} - e^{-N_2't})))}{[V_2CO_{B2}D\ (N_2'-N_1')]^2} \qquad (4.4.23)$$

$$\frac{\partial N_2}{\partial N_2'} = \frac{(Q_{12}CO_{B1}te^{-N_2't})(V_2CO_{B2}D(N_2'-N_1')) - (V_2CO_{B2}D(Q_{12}CO_{B1}(e^{-N_1't} - e^{-N_2't})))}{[V_2CO_{B2}D\ (N_2' - N_1')]^2} \qquad (4.4.24)$$

$$\frac{\partial N_2}{\partial CO_{B1}} = \frac{Q_{12}}{V_2 CO_{B2} D}\left[\frac{e^{-N_1' t} - e^{-N_2' t}}{N_2' - N_1'}\right] \qquad (4.4.25)$$

$$\frac{\partial N_2}{\partial CO_{B2}} = \frac{\tilde{C}_{B2}}{CO_{B2}^2 D} - \frac{Q_{12} CO_{B1}}{V_2 CO_{B2}^2 D}\left[\frac{e^{-N_1' t} - e^{-N_2' t}}{N_2' - N_1'}\right] \qquad (4.4.26)$$

$$\frac{\partial N_2}{\partial C_{B2}} = -\frac{1}{CO_{B2} D} \qquad (4.4.27)$$

$$\frac{\partial N_2}{\partial V_2} = -\frac{Q_{12} CO_{B1}}{V_2^2 CO_{B2} D}\left[\frac{e^{-N_1' t} - e^{-N_2' t}}{N_2' - N_1'}\right] \qquad (4.4.28)$$

$$\frac{\partial N_2}{\partial Q_{12}} = \frac{CO_{B1}}{V_2 CO_{B2} D}\left[\frac{e^{-N_1' t} - e^{-N_2' t}}{N_2' - N_1'}\right] \qquad (4.4.29)$$

$$\frac{\partial N_2}{\partial D} = \left[-\frac{1}{D^2} + \frac{\tilde{C}_{B2}}{CO_{B2} D^2}\right] - \frac{Q_{12} CO_{B1}}{V_2 CO_{B2} D^2}\left[\frac{e^{-N_1' t} - e^{-N_2' t}}{N_2' - N_1'}\right] \qquad (4.4.30)$$

Equation (4.3.19) gives for Q_{12}:

$$Q_{12} = \frac{(\tilde{C}_{A2} + CO_{A2}(DN_2 - 1))\, V_2 (N_2' - N_1')}{CO_{A1}(e^{-N_1' t} - e^{-N_2' t})} \qquad (4.4.31)$$

The absolute error in Q_{21} is found from:

$$(\Delta Q_{12})^2 = \left|\frac{\partial Q_{12}}{\partial N_1'}\Delta N_1'\right|^2 + \left|\frac{\partial Q_{12}}{\partial N_2'}\Delta N_2'\right|^2 + \left|\frac{\partial Q_{12}}{\partial CO_{A1}}\Delta CO_{A1}\right|^2 + \left|\frac{\partial Q_{12}}{\partial CO_{A2}}\Delta CO_{A2}\right|^2 + \left|\frac{\partial Q_{12}}{\partial \tilde{C}_{A_2}}\Delta \tilde{C}_{A2}\right|^2 +$$

$$\left|\frac{\partial Q_{12}}{\partial N_2}\Delta N_2\right|^2 + \left|\frac{\partial Q_{12}}{\partial V_2}\Delta V_2\right|^2 + \left|\frac{\partial Q_{12}}{\partial D}\Delta D\right|^2 \qquad (4.4.32)$$

where

$$\frac{\partial Q_{12}}{\partial N_1'} = \frac{-V_2(\tilde{C}_{A2}+CO_{A2}(N_2D-1))(CO_{A1}(e^{-N_1't-N_2't}))-(-tCO_{A1}e^{-N_1't})(V_2(N_2'-N_1'))(C_{A2}+CO_{A2}(DN_2-1))}{[CO_{A1}(e^{-N_1't}-e^{-N_2't})]^2} \qquad (4.4.33)$$

$$\frac{\partial Q_{12}}{\partial N_2'} = \frac{-V_2(\tilde{C}_{A2}+CO_{A2}(N_2D-1))(CO_{A1}(e^{-N_1't-N_2't}-e^{-N_2't}))-(tCO_{A1}e^{-N_2't})(V_2(N_2'-N_1'))(C_{A2}+CO_{A2}(DN_2-1))}{[CO_{A1}(e^{-N_1't}-e^{-N_2't})]^2} \qquad (4.4.34)$$

$$\frac{\partial Q_{12}}{\partial CO_{A1}} = -\frac{(\tilde{C}_{A2}+CO_{A2}(DN_2-1)(V_2(N_2'-N_1'))}{CO_{A1}^2(e^{-N_1't}-e^{-N_2't})} \qquad (4.4.35)$$

$$\frac{\partial Q_{12}}{\partial CO_{A2}} = \frac{(N_2D-1)\,V_2(N_2'-N_1')}{CO_{A1}(e^{-N_1't}-e^{-N_2't})} \qquad (4.4.36)$$

$$\frac{\partial Q_{12}}{\partial C_{A2}} = \frac{V_2(N_2' - N_1')}{CO_{A1}(e^{-N_1't} - e^{-N_2't})} \qquad (4.4.37)$$

$$\frac{\partial Q_{12}}{\partial N_2} = \frac{CO_{A2} D\ V_2(N_2' - N_1')}{CO_{A1}(e^{-N_1't} - e^{-N_2't})} \qquad (4.4.38)$$

$$\frac{\partial Q_{12}}{\partial V_2} = \frac{(\tilde{C}_{A2} + CO_{A2}(DN_2 - 1))(N_2' - N_1')}{CO_{A1}(e^{-N_1't} - e^{-N_2't})} \qquad (4.4.39)$$

$$\frac{\partial Q_{12}}{\partial D} = \frac{CO_{A2} N_2 V_2(N_2' - N_1')}{CO_{A1}(e^{-N_1't} - e^{-N_2't})} \qquad (4.4.40)$$

The relative contribution of errors in each variable to the total error in calculated values of N_1, Q_{21}, N_2 and Q_{12} are most clearly seen where known airflows and tracer gas concentrations can be directly compared with airflows calculated from site concentration data which is subject to random measurement errors.

4.5) Calculating N1, Q21, N2, Q12 using a worked example for 2 cells

4.5.1) General

Figure (10) shows the theoretical time variations of a tracer gas (A) released in Cell (1) and connected by two directional airflows to Cell (2). The data is derived from the fundamental tracer equation

(4.2.1) for known airflows N_1, Q_{21}, N_2, Q_{12} and initial tracer gas concentrations. The data points scattered around the theoretical curve shapes for C_{A1} and C_{A2} are the result of imposing a random measurement error of $\pm$ 5% on each data point. Using this data and similar data created for tracer gas (B) (released in Cell (2)),we can quantify the resulting errors on calculated airflows using the method outlined in section (4.3).

4.5.2) First order estimates of N1 and N2

Taking the first six C_{A1}, time points from figure (10) it is possible to obtain a crude estimate of Cell (1) air change rate (N_1'). This is obtained quite simply from a least squares fit of LnC_{A1} versus time. The gradient of the resulting straight line is the estimate (N_1'). A similar process using C_{B2}, time data from figure (11) gives an estimate of Cell (2) air change rate (N_2').

It is worth remembering that the estimates (N_1'), (N_2') will, if two directional airflows exist, be under-estimates of the actual cell air change rates because of recirculation of tracer gas between cells.

Appendix (D) should be consulted in the following discussion.
Least squares fits for (N_1') and (N_2') yields:

N_1' = 1.71 air changes/hour CO_{A1} = 10 ppm

N_2' = 2.77 air changes/hour CO_{B2} = 8.27 ppm.

$N_1 = 2{\cdot}75$ A.C./HR, $N_2 = 2{\cdot}5$ A.C./HR

$Q_{12} = 200\ M^3/HR$, $Q_{21} = 200\ M^3/HR$

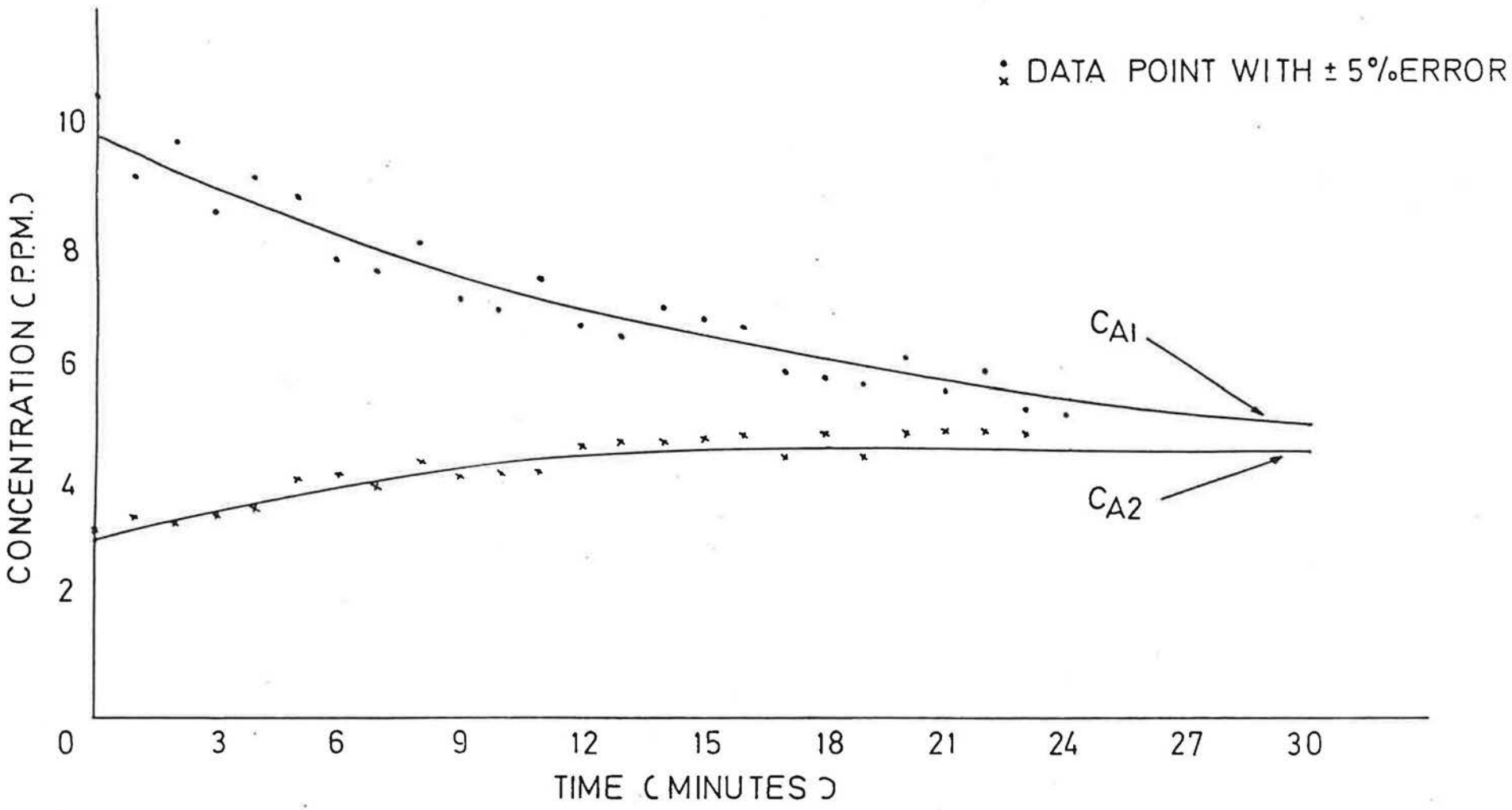

FIGURE 10 CA(t) VARYING WITH TIME FOR KNOWN AIRFLOWS

$N_1 = 2{\cdot}75$ AC/HR, $N_2 = 2{\cdot}5$ AC/HR

$Q_{12} = 200\ M^3/HR$, $Q_{21} = 200\ M^3/HR$

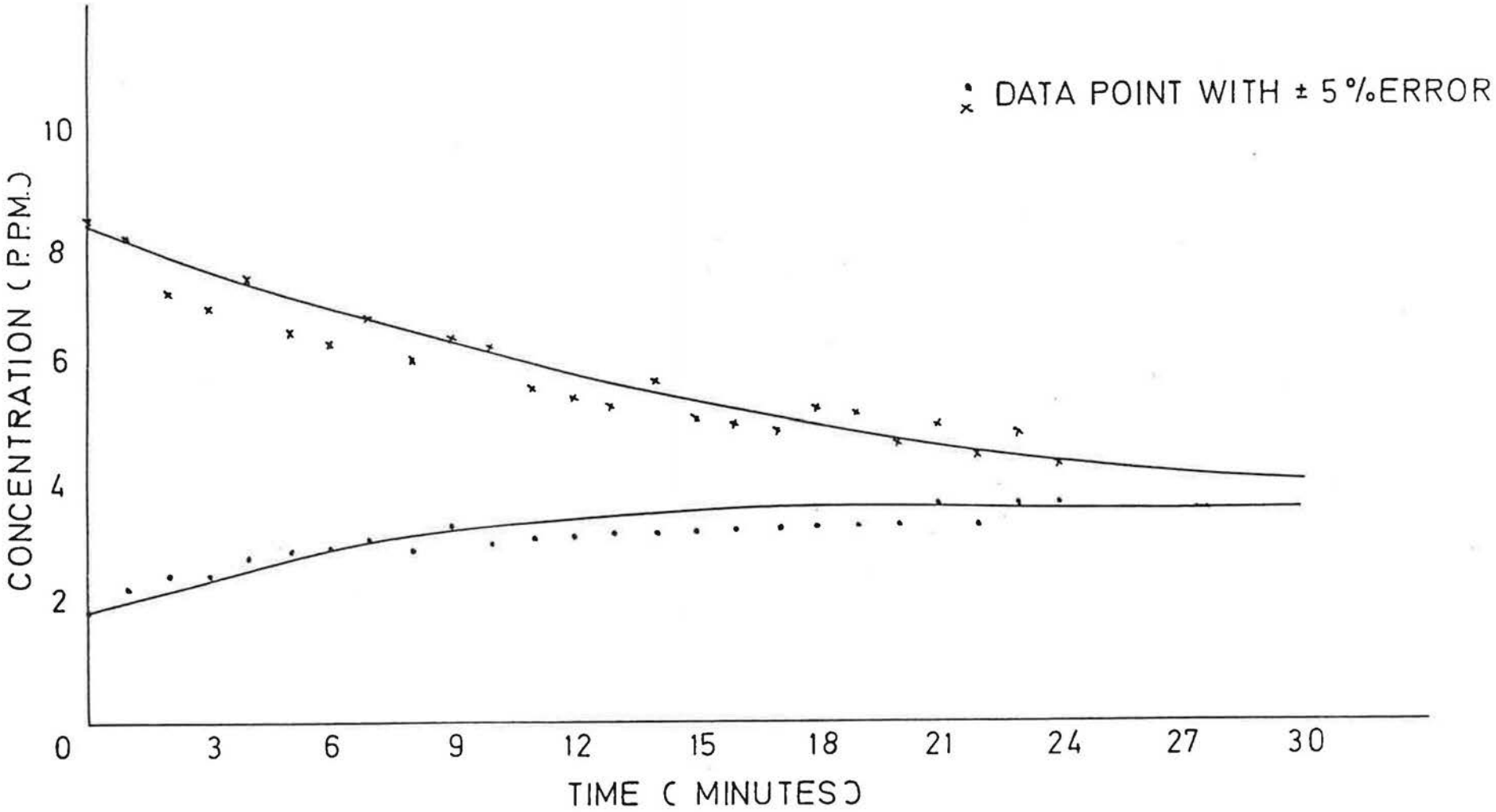

FIGURE 11 C B(t) VARYING WITH TIME FOR KNOWN AIRFLOWS

4.5.3) Calculating N1 Q21, Q12 and N2

Using the first 16 tracer concentration data points for C_{A1}, C_{A2}, C_{B1} and C_{B2}, numerical integration yields:

$\tilde{C}_{A1}$ = 7.65 ppm, $\tilde{C}_{A2}$ = 4.1 ppm

$\tilde{C}_{B1}$ = 3 ppm , $\tilde{C}_{B2}$ = 6.4 ppm

Figures (10) and (11) give values for CO_{A2} and CO_{B1} of

CO_{A2} = 3.15 ppm, CO_{B1} = 1.9 ppm.

The maclaurin series expansion for N_1' and N_2' gives

A = 0.113, D = 0.105

Substituting these values into equation (4.3.16) for N_1 and equation (4.3.17) for Q_{21} :

$$N_1 = 2.07 + 0.0026\ Q_{21} \qquad (4.5.1)$$

$$Q_{21} = 142 + 28\ N_1 \qquad (4.5.2)$$

Iterating the above equations using the Gauss-Seidel technique gives:

N_1 = 2.63 air change/hour, Q_{21} = 215 m^3/hour

Solving equations (4.3.18) and (4.3.19) in similar manner gives:

N_2 = 2.54 air changes/hour, Q_{12} = 190 m^3/hour

The calculated values of N_1, Q_{21}, N_2 and Q_{12} are used in equations (4.2.6) and (4.2.8) to calculate theoretical time variations in tracer gas concentrations C_{A1} and C_{A2}. The curves resulting from these equations are compared with the observed values of tracer concentration in figure (12). A similar comparison is made in figure (13) for tracer gas (B) concentrations C_{B1} and C_{B2}.

Examination of these figures shows the goodness of fit attained with this method of analysis.

4.6) Estimating errors in calculated values of N1, Q21, N2, Q21

Let us consider the error in the calculated value of N_1, from section (4.4), equation (4.4.2), the absolute standard error in N_1 may be found from:

$$(\Delta N_1)^2 = \left|\frac{\partial N_1}{\partial N_1'}\Delta N_1'\right|^2 + \left|\frac{\partial N_1}{\partial N_2}\Delta N_2'\right|^2 + \left|\frac{\partial N_1}{\partial CO_{A1}}\Delta CO_{A1}\right|^2 + \left|\frac{\partial N_1}{\partial CO_{A2}}\Delta CO_{A2}\right|^2 + \left|\frac{\partial N_1}{\partial \tilde{C}_{A1}}\Delta \tilde{C}_{A1}\right|^2$$

$$+ \left|\frac{\partial N_1}{\partial V_1}\Delta V_1\right|^2 + \left|\frac{\partial N_1}{\partial Q_{21}}\Delta Q_{21}\right|^2 + \left|\frac{\partial N_1}{\partial A}\Delta A\right|^2 \qquad (4.6.1)$$

The partial derivatives in equation (4.6.1) can be calculated from the data given in the 2 cell worked example using equations (4.4.3) to (4.4.10). These calculations are shown in Appendix (D) and give the following values:

$N_1 = 2{\cdot}63$ A.C/HR , $N_2 = 2{\cdot}54$ A.C/HR

$Q_{12} = 190\ M^3/HR$, $Q_{21} = 215\ M^3/HR$

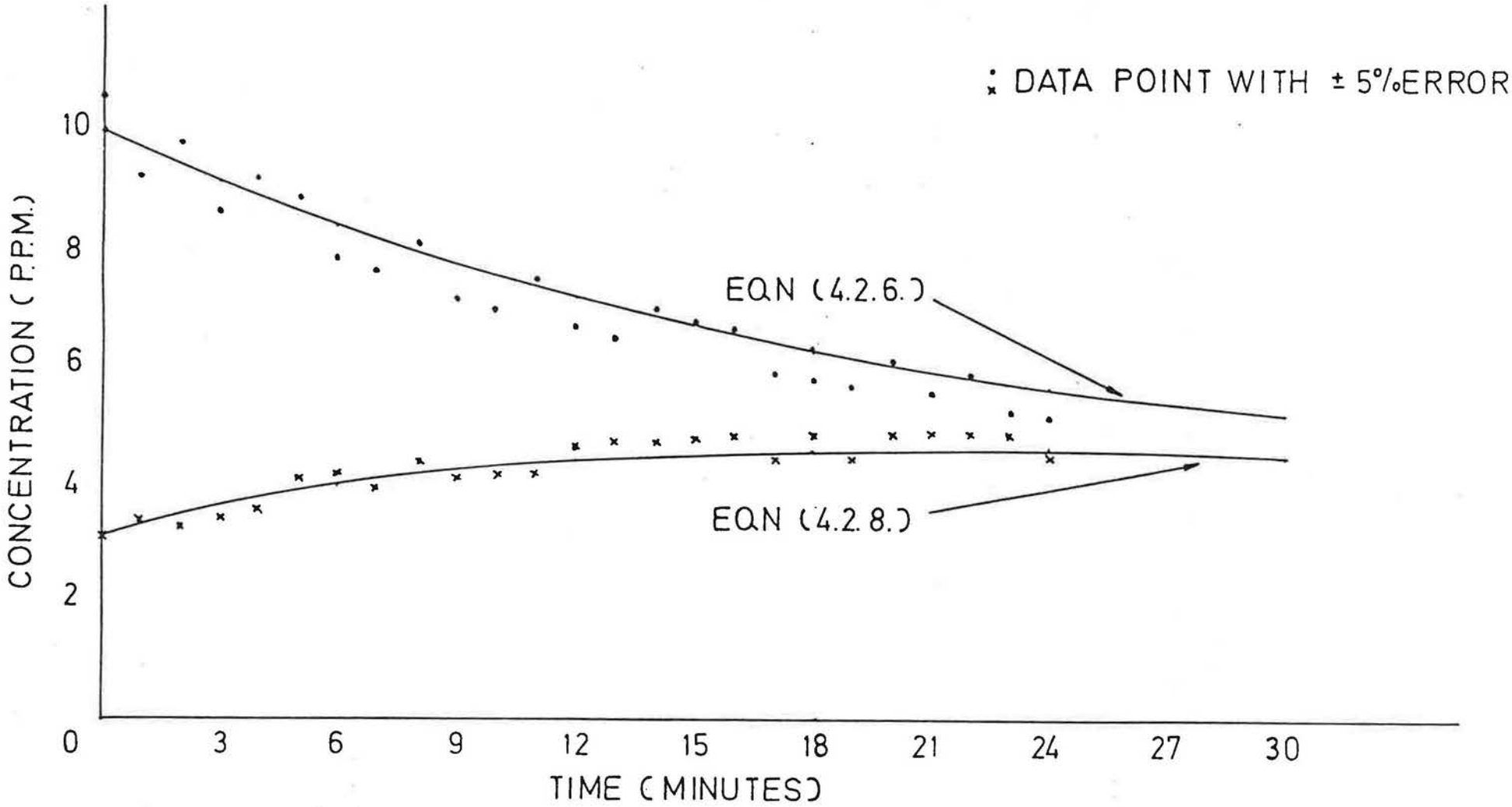

FIGURE 12 CA(t) VARYING WITH TIME FOR CALCULATED AIRFLOWS

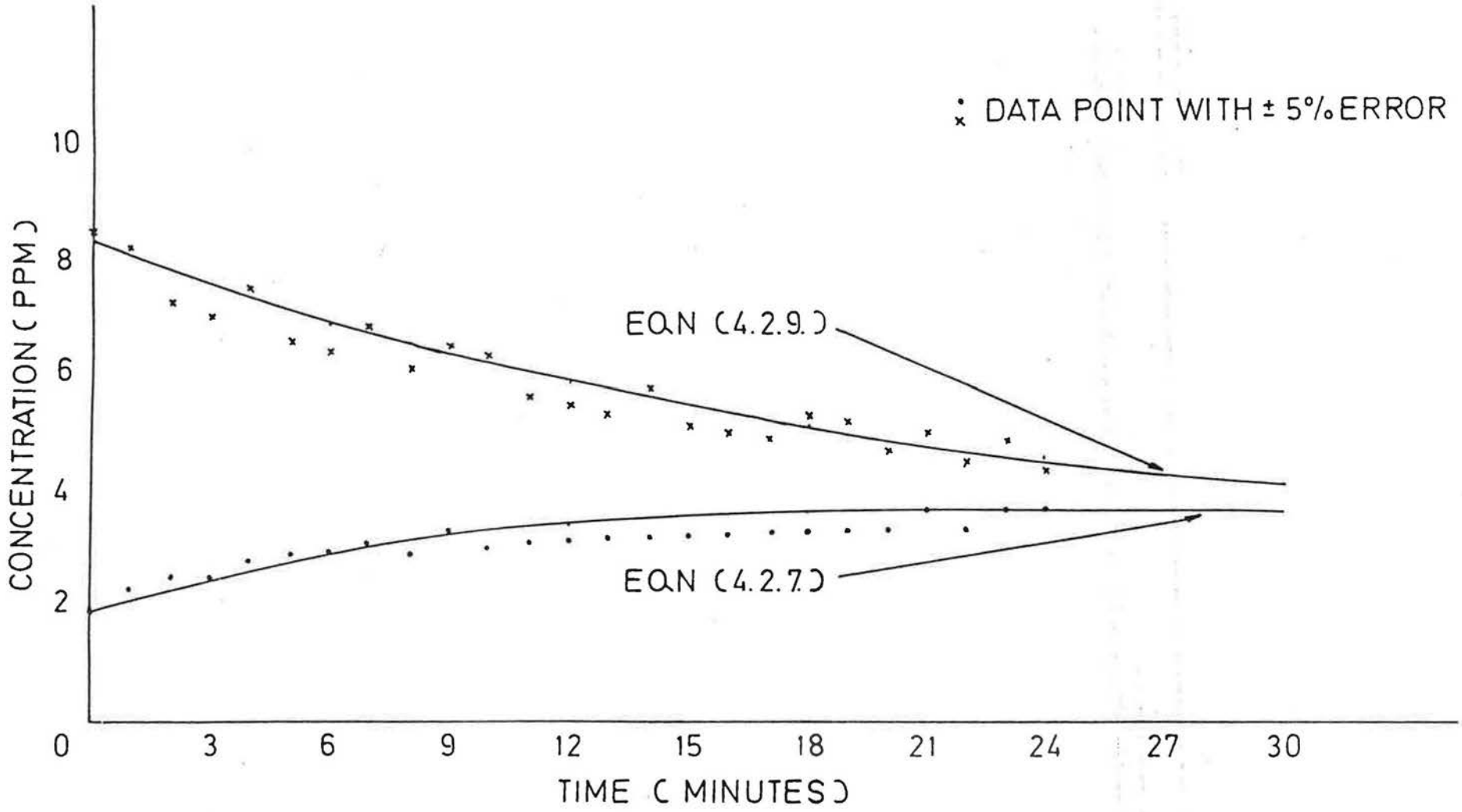

FIGURE 13 CB(t) VARYING WITH TIME FOR CALCULATED AIRFLOWS

$$\frac{\partial N_1}{\partial N_1'} = 0.04,\ \frac{\partial N_1}{\partial N_2'} = 0.04,\ \frac{\partial N_1}{\partial CO_{A1}} = 0.125,\ \frac{\partial N_1}{\partial CO_{A2}} = 0.152,$$

$$\frac{\partial N_1}{\partial \tilde{C}_{A1}} = 0.8,\ \frac{\partial N_1}{\partial V_1} = 0.005,\ \frac{\partial N_1}{\partial Q_{21}} = 0.0024,\ \frac{\partial N_1}{\partial A} = 21.43$$

Substituting these values into equation (4.6.1) gives

$$(\Delta N_1^2) = |0.04\ N_1|^2 + |0.04\ N_2|^2 + |0.125\ CO_{A1}|^2 + |0.152\ CO_{A2}|^2 + 0.8\ C_{A1}|^2 +$$

$$|0.005\ V_1|^2 + |0.0024\ Q_{21}|^2 + |21.43\ A|^2 \qquad (4.6.2)$$

The exact data from which the worked example has been taken enables us to calculate the absolute errors in all variables of equation (4.6.2). These are:

N_1	$=\|2.75 - 2.63\| = 0.12$		
N_2	$= 0.04$	V_1	$= 0$
CO_{A1}	$= 0$	Q_{21}	$= 15$
CO_{A2}	$= 0.15$	A	$= 0.007$
C_{A1}	$= 0.18$		

Substituting for these values in equation (4.6.2) gives:

$$(\Delta N_1)^2 = |0.0048|^2 + |0.0016|^2 + |0.023|^2 + |0.144|^2 + |0.031|^2 + |0.15|^2 \qquad (4.6.3)$$

$\Delta N_1 = \pm 0.21$ air changes/hour

Therefore the error calculation suggests $N_1 = 2.63 \pm 0.21$ air changes/hour

A similar calculation for ΔQ_{21} from equation (4.4.12) gives:

$$(\Delta Q_{21})^2 = |14\Delta N_1'|^2 + |10\Delta N_2'|^2 + |104\Delta CO_{B1}|^2 + |234\Delta CO_{B2}|^2 + |1294\Delta \tilde{C}_{B1}|^2 + |28\Delta N_1|^2$$

$$+ |1.9\Delta V_1|^2 + |654\Delta A|^2 \qquad (4.6.4)$$

Inserting absolute errors for each variable yields:

$\Delta Q_{21} = \pm 15$ m^3/hour

therefore

$Q_{21} = 215 \pm 15$ m^3/hr.

Using identical procedures equations (4.4.21) and (4.4.32) enable error bounds to be calculated for N_2 and Q_{12}, these are

$N_2 = 2.54 \pm 0.25$ air changes/hour

$Q_{12} = 190 \pm 16$ m^3/hr

The worked example shows that using the preceeding method of data analysis, a random $\pm$ 5% error on site data points creates a $\pm$ 10% uncertainty in calculated airflows derived from such data.

4.7) Estimating errors in "Real" airflows

Site measurements of tracer concentrations varying with time between connected cells are used to calculate cell air change rates and connecting airflows. To establish the most probable errors on such calculated values is very difficult where the absolute error between "real" values

and calculated values are unknown.

The major sources of error can be divided into two categories:

Type (1) Errors in collected Ci(t) data, such errors are dependent upon type of measurement system used, operator errors, incomplete mixing of air and tracer gas.

Type (2) The analysis method described in section (4.3) is dependent upon the assumption that recirculation of tracer gas between connected cells is time dependent, so that the proportion of recirculated tracer gas to the measured value of tracer concentration is $\leq 15\%$ of Ci(t) at time (t). A further source of error in the analysis method is the use of a maclaurin series expansion for $e^{-N_1 t}$ and $e^{-N_2 t}$. As time (t) increases from zero the maclaurin series approximation will have increasing errors and will eventually fail completely.

To evaluate type (1) and (2) errors the measurement system used for site data collection can be validated in the laboratory. Under controlled conditions cell air change rates and inter-connecting airflows can be given predetermined values. Using multiple tracer gas measurements and the analysis method of section (4.3), direct comparison between "real" and calculated airflows can be made, such a validation procedure is described in Chapter (6).

Type (2) errors are minimised if the time required to collect sufficient data points (usually 10 points per concentration/time curve) is kept as small as possible. Clearly if type (2) errors become significant

the theoretical curve shapes derived from calculated airflows will show a poor "goodness-of-fit" when compared with the site tracer concentration data points.

The rapid sampling multiple tracer gas technique described in Chapter (6) has been designed to minimise the time required to collect tracer concentration data.

If recirculation of tracer gas between connected spaces is causing a poor "goodness-of-fit", the calculated airflows and air change rates N_1, Q_{21}, N_2, Q_{12} can be used in the exact equations (4.2.16)-(4.2.20) to estimate the likely contributions of recirculating tracer gas. Let this be defined as $C_{R(t)}$, then considering $C_{A1(t)}$, from equation (4.2.16).

$$C_{A1R(t)} = \frac{Q_{21}Q_{12}CO_{A1}}{V_1V_2(N_2-N_1)} \left[te^{-N_1t} + \frac{(e^{-N_2t} - e^{-N_1t})}{(N_2 - N_1)} \right] \qquad (4.7.1)$$

The calculated value of $C_{A1R(t)}$ can then be used in the simplified equation for $C_{A1(t)}$ described by equation (4.3.11).

It should be stated that for the air movement tests carried out by the author in a variety of dwellings, recirculation of tracer gas does not create significant errors in the calculation of N_1, Q_{21}, N_2, Q_{12} provided the total test time does not exceed 20 minutes.

Chapter 5: AN ALTERNATIVE ANALYSIS METHOD FOR CALCULATING AIR-FLOWS : THREE CELL CASE

5.1) General

The analytical solution of the fundamental tracer equations discussed in Chapter (4), section (4.2) can be used to derive solutions for any number of cells. The complexity and size of the resulting equations make them clumsy to use without some simplifying assumptions being made.

To illustrate this let us derive sets of equations which describe the time variations in tracer gas concentrations which occurs between three connected cells.

5.2) Analytical solution of the fundamental tracer gas equations

With reference to figure (14), tracer gas (A) is released in Cell (1), tracer gas (B) is released in Cell (2) and tracer gas (C) released in Cell (3).

The fundamental tracer gas equation is for the N = 3 cell case, expressed as:

$$Vi \frac{dCi}{dt} = f(i) + \left[\sum_{j=1}^{3} Qji Cj \ (1 - \delta ij) \right] - SiCi \qquad (5.2.1)$$

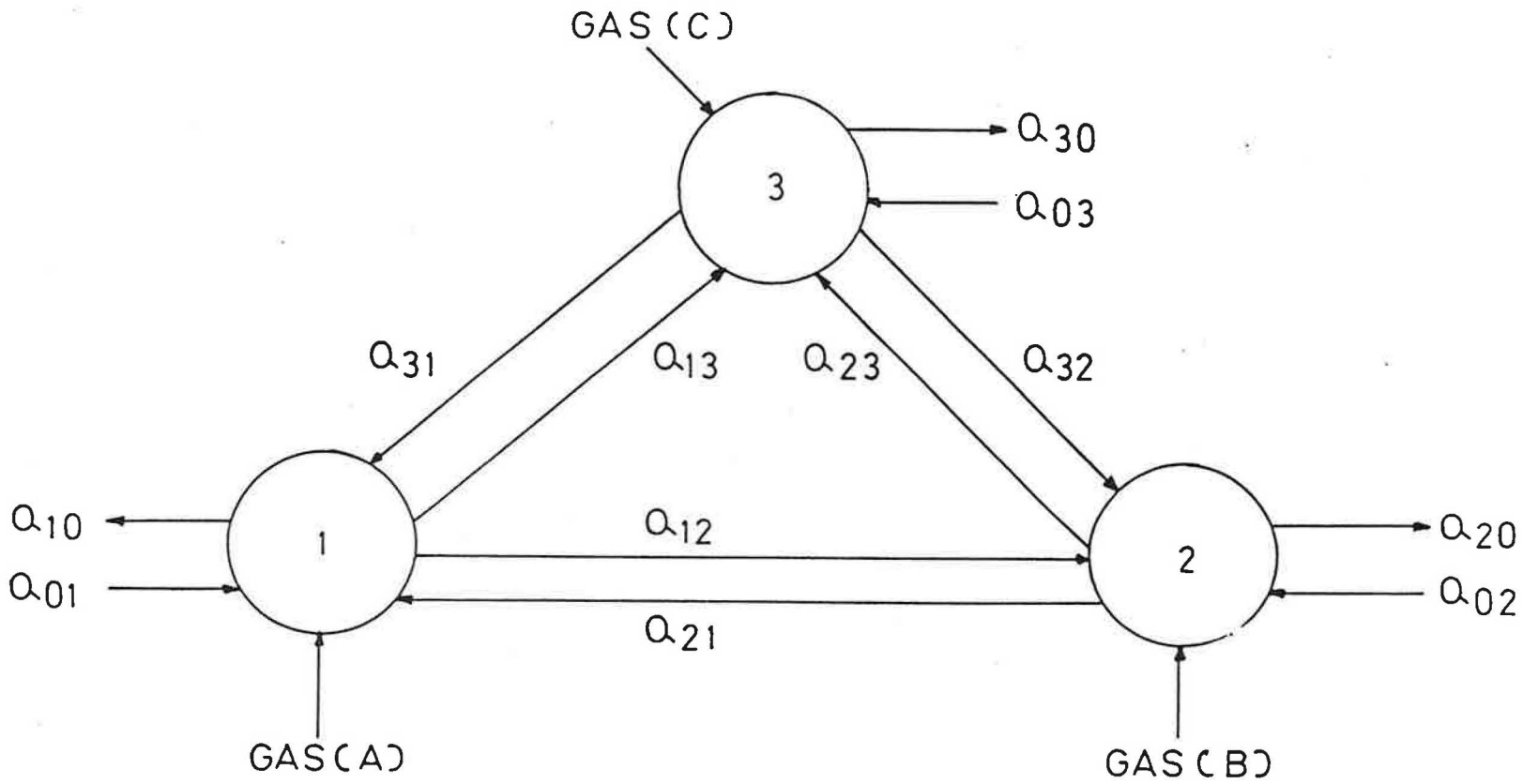

FIGURE 14 THREE CELL AIRFLOWS

If a single pulse of tracer gas (A),(B) and (C) is released in Cell (1), (2) and (3) respectively at time zero, equation (5.2.1) becomes:

For Cell (1)

Gas (A)

$$V_1 \frac{dC_{A1}}{dt} = Q_{21}C_{A2} + Q_{31}C_{A3} - S_1C_{A1} \qquad (5.2.2)$$

Gas (B)

$$V_1 \frac{dC_{B1}}{dt} = Q_{21}C_{B2} + Q_{31}C_{B3} - S_1C_{B1} \qquad (5.2.3)$$

Gas (C)

$$V_1 \frac{dC_{C1}}{dt} = Q_{21}C_{C2} + Q_{31}C_{C3} - S_1C_{C1} \qquad (5.2.4)$$

For Cell (2):

Gas (A)

$$V_2 \frac{dC_{A2}}{dt} = Q_{12}C_{A1} + Q_{32}C_{A3} - S_2C_{A2} \qquad (5.2.5)$$

Gas (B)

$$V_2 \frac{dC_{B2}}{dt} = Q_{12}C_{B1} + Q_{32}C_{B3} - S_2C_{B2} \qquad (5.2.6)$$

Gas (C)

$$V_2 \frac{dC_{C2}}{dt} = Q_{12}C_{C1} + Q_{32}C_{C3} - S_2C_{C2} \qquad (5.2.7)$$

For Cell (3)

Gas (A)

$$V_3 \frac{dC_{A3}}{dt} = Q_{13}C_{A1} + Q_{23}C_{A2} - S_3C_{A3} \qquad (5.2.8)$$

Gas (B)

$$V_3 \frac{dC_{B3}}{dt} = Q_{13}C_{B1} + Q_{23}C_{B2} - S_3C_{B3} \qquad (5.2.9)$$

Gas (C)

$$V_3 \frac{dC_{C3}}{dt} = Q_{13}C_{C1} + Q_{23}C_{CC2} - S_3C_{C3} \qquad (5.2.10)$$

Defining cell air change rate as $N_1 = \frac{S_1}{V_1}$, $N_2 = \frac{S_2}{V_2}$, $N_3 = \frac{S_3}{V_3}$

Substituting for N_1, N_2, and N_3 in equations (5.2.2.) - (5.2.10) and re-arranging we obtain:

For Cell (1)

$$\frac{dC_{A1}}{dt} + N_1 C_{A1} = \frac{Q_{21}}{V_1} C_{A2} + \frac{Q_{31}}{V_1} C_{A3} \qquad (5.2.11)$$

$$\frac{dC_{B1}}{dt} + N_1 C_{B1} = \frac{Q_{21}}{V_1} C_{B2} + \frac{Q_{31}}{V_1} C_{B3} \qquad (5.2.12)$$

$$\frac{dC_{C1}}{dt} + N_1 C_{C1} = \frac{Q_{21} C_{C2}}{V_1} + \frac{Q_{31}}{V_1} C_{C3} \qquad (5.2.13)$$

For Cell (2)

$$\frac{dC_{A2}}{dt} + N_2 C_{A2} = \frac{Q_{12}}{V_2} C_{A1} + \frac{Q_{32}}{V_2} C_{A3} \qquad (5.2.14)$$

$$\frac{dC_{B2}}{dt} + N_2 C_{B2} = \frac{Q_{12} C_{B1}}{V_2} + \frac{Q_{32}}{V_2} C_{B3} \qquad (5.2.15)$$

$$\frac{dC_{C2}}{dt} + N_2 C_{C2} = \frac{Q_{12}}{V_2} C_{C1} + \frac{Q_{32} C_{C3}}{V_2} \qquad (5.2.16)$$

For Cell (3)

$$\frac{dC_{A3}}{dt} + N_3 C_{A3} = \frac{Q_{13}}{V_3} C_{A1} + \frac{Q_{23}}{V_3} C_{A2} \qquad (5.2.17)$$

For Cell (3)

$$\frac{dC_{B3}}{dt} + N_3 C_{B3} = \frac{Q_{13}}{V_3} C_{B1} + \frac{Q_{23}}{V_3} C_{B2} \qquad (5.2.18)$$

$$\frac{dC_{C3}}{dt} + N_3 C_{C3} = \frac{Q_{13}}{V_3} C_{C1} + \frac{Q_{23}}{V_3} C_{C2} \qquad (5.2.19)$$

Equations (5.2.11) - (5.2.19) are first order differential equations which can be solved using an integrating factor.

The integrating factor for equations (5.2.11) - (5.2.13) is $e^{N_1 t}$.

For convenience let us consider tracer gas (A) equations only.

$$C_{A1} e^{N_1 t} = \int \frac{Q_{21}}{V_1} C_{A2} \, e^{N_1 t} \, dt + \int \frac{Q_{31}}{V_1} C_{A3} \, e^{N_1 t} \, dt + A \qquad (5.2.20)$$

Similarly, equation (5.2.14) which describes tracer gas (A) concentration in cell (2) is solved using $e^{N_2 t}$ as the integrating factor.

$$C_{A2} e^{N_2 t} = \int \frac{Q_{12}}{V_2} C_{A1} \, e^{N_2 t} \, dt + \int \frac{Q_{32}}{V_2} C_{A3} \, e^{N_2 t} \, dt + B \qquad (5.2.21)$$

and for tracer gas (A) concentration in Cell (3) equation (5.2.17) becomes

$$C_{A3}e^{N_3t} = \int \frac{Q_{13}}{V_3} C_{A1} e^{N_3t} dt + \int \frac{Q_{23}}{V_3} C_{A2} e^{N_3t} dt + C \qquad (5.2.22)$$

Equations (5.2.20) - (5.2.22) can only be solved where the time variations in C_{A1}, C_{A2} and C_{A3} are assumed. Assuming a one directional airflow between cell (1) and cell (2), then using Dick's equations

$$C_{A2} = CO_{A2}e^{-N_2t} + \frac{Q_{12}CO_{A1}}{V_2(N_2-N_1)} [e^{-N_1t} - e^{-N_2t}] \qquad (5.2.23)$$

and assuming one directional airflow between cell (1) and cell (3)

$$C_{A3} = CO_{A3}e^{-N_3t} + \frac{Q_{13}CO_{A1}}{V_3(N_3-N_1)} [e^{-N_1t} - e^{-N_3t}] \qquad (5.2.24)$$

where CO_{A1}, CO_{A2}, CO_{A3} are the initial tracer gas (A) concentrations in cells (1), (2), and (3) respectively at time zero.

Substituting for C_{A2} from equation (5.2.23) and for C_{A3} from equation (5.2.24) into equation (5.2.20) we obtain:

$$C_{A1}e^{N_1t} = \int \frac{Q_{21}}{V_1} (CO_{A2}e^{-N_2t} + \frac{Q_{12}CO_{A1}}{V_2(N_2-N_1)} [e^{-N_1t} - e^{-N_2t}])e^{N_1t} dt +$$

$$\int \frac{Q_{31}}{V_1} (CO_{A3}e^{-N_3t} + \frac{Q_{13}CO_{A1}}{V_3(N_3-N_1)} (e^{-N_1t} - e^{-N_3t}))e^{N_1t} dt + A \qquad (5.2.25)$$

Integrating equation (5.2.25) and imposing the boundary condition that $C_{A1} = CO_{A1}$ at time = zero we obtain

$$C_{A1} = CO_{A1}e^{-N_1t} + \frac{Q_{21}CO_{A2}}{V_1(N_1-N_2)}\left[e^{-N_2t} - e^{-N_1t}\right] + \frac{Q_{21}Q_{12}CO_{A1}}{V_1V_2(N_2-N_1)}\left[\frac{(e^{-N_2t} - e^{-N_1t})}{(N_2-N_1)} + te^{-N_1t}\right]$$

$$+\frac{Q_{31}CO_{A3}}{V_1(N_1-N_3)}\left[e^{-N_3t} - e^{-N_1t}\right] + \frac{Q_{31}Q_{13}CO_{A1}}{V_1V_3(N_3-N_1)}\left[\frac{(e^{-N_3t} - e^{-N_1t})}{(N_3 - N_1)} + te^{-N_1t}\right] \qquad (5.2.26)$$

Equation (5.2.21) can be solved for C_{A2} by substituting for C_{A1} from equation (5.2.26) and for C_{A3} from equation (5.2.24).

Equation (5.2.21) becomes

$$C_{A2}e^{N_2t} = \int \frac{Q_{12}}{V_1}\left[CO_{A1}e^{-N_1t} + \frac{Q_{21}CO_{A2}}{V_1(N_1-N_2)}\left[e^{-N_2t} - e^{-N_1t}\right] + \frac{Q_{21}Q_{12}CO_{A1}}{V_1V_2(N_2-N_1)}\left[\frac{(e^{-N_2t} - e^{-N_1t})}{(N_2 - N_1)} + te^{-N_1t}\right]\right.$$

$$\left. + \frac{Q_{31}CO_{A3}}{V_1(N_1-N_3)}(e^{-N_3t} - e^{-N_1t}) + \frac{Q_{31}Q_{13}CO_{A1}}{V_1V_3(N_3-N_1)}\left[\frac{(e^{-N_3t} - e^{-N_1t})}{(N_3 - N_1)} + te^{-N_1t}\right]\right] e^{N_2t}\,dt$$

$$+\int \frac{Q_{32}}{V_2}\left[CO_{A3}e^{-N_3t} + \frac{Q_{13}CO_{A1}}{V_3(N_3-N_1)}(e^{-N_1t} - e^{-N_3t})\,e^{N_2t}\right]dt + B \qquad (5.2.27)$$

Integrating equation (5.2.27) and imposing the boundary condition that $C_{A2} = CO_{A2}$ at time = zero we obtain:

$$C_{A2}=CO_{A2}e^{-N_2t} + \frac{+Q_{12}CO_{A1}}{V_2(N_2-N_1)}(e^{-N_1t}-e^{-N_2t}) + \frac{+Q_{32}CO_{A3}}{V_2(N_2-N_3)}(e^{-N_3t}-e^{-N_2t}) +$$

$$\frac{Q_{12}Q_{21}CO_{A2}}{V_2V_1(N_1-N_2)}\left[(te^{-N_2t} + \frac{(e^{-N_2t}-e^{-N_1t})}{(N_2-N_1)}\right] + \frac{Q_{12}Q_{31}CO_{A3}}{V_2V_1(N_1-N_3)}\left[\frac{(e^{-N_3t}-e^{-N_2t})}{(N_2-N_3)} + \frac{(e^{-N_2t}-e^{-N_1t})}{(N_2-N_1)}\right]$$

$$+ \frac{Q_{32}Q_{13}CO_{A1}}{V_2V_3(N_3-N_1)}\left[\frac{(e^{-N_1t}-e^{-N_2t})}{(N_2-N_1)} + \frac{(e^{-N_2t}-e^{-N_3t})}{(N_2-N_3)}\right] +$$

$$\frac{Q_{21}Q_{12}^2CO_{A1}}{V_1V_2^2(N_2-N_1)}\left[\frac{(te^{-N_1t}+te^{-N_2t})}{(N_2-N_1)} + \frac{(2e^{-N_2t}-2e^{-N_1t})}{(N_2-N_1)^2}\right] +$$

$$\frac{Q_{12}Q_{31}Q_{13}CO_{A1}}{V_1V_2V_3(N_3-N_1)}\left[\frac{(e^{-N_2t}-e^{-N_1t})}{(N_2-N_1)^2} + \frac{(e^{-N_2t}-e^{-N_1t})}{(N_3-N_1)(N_2-N_1)} + \frac{(e^{-N_3t}-e^{-N_2t})}{(N_3-N_1)(N_2-N_3)} + \frac{te^{-N_1t}}{(N_2-N_1)}\right]$$

(5.2.28)

C_{A3} can be found by substituting for C_{A1}, equation (5.2.26) and C_{A2}, equation (5.2.28) into equation (5.2.22). Therefore equation (5.2.22) becomes:

$$C_{A3}e^{N_3t} = \int \frac{Q_{13}}{V_3} C_{A1}e^{N_3t}dt + \int \frac{Q_{23}}{V_3} C_{A2}e^{N_3t}dt + C \qquad (5.2.29)$$

and integrating with respect to time and by applying the boundary condition $C_{A3} = CO_{A3}$ at time zero we obtain:

$$C_{A3} = CO_{A3}e^{-N_3t} + \frac{Q_{13}CO_{A1}}{V_3(N_3-N_1)}(e^{-N_1t} - e^{-N_3t}) + \frac{Q_{23}CO_{A2}}{V_3(N_3-N_2)}(e^{-N_2t} - e^{-N_3t})$$

$$+ \frac{Q_{13}Q_{21}CO_{A2}}{V_3(N_1-N_2)}\left[\frac{(e^{-N_2t} - e^{-N_3t})}{(N_3-N_2)} + \frac{(e^{-N_3t} - e^{-N_1t})}{(N_3-N_1)}\right] + \frac{Q_{13}Q_{31}CO_{A3}}{V_3V_1(N_1-N_3)}\left[te^{-N_3t} + \frac{(e^{-N_3t} - e^{-N_1t})}{(N_3-N_1)}\right]$$

$$+ \frac{Q_{23}Q_{12}CO_{A1}}{V_3V_2(N_2-N_1)}\left[\frac{(e^{-N_1t} - e^{-N_3t})}{(N_3-N_1)} + \frac{(e^{-N_3t} - e^{-N_2t})}{(N_3-N_2)}\right] + \frac{Q_{23}Q_{32}CO_{A3}}{V_3V_2(N_2-N_3)}\left[te^{-N_3t} + \frac{(e^{-N_3t} - e^{-N_2t})}{(N_3-N_2)}\right]$$

$$+ \frac{Q_{13}Q_{21}Q_{12}CO_{A2}}{V_3V_2V_1(N_2-N_1)}\left[\frac{te^{-N_1t}}{N_3-N_1} + \frac{(e^{-N_3t} - e^{-N_1t})}{(N_3-N_1)^2} + \frac{(e^{-N_2t} - e^{-N_3t})}{(N_2-N_1)(N_3-N_2)}\right] +$$

$$\frac{Q_{31}Q_{13}^2\,CO_{A1}}{V_1V_3^2(N_3-N_1)}\left[\frac{(te^{-N_1t} + te^{-N_3t})}{(N_3-N_1)} + \frac{(2e^{-N_3t} - 2e^{-N_1t})}{(N_3-N_1)^2}\right] +$$

$$\frac{Q_{23}Q_{32}Q_{13}CO_{A1}}{V_3^2V_2(N_3-N_1)}\left[\frac{(e^{-N_1t} - e^{-N_3t})}{(N_2-N_1)(N_3-N_1)} + \frac{(e^{-N_3t} - e^{-N_2t})}{(N_2-N_1)(N_3-N_2)} + \frac{(e^{-N_2t} - e^{-N_3t})}{(N_2-N_3)(N_3-N_2)} - \frac{te^{-N_3t}}{(N_2-N_3)}\right]$$

(5.2.30)

Equations (5.2.30) has been rounded to the first 10 terms.

Typical curve shapes for C_{A1} (equation (5.2.26)), C_{A2} (equation (5.2.28)) and C_{A3} (equation 5.2.30) are shown in figure (15) where comparison is made with the fundamental tracer equation (5.2.1) solved for known airflows and initial tracer gas concentrations.

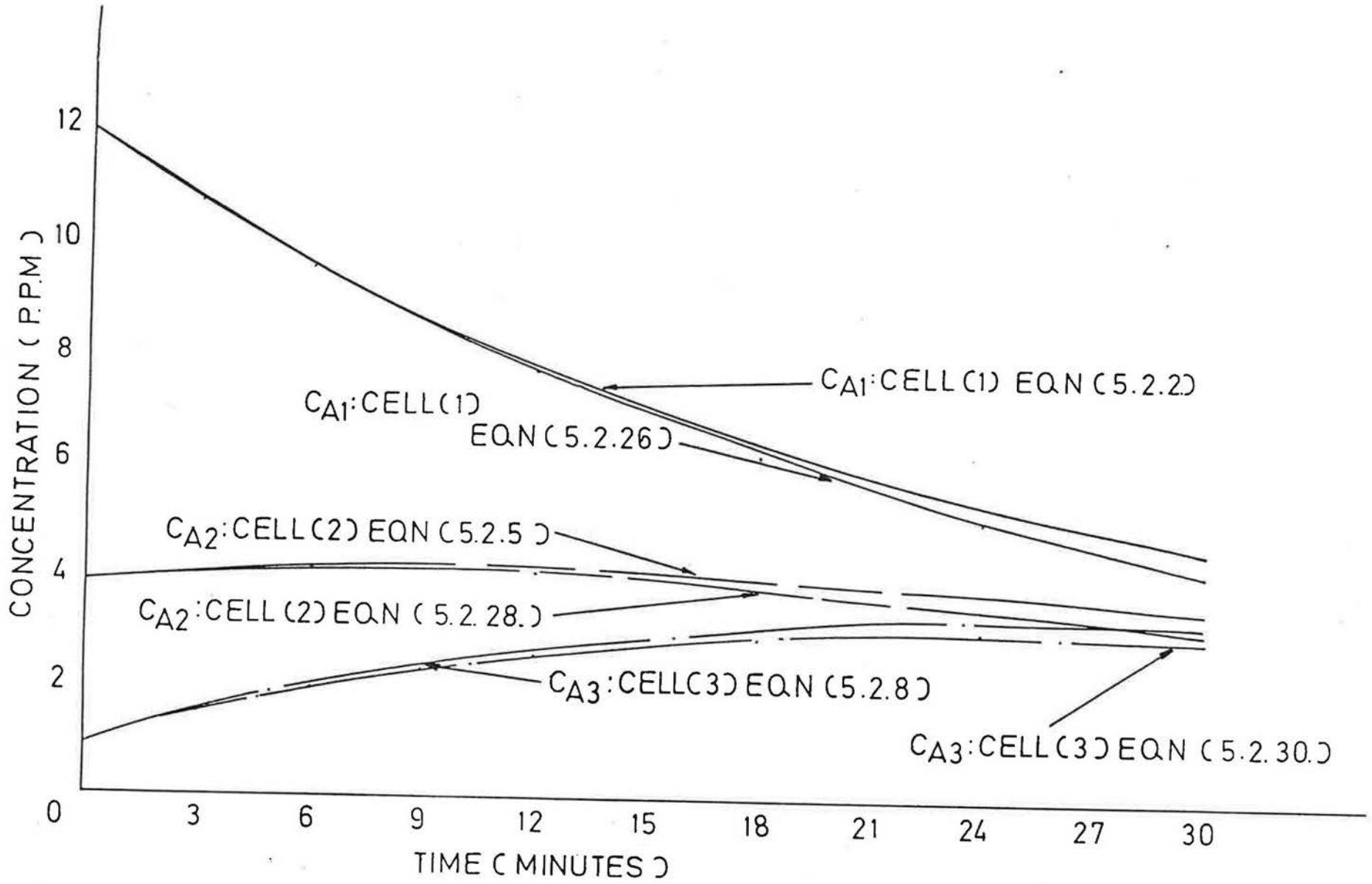

FIGURE 15 VARIATIONS IN CA (t) CONCENTRATION : THREE CELL CASE

Using an identical analysis, theoretical equations for tracer gas (B) and tracer gas (c) can be derived.

5.3) Calculating N1, N2, N3, Q12, Q32, Q13, Q23, Q21, Q31

The method of calculating all unknown airflows and cell air change rates is an identical procedure to the two cell case discussed in Chapter (4), Section (4.3)

The simplified tracer gas equations can be written:

For Cell (1)

$$\tilde{C}_{A1}=CO_{A1}(1-AN_1)+\frac{Q_{21}CO_{A2}}{V_1}\left(\frac{e^{-N_2't}-e^{-N_1't}}{(N_1'-N_2')}\right)+\frac{Q_{31}CO_{A3}}{V_1}\left(\frac{e^{-N_3't}-e^{-N_1't}}{(N_1'-N_3')}\right) \quad (5.3.1)$$

$$\tilde{C}_{B1}=CO_{B1}\ (1-AN_1)+\frac{Q_{21}CO_{B2}}{V_1}\left(\frac{e^{-N_2't}-e^{-N_1't}}{(N_1'-N_2')}\right)+\frac{Q_{31}CO_{B3}}{V_1}\left(\frac{e^{-N_3't}-e^{-N_1't}}{(N_1'-N_3')}\right) \quad (5.3.2)$$

$$\tilde{C}_{C1}=CO_{C1}\ (1-AN_1)+\frac{Q_{21}CO_{C2}}{V_1}\left(\frac{e^{-N_2't}-e^{-N_1't}}{(N_1'-N_2')}\right)+\frac{Q_{31}CO_{C3}}{V_1}\left(\frac{e^{-N_3't}-e^{-N_1't}}{(N_1'-N_3')}\right) \quad (5.3.3.)$$

For Cell (2)

$$\tilde{C}_{A2}=CO_{A2}(1-BN_2)+\frac{Q_{12}CO_{A1}}{V_2}\left(\frac{e^{-N_1't}-e^{-N_2't}}{(N_2'-N_1')}\right)+\frac{Q_{32}CO_{A3}}{V_2}\left(\frac{e^{-N_3't}-e^{-N_2't}}{(N_2'-N_3')}\right) \quad (5.3.4)$$

$$\tilde{C}_{B2}=CO_{B2}(1-BN_2)+\frac{Q_{12}CO_{B1}}{V_2}\left(\frac{e^{-N_1't}-e^{-N_2't}}{(N_2'-N_1')}\right)+\frac{Q_{32}CO_{B3}}{V_2}\left(\frac{e^{-N_3't}-e^{-N_2't}}{(N_2'-N_3')}\right) \quad (5.3.5)$$

$$\tilde{C}_{C2}=CO_{C2}(1-BN_2)+\frac{Q_{12}CO_{C1}}{V_2}\left(\frac{e^{-N_1't}-e^{-N_2't}}{(N_2'-N_1')}\right)+\frac{Q_{32}CO_{C3}}{V_2}\left(\frac{e^{-N_3't}-e^{-N_2't}}{(N_2'-N_3')}\right) \quad (5.3.6)$$

For Cell (3) :

$$\tilde{C}_{A3} = CO_{A3}(1-EN_3) + \frac{Q_{13}CO_{A1}}{V_3}\frac{(e^{-N_1't} - e^{-N_3't})}{(N_3'-N_1')} + \frac{Q_{23}CO_{A2}}{V_3}\frac{(e^{N_2't} - e^{-N_3't})}{(N_3'-N_2')} \quad (5.3.7)$$

$$\tilde{C}_{B3} = CO_{B3}(1-EN_3) + \frac{Q_{13}CO_{B1}}{V_3}\frac{(e^{-N_1't} - e^{-N_3't})}{(N_3'-N_1')} + \frac{Q_{23}CO_{B2}}{V_3}\frac{(e^{-N_2't} - e^{-N_3't})}{(N_3'-N_2')} \quad (5.3.8)$$

$$\tilde{C}_{C3} = CO_{C3}(1-EN_3) + \frac{Q_{13}CO_{C1}}{V_3}\frac{(e^{-N_1't} - e^{-N_3't})}{(N_3'-N_1')} + \frac{Q_{23}CO_{C2}}{V_3}\frac{(e^{-N_2't} - e^{-N_3't})}{(N_3'-N_2')} \quad (5.3.9)$$

Where $\tilde{C}_A$, $\tilde{C}_B$, $\tilde{C}_C$ are mean tracer gas concentrations derived from site data and calculated by numerical integration

$$A = -t + \frac{N_1't^2}{2!} - \frac{N_1'^2t^3}{3!} + \frac{N_1'^3t^4}{4!} - \frac{N_1'^4t^5}{5!} \quad x(-1)$$

$$B = -t + \frac{N_2't^2}{2!} - \frac{N_2'^2t^3}{3!} + \frac{N_2'^3t^4}{4!} - \frac{N_2'^4t^5}{5!} \quad x(-1)$$

$$E = -t + \frac{N_3't^2}{2!} - \frac{N_3'^2t^3}{3!} + \frac{N_3'^3t^4}{4!} - \frac{N_3'^4t^5}{5!} \quad x(-1)$$

For Cell (1), equations (5.3.1) - (5.3.3) are re-arranged for N_1, Q_{21} and Q_{31} as follows:

$$N_1 = \left[\frac{1}{A} - \frac{\tilde{C}_{A1}}{CO_{A1}A}\right] + \frac{Q_{21}CO_{A2}}{V_1CO_{A1}A}\left[\frac{e^{-N_2't} - e^{-N_1't}}{N_1' - N_2'}\right] + \frac{Q_{31}CO_{A3}}{V_1CO_{A1}A}\left[\frac{e^{-N_3't} - e^{-N_1't}}{N_1' - N_3'}\right] \quad (5.3.10)$$

$$Q_{21} = \frac{\left[\tilde{C}_{B1} - CO_{B1} + CO_{B1}N_1A - \frac{Q_{31}CO_{B3}}{V_1}\left(\frac{e^{-N_3't} - e^{-N_1't}}{N_1' - N_3'}\right)\right] V_1(N_1' - N_2')}{CO_{B2}(e^{-N_2't} - e^{-N_1't})} \quad (5.3.11)$$

$$Q_{31} = \frac{\left[\tilde{C}_{C1} - CO_{C1} + CO_{C1}N_1A - \frac{Q_{21}CO_{C2}}{V_1}\left(\frac{e^{-N_2't} - e^{-N_1't}}{(N_1' - N_2')}\right)\right] V_1(N_1' - N_3')}{CO_{C3}(e^{-N_3't} - e^{-N_1't})} \quad (5.3.12)$$

For Cell (2)

Equations (5.3.4), (5.3.5) and (5.3.6) are solved for Q_{12}, N_2 and Q_{32} in a similar manner.

$$N_2 = \left[\frac{1}{B} - \frac{\tilde{C}_{B2}}{CO_{B2}B}\right] + \frac{Q_{12}CO_{B1}}{V_2CO_{B2}B}\left[\frac{(e^{-N_1't} - e^{-N_2't})}{(N_2' - N_1')}\right] + \frac{Q_{32}CO_{B3}}{V_2CO_{B2}B}\left[\frac{(e^{-N_3't} - e^{-N_2't})}{(N_2' - N_3')}\right] \quad (5.3.13)$$

$$Q_{12} = \frac{\left[(\tilde{C}_{A2} - CO_{A2} + CO_{A2}BN_2) - \frac{Q_{32}CO_{A3}}{V_2}\left(\frac{e^{-N_3't} - e^{-N_2't}}{N_2' - N_3'}\right)\right] V_2(N_2' - N_1')}{CO_{A1}(e^{-N_1't} - e^{-N_2't})} \quad (5.3.14)$$

and

$$Q_{32} = \frac{\left[\tilde{C}_{C2} - CO_{C2} + CO_{C2}BN_2 - \frac{Q_{12}CO_{C1}}{V_2}\left(\frac{e^{-N_1't} - e^{-N_2't}}{(N_2'-N_1')}\right)\right](V_2(N_2'-N_3'))}{CO_{C3}\,(e^{-N_3't} - e^{-N_2't})} \qquad (5.3.15)$$

Finally equations (5.3.7) (5.3.8) and (5.3.9) are solved for Q_{13}, Q_{23} and N_3 in Cell (3)

$$N_3 = \left[\frac{1}{E} - \frac{\tilde{C}_{C3}}{CO_{C3}E}\right] + \frac{Q_{13}CO_{C1}}{V_3CO_{C3}E}\left[\frac{e^{-N_1't} - e^{-N_3't}}{N_3'-N_1'}\right] + \frac{Q_{23}CO_{C2}}{V_3CO_{C3}E}\left[\frac{e^{-N_2't} - e^{-N_3't}}{N_3'-N_2'}\right] \qquad (5.3.16)$$

$$Q_{13} = \frac{\left[\tilde{C}_{A3} - CO_{A3} + CO_{A3}N_3E - \frac{Q_{23}CO_{A2}}{V_3}\left(\frac{e^{-N_2't} - e^{-N_3't}}{(N_3'-N_2')}\right)\right]V_3(N_3'-N_1')}{CO_{A1}\,(e^{-N_1't} - e^{-N_3't})} \qquad (5.3.17)$$

$$Q_{23} = \frac{\left[\tilde{C}_{B3} - CO_{B3} + CO_{B3}N_3E - \frac{Q_{13}CO_{B1}}{V_3}\left(\frac{e^{-N_1't} - e^{-N_3't}}{(N_3'-N_1')}\right)\right]V_3\,(N_3'-N_2')}{CO_{B2}\,(e^{-N_2't} - e^{-N_3't})} \qquad (5.3.18)$$

First order estimates of N_1', N_2' and N_3' are obtained from an LnC(t) plot versus time from the first six data points of C_{A1}, C_{B2}, and C_{C3} respectively.

The calculated values of N_1, N_2, N_3, Q_{12}, Q_{13}, Q_{21}, Q_{23}, Q_{31} and Q_{32} are used in equations (5.2.2) - (5.2.10) to calculate the theoretical time variations in tracer concentrating for known airflows and initial gas concentrations at time zero. The resulting curves can then be compared with site data and direct comparison made.

5.4) Estimating errors in N1, N2, N3, Q12, Q32, Q13, Q23, Q21, and Q32

The following discussion assumes that all variables in equations (5.3.10) - (5.3.18) vary independantly of each other and there is no error in measured values of time.

Considering equation (5.3.10) for N_1:

$$N_1 = \left[\frac{1}{A} - \frac{\tilde{C}_{A1}}{CO_{A1}A}\right] + \frac{Q_{21}CO_{A2}}{V_1 CO_{A1}A}\left[\frac{e^{-N_2't} - e^{-N_1't}}{(N_1'-N_2')}\right] + \frac{Q_{31}CO_{A3}}{V_1 CO_{A1}A}\left[\frac{e^{-N_3't} - e^{-N_1't}}{N_1' - N_3'}\right] \quad (5.4.1)$$

The absolute standard error in N_1 can be estimated from:

$$(\Delta N_1)^2 = \left|\frac{\partial N_1}{\partial N_1'}\Delta N_1'\right|^2 + \left|\frac{\partial N_1}{\partial N_2'}\Delta N_2'\right|^2 + \left|\frac{\partial N_1}{\partial N_3'}\Delta N_3'\right|^2 + \left|\frac{\partial N_1}{\partial CO_{A1}}\Delta CO_{A1}\right|^2 +$$

$$\left|\frac{\partial N_1}{\partial CO_{A2}}\Delta CO_{A2}\right|^2 + \left|\frac{\partial N_1}{\partial CO_{A3}}\Delta CO_{A3}\right|^2 + \left|\frac{\partial N_1}{\partial \tilde{C}_{A1}}\Delta \tilde{C}_{A1}\right|^2 + \left|\frac{\partial N_1}{\partial A}\Delta A\right|^2 +$$

$$\left|\frac{\partial N_1}{\partial Q_{21}}\Delta Q_{21}\right|^2 + \left|\frac{\partial N_1}{\partial Q_{31}}\Delta Q_{31}\right|^2 + \left|\frac{\partial N_1}{\partial V_1}\Delta V_1\right|^2 \quad (5.4.2)$$

where

$$\frac{\partial N_1}{\partial N_1'} = \frac{(CO_{A1}AV_1)(N_1'-N_2')(Q_{21}CO_{A2}te^{-N_1't}) - (Q_{21}CO_{A2}(e^{-N_2't} - e^{-N_1't})(CO_{A1}AV_1))}{[CO_{A1}AV_1(N_1' - N_2')]^2}$$

$$+ \frac{(CO_{A1}AV_1)(N_1'-N_3')(Q_{31}CO_{A3}te^{-N_1't}) - (Q_{31}CO_{A3}(e^{-N_3't} - e^{-N_1't})(CO_{A1}AV_1))}{[CO_{A1}AV_1\ (N_1' - N_3')]^2} \qquad (5.4.3)$$

$$\frac{\partial N_1}{\partial N_2'} = \frac{(CO_{A1}AV_1)(N_1'-N_2')(-te^{-N_2't}Q_{21}CO_{A2}) - (Q_{21}CO_{A2}(e^{-N_2't} - e^{-N_1't})(-CO_{A1}AV_1))}{[CO_{A1}\ A\ V_1(N_1'-N_2')]^2} \qquad (5.4.4)$$

$$\frac{\partial N_1}{\partial N_3'} = \frac{(CO_{A1}AV_1)(N_1'-N_3')(Q_{31}CO_{A3}x\ -te^{-N_3't}) - (Q_{31}CO_{A3}(e^{-N_3't} - e^{-N_1't})(-V_1CO_{A1}A))}{(V_1CO_{A1}A(N_1' - N_3'))^2} \qquad (5.4.5)$$

$$\frac{\partial N_1}{\partial CO_{A1}} = \frac{\tilde{C}_{A1}}{CO_{A1}^2A} - \frac{Q_{21}CO_{A2}}{V_1CO_{A1}^2A}\left[\frac{e^{-N_2't} - e^{-N_1't}}{(N_1'-N_2')}\right] - \frac{Q_{31}CO_{A3}}{V_1CO_{A1}^2A}\left[\frac{e^{-N_3't} - e^{-N_1't}}{(N_1' - N_3')}\right] \qquad (5.4.6)$$

$$\frac{\partial N_1}{\partial CO_{A2}} = \frac{Q_{21}}{CO_{A1}V_1A}\left[\frac{e^{-N_2't} - e^{-N_1't}}{(N_1' - N_2')}\right] \qquad (5.4.7)$$

$$\frac{\partial N_1}{\partial CO_{A3}} = \frac{Q_{31}}{CO_{A1}V_1A}\left(\frac{e^{-N_3't} - e^{-N_1't}}{(N_1'-N_3')}\right) \qquad (5.4.8)$$

$$\frac{\partial N_1}{\partial C_{A1}} = -\frac{1}{CO_{A1}A} \qquad (5.4.9)$$

$$\frac{\partial N_1}{\partial A} = \left[\frac{-1}{A^2} + \frac{\tilde{C}_{A1}}{CO_{A1}A^2}\right] - \frac{Q_{21}CO_{A2}}{V_1CO_{A1}A^2}\left[\frac{e^{-N_2't} - e^{-N_1't}}{(N_1' - N_2')}\right] - \frac{Q_{31}CO_{A3}}{V_1CO_{A1}A^2}\left[\frac{e^{-N_3't} - e^{-N_1't}}{(N_1'-N_3')}\right] \qquad (5.4.10)$$

$$\frac{\partial N_1}{\partial Q_{21}} = \frac{CO_{A2}}{V_1CO_{A1}A}\left(\frac{e^{-N_2't} - e^{-N_1't}}{(N_1'-N_2')}\right) \qquad (5.4.11)$$

$$\frac{\partial N_1}{\partial Q_{31}} = \frac{CO_{A3}}{V_1CO_{A1}A}\left(\frac{e^{-N_3't} - e^{-N_1't}}{(N_1'-N_3')}\right) \qquad (5.4.12)$$

$$\frac{\partial N_1}{\partial V_1} = \frac{-Q_{21}CO_{A2}}{V_1^2\,CO_{A1}A}\left(\frac{e^{-N_2't} - e^{-N_1't}}{(N_1'-N_2')}\right) - \frac{Q_{31}CO_{A3}}{V_1^2CO_{A1}A}\left(\frac{e^{-N_3't} - e^{-N_1't}}{(N_1' - N_3')}\right) \qquad (5.4.13)$$

The absolute error in Q_{21} is found by considering equation (5.3.11)

$$Q_{21} = \left[\tilde{C}_{B1} + CO_{B1}(N_1A-1) - \frac{Q_{31}CO_{B3}}{V_1}\left(\frac{e^{-N_3't} - e^{-N_1't}}{(N_1'-N_3')}\right)\right]\frac{V_1(N_1'-N_2')}{CO_{B2}(e^{-N_2't} - e^{-N_1't})} \qquad (5.4.14)$$

$$(\Delta Q_{21})^2 = \left|\frac{\partial Q_{21}}{\partial N_1'}\Delta N_1'\right|^2 + \left|\frac{\partial Q_{21}}{\partial N_2'}\Delta N_2'\right|^2 + \left|\frac{\partial Q_{21}}{\partial N_3'}\Delta N_3'\right|^2 + \left|\frac{\partial Q_{21}}{\partial CO_{B1}}\Delta CO_{B1}\right|^2 + \left|\frac{\partial Q_{21}}{\partial CO_{B2}}\Delta CO_{B2}\right|^2 +$$

$$\left|\frac{\partial Q_{21}}{\partial CO_{B3}}\Delta CO_{B3}\right|^2 + \left|\frac{\partial Q_{21}}{\partial \tilde{C}_{B1}}\tilde{C}_{B1}\right|^2 + \left|\frac{\partial Q_{21}}{\partial A}\Delta A\right|^2 + \left|\frac{\partial Q_{21}}{\partial Q_{31}}\Delta Q_{31}\right|^2 + \left|\frac{\partial Q_{21}}{\partial N_1}\Delta N_1\right|^2 +$$

$$\left|\frac{\partial Q_{21}}{\partial V_1}\Delta V_1\right|^2 \qquad (5.4.15)$$

where

$$\frac{\partial Q_{21}}{\partial N_1'} = \frac{V_1(\tilde{C}_{B1}-CO_{B1}+CO_{B1}N_1A)(CO_{B2}(e^{-N_2't}-e^{-N_1't}))}{[CO_{B2}(e^{-N_2't}-e^{-N_1't})]^2} -$$

$$\frac{(CO_{B2}te^{-N_1't})(\tilde{C}_{B1}-CO_{B1}+CO_{B1}N_1A)(V_1(N_1'-N_2'))}{[CO_{B2}(e^{-N_2't}-e^{-N_1't})]^2}$$

$$+\left[\frac{(N_1'-N_2')}{CO_{B2}(e^{-N_2't}-e^{-N_1't})}\right]\left[\frac{-Q_{31}CO_{B3}te^{-N_1't}(N_1'-N_3') + Q_{31}CO_{B3}(e^{-N_3't}-e^{-N_1't})}{(N_1'-N_3')^2}\right] +$$

$$\left[\frac{-Q_{31}CO_{B3}(e^{-N_3't}-e^{-N_1't})}{(N_1'-N_3')}\right]\left[\frac{CO_{B2}(e^{-N_2't}-e^{-N_1't}) - CO_{B2}te^{-N_1't}(N_1'-N_2')}{[CO_{B2}(e^{-N_2't}-e^{-N_1't})]^2}\right]$$

(5.4.16)

$$\frac{\partial Q_{21}}{\partial N_2'} = \left[\frac{(-V_1(\tilde{C}_{B1}-CO_{B1}+CO_{B1}N_1A-\frac{Q_{31}CO_{B3}}{V_1}(e^{N_3't}-e^{-N_1't}))(CO_{B2}(e^{-N_2't}-e^{-N_1't}))}{[CO_{B2}(e^{-N_2't}-e^{-N_1't})]^2}\right] +$$

$$\left[\frac{CO_{B2}te^{-N_2't}(\tilde{C}_{B1}-CO_{B1}+CO_{B1}N_1A-\frac{Q_{31}CO_{B3}}{V_1}(e^{-N_3't}-e^{-N_1't}))(V_1(N_1'-N_2'))}{[CO_{B2}(e^{-N_2't}-e^{-N_1't})]^2}\right]$$

(5.4.17)

$$\frac{\partial Q_{21}}{\partial N_3'} = \frac{-(N_1'-N_2')Q_{31}CO_{B3}}{CO_{B2}(e^{-N_2't}-e^{-N_1't})} \left[\frac{-te^{-N_3't}(N_1'-N_3') + (e^{-N_3't}-e^{-N_1't})}{(N_1'-N_3')^2} \right] \quad (5.4.18)$$

$$\frac{\partial Q_{21}}{\partial N_1} = \frac{CO_{B1}AV_1(N_1'-N_2')}{CO_{B2}(e^{-N_2't}-e^{-N_1't})} \quad (5.4.19)$$

$$\frac{\partial Q_{21}}{\partial CO_{B1}} = \frac{(-1+N_1A)\,V_1(N_1'-N_2')}{CO_{B2}(e^{-N_2't}-e^{-N_1't})} \quad (5.4.20)$$

$$\frac{\partial Q_{21}}{\partial CO_{B2}} = -\frac{\left[\tilde{C}_{B1}-CO_{B1}+CO_{B1}N_1A - \frac{Q_{31}CO_{B3}}{V_1}\left(\frac{e^{-N_3't}-e^{-N_1't}}{(N_1'-N_3')}\right)\right] V_1(N_1'-N_2')}{CO_{B2}^2\,(e^{-N_2't}-e^{-N_1't})} \quad (5.4.21)$$

$$\frac{\partial Q_{21}}{\partial CO_{B3}} = \frac{-Q_{31}(e^{-N_3't}-e^{-N_1't})\,(N_1'-N_2')}{(N_1'-N_3')\,CO_{B2}(e^{-N_2't}-e^{-N_1't})} \quad (5.4.22)$$

$$\frac{\partial Q_{21}}{\partial \tilde{C}_{B1}} = \frac{V_1(N_1'-N_2')}{CO_{B2}(e^{-N_2't}-e^{-N_1't})} \quad (5.4.23)$$

$$\frac{\partial Q_{21}}{\partial A} = \frac{CO_{B1}N_1V_1(N_1'-N_2')}{CO_{B2}(e^{-N_2't}-e^{-N_1't})} \quad (5.4.24)$$

$$\frac{\partial Q_{21}}{\partial Q_{31}} = \left[\frac{-CO_{B3}}{V_1} \quad \frac{e^{-N_3't} - e^{-N_1't}}{(N_1' - N_3')}\right] \frac{V_1(N_1' - N_2')}{CO_{B2}(e^{-N_2't} - e^{-N_1't})} \qquad (5.4.25)$$

$$\frac{\partial Q_{21}}{\partial V_1} = \left[(\tilde{C}_{B1} + CO_{B1}(N_1A - 1))\right] \frac{(N_1' - N_2')}{CO_{B2}(e^{-N_2't} - e^{-N_1't})} \qquad (5.4.27)$$

Considering equation (5.3.12) for Q_{31}:

$$Q_{31} = \left[(\tilde{C}_{C1} + CO_{C1}(N_1A - 1) - \frac{Q_{21}CO_{C2}}{V_1} \quad \frac{(e^{-N_2't} - e^{-N_1't})}{(N_1' - N_2')}\right] \frac{V_1(N_1' - N_3')}{CO_{C3}(e^{-N_3't} - e^{-N_1't})} \qquad (5.4.28)$$

The absolute error in Q_{31} is found from:

$$(\Delta Q_{31})^2 = \left|\frac{\partial Q_{31}}{\partial N_1'} \Delta N_1'\right|^2 + \left|\frac{\partial Q_{31}}{\partial N_2'} \Delta N_2'\right|^2 + \left|\frac{\partial Q_{31}}{\partial N_3'} \Delta N_3'\right|^2 + \left|\frac{\partial Q_{31}}{\partial CO_{C1}} \Delta CO_{C1}\right|^2 + \left|\frac{\partial Q_{31}}{\partial CO_{C2}} \Delta CO_{C2}\right|^2$$

$$+ \left|\frac{\partial Q_{31}}{\partial N_1} \Delta N_1\right|^2 + \left|\frac{\partial Q_{31}}{\partial CO_{C3}} \Delta CO_{C3}\right|^2 + \left|\frac{\partial Q_{31}}{\partial \tilde{C}_{C3}} \Delta \tilde{C}_{C3}\right|^2 + \left|\frac{\partial Q_{31}}{\partial N_1} \Delta N_1\right|^2 + \left|\frac{\partial Q_{31}}{\partial A} \Delta A\right|^2 + \left|\frac{\partial Q_{31}}{\partial Q_{21}} \Delta Q_{21}\right|^2$$

(5.4.29)

where

$$\frac{\partial Q_{31}}{\partial N_1'} = \frac{V_1(\tilde{C}_{C1}-CO_{C1}+CO_{C1}N_1A)CO_{C3}(e^{-N_3't}-e^{-N_1't})-CO_{C3}te^{-N_1't}(\tilde{C}_{C1}-CO_{C1}+CO_{C1}N_1A)(V_1(N_1'-N_2'))}{[CO_{C3}(e^{-N_3't}-e^{-N_1't})]^2}$$

$$+\frac{(N_1'-N_3')}{CO_{C3}(e^{-N_3't}-e^{-N_1't})}\left(\frac{-(N_1'-N_2')Q_{21}CO_{C2}te^{-N_1't}+Q_{21}CO_{C2}(e^{-N_2't}-e^{-N_1't})}{(N_1'-N_2')^2}\right)$$

$$+\left[\frac{-Q_{21}CO_{C2}(e^{-N_2't}-e^{-N_1't})}{(N_1'-N_2')}\right]\left[\frac{CO_{C3}(e^{-N_3't}-e^{-N_1't})-CO_{C3}te^{-N_1't}(N_1'-N_3')}{[CO_{C3}(e^{-N_3't}-e^{-N_1't})]^2}\right]$$

(5.4.30)

$$\frac{\partial Q_{31}}{\partial N_2'} = \frac{(N_1'-N_3')}{CO_{C3}(e^{-N_3't}-e^{-N_1't})}\left[\frac{Q_{21}CO_{C2}te^{-N_2't}(N_1'-N_2')+(Q_{21}CO_{C2}(e^{-N_2't}-e^{-N_1't}))}{(N_1'-N_2')^2}\right]$$

(5.4.31)

$$\frac{\partial Q_{31}}{\partial N_3'} = \frac{\left[-V_1(\tilde{C}_{C1}-CO_{C1}+CO_{C1}N_1A-\frac{Q_{21}CO_{C2}}{V_1}\frac{(e^{-N_2't}-e^{-N_1't})}{(N_1'-N_2')}\right](CO_{C3}(e^{-N_3't}-e^{-N_1't}))}{[CO_{C3}(e^{-N_3't}-e^{-N_1't})]^2} +$$

$$\frac{\left[\tilde{C}_{C1}-CO_{C1}+CO_{C1}N_1A-\frac{Q_{21}CO_{C2}}{V_1}\frac{(e^{-N_2't}-e^{-N_1't})}{(N_1-N_2)}\right]V_1(N_1'-N_2')(CO_{C3}x-te^{-N_3't})}{[CO_{C3}(e^{-N_3't}-e^{-N_1't})]^2}$$

(5.4.32)

$$\frac{\partial Q_{31}}{\partial N_1} = \frac{CO_{C1}AV_1(N_1'-N_2')}{CO_{C3}(e^{-N_3't}-e^{-N_1't})} \qquad (5.4.33)$$

$$\frac{\partial Q_{31}}{\partial CO_{C1}} = \frac{(-1+N_1A)V_1(N_1'-N_3')}{CO_{C3}(e^{-N_3't} - e^{-N_1't})} \qquad (5.4.34)$$

$$\frac{\partial Q_{31}}{\partial CO_{C2}} = \frac{-Q_{21}(N_1'-N_3')(e^{-N_2't} - e^{-N_1't})}{(N_1'-N_2')\ CO_{C3}(e^{-N_3't} - e^{-N_1't})} \qquad (5.4.35)$$

$$\frac{\partial Q_{31}}{\partial \omega_{C3}} = -(\tilde{C}_{C1} - CO_{C1} + CO_{C1}N_1A - \frac{Q_{21}CO_{C2}}{V_1}(e^{-N_2't} - e^{-N_1't}))\left[\frac{V_1(N_1'-N_3')}{CO_{C3}^2(e^{-N_3't} - e^{-N_1't})}\right] \qquad (5.4.36)$$

$$\frac{\partial Q_{31}}{\partial \tilde{C}_{C1}} = \frac{V_1(N_1'-N_3')}{CO_{C3}(e^{-N_3't} - e^{-N_1't})} \qquad (5.4.37)$$

$$\frac{\partial Q_{31}}{\partial A} = \frac{CO_{C1}N_1V_1(N_1'-N_3')}{CO_{C3}(e^{-N_3't} - e^{-N_1't})} \qquad (5.4.38)$$

$$\frac{\partial Q_{31}}{\partial Q_{21}} = -CO_{C2}\ \frac{e^{-N_2't} - e^{-N_1't}}{(N_1' - N_2')}\ \frac{(N_1' - N_3')}{CO_{C3}(e^{-N_3't} - e^{-N_1't})} \qquad (5.4.39)$$

Considering Cell (2) :

Equation (5.3.13) for N_2 is:

$$N_2 = \left[\frac{1}{B} - \frac{\tilde{C}_{B2}}{CO_{B2}B}\right] + \frac{Q_{12}CO_{B1}}{V_2CO_{B2}B}\left[\frac{e^{-N_1't} - e^{-N_2't}}{(N_2' - N_1')}\right] + \frac{Q_{32}CO_{B3}}{V_2CO_{B2}B}\left[\frac{e^{-N_3't} - e^{-N_2't}}{(N_2' - N_3')}\right] \qquad (5.4.40)$$

The absolute error in N_2 is found from:

$$(\Delta N_2)^2 = \left|\frac{\partial N_2}{\partial N_1'}\Delta N_1'\right|^2 + \left|\frac{\partial N_2}{\partial N_2'}\Delta N_2'\right|^2 + \left|\frac{\partial N_2}{\partial N_3'}\Delta N_3'\right|^2 + \left|\frac{\partial N_2}{\partial CO_{B1}}\Delta CO_{B1}\right|^2 + \left|\frac{\partial N_2}{\partial CO_{B2}}\Delta CO_{B2}\right|^2$$

$$+\left|\frac{\partial N_2}{\partial CO_{B3}}\Delta CO_{B3}\right|^2 + \left|\frac{\partial N_2}{\partial \tilde{C}_{B2}}\Delta \tilde{C}_{B2}\right|^2 + \left|\frac{\partial N_2}{\partial Q_{12}}\Delta Q_{12}\right|^2 + \left|\frac{\partial N_2}{\partial Q_{32}}\Delta Q_{32}\right|^2 +$$

$$\left|\frac{\partial N_2}{\partial B}\Delta B\right|^2 + \left|\frac{\partial N_2}{\partial V_2}\Delta V_2\right|^2 \qquad (5.4.41)$$

$$\frac{\partial N_2}{\partial N_1'} = \frac{Q_{12}CO_{B1}(-te^{-N_1't})(V_2CO_{B2}B)(N_2'-N_1')-(-V_2CO_{B2}BQ_{12}CO_{B1}(e^{-N_1't}-e^{-N_2't}))}{[V_2CO_{B2}B\ (N_2'-N_1')]^2}$$

(5.4.42)

$$\frac{\partial N_2}{\partial N_2'} = \frac{(Q_{12}CO_{B1}te^{-N_2't})(V_2CO_{B2}B(N_2'-N_1'))-(V_2CO_{B2}B)(Q_{12}CO_{B1}(e^{-N_1't}-e^{-N_2't}))}{[V_2CO_{B2}B(N_2'-N_1')]^2}$$

$$+\frac{(Q_{32}CO_{B3}te^{-N_2't}V_2CO_{B2}B(N_2'-N_3')-(Q_{32}CO_{B3}(e^{-N_3't}-e^{-N_2't})\ V_2CO_{B2}B))}{[V_2CO_{B2}B\ (N_2'-N_3')]^2}$$

(5.4.43)

$$\frac{\partial N_2}{\partial N_3} = \frac{(-te^{-N_3't} Q_{32}CO_{B3})(V_2CO_{B2}B(N_2'-N_3')) - Q_{32}CO_{B2}(e^{-N_3't} - e^{-N_2't})(-V_2CO_{B2}B)}{[V_2CO_{B2}B\ (N_2' - N_3')]^2} \quad (5.4.44)$$

$$\frac{\partial N_2}{\partial CO_{B1}} = \frac{Q_{12}}{V_2CO_{B2}B} \frac{[e^{-N_1't} - e^{-N_2't}]}{(N_2'-N_1')} \quad (5.4.45)$$

$$\frac{\partial N_2}{\partial CO_{B2}} = \frac{\tilde{C}_{B2}}{CO_{B2}^2B} - \frac{Q_{12}CO_{B1}}{V_2CO_{B2}^2B} \frac{(e^{-N_1't} - e^{-N_2't})}{(N_2'-N_1')} - \frac{Q_{32}CO_{B3}}{V_2CO_{B2}^2B} \frac{(e^{-N_3't} - e^{-N_2't})}{(N_2' - N_3')} \quad (5.4.46)$$

$$\frac{\partial N_2}{\partial CO_{B3}} = \frac{Q_{32}}{V_2CO_{B2}B} \frac{[e^{-N_3't} - e^{-N_2't}]}{(N_2' - N_3')} \quad (5.4.47)$$

$$\frac{\partial N_2}{\partial \tilde{C}_{B2}} = -\frac{1}{CO_{B2}B} \quad (5.4.48)$$

$$\frac{\partial N_2}{\partial Q_{12}} = \frac{CO_{B1}}{V_2CO_{B2}B} \frac{[e^{-N_1't} - e^{-N_2't}]}{(N_2' - N_1')} \quad (5.4.49)$$

$$\frac{\partial N_2}{\partial Q_{32}} = \frac{CO_{B3}}{V_2CO_{B2}B} \frac{e^{-N_3't} - e^{-N_2't}}{(N_2' - N_3')} \quad (5.4.50)$$

$$\frac{\partial N_2}{\partial B} = -\frac{1}{B^2} + \frac{\tilde{C}_{B2}}{CO_{B2}B^2} - \frac{Q_{12}CO_{B1}}{V_2CO_{B2}B^2} \frac{[e^{-N_1't} - e^{-N_2't}]}{(N_2'-N_1')} - \frac{Q_{32}CO_{B3}}{V_2CO_{B2}B^2} \frac{[e^{-N_3't} - e^{-N_2't}]}{(N_2'-N_3')} \quad (5.4.51)$$

$$\frac{\partial N_2}{\partial V_2} = \frac{-Q_{12}CO_{B1}}{V_2^2 CO_{B1} B}\left(\frac{e^{-N_1't} - e^{-N_2't}}{(N_2'-N_1')}\right) - \frac{Q_{32}CO_{B3}}{V_2^2 CO_{B2} B}\left(\frac{e^{-N_3't} - e^{-N_2't}}{(N_2' - N_3')}\right) \qquad (5.4.52)$$

Equation (5.3.14) for Q_{12} is :

$$Q_{12} = (\tilde{C}_{A2} + CO_{A2}(BN_2 - 1) - \frac{Q_{32}CO_{A3}}{V_2}\left(\frac{e^{-N_3't} - e^{-N_2't}}{(N_2'-N_3')}\right)\frac{V_2(N_2'-N_1')}{CO_{A1}(e^{-N_1't} - e^{-N_2't})} \qquad (5.4.53)$$

The absolute error in Q_{12} can be estimated from :

$$(\Delta Q_{12})^2 = \left|\frac{\partial Q_{12}}{\partial N_1'}\Delta N_1'\right|^2 + \left|\frac{\partial Q_{12}}{\partial N_2'}\Delta N_2'\right|^2 + \left|\frac{\partial Q_{12}}{\partial N_3'}\Delta N_3'\right|^2 + \left|\frac{\partial Q_{12}}{\partial N_2}\Delta N_2\right|^2 +$$

$$\left|\frac{\partial Q_{12}}{\partial CO_{A1}}\Delta CO_{A1}\right|^2 + \left|\frac{\partial Q_{12}}{\partial CO_{A2}}\Delta CO_{A2}\right|^2 + \left|\frac{\partial Q_{12}}{\partial CO_{A3}}\Delta CO_{A3}\right|^2 + \left|\frac{\partial Q_{12}}{\partial C_{A2}}\Delta C_{A2}\right|^2 +$$

$$\left|\frac{\partial Q_{12}}{\partial Q_{32}}\Delta Q_{32}\right|^2 + \left|\frac{\partial Q_{12}}{\partial B}\Delta B\right|^2 + \left|\frac{\partial Q_{12}}{\partial V_2}\Delta V_2\right|^2 \qquad (5.4.54)$$

where

$$\frac{\partial Q_{12}}{\partial N_1'} = \frac{\left[(-V_2)(\tilde{C}_{A2} - CO_{A2} + N_2 BCO_{A2} - \frac{Q_{32}CO_{A3}(e^{-N_3't} - e^{-N_2't})}{V_2(N_2'-N_3')}\right](CO_{A1}(e^{-N_1't} - e^{-N_2't}))}{[CO_{A1}(e^{-N_1't} - e^{-N_2't})]^2}$$

$$- \frac{((-te^{-N_1't}CO_{A1})(V_2(N_2'-N_1'))(\tilde{C}_{A2} - CO_{A2} + N_2 BCO_{A2} - \frac{Q_{32}CO_{A3}(e^{-N_3't} - e^{-N_1't})}{V_2(N_2'-N_3')})}{[CO_{A1}(e^{-N_1't} - e^{-N_2't})]^2} \qquad (5.4.55)$$

$$\frac{\partial Q_{12}}{\partial N_2'} = -\frac{V_2(N_2'-N_1')}{CO_{A1}(e^{-N_1't-N_2't})}\left[\frac{(Q_{32}CO_{A3}te^{-N_2't}V_2(N_2'-N_3')) - (V_2 Q_{31}CO_{A3}(e^{-N_3't} - e^{-N_2't}))}{(V_2(N_2' - N_3'))^2}\right.$$

$$\left. + \frac{Q_{32}CO_{A3}(e^{-N_3't} - e^{-N_2't})}{V_2(N_2'-N_3')}\left[\frac{(V_2CO_{A1}(e^{-N_1't} - e^{-N_2't}) - (CO_{A1}te^{-N_2't}V_2(N_2'-N_1')))}{[CO_{A1}(e^{-N_1't} - e^{-N_2't})]^2}\right]\right] \tag{5.4.56}$$

$$\frac{\partial Q_{12}}{\partial N_3'} = -\frac{V_2(N_2'-N_1')}{CO_{A1}(e^{-N_1't-N_2't})}\left[\frac{-Q_{32}CO_{A3}te^{-N_3't}V_2(N_2'-N_3') - (-V_2Q_{32}CO_{A3}(e^{-N_3't} - e^{-N_2't}))}{(V_2(N_2'-N_3'))^2}\right] \tag{5.4.57}$$

$$\frac{\partial Q_{12}}{\partial CO_{A1}} = -\left[(\tilde{C}_{A2} - CO_{A2} + CO_{A2}BN_2 - \frac{Q_{32}CO_{A3}}{V_2}\frac{(e^{-N_3't} - e^{-N_2't})}{(N_2'-N_3')}\right]\frac{V_2(N_2'-N_1')}{CO_{A1}^2(e^{-N_1't} - e^{-N_2't})} \tag{5.4.58}$$

$$\frac{\partial Q_{12}}{\partial CO_{A2}} = (-1 + BN_2)\frac{V_2(N_2'-N_1')}{CO_{A1}(e^{-N_1't} - e^{-N_2't})} \tag{5.4.59}$$

$$\frac{\partial Q_{12}}{\partial CO_{A3}} = -\frac{Q_{32}}{V_2}\frac{(e^{-N_3't} - e^{-N_2't})}{(N_2' - N_3')}\frac{V_2(N_2'-N_1')}{CO_{A1}(e^{-N_1't} - e^{-N_2't})} \tag{5.4.60}$$

$$\frac{\partial Q_{12}}{\partial N_2} = \frac{CO_{A2}\, B\, V_2(N_2' - N_1')}{CO_{A1}(e^{-N_1't} - e^{-N_2't})} \tag{5.4.61}$$

$$\frac{\partial Q_{12}}{\partial \tilde{C}_{A2}} = \frac{V_2(N_2' - N_1')}{CO_{A1}\,(e^{-N_1't} - e^{-N_2't})} \qquad (5.4.62)$$

$$\frac{\partial Q_{12}}{\partial Q_{32}} = \frac{-CO_{A3}}{V_2}\,\frac{e^{-N_3't} - e^{-N_2't})}{(N_2' - N_3')}\,\frac{V_2(N_2' - N_1')}{CO_{A1}(e^{-N_1't} - e^{-N_2't})} \qquad (5.4.63)$$

$$\frac{\partial Q_{12}}{\partial B} = \frac{CO_{A2}N_2V_2(N_2' - N_1')}{CO_{A1}(e^{-N_1't} - e^{-N_2't})} \qquad (5.4.64)$$

$$\frac{\partial Q_{12}}{\partial V_2} = (\tilde{C}_{A2} + CO_{A2}\,(BN_2 - 1))\,\frac{(N_2' - N_1')}{CO_{A1}(e^{-N_1't} - e^{-N_2't})} \qquad (5.4.65)$$

Considering equation (5.3.15) for Q_{32}:

$$Q_{32} = (\tilde{C}_{C2} + CO_{C2}(BN_2 - 1) - \frac{Q_{12}CO_{C1}}{V_2}\,\frac{(e^{-N_1't} - e^{-N_2't})}{(N_2' - N_1')}\,\frac{V_2(N_2' - N_3')}{CO_{C3}(e^{-N_3't} - e^{-N_2't})} \qquad (5.4.66)$$

The absolute error in Q_{32} is found from:

$$(\Delta Q_{32})^2 = \left|\frac{\partial Q_{32}}{\partial N_1'}\Delta N_1'\right|^2 + \left|\frac{\partial Q_{32}}{\partial N_2'}\Delta N_2'\right|^2 + \left|\frac{\partial Q_{32}}{\partial N_3'}\Delta N_3'\right|^2 + \left|\frac{\partial Q_{32}}{\partial N_2}\Delta N_2\right|^2 + \left|\frac{\partial Q_{32}}{\partial CO_{C1}}\Delta CO_{C1}\right|^2$$

$$+ \left|\frac{\partial Q_{32}}{\partial CO_{C2}}\Delta CO_{C2}\right|^2 + \left|\frac{\partial Q_{32}}{\partial CO_{C3}}\Delta CO_{C3}\right|^2 + \left|\frac{\partial Q_{32}}{\partial \tilde{C}_{C2}}\Delta \tilde{C}_{C2}\right|^2 + \left|\frac{\partial Q_{32}}{\partial Q_{12}}\Delta Q_{12}\right|^2 + \left|\frac{\partial Q_{32}}{\partial B}\Delta B\right|^2$$

$$+ \left|\frac{\partial Q_{32}}{\partial V_2}\Delta V_2\right|^2 \qquad (5.4.67)$$

value

$$\frac{\partial Q_{32}}{\partial N_1'} = -\frac{V_2(N_2'-N_3')}{CO_{C3}(e^{-N_3't-N_2't})}\left[\frac{-(Q_{12}CO_{C1}\,te^{-N_1't}V_2(N_2'-N_1')) - (-V_2Q_{12}CO_{C1}(e^{-N_1't}-e^{-N_2't}))}{(V_2(N_2'-N_1'))^2}\right] \quad (5.4.68)$$

$$= \frac{V_2(\tilde{C}_{C2}-CO_{C2}+CO_{C2}BN_2)(CO_{C3}(e^{-N_3't}-e^{-N_2't})) - ((\tilde{C}_{C2}-CO_{C2}+CO_{C2}BN_2)V_2(N_2'-N_3'))(CO_{C3}te^{-N_2't})}{(CO_{C3}(e^{-N_3't}-e^{-N_2't}))^2}$$

$$+\left[\frac{-(V_2(N_2'-N_3')}{CO_{C3}(e^{-N_3't-N_2't})}\;\frac{((Q_{12}CO_{C1}te^{-N_2't}V_2(N_2'-N_1')) - (V_2Q_{12}CO_{C1}(e^{-N_1't}-e^{-N_2't})))}{(V_2(N_2'-N_1'))^2}\right]$$

$$+\left[\frac{(-Q_{12}CO_{C1}(e^{-N_1't}-e^{-N_2't})}{V_2(N_2'-N_1')}\;\frac{(V_2CO_{C3}(e^{-N_3't}-e^{-N_2't}) - (te^{-N_2't}CO_{C3}V_2(N_2'-N_3')))}{(CO_{C3}(e^{-N_3't}-e^{-N_2't}))^2}\right] \quad (5.4.69)$$

$$\frac{\partial Q_{32}}{\partial N_3'} = \left[\frac{(\tilde{C}_{C2} - CO_{C2} + CO_{C2}BN_2 - \frac{Q_{12}CO_{C1}}{V_2}(e^{-N_1't}-e^{-N_2't}))(-V_2)(CO_{C3}(e^{-N_3't}-e^{-N_2't}))}{(N_2'-N_1')}}{(CO_{C3}(e^{-N_3't}-e^{-N_2't}))^2}\right]$$

$$+\left[\frac{(-CO_{C3}te^{-N_3t})(\tilde{C}_{C2}-CO_{C2}+CO_{C2}BN_2 - \frac{Q_{12}CO_{C1}(e^{-N_1't}-e^{-N_2't}))}{V_2(N_2'-N_1')}}{(CO_{C3}(e^{-N_3't}-e^{-N_2't}))^2}\right] \quad (5.4.70)$$

$$\frac{\partial Q_{32}}{\partial N_2} = \frac{CO_{C2}BV_2(N_2'-N_3')}{CO_{C3}(e^{-N_3't}-e^{-N_2't})} \quad (5.4.71)$$

$$\frac{\partial Q_{32}}{\partial CO_{C1}} = \frac{-Q_{12}}{V_2}\,\frac{(e^{-N_1't} - e^{-N_2't})}{(N_2'-N_1')}\,\frac{(V_2(N_2'-N_3'))}{CO_{C3}(e^{-N_3't} - e^{-N_2't})} \qquad (5.4.72)$$

$$\frac{\partial Q_{32}}{\partial CO_{C2}} = (-1+BN_2)\,\frac{V_2(N_2'-N_3')}{CO_{C3}(e^{-N_3't} - e^{-N_2't})} \qquad (5.4.73)$$

$$\frac{\partial Q_{32}}{\partial CO_{C3}} = -(\tilde{C}_{C2}-CO_{C2}+CO_{C2}BN_2-\frac{Q_{12}CO_{C1}(e^{-N_1't} - e^{-N_2't})}{V_2(N_2'-N_1')})\,\frac{V_2(N_2'-N_3')}{CO_{C3}^2(e^{-N_3't} - e^{-N_2't})} \qquad (5.4.74)$$

$$\frac{\partial Q_{32}}{\partial \tilde{C}_{C2}} = \frac{(V_2(N_2'-N_3'))}{CO_{C3}(e^{-N_3't} - e^{-N_2't})} \qquad (5.4.75)$$

$$\frac{\partial Q_{32}}{\partial Q_{12}} = \frac{-CO_{C1}}{V_2}\,\frac{(e^{-N_1't} - e^{-N_2't})}{(N_2'-N_1')}\,\frac{V_2(N_2'-N_3')}{CO_{C3}(e^{-N_3't} - e^{-N_1't})} \qquad (5.4.76)$$

$$\frac{\partial Q_{32}}{\partial B} = \frac{CO_{C2}N_2V_2\,(N_2'-N_3')}{CO_{C3}(e^{-N_3't} - e^{-N_2't})} \qquad (5.4.77)$$

$$\frac{\partial Q_{32}}{\partial V_2} = (\tilde{C}_{C2} + CO_{C2}(BN_2-1))\,\frac{(N_2' - N_3')}{CO_{C3}(e^{-N_3't} - e^{-N_2't})} \qquad (5.4.78)$$

Considering Cell (3)

Equation (5.3.16) gives for N_3:

$$N_3 = \frac{1}{E} - \frac{\tilde{C}_{C3}}{CO_{C3}E} + \frac{Q_{13}CO_{C1}}{V_3CO_{C3}E}\left(\frac{e^{-N_1't} - e^{-N_3't}}{(N_3' - N_1')}\right) + \frac{Q_{23}CO_{C2}}{V_3CO_{C3}E}\left(\frac{e^{-N_2't} - e^{-N_3't}}{(N_3' - N_2')}\right) \quad (5.4.79)$$

The absolute error in N_3 is found from:

$$(\Delta N_3)^2 = \left|\frac{\partial N_3}{\partial N_1'}\Delta N_1'\right|^2 + \left|\frac{\partial N_3}{\partial N_2'}\Delta N_2'\right|^2 + \left|\frac{\partial N_3}{\partial N_3'}\Delta N_3'\right|^2 + \left|\frac{\partial N_3}{\partial CO_{C1}}\Delta CO_{C1}\right|^2 + \left|\frac{\partial N_3}{\partial CO_{C2}}\Delta CO_{C2}\right|^2 + \left|\frac{\partial N_3}{\partial CO_{C3}}\Delta CO_{C3}\right|^2$$

$$+ \left|\frac{\partial N_3}{\partial \tilde{C}_{C3}}\Delta \tilde{C}_{C3}\right|^2 + \left|\frac{\partial N_3}{\partial Q_{13}}\Delta Q_{13}\right|^2 + \left|\frac{\partial N_3}{\partial Q_{23}}\Delta Q_{23}\right|^2 + \left|\frac{\partial N_3}{\partial E}\Delta E\right|^2 + \left|\frac{\partial N_3}{\partial V_3}\Delta V_3\right|^2 \quad (5.4.80)$$

$$\frac{\partial N_3}{\partial N_1'} = \frac{(-te^{-N_1't}Q_{13}CO_{C1}V_3CO_{C3}E(N_3' - N_1')) + (V_3CO_{C3}EQ_{13}CO_{C1}(e^{-N_1't} - e^{-N_3't}))}{(V_3CO_{C3}E(N_3' - N_1'))^2} \quad (5.4.81)$$

$$\frac{\partial N_3}{\partial N_2'} = \frac{(te^{-N_2't}Q_{23}CO_{C2}V_3CO_{C3}E(N_3' - N_1')) + (V_3CO_{C3}Q_{23}CO_{C2}(e^{-N_2't} - e^{-N_1't}))}{(V_3CO_{C3}E(N_3' - N_2'))^2} \quad (5.4.82)$$

$$\frac{\partial N_3}{\partial N_3'} = \frac{(te^{-N_3't} Q_{13}CO_{C1}V_3CO_{C3}E(N_3'-N_1')) - (V_3CO_{C3}EQ_{13}CO_{C1}(e^{-N_1't} - e^{-N_3't}))}{(V_3CO_{C3}E(N_3'-N_1'))^2}$$

$$+ \frac{(te^{-N_3't} Q_{23}CO_{C2}V_3CO_{C3}E(N_3'-N_2')) - (V_3CO_{C3}EQ_{23}CO_{C2}(e^{-N_2't} - e^{-N_1't}))}{(V_3CO_{C3}E(N_3'-N_2'))^2} \qquad (5.4.83)$$

$$\frac{\partial N_3}{\partial CO_{C1}} = \frac{Q_{13}}{V_3CO_{C3}E(N_3'-N_1')} \frac{(e^{-N_1't} - e^{-N_3't})}{} \qquad (5.4.84)$$

$$\frac{\partial N_3}{\partial CO_{C2}} = \frac{Q_{23}}{V_3CO_{C3}E(N_3'-N_2')} \frac{(e^{-N_2't} - e^{-N_3't})}{} \qquad (5.4.85)$$

$$\frac{\partial N_3}{\partial CO_{C3}} = \frac{\tilde{C_{C3}}}{CO_{C3}^2E} - \frac{Q_{13}CO_{C1}}{V_3CO_{C3}^2E} \frac{(e^{-N_1't} - e^{-N_3't})}{(N_3'-N_1')} - \frac{Q_{23}CO_{C2}}{V_3CO_{C3}^2E} \frac{(e^{-N_2't} - e^{-N_3't})}{(N_3'-N_2')} \qquad (5.4.86)$$

$$\frac{\partial N_3}{\partial \tilde{C_{C3}}} = -\frac{1}{CO_{C3}E} \qquad (5.4.87)$$

$$\frac{\partial N_3}{\partial Q_{13}} = \frac{CO_{C1}}{V_3CO_{C3}E} \frac{(e^{-N_1t} - e^{-N_3t})}{(N_3-N_1)} \qquad (5.4.88)$$

$$\frac{\partial N_3}{\partial Q_{23}} = \frac{CO_{C2}}{V_3 CO_{C3} E} \frac{(e^{-N_1' t} - e^{-N_3' t})}{(N_3' - N_2')} \qquad (5.4.89)$$

$$\frac{\partial N_3}{\partial E} = \frac{-1}{\epsilon^2} + \frac{\tilde{C}_{C3}}{CO_{C3} E^2} - \frac{Q_{13} CO_{C1}}{V_3 CO_{C3} E^2} \frac{(e^{-N_1' t} - e^{-N_3' t})}{(N_3' - N_1')} - \frac{Q_{23} CO_{C2}}{V_3 CO_{C3} E^2} \frac{(e^{-N_2' t} - e^{-N_3' t})}{(N_3' - N_2')} \qquad (5.4.90)$$

$$\frac{\partial N_3}{\partial V_3} = \frac{-Q_{13} CO_{C1}}{V_3^2 CO_{C3} E} \frac{(e^{-N_1' t} - e^{-N_3' t})}{(N_3' - N_1')} - \frac{Q_{23} CO_{C2}}{V_3^2 CO_{C3} E} \frac{(e^{-N_2' t} - e^{-N_3' t})}{(N_3' - N_2')} \qquad (5.4.91)$$

Equation (5.3.17) gives for Q_{13} :

$$Q_{13} = \left(\tilde{C}_{A3} + CO_{A3}(N_3 E - 1) - \frac{Q_{23} CO_{A2}}{V_3} \frac{(e^{-N_2 t} - e^{-N_3 t})}{(N_3' - N_2')}\right) \frac{V_3 (N_3' - N_1')}{CO_{A1} (e^{-N_1' t} - e^{-N_3' t})} \qquad (5.4.92)$$

The absolute error in Q_{13} is estimated from:

$$(\Delta Q_{13})^2 = \left|\frac{\partial Q_{13}}{\partial N_1'} \Delta N_1'\right|^2 + \left|\frac{\partial Q_{13}}{\partial N_2'} \Delta N_2'\right|^2 + \left|\frac{\partial Q_{13}}{\partial N_3'} \Delta N_3'\right|^2 + \left|\frac{\partial Q_{13}}{\partial CO_{A1}} \Delta CO_{A1}\right|^2 + \left|\frac{\partial Q_{13}}{\partial CO_{A2}} \Delta CO_{A2}\right|^2$$

$$+ \left|\frac{\partial Q_{13}}{\partial CO_{A3}} \Delta CO_{A3}\right|^2 + \left|\frac{\partial Q_{13}}{\partial N_3} \Delta N_3\right|^2 + \left|\frac{\partial Q_{13}}{\partial C_{A3}} \Delta C_{A3}\right|^2 + \left|\frac{\partial Q_{13}}{\partial Q_{23}} \Delta Q_{23}\right|^2 + \left|\frac{\partial Q_{13}}{\partial E} \Delta E\right|^2 +$$

$$\left|\frac{\partial Q_{13}}{\partial V_3} \Delta V_3\right|^2 \qquad (5.4.93)$$

where

$$\frac{\partial Q_{13}}{\partial N_1'} = \left[\frac{-V_3(\tilde{C}_{A3} - CO_{A3} + CO_{A3}N_3E - \frac{Q_{23}CO_{A2}(e^{-N_2't} - e^{-N_3't})}{V_3(N_3' - N_2')})CO_{A1}(e^{-N_1't} - e^{-N_3't})}{[CO_{A1}(e^{-N_1't} - e^{-N_3't})]^2} \right]$$

$$+ \left[\frac{te^{-N_1t}CO_{A1}(\tilde{C}_{A3} - CO_{A3} + CO_{A3}N_3 \frac{-Q_{23}CO_{A2}(e^{-N_2't} - e^{-N_3't})}{V_3 (N_3' - N_2')})(V_3(N_3' - N_1'))}{[CO_{A1}(e^{-N_1't} - e^{-N_3't})]^2} \right] \quad (5.4.94)$$

$$\frac{\partial Q_{13}}{\partial N_2'} = \frac{-V_3(N_3' - N_1')}{CO_{A1}(e^{-N_1t} - e^{-N_3t})} \left[\frac{[-Q_{23}CO_{A2}te^{-N_2't}V_3(N_3' - N_2') + V_3Q_{23}CO_{A2}(e^{-N_2't} - e^{-N_3't})]}{[V_3(N_3' - N_2')]^2} \right] \quad (5.4.95)$$

$$\frac{\partial Q_{13}}{\partial N_3'} = \left[\frac{V_3(\tilde{C}_{A3} - CO_{A3} + CO_{A3}N_3E)(CO_{A1}(e^{-N_1't} - e^{-N_3't})) - CO_{A1}te^{-N_3't}(\tilde{C}_{A3} - CO_{A3} + CO_{A3}N_3E)}{[CO_{A1}(e^{-N_1't} - e^{-N_3't})]^2} \right]$$

$$- \left[\frac{V_3(N_3' - N_1')}{CO_{A1}(e^{-N_1't} - e^{-N_3't})} \frac{[Q_{23}CO_{A2}te^{-N_3't}V_3(N_3' - N_2') - V_3Q_{23}CO_{A2}(e^{-N_2't} - e^{-N_3't})]}{[V_3(N_3' - N_2')]^2} \right]$$

$$- \left[\frac{Q_{23}CO_{A2}(e^{N_2't} - e^{-N_1't})}{V_3(N_3' - N_2')} \frac{[V_3CO_{A1}(e^{-N_1't} - e^{-N_3't}) - te^{-N_3't}CO_{A1}V_3(N_3' - N_1')]}{[CO_{A1}(e^{-N_1't} - e^{-N_3't})]^2} \right] \quad (5.4.96)$$

$$\frac{\partial Q_{13}}{\partial CO_{A1}} = \left[\frac{-\left[\tilde{C}_{A3} - CO_{A3} + CO_{A3} N_3 E - \frac{Q_{23} CO_{A2} (e^{-N_2' t} - e^{-N_3' t})}{V_3 (N_3' - N_2')} \right] V_3 (N_3' - N_1')}{CO_{A1}^2 (e^{-N_1' t} - e^{-N_3' t})} \right] \tag{5.4.97}$$

$$\frac{\partial Q_{13}}{\partial CO_{A2}} = - \frac{Q_{23} (e^{-N_2' t} - e^{-N_3' t})}{V_3 (N_3' - N_2')} \frac{V_3 (N_3' - N_1')}{CO_{A1} (e^{-N_1' t} - e^{-N_3' t})} \tag{5.4.98}$$

$$\frac{\partial Q_{13}}{\partial CO_{A3}} = \frac{(-1 + N_3 E) V_3 (N_3' - N_1')}{CO_{A1} (e^{-N_1' t} - e^{-N_3' t})} \tag{5.4.99}$$

$$\frac{\partial Q_{13}}{\partial \tilde{C}_{A3}} = \frac{V_3 (N_3' - N_1')}{CO_{A1} (e^{-N_1' t} - e^{-N_3' t})} \tag{5.4.100}$$

$$\frac{\partial Q_{13}}{\partial N_3} = \frac{CO_{A3} E V_3 (N_3' - N_1')}{CO_{A1} (e^{-N_1' t} - e^{N_3' t})} \tag{5.4.101}$$

$$\frac{\partial Q_{13}}{\partial Q_{23}} = - \frac{CO_{A2}}{V_3} \left[\frac{e^{-N_2' t} - e^{-N_3' t}}{(N_3' - N_2')} \right] \frac{V_3 (N_3' - N_1')}{CO_{A1} (e^{-N_1' t} - e^{-N_3' t})} \tag{5.4.102}$$

$$\frac{\partial Q_{13}}{\partial E} = \frac{CO_{A3} N_3 V_3 (N_3' - N_1')}{CO_{A1} (e^{-N_1' t} - e^{-N_3' t})} \tag{5.4.103}$$

Equation (5.3.18) gives for Q_{23}:

$$Q_{23} = [\tilde{C}_{B3} + CO_{B3}(N_3E-1) - \frac{Q_{13}CO_{B1}}{V_3}\left(\frac{e^{-N_1't} - e^{-N_3't}}{(N_3'-N_1')}\right)] \frac{V_3(N_3'-N_2')}{CO_{B2}(e^{-N_2't} - e^{-N_3't})} \qquad (5.4.105)$$

The absolute error in Q_{23} is estimated from:

$$(\Delta Q_{23})^2 = \left|\frac{\partial Q_{23}}{\partial N_1'}\Delta N_1'\right|^2 + \left|\frac{\partial Q_{23}}{\partial N_2'}\Delta N_2'\right|^2 + \left|\frac{\partial Q_{23}}{\partial N_3'}\Delta N_3'\right|^2 + \left|\frac{\partial Q_{23}}{\partial CO_{B1}}\Delta CO_{B1}\right|^2 + \left|\frac{\partial Q_{23}}{\partial CO_{B2}}\Delta CO_{B2}\right|^2$$

$$\left|\frac{\partial Q_{23}}{\partial CO_{B3}}\Delta CO_{B3}\right|^2 + \left|\frac{\partial Q_{23}}{\partial \tilde{C}_{B3}}\Delta \tilde{C}_{B3}\right|^2 + \left|\frac{\partial Q_{23}}{\partial N_3}\Delta N_3\right|^2 + \left|\frac{\partial Q_{23}}{\partial Q_{13}}\Delta Q_{13}\right|^2 + \left|\frac{\partial Q_{23}}{\partial E}\Delta E\right|^2 +$$

$$\left|\frac{\partial Q_{23}}{\partial V_3}\Delta V_3\right|^2 \qquad (5.4.106)$$

where

$$\frac{\partial Q_{23}}{\partial N_1'} = \frac{-V_3(N_3'-N_2')}{CO_{B2}(e^{-N_2't} - e^{-N_3't})}\left[\frac{-Q_{13}CO_{B1}te^{-N_1't}V_3(N_3'-N_1') + V_3Q_{13}CO_{B1}(e^{-N_1't} - e^{-N_3't})}{[V_3(N_3'-N_1')]^2}\right] \qquad (5.4.107)$$

$$\frac{\partial Q_{23}}{\partial N_2'} = \left[\frac{-V_3[\tilde{C}_{B3} - CO_{B3} + CO_{B3}N_3E - \frac{Q_{13}CO_{B1}(e^{-N_1't} - e^{-N_3't})}{V_3(N_3'-N_1')}](CO_{B2}(e^{-N_2't} - e^{-N_3't})}{[CO_{B2}(e^{-N_2't} - e^{-N_3't})]^2}\right]$$

$$+ \left[\frac{CO_{B2}te^{-N_2t}[\tilde{C}_{B3} - CO_{B3} + CO_{B3}N_3E - \frac{Q_{13}CO_{B1}}{V_3}\left(\frac{e^{-N_1't} - e^{-N_3't}}{(N_3'-N_1')}\right)]V_3(N_3'-N_2')}{[CO_{B_2}(e^{-N_2't} - e^{-N_3't})]^2}\right] \qquad (5.4.108)$$

$$\frac{\partial Q_{23}}{\partial N_3'} = \left[\frac{V_3(\tilde{C}_{B3} - CO_{B3} + CO_{B3}N_3E)(CO_{B2}(e^{-N_2't} - e^{-N_3't}))}{[CO_{B2}(e^{-N_2't} - e^{-N_3't})]^2} \right.$$

$$- \frac{CO_{B2}te^{-N_3t}(\tilde{C}_{B3} - CO_{B3} + CO_{B3}N_3E)\ V_3(N_3' - N_2')}{[CO_{B2}(e^{-N_2't} - e^{-N_3't})]^2}$$

$$+ \frac{(-V_3(N_3' - N_2'))}{CO_{B2}(e^{-N_2't} - e^{-N_3't})} \left[\frac{(Q_{13}CO_{B1}te^{-N_3't} V_3(N_3' - N_1') - V_3Q_{13}CO_{B1}(e^{-N_1't} - e^{-N_3't}))}{[V_3(N_3' - N_1')]^2} \right]$$

$$\left. + \frac{(-Q_{13}CO_{B1}(e^{-N_1't} - e^{-N_3't}))}{V_3(N_3' - N_1')} \left[\frac{(V_3CO_{B2}(e^{-N_2't} - e^{-N_3't}) - CO_{B2}te^{-N_3't} V_3(N_3' - N_2'))}{[CO_{B2}(e^{-N_2't} - e^{-N_3't})]^2} \right] \right] \tag{5.4.109}$$

$$\frac{\partial Q_{23}}{\partial CO_{B1}} = \frac{V_3(N_3' - N_2')}{CO_{B2}(e^{-N_2't} - e^{-N_3't})} \left[\frac{-Q_{13}(e^{-N_1't} - e^{-N_3't})}{V_3(N_3' - N_1')} \right] \tag{5.4.110}$$

$$\frac{\partial Q_{23}}{\partial CO_{B2}} = \frac{-\left(\tilde{C}_{B3} - CO_{B3} + CO_{B3}N_3E - \frac{Q_{13}CO_{B1}(e^{-N_1't} - e^{-N_3't})}{V_3(N_3' - N_1')}\right) V_3(N_3' - N_2')}{CO_{B2}^2\ (e^{-N_2't} - e^{-N_3't})} \tag{5.4.111}$$

$$\frac{\partial Q_{23}}{\partial CO_{B3}} = (-1 + N_3E)\ \frac{V_3(N_3' - N_2')}{CO_{B2}(e^{-N_2't} - e^{-N_3't})} \tag{5.4.112}$$

$$\frac{\partial Q_{23}}{\partial \tilde{C}_{B3}} = \frac{V_3(N_3' - N_2')}{CO_{B2}(e^{-N_2't} - e^{-N_3't})} \qquad (5.4.113)$$

$$\frac{\partial Q_{23}}{\partial N_3} = \frac{CO_{B3} E\, V_3(N_3' - N_2')}{CO_{B2}(e^{-N_2't} - e^{-N_3't})} \qquad (5.4.114)$$

$$\frac{\partial Q_{23}}{\partial Q_{13}} = -CO_{B1} \frac{(e^{-N_1't} - e^{-N_3't})}{(N_3' - N_1')} \frac{(N_3' - N_2')}{CO_{B2}(e^{-N_2't} - e^{-N_3't})} \qquad (5.4.115)$$

$$\frac{\partial Q_{23}}{\partial E} = \frac{CO_{B3} N_3 V_3(N_3' - N_2')}{CO_{B2}(e^{-N_2't} - e^{-N_3't})} \qquad (5.4.116)$$

$$\frac{\partial Q_{23}}{\partial V_3} = \frac{(\tilde{C}_{B3} + CO_{B3}(N_3 E - 1))\ (N_3' - N_2')}{CO_{B2}(e^{-N_2't} - e^{-N_3't})} \qquad (5.4.117)$$

The relative contribution of errors in each variable to the total error in calculated values of N_1, N_2, N_3, Q_{12}, Q_{13}, Q_{23}, Q_{32}, Q_{31} and Q_{21} are most clearly seen where known airflows and tracer gas concentrations can be directly compared with airflows calculated from site concentration data which is subject to random measurement errors.

5.5) Calculating airflows and cell air change rates using a worked example

5.5.1) General

Figure (16) shows the theoretical time variations of a tracer gas (A) released in cell (1) only and connected by inter-cell airflows to cell (2) and cell (3). The data is derived from the fundamental tracer equations

(5.2.1) for known airflows, cell air change rates and initial tracer gas concentrations. The data points scattered around the theoretical curve shapes for C_{A1}, C_{A2} and C_{A3} are the result of imposing a random measurement error of $\pm 5\%$ on each data point. Using this data and similar data created for tracer gases (B) figure (17 and (C) Figure (18) (released in cells(2) and (3) respectively) we can quantify the resulting errors on calculated airflows using the method outlined in section (5.3.).

5.5.2) Calculating intercell airflows and airchange rates

The first requirement is to estimate approximate values for N_1, N_2 and N_3. Using the first six concentration, time points of C_{A1}, C_{B2} and C_{C3} data, "first order" estimates of N_1', N_2', and N_3' are obtained by taking Ln C (t) versus time plots, the gradient of the straight line which best fits the data points is an estimate of cell air change rate.

Appendix(E) should be consulted in the following discussion

Using the first 10 tracer gas concentration data points for tracer gases (A), (B) and (C) enables equations (5.3.10) -(5.3.18) to be solved for the unknown inter-cell airflows and cell air change rates.

Equations (5.3.10)-(5.3.12) become for N_1, Q_{21} and Q_{31} respectively

$$N_1 = 2.90 + 0.0028\ Q_{21} + 0.00076\ Q_{31} \quad (5.5.1)$$

$$Q_{21} = 9.63\ N_1 + 105 - 0.29\ Q_{31} \quad (5.5.2)$$

$$Q_{31} = 39.7\ N_1 - 36.3 - 0.14\ Q_{21} \quad (5.5.3)$$

Iterating these equations using the Gauss-Seidel technique gives:

N_1 = 3.25 air changes/hour

Q_{21} = 113 m^3/hour

Q_{31} = 77 m^3/hour

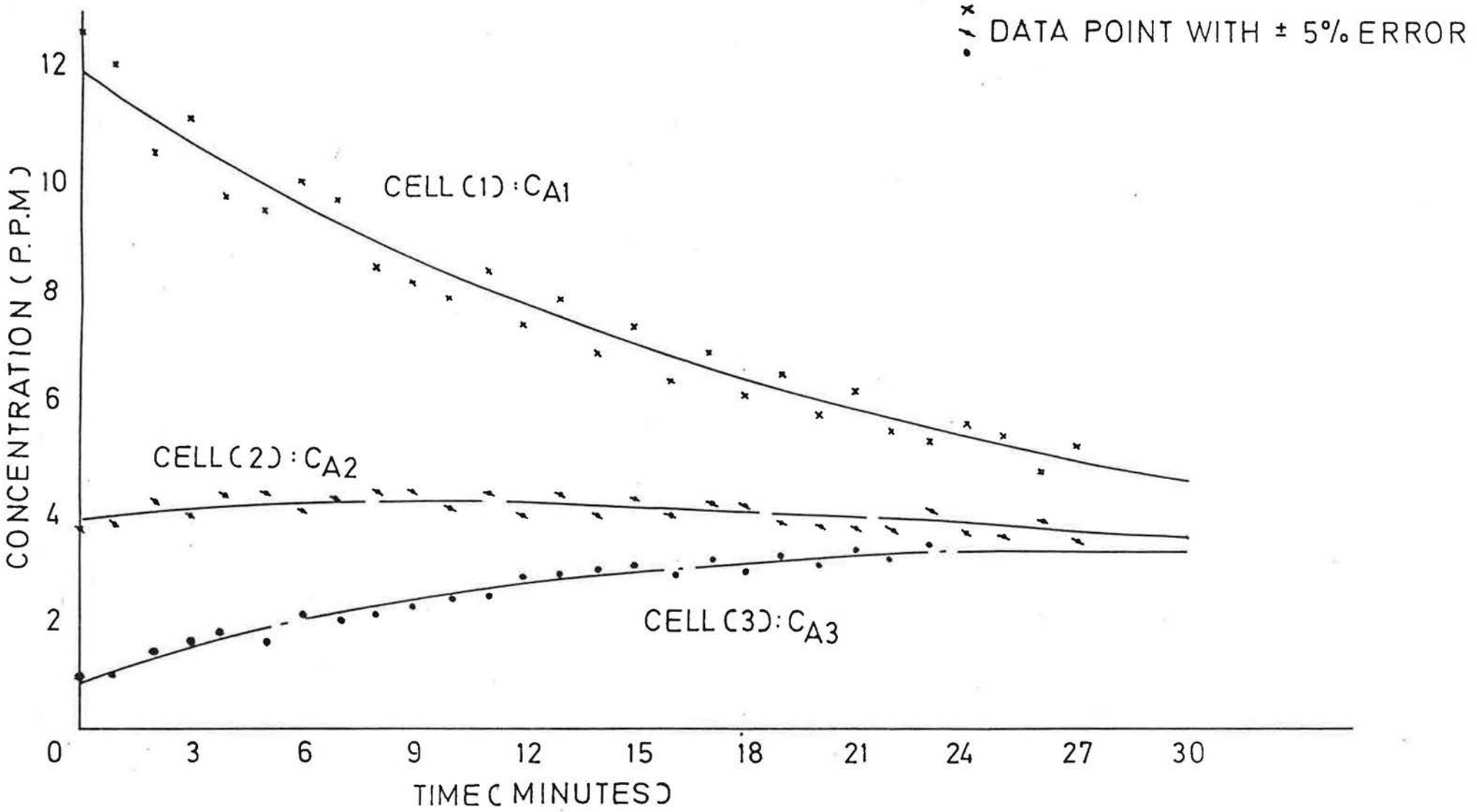

FIGURE 16 CA (t) VARYING WITH TIME FOR KNOWN AIRFLOWS : THREE CELL CASE

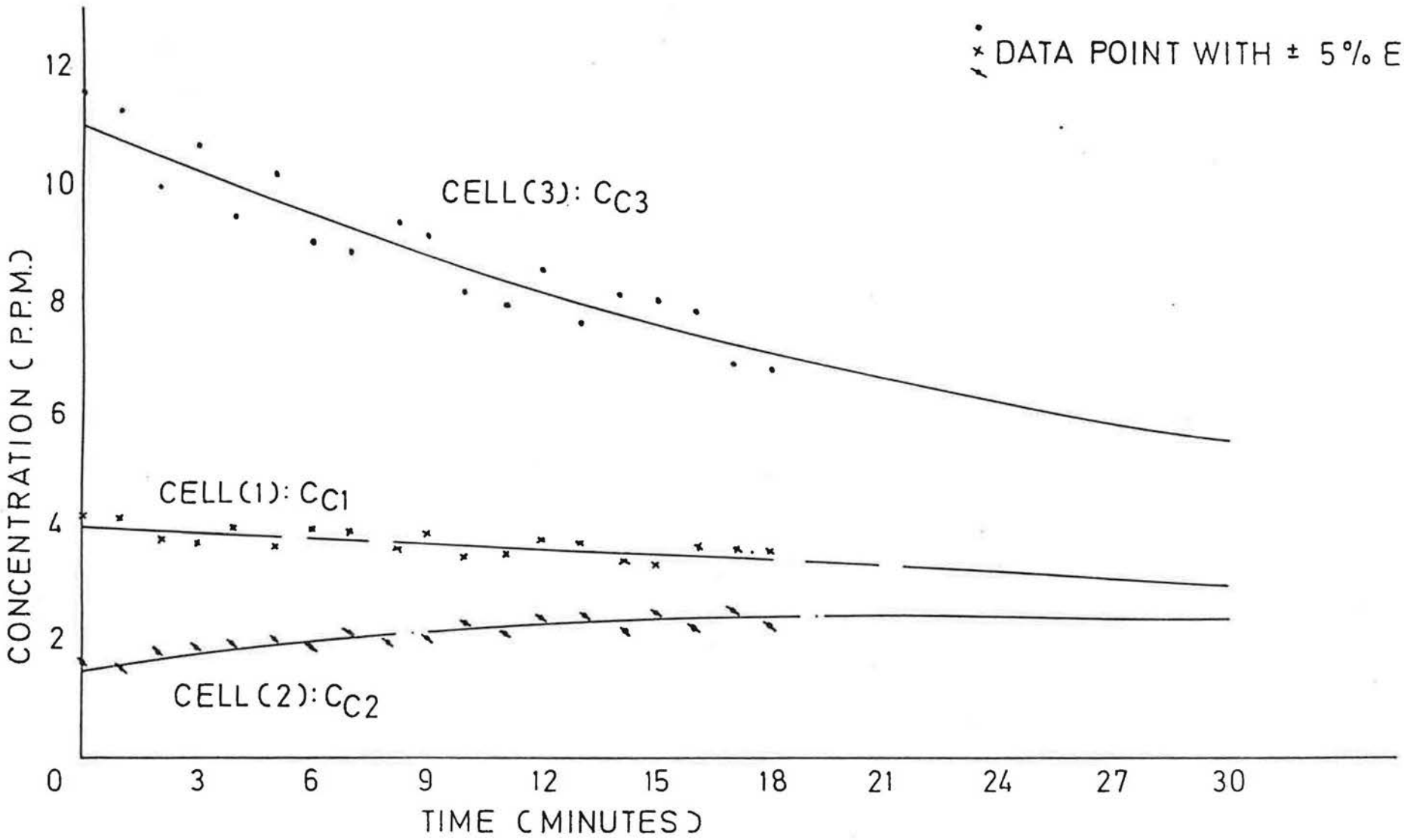

FIGURE 18 CC(t) VARYING WITH TIME FOR KNOWN AIRFLOWS: THREE CELL CASE

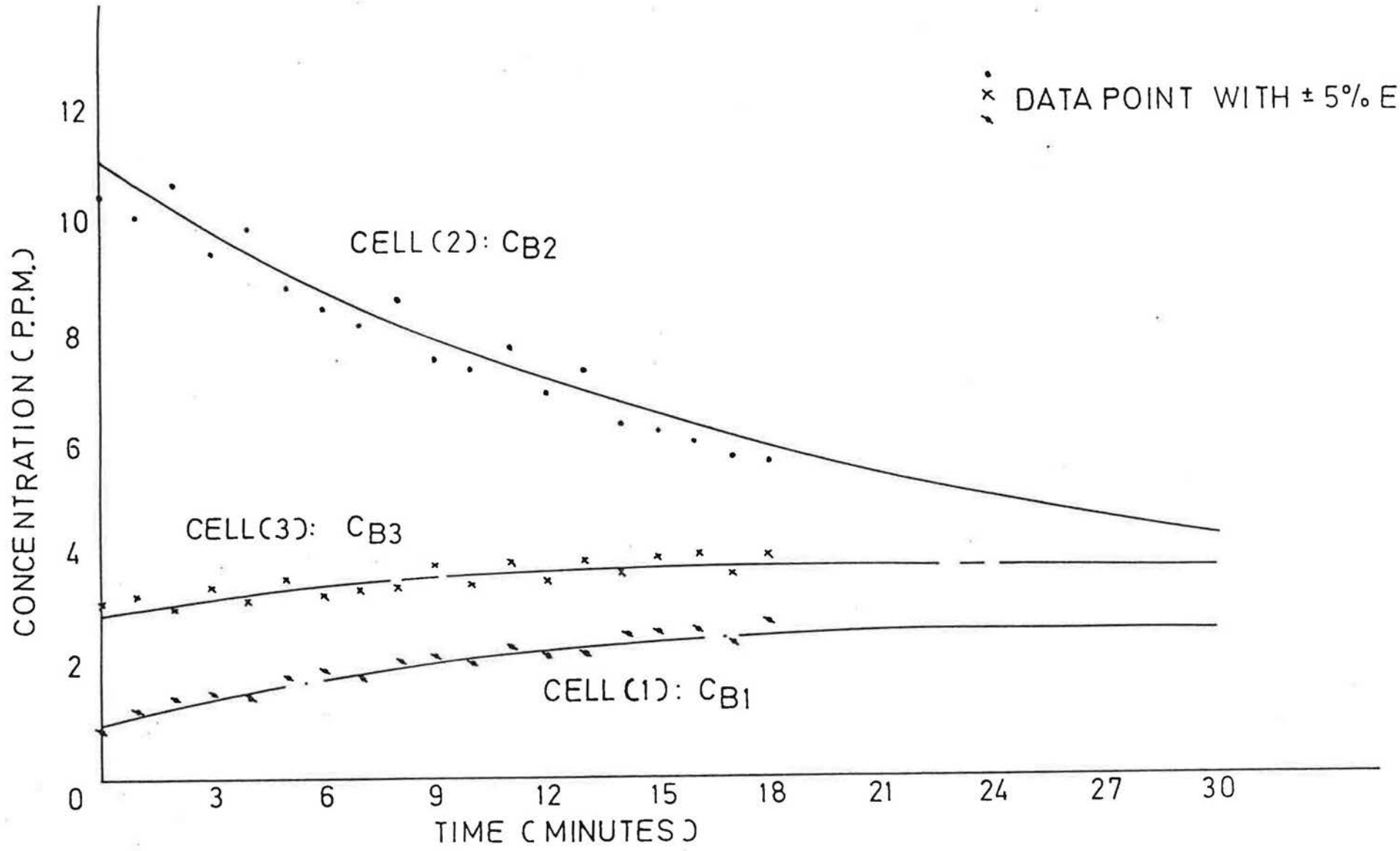

FIGURE 17 CB (t) VARYING WITH TIME FOR KNOWN AIRFLOWS: THREE CELL CASE

Solving equations (5.3.13)-(5.3.15) for N_2, Q_{21} and Q_{32} gives:

$$N_2 = 1.87 + 0.000785\ Q_{12} + 0.00276\ Q_{32} \qquad (5.5.4)$$

$$Q_{12} = 37.16 + 34.92\ N_2 - 0.088\ Q_{32} \qquad (5.5.5)$$

$$Q_{32} = 46.27 - 0.34\ Q_{12} + 14.84\ N_2 \qquad (5.5.6)$$

Iterating these equations gives:

N_2 = 2.07 changes/hour

Q_{12} = 106 m^3/hour

Q_{32} = 42 m^3/hr

Solving equations (5.3.16)-(5.3.18) for N_3, Q_{13} and Q_{23} gives:

$$N_3 = 1.95 + 0.0031Q_{13} + 0.00128Q_{23} \qquad (5.5.7)$$

$$Q_{13} = 9.68N_3 + 89.7 - 0.33\ Q_{23} \qquad (5.5.8)$$

$$Q_{23} = 32N_3 + 42.24 - 0.083\ Q_{13} \qquad (5.5.9)$$

Iterating these equations gives:

N_3 = 2.34 air changes/hour

Q_{13} = 75 m^3/hour

Q_{23} = 111 n^3/hour

The calculated values of inter-cell airflows and cell air change rates are used in equations (5.2.2) -(5.2.10) to calculated theoretical time variations in tracer gas concentrations. Figures (19), (20) and (21) shows a comparison between the observed values of tracer gas concentration and the curves resulting from the solution of equations (5.2.2) - (5.2.10) using the calculated airflows found from site data.

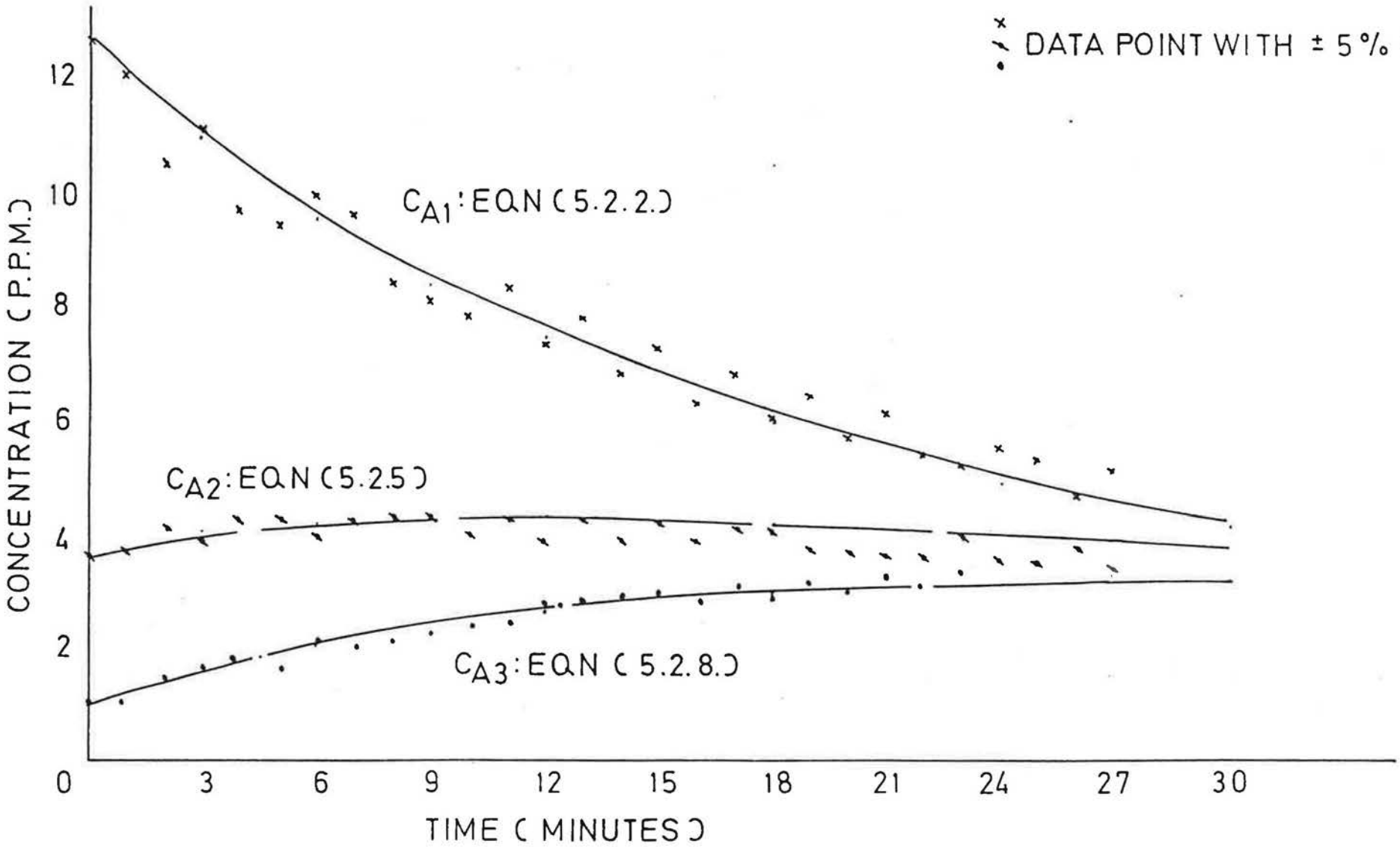

FIGURE 19 CA(t) VARYING WITH TIME FOR CALCULATED AIRFLOWS : THREE CELL CASE

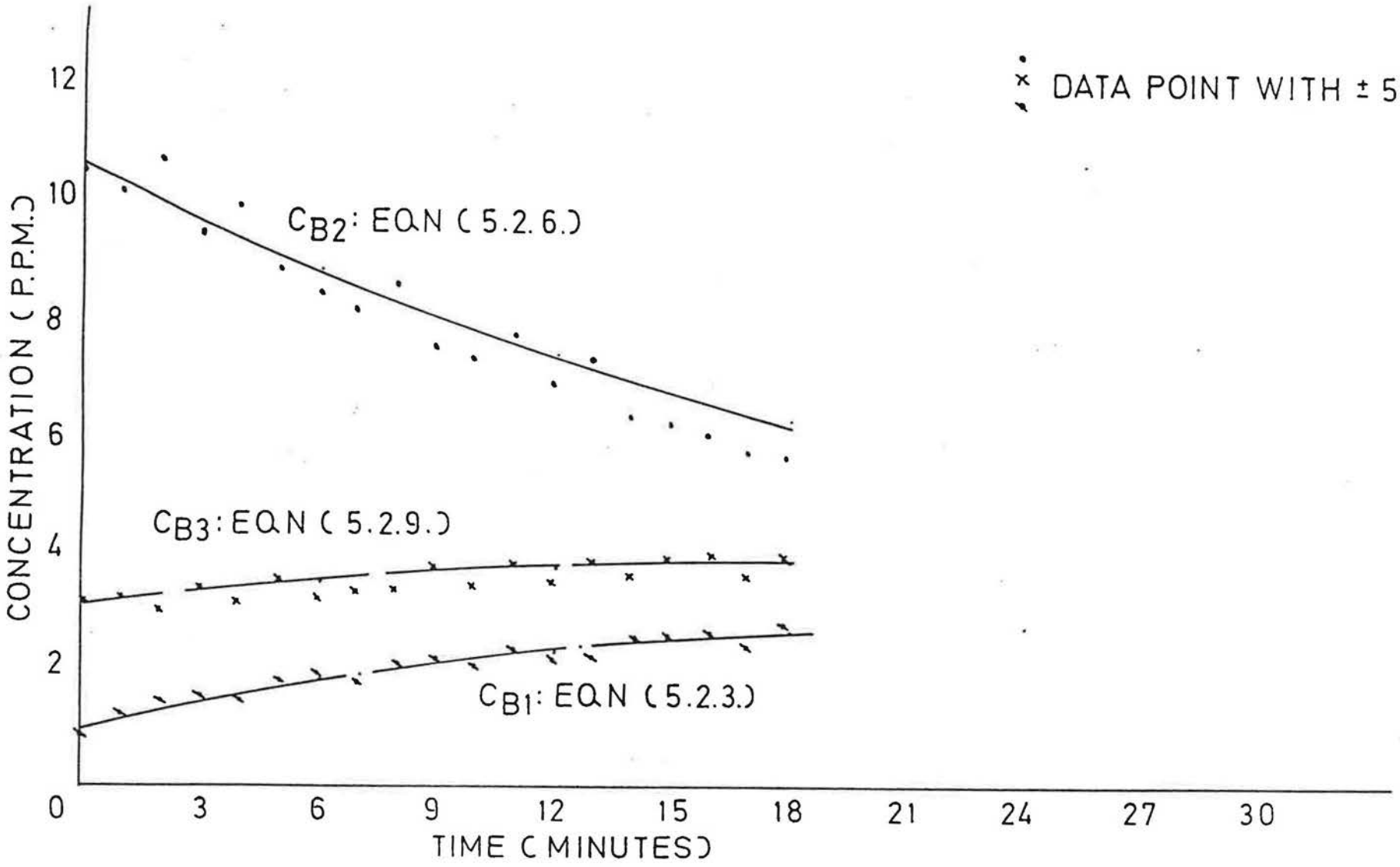

FIGURE 20 CB(t) VARYING WITH TIME FOR CALCULATED AIRFLOWS : THREE CELL CASE

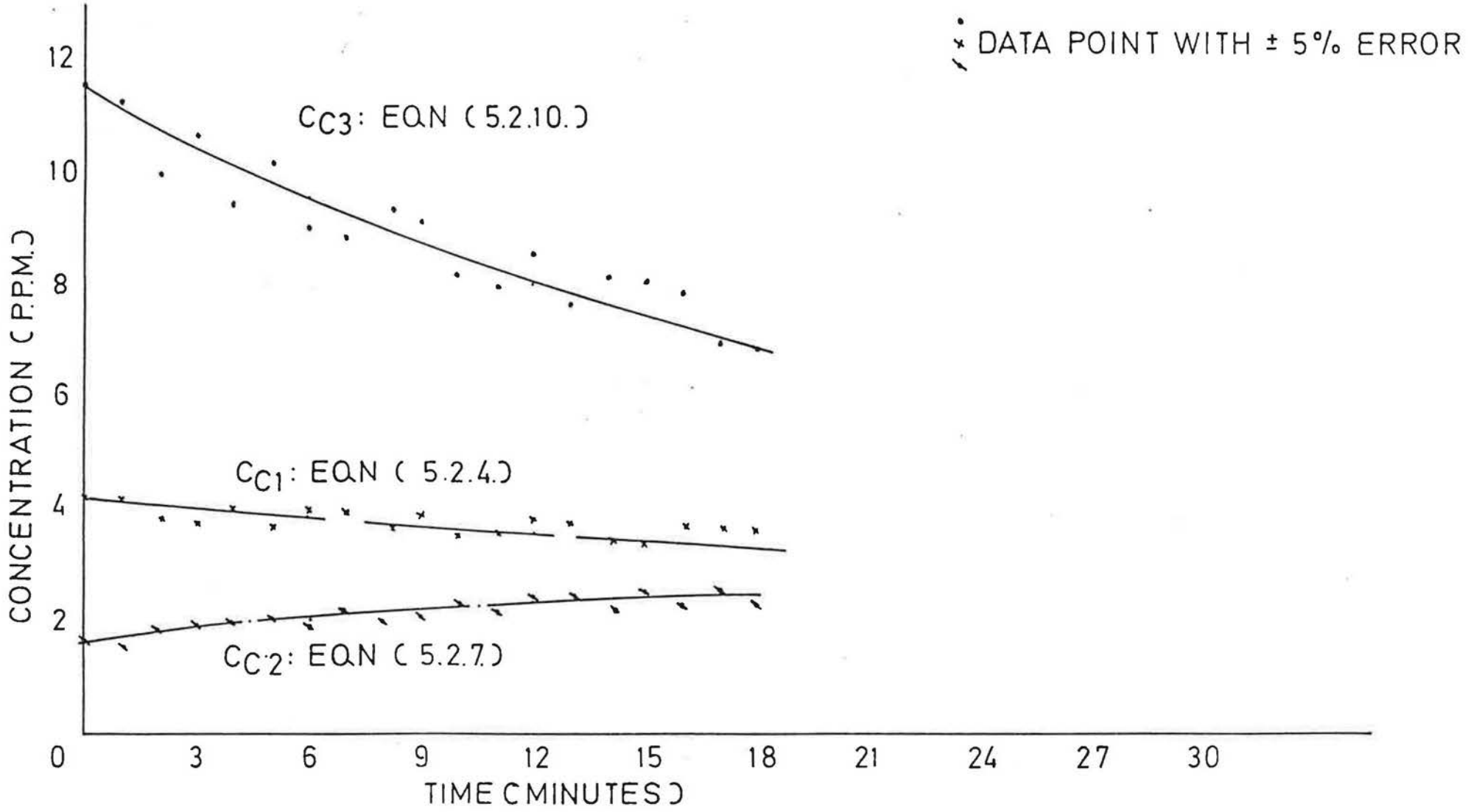

FIGURE 21 CC(t) VARYING WITH TIME FOR CALCULATED AIRFLOWS: THREE CELL CASE

5.6) Estimating Errors in calculated airflows using "real" data

The following analysis is concerned with "real" data where the absolute values of initial tracer gas concentrations and inter-cell airflows are unknown.

The for worked example given, the major sources of error in the calculated value of cell (1) air change rate N_1, are:

$$(\Delta N_1)^2 = \left|\frac{\partial N_1}{\partial CO_{A1}} CO_{A1}\right|^2 + \left|\frac{\partial N_1}{\partial CO_{A2}} \Delta CO_{A2}\right|^2 + \left|\frac{\partial N_1}{\partial CO_{A3}} \Delta CO_{A3}\right|^2 + \left|\frac{\partial N_1}{\partial \tilde{C}_{A1}} \Delta \tilde{C}_{A1}\right|^2 + \left|\frac{\partial N_1}{\partial A} \Delta A\right|^2 \qquad (5.6.1)$$

Similarly for Q_{21}, the major source of errors are:

$$(\Delta Q_{21})^2 = \left|\frac{\partial Q_{21}}{\partial CO_{B1}} \Delta CO_{B1}\right|^2 + \left|\frac{\partial Q_{21}}{\partial CO_{B2}} \Delta CO_{B2}\right|^2 + \left|\frac{\partial Q_{21}}{\partial CO_{B3}} \Delta CO_{B3}\right|^2 + \left|\frac{\partial Q_{21}}{\partial \tilde{C}_{B1}} \Delta \tilde{C}_{B1}\right|^2 + \left|\frac{\partial Q_{21}}{\partial N_1} N_1\right|^2$$

$$+ \left|\frac{\partial Q_{21}}{\partial A} \Delta A\right|^2 \qquad (5.6.2)$$

and for Q_{31} the major source of errors are:

$$(\Delta Q_{31})^2 = \left|\frac{\partial Q_{31}}{\partial CO_{C1}} \Delta CO_{C1}\right|^2 + \left|\frac{\partial Q_{31}}{\partial CO_{C2}} \Delta CO_{C2}\right|^2 + \left|\frac{\partial Q_{31}}{\partial CO_{C3}} \Delta CO_{C3}\right|^2 + \left|\frac{\partial Q_{31}}{\partial \tilde{C}_{C1}} \Delta \tilde{C}_{C1}\right|^2 +$$

$$\left|\frac{\partial Q_{31}}{\partial N_1} \Delta N_1\right|^2 + \left|\frac{\partial Q_{31}}{\partial Q_{21}} \Delta Q_{21}\right|^2 + \left|\frac{\partial Q_{31}}{\partial A} \Delta A\right|^2 \qquad (5.6.3)$$

Considering tracer gas (A),

when site data is being analysed, estimating CO_{A1}, CO_{A2}, CO_{A3} is difficult because the "real" value of initial tracer gas concentrations are unknown.

Taking the uncertainty in CO_{A1}, i.e. ΔCO_{A1}, let us estimate this error from

$$\Delta CO_{A1} = \frac{\sum_{1}^{P} \left| C_{A1}(s) - C_{A1}(c) \right|}{P} \qquad (5.6.4)$$

where $C_{A1}(s)$ is the measured value of C_{A1} concentration at time (t)

$C_{A1}(c)$ is the calculated value of C_{A1} concentration at time (t)

P is the total number of points considered.

Similarly the uncertainties in CO_{A2} and CO_{A3} may also be estimated.

To estimate the uncertainty in C_{A1} at time (t) let

$$\Delta \tilde{C}_{A1}(t) = \left| \tilde{C}_{A1(t)(s)} - C_{A1(t)}(c) \right| \qquad (5.6.5)$$

where $\tilde{C}_{A1(t)(s)}$ is found from numerical integration of site data.

$C_{A1(t)}(c)$ is calculated from the fundamental tracer equations using calculated airflows derived from site data.

The uncertainty in A, the maclaurin expansion can be estimated from

$$\Delta A = \left| A - \frac{(1 - e^{-N_1 t})}{N_1} \right| \qquad (5.6.6)$$

where A is estimated from $(-t + \frac{N_1' t^2}{2!} - \frac{N_1'^2 t^3}{3!} + \frac{N_1'^3 t^4}{4!} - \frac{N_1'^4 t^5}{5!})$ $(x - 1)$

N_1' is the "first order" estimate of cell (1) airchange rate

N_1 is the calculated value of cell (1) airchange rate found from site data

The uncertainties in tracer gas (B) and tracer gas (C) concentrations can be estimated in a similar manner together with the maclaurin series approximation for (B) and (E).

Using the data given in the 3 cell worked example let us estimate the errors in the calculated airflows given in section (5.5).

Let us initially consider the error in N_1, referring to equation (5.6.1)

$$(\Delta N_1)^2 = \left|\frac{\partial N_1}{\partial CO_{A1}} \Delta CO_{A1}\right|^2 + \left|\frac{\partial N_1}{\partial CO_{A2}} \Delta CO_{A2}\right|^2 + \left|\frac{\partial N_1}{\partial CO_{A3}} \Delta CO_{A3}\right|^2 + \left|\frac{\partial N_1}{\partial C_{A1}} \Delta C_{A1}\right|^2 + \left|\frac{\partial N_1}{\partial A} \Delta A\right|^2$$

The partial derivates can be calculated from equations (5.4.6) - (5.4.10), the calculations are shown in Appendix (E).

The calculated value for $\Delta N_1 = \pm 0.28$ air changes/hour.

From equation (5.6.2) the uncertainty in Q_{21} is calculated in Appendix (E) as $\Delta Q_{21} = \pm 9$ m^3/hour

Similarly ΔQ_{31} is $= \pm 20$ m^3/hour.

The error estimates for calculated airflows in the 3-cell worked example are shown in Appendix (E).

The calculated values of inter-cell airflows and cell air change rates with their error bounds are summarized below:

N_1 = 3.25 $\pm$ 0.28 air changes/hour

N_2 = 2.07 $\pm$ 0.37 " " "

N_3 = 2.34 $\pm$ 0.35 " " "

Q_{12} = 106 $\pm$ 22 m^3/hour $\quad$ Q_{32} = 42 $\pm$ 11 m^3/hour

Q_{21} = 113 $\pm$ 9 m^3/hour $\quad$ Q_{13} = 75 $\pm$ 9m^3/hour

Q_{31} = 77 $\pm$ 20 m^3/hour $\quad$ Q_{23} = 111 $\pm$ 20 m^3/hour

The error bounds calculated from the preceeding equations suggest that a random $\pm$5%error on individual site data creates a $\pm$ 8% to $\pm$ 25 error in calculated airflows derived from such data.

Unlike "Real" site data where the exact value of inter-cell airflows are unknown, the 3 cell worked example enables comparison of calculated error bounds and actual error bounds. The calculated error bands found using equations (5.4.1) - (5.4.117) suggest errors of $\pm$ 8% to $\pm$ 26% on calculated airflows and cell air change rates, which compares quite well with the known errors of 6% to 20%

The use of a 3 cell worked example shows the ability of the analysis method in coping with random measurement errors. If the comparison between site data and theoretical tracer concentration curves shows a poor goodness-of-fit or calculated error bounds are unacceptably large,

the method of analysis could, of course, be re-applied by analysing a different part of the tracer concentration data obtained from site measurement.

The basic principle which must be applied with this method of analysis is that the tracer concentration, time histories under measurement must be obtained within 30 minutes of the commencement of any test run.

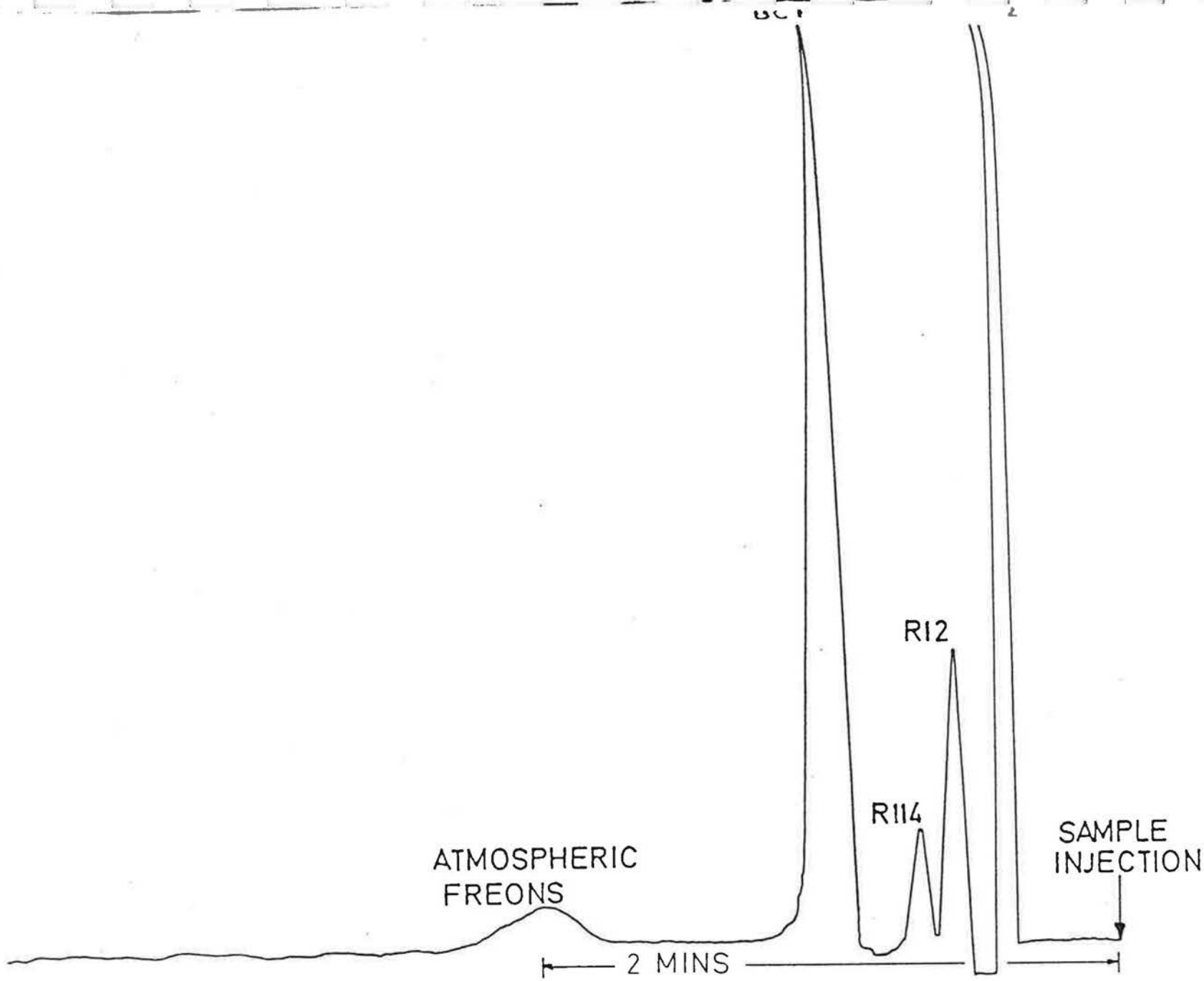

FIGURE 24 TYPICAL OUTPUT FROM ELECTRON CAPTURE DETECTOR

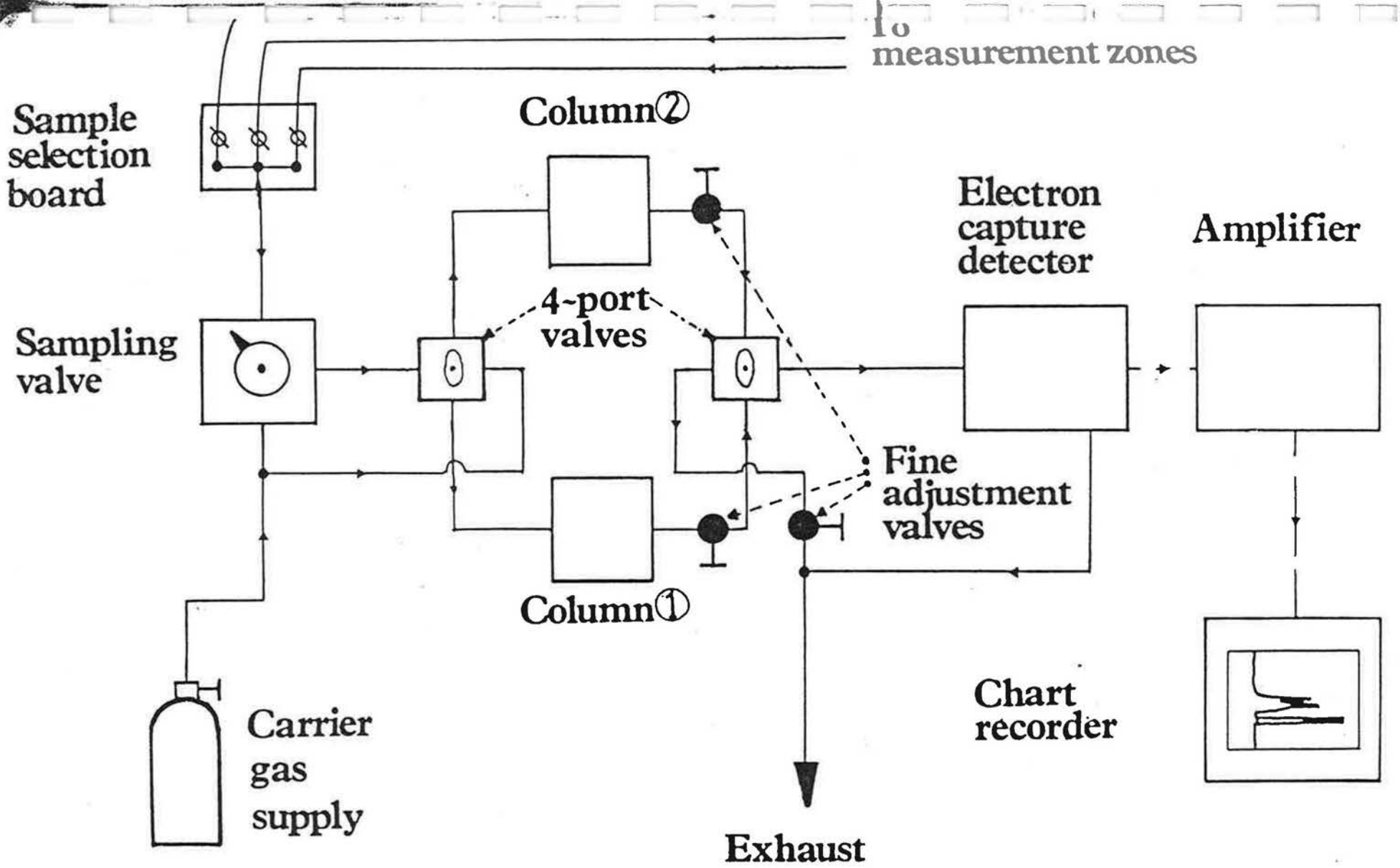

FIGURE 25 GAS CHROMATOGRAPHY USING PARALLEL COLUMNS

6.4) Optimisation of equipment using several tracer gases

Work carried out by Clemons and Altshuller [32] gives a guide to the electron absorbing tracer gases which are suitable for use with an electron capture detector. A particularly suitable family of non-toxic gases are Freons, table (6.1) shows a summary of these gases.

Laboratory experiments were carried out using eight of the nine freons given in table (6.1); Freon C318 is no longer manufactured. Of the remaining eight gases, three were found to be relatively insensitive to measurement using electron capture detection; Freon 115, Freon 22 and Freon 13. The remaining five gases are highly electron capturing and are separable using a variety of different chromatographic separating column packings.

When a single pulse of tracer gas is used to detect intercell airflows and cell air change rates, the most important consideration for the concentration measuring system used is the time interval between sampling consecutive air tracer gas concentration points. To achieve such rapid sampling of data, the delay time required for the slowest tracer gas to be separated by the column, directly influences the sampling interval between data points which can be used.

The time taken for a tracer gas to be separated in a chromatographic separation column is dependant on three factors:

Chapter 6: EXPERIMENTAL TECHNIQUE FOR MEASURING MULTIPLE TRACER GAS CONCENTRATIONS.

6.1) General

There are three existing measuring systems which are capable of measuring multiple tracer gas concentrations in air.

The first system developed by Perera [25] at the B.R.E measures continuously the concentrations of carbon dioxide, sulphurhexafluoride and nitrous oxide using a multi-cell infra red gas analyser.

Prior et al [19] uses gas chromatography coupled with a flame ionization detector to measure the concentrations of four perfluoro hoxanes and decalins, these chemicals being liquids at room temperature.

The third measuring system also uses gas chromatography coupledwith an electron capture detector. The original system was used by Saltzman et al [30] in meteorological tracer experiments in the mid-nineteen sixties. Foord and Lidwell [31] later used a portable electron capture detector to measureair movements in hospitals using three hydrofluorocarbon tracer gases, these are Freon 12 (dichorodifluoromethane), Freon 114 (dichlorotetrafluoroethane) and B.C.F.(bromochlorodifluoromethane) I'Anson et al [21] modified this system and applied it to the measurement of airflows in dwellings; Extensive improvements have been carried out by the author and are described here.

The time interval between consecutive samples of air-tracer gas mixtures have been reduced from two minutes to thirty seconds. This seventy five percent reduction in sampling interval is achieved by use of parallel gas chromatographic separation columns. Rapid sampling of tracer gas concentrations improves the versatility of the technique in measuring a wide range of airflows of variable size.

Existing Measurment systems

The major advantages of the multi-cell infra red analyser used by Perera, is its ability to measure the concentrations of up to nine different tracer gases in air. Further, the continuous output from each cell means a continuous record of tracer gas concentration histories are used to estimate air movements. Consequently, any variations in tracer concentrations which could effect the calculated airflows obtained from such data can be easily seen.

The use of a multi-cell, multi-component infra-red analyser has two basic disadvantages when used as a site tool. Firstly the physical size and cost of such an instrument makes it difficult to transport and expensive to replace if damaged. A multi-cell analyser is primarily designed for laboratory use. Secondly calibration of a multi-cell analyser so that each cell responds identically to known tracer gas concentrations is very difficult to achieve in practice.

The system adopted by Prior et al is shown in figure (22). Four perfluoro hexanes and decalin liquids are used as tracers; an electrically heated plate is required to evaporate these liquids. Once evaporation

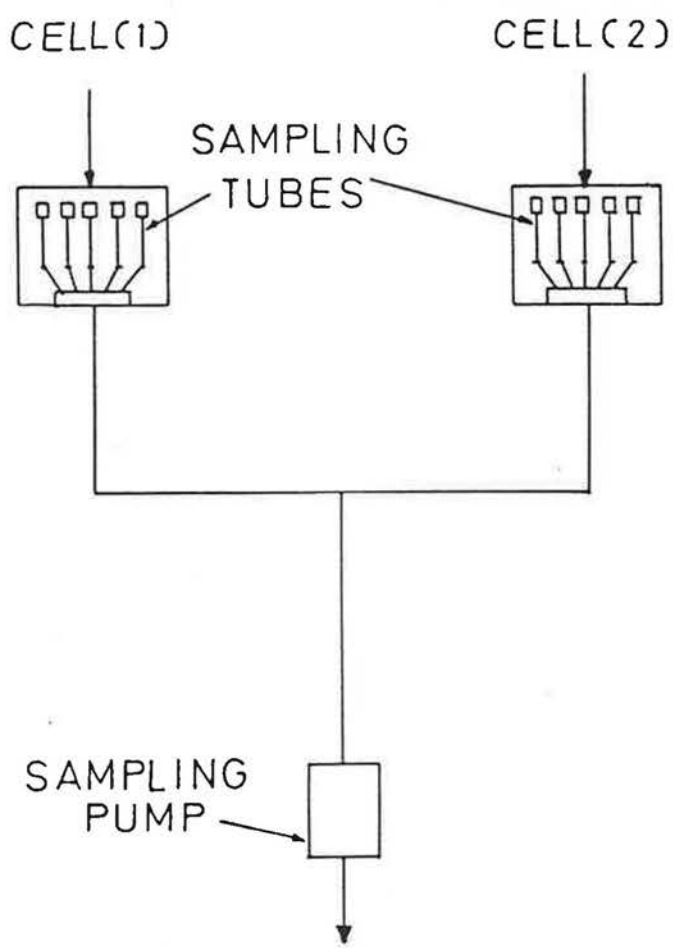

(SITE USAGE)

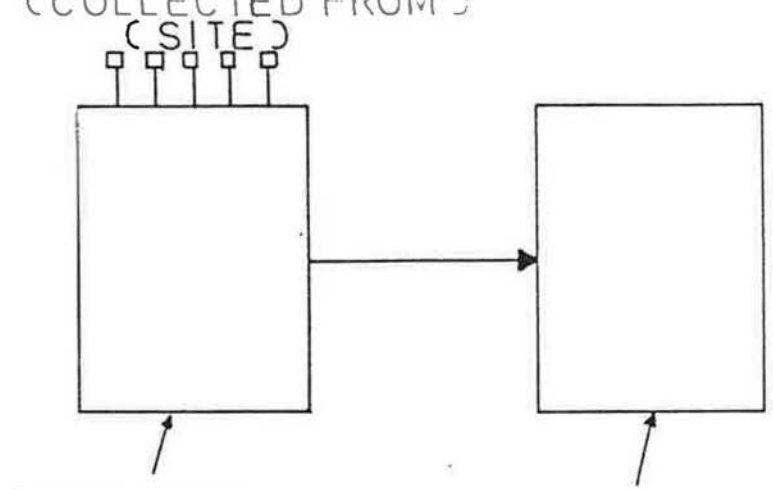

(LABORATORY BASED)

FIGURE 22 SCHEMATIC LAYOUT OF PRIOR'S EQUIPMENT

has taken place and mixing of the tracers in air is complete, the tracer gas concentrations in air are monitored by drawing a fixed volume of air through an absorbent tube for a period of approximately 5 minutes. Use of a sampling pump and timer enables a fixed number of such tubes to be sampled at a pre-determined time after commencement of a test run. This system does not require the extensive air sampling tubes that other tracer gas system require. The exposed tubes are then collected and transported back to the laboratory for analysis using a thermal desorbtion unit, which is connected in series with the gas chromatographic separation column and flame ionization detector.

Consequently, actual tracer gas concentrations during a test run are unknown at the time of the test, therefore if too great a volume of tracer were released and flame ionization detector saturation occurred insufficient numbers of usable data points could invalidate the measurements carried out.

The third measurement system used by I'Anson et al is shown in figure (23). A portable gas chromatograph fitted with an electron capture detector is used to measure the concentration of three fluorinated gases. The instrument is simple to use, portable and relatively inexpensive to buy. However, the portable gas chromatograph used operates at ambient temperature and any random variations in ambient conditions will affect the instrument's stability. A further consequence of operating at ambient temperature is the throughput time required between consecutive air tracer gas samples. For the three freon tracer gases used the minimum time between samples is approximately 2 minutes.

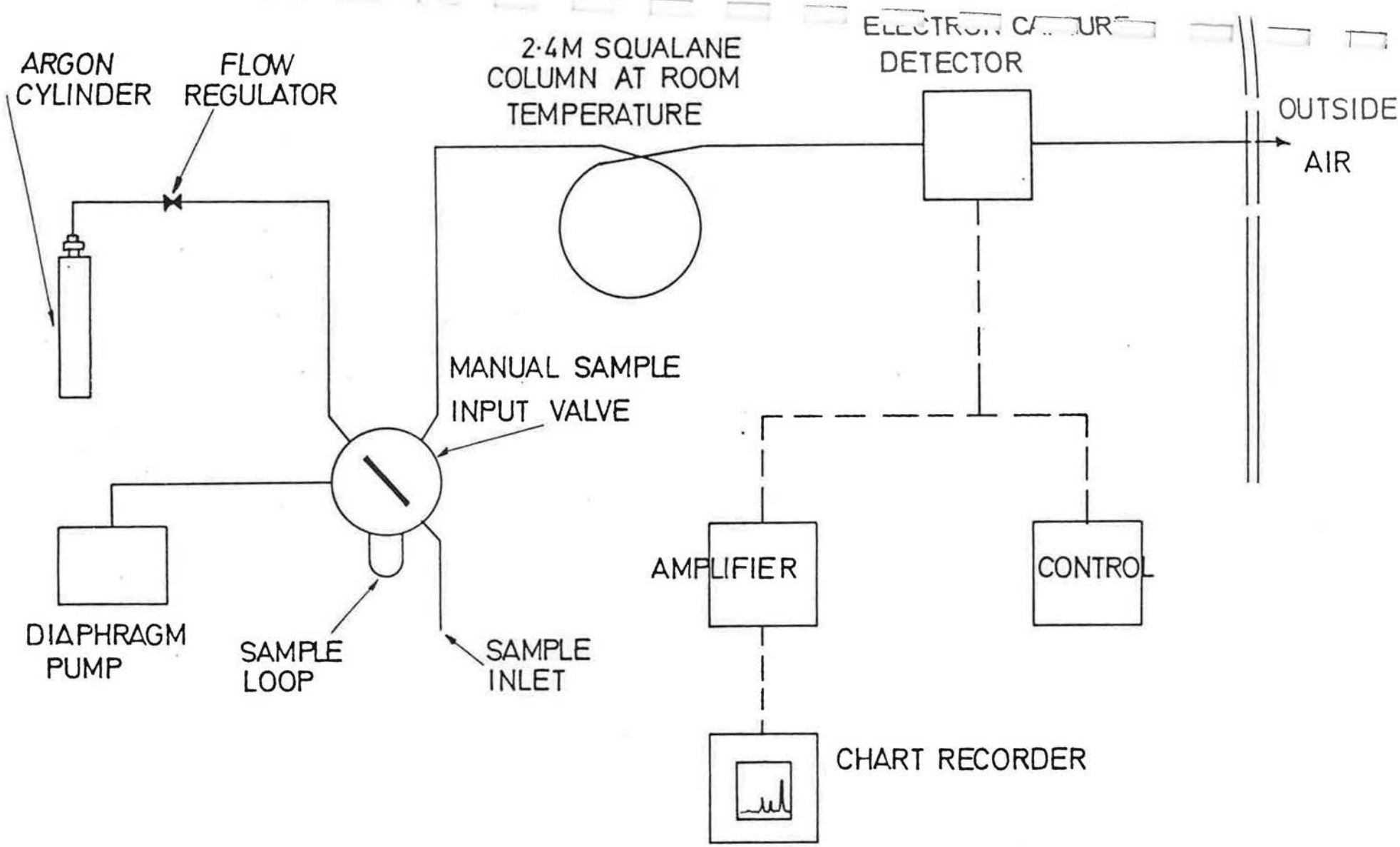

FIGURE 23 SCHEMATIC LAYOUT OF IANSONS EQUIPMENT

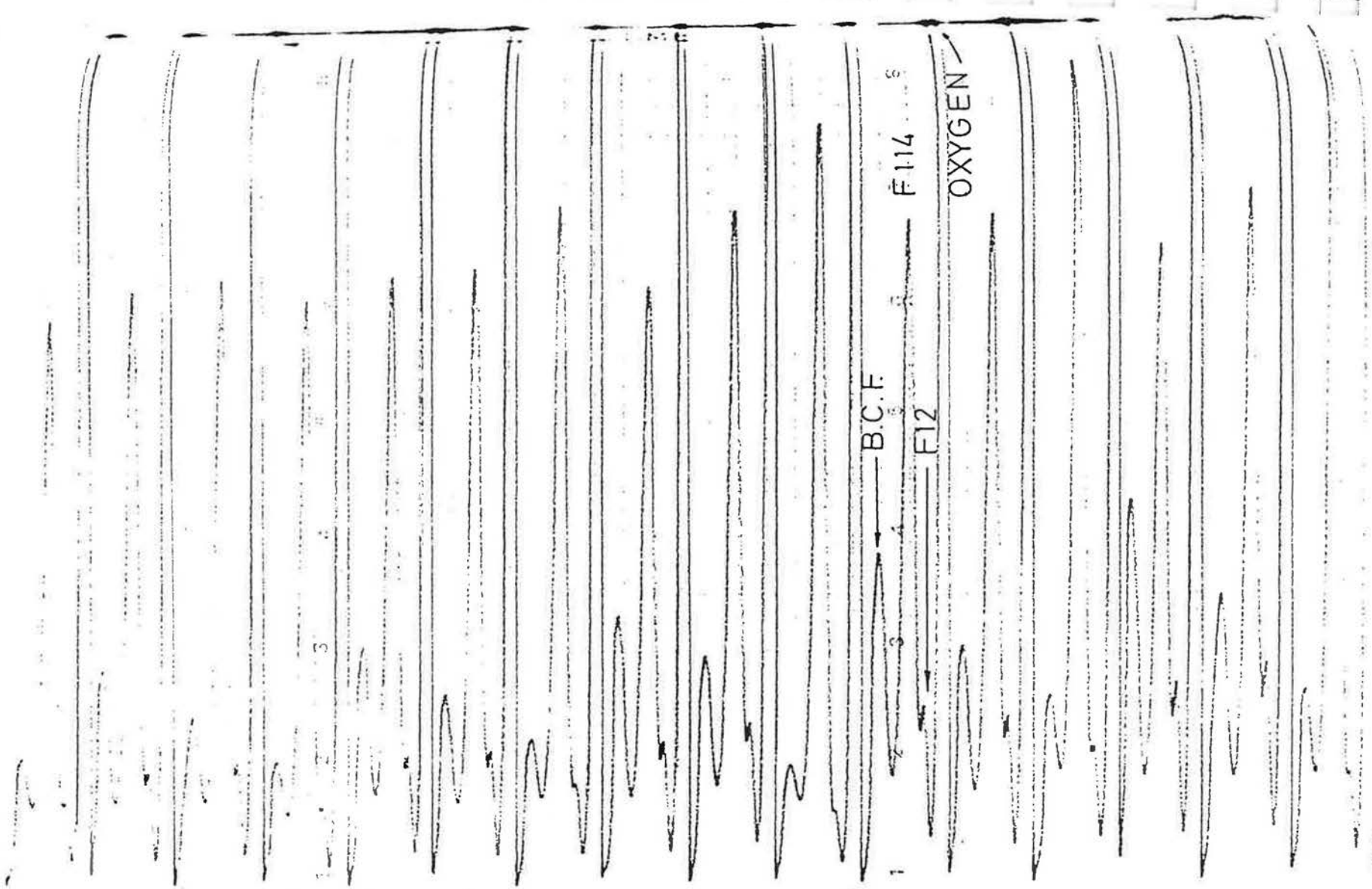

FIGURE 28 OUTPUT FROM ELECTRON CAPTURE DETECTOR (30 SECOND SAMPLING)

The experimental technique adopted by I'Anson has been unproved and extended to overcome these difficulties.

.3) Gas chromatography using heating parallel columns

The portable gas chromatograph* used by I'Anson comprises of an internal diaphragm pump to draw air from the cell under test. A six part sampling valve (Manually operated) isolates a fixed volume (0.5cc) of the air-tracer gas mixture. The sample is then carried through a sing le squalane chromatographic separating column using argon as a carrier gas. In the column each gas is absorbed and desorbed at different rates by the squalane, causing the component gases to arrive at the other end of the column at different times. The separated gas mixture passes through the electron capture detector, where each component gas is detected in turn. The electron capture detector comprises of two oppositely charged electric plates and a radioactive β particle source (10 Mc). The β source causes an excess of negative ions in the detector, which are collected at the positively charged plate causing a current flow (standing current). When an electron absorbing gas passes through the detector cell it captures a quantity of electrons. The standing current drops, this drop in standing current can be measured and related to the concentration of this gas. Once clear of the detector cell this electron absorbing gas is exhausted to atmosphere, the inert argon carrier gas continuously flows through the column and detector, to keep them free from oxygen and other electron-capturing gases, until the next sample is injected.

* Analytical Instruments Ltd. Model 505.

A typical trace of chromatographic output is shown in figure (24). Two points are of great interest, the 30 second time delay, after sample injection, before the emergence of the oxygen peak and the presence of a small peak 2 minutes after sample injection.

Using two parallel separation columns instead of one enables the 30 second delay time between sample injection and emergence of the oxygen peak to be effectively reduced to zero. This is achieved by injecting air tracer gas samples through each column with a 30 second time delay between each injection. A schematic layout of the modified system is shown in figure (25), parallel column operation is achieved using two zero-dead volume 4 port valves. Valve (1) determines column selection and valve (2) diverts the separated air-tracer gas mixture either to the detector cell or exhausting to atmosphere.

The fine adjustment valves located after each column are used to equalise the pressure in both legs of the system. Electron capture detectors are sensitive to pressure differences between each column. A further adjustment valve is located in the exhaust line, the resistance of the detector cell to carrier gas flow is considerably higher than the resistance of the exhaust pipework.

To overcome the difficulty of atmospheric freons emerging 2 minutes after sample injection and any variations in ambient temperature affecting instrument stability (base line drift), the temperature of the two parallel columns is controlled, above ambient temperature, using an electrically heated water bath.

the emergence of Freon 12 and Freon 114 peaks is less than 4 seconc This increases the risk of losing the Freon 114 peak were high concent rations of Freon 12 are encountered. Figure (28) shows that for a three cell, three tracer gas concentration measurement system, the three tracer gases most suitable are Freon 12, Freon 114 and B.C.F. The operating conditions required are an argon carrier gas pressure of 3 bar and a column temperature of 30°C; the total throughput time from sample injection to emergence of B.C.F. peak being 60 seconds.

Using two columns of identical length and packing material, operating in parallel, enables a 30 second sampling interval to be obtained when the concentrations of three Freon tracer gases in air are being examined.

6.5) Calibration of Electron Capture Detector

The common practice in gas chromatography is to relate the area under a peak to the concentration of tracer gas being measured. However, assessment of peak areas in field measurements is time consuming, an alternative approach is to measure peak heights which are calibrated using mixtures of known concentration. The response of the electron capture detector is not linear over its full working range, to determine the instruments linear range for peak heights the following calibration procedure was adopted.

Dilutions of the three tracer gases being made in high purity argon, over water in a five litre measuring cylinder. The argon is introduced through a nylon tube, fitted in the tube is a septum port where a gas tight syringe injects a known volume of tracer gas. The mixed air-tracer gas is then drawn into the instrument using the sampling pump, several dilutions for each tracer gas were made. A schematic layout of the calibration system is shown in figure (29).

The linearity of the electron capture detector gives a ratio of approximately 100 between the highest and lowest gas concentrations which can be measured. The minimum concentrations of the three tracer gases which can be measured are approximately:

Freon 12 60 p.p. 10^{-9} parts air

Freon 114 135 pp 10^{-9} parts air

B.C.F. 0·5 pp 10^{-9} parts air.

The electron capture detector has a different sensitivity for each tracer gas, in determining inter-cell airflows from such measurements, the ratio of the tracer gas concentration to its initial concentration in each cell is important and not the absolute values of tracer gas concentration.

The procedure discussed here is based on the calibration method suggested by I'Anson et al [21].

6.6) Validation of measuring system

To evaluate the effects of systematic measurement errors using this rapid

sampling multiple tracer gas system, air movement tests were carried out using two adjacent environmental chambers see figure (30). The results of this validation work have been published [33]: air movement between the two chambers took place through two 100 mm dia holes in a partition wall which separates them. Controlling the mechanical supply and extract ductwork to each chamber enable a steady airflow from chamber (2) to chamber (1). A ducted low speed fan mounted in one of the 100mm dia holes induced air movement from chamber (1) to chamber (2). Air velocities in the supply ductwork were measured using a pitot tube and inclined "U" tube manometer. Air velocities in the openings on the partition wall were measured using a hot wire anemometer. Two of the three available tracer gases were injected manually into each chamber and initial mixing achieved using oscillating desk fans.

There were three objectives in carrying out these validation tests:

(i) Compatability of two columns

(ii) The effects of mixing dense tracer gases in air.

(iii) measurement errors of parallel column/electron capture system on two cell air movement measurements.

(i) Compatability of two columns is tested by releasing a tracer gas in a single volumne and monitoring the decay of concentration of tracer gas with time. Column compatability is attained if no significant difference between alternate samples for each column occurs. Figure (31) shows the exponential decay of tracer gas concentration using parallel columns.

(ii) The time taken for Freon 12 to mix with air in a single chamber without the aid of mixing fans is shown in figure (32). A pulse of tracer gas is released at floor level and allowed to disperse. The tracer gas concentration being monitored at low level, intermediate level (desk height) and high level in the chamber, equilibrium concentration being reached after approximately 10 minutes. Identical tests were carried out using Freons 114 and B.C.F.

A one directional airflow was induced from chamber (2) to (1) by switching off the air supply system to chamber (1). Freon 12, 114 and B.C.F. were released in chamber (2), mixed, and the growth of tracer concentration monitored at the three different levels in chamber (1). Figure (33) shows the three growth curves for Freon 12; the three estimates of air movement suggest non-uniform mixing errors of approximately $\pm$7%

(iii) To examine the effects of systematic measurement errors on inter-cell air movements by comparing calculated airflows with measured airflows under controlled environmental conditions.

The first three tests examined a one directional airflow induced from chamber (2) to chamber (1). Comparison between measured airflows and those calculated from tracer gas concentration data suggest systematic errors between 2% - 6%.

The remaining six tests examined two directional air movements between both chambers. The systematic errors found between calculated inter-cell airflows lies between 1% - 8%.

The ventilation rates of both chambers measured directly using a pitot tube in the supply air input ducts and calculated from tracer concentration data have a systematic measurement error between 4% - 10%.

To determine if any significant differences existed between the three different tracer gases used, each air movement test was carried out using different combinations of tracer gases. No significant differences between tracer gases being found.

(6.7) Experimental technique in site measurements

When a site test is performed the tracer gases are introduced into the space in one of two ways. The first being to inject the gas using a gas tight syringe, via a septum port into a polythene tube so that it can be driven into the test space using compressed air. The second method is to manually inject tracer gas directly from the cylinder in the appropriate space by briefly opening the cylinder valve.

After injection the tracer gases are mixed using oscillating desk fans (minimum two per cell). Mixing is generally found to be adequate five minutes after initial tracer gas injection. Sampling of the air tracer gas mixture is achieved by drawing air through polythene tubes (8mm O.D) from each cell under test. Each sample tube terminates in a "spider", from which three tubes are placed at different heights and locations in the cell under test. This sampling manifold is intended to lessen the effects of any concentration gradients, within a cell, which may have developed from stratification of tracer gases.

The technique described is able to measure the concentration of two tracer gases using a sample interval of 30 seconds. The minimum number of tracer gas concentration data points taken per cell is 10 No, the total test time being therefore 15 minutes (includes a 5 minute mixing period). When applied to three cell measurements, the sample interval is 30 seconds and the total test time, assuming 10 No. data points is 20 minutes (includes 5 minutes mixing period). When the required data points have been obtained, the results are fed into an Apple II/e micro-computer for analysis using the methods shown in Chapters (4) and (5). Appendix (G) has the program listings for two and three cell analysis.

Photographs of the gas chromatograph and sampling equipment are shown in figure (34).

6.8) Experimental Difficulties

The three difficulties encountered with this tracer gas measuring system are:

(i) Ensuring that two separation columns behave in identical manner.

(ii) Contamination of instrument components and pipework

(iii) Contamination of Argon carrier gas.

Considering compatability of the two columns; the column manufacturers supplied both columns from the same production batch, each pair of columns used being conditioned at the same time and generally treated

in an identical manner. Both squalane columns have to be subject to a continuous trickle of argon carrier gas when not in use. Provided the separation columns are treated in this manner, the maximum difference in response between any pair of columns used is generally less than 1% of the available standing current.

(ii) contamination of instrument components and pipework is easily overcome by a policy of thorough cleaning of all pipework and fittings. Carrier gas pressure regulators and pipework being kept thoroughly clean at all times.

(iii) Occasional difficulties were encountered with the high purity argon supplied. Large reductions in electron capture detector standing current and random variations in baseline during tests indicating a problem. In all cases this problem occurred when the high purity argon was found to be contaminated with sulphur hexafluoride.

Table (6.1) Freons suitable for Electron Capture Detection

Gas	Formula	Boiling Point °C	Relative sensitivity to E.C.D.
B.C.F.	($CBrCLF_2$)	-3	most sensitive
Freon 11	(CCL_3F)	24	
Freon C318	($CF_2CF_2CF_2CF_2$)	-6	
Freon 13B1	($CBrF_3$)	-57.8	
Freon 12	(CF_2CL_2)	-30	
Freon 114	($CCLF_2CCLF_2$)	4	
Freon 115	($CCLF_2CF_3$)	-38	
Freon 22	(CHF_2CL)	-41	
Freon 13	($CCLF_3$)	-81.4	Least sensitive

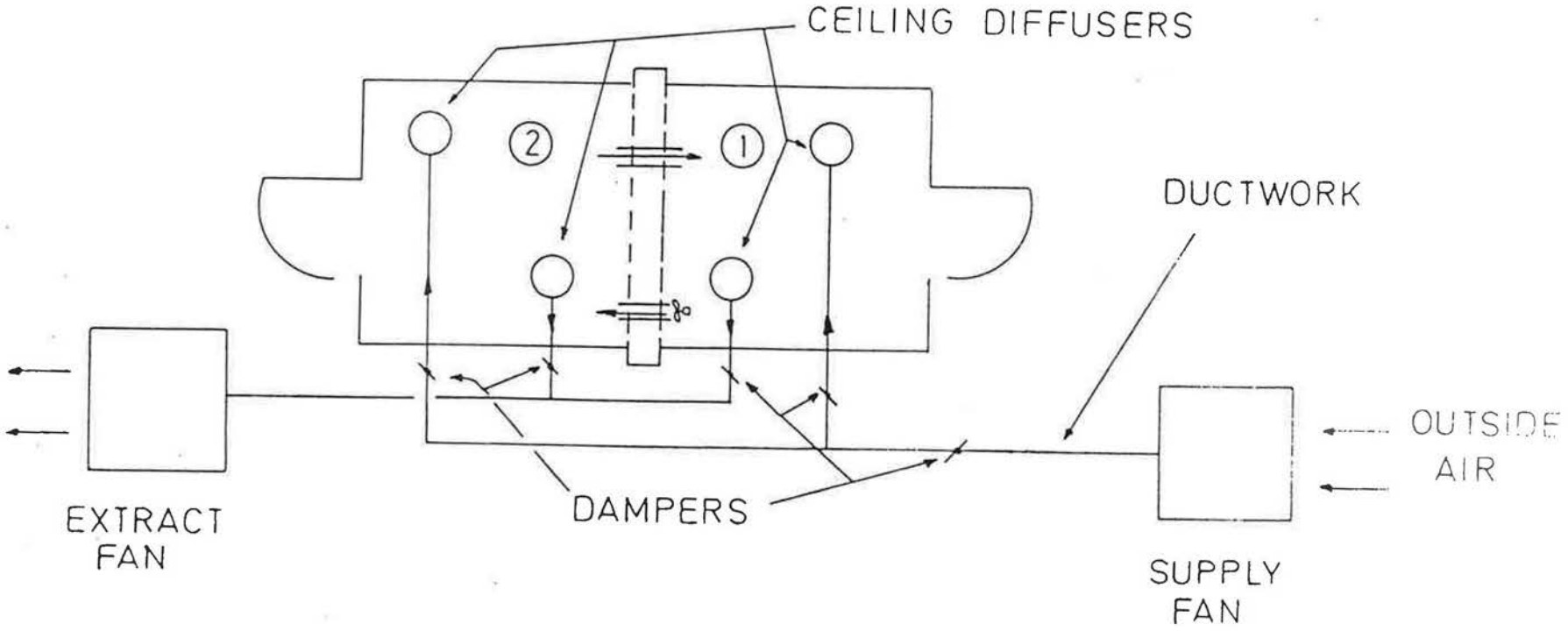

FIGURE 30 TWO CONNECTED CHAMBERS : 2 WAY AIRFLOW VALIDATION

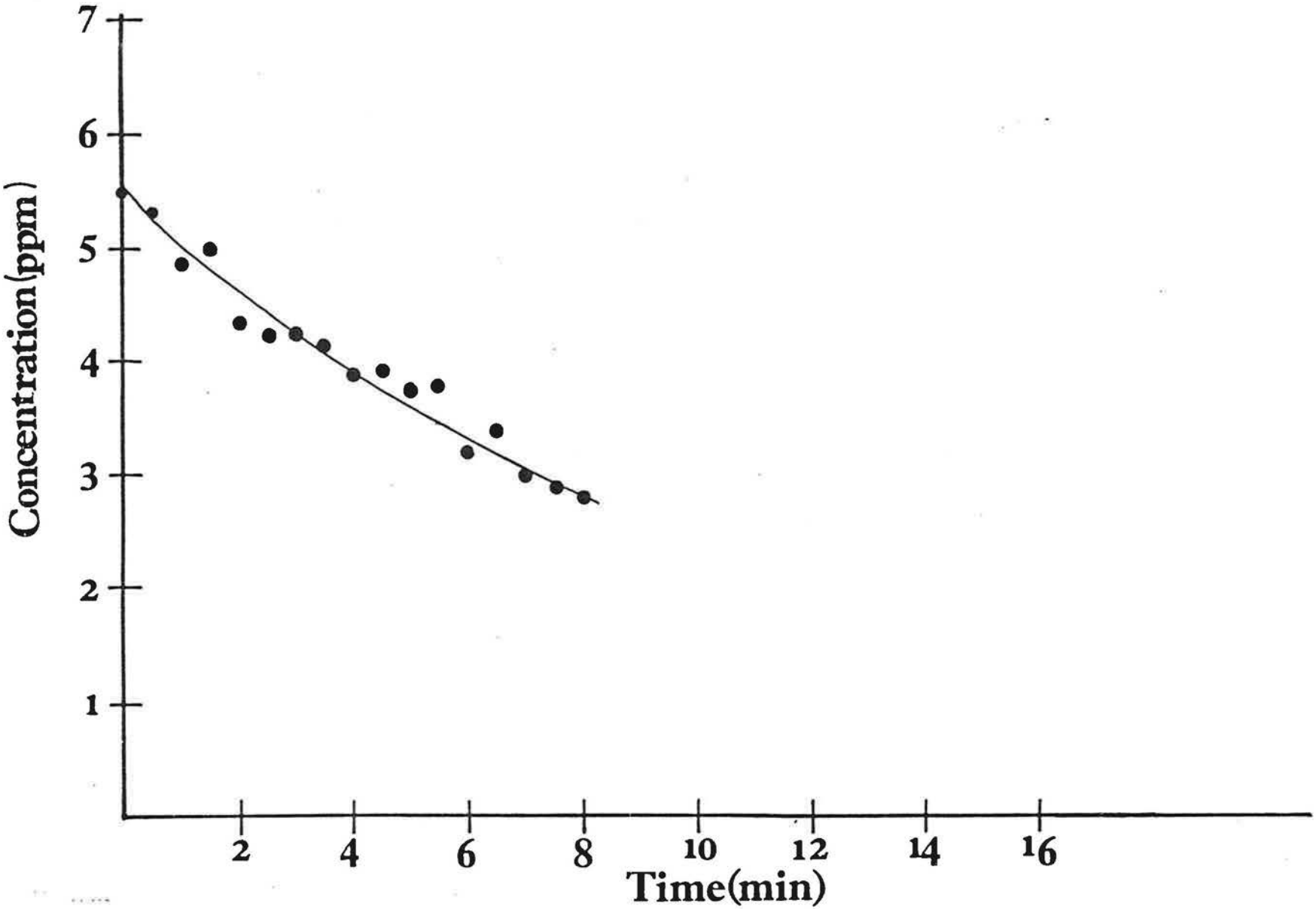

FIGURE 31 TRACER GAS DECAY USING PARALLEL COLUMNS

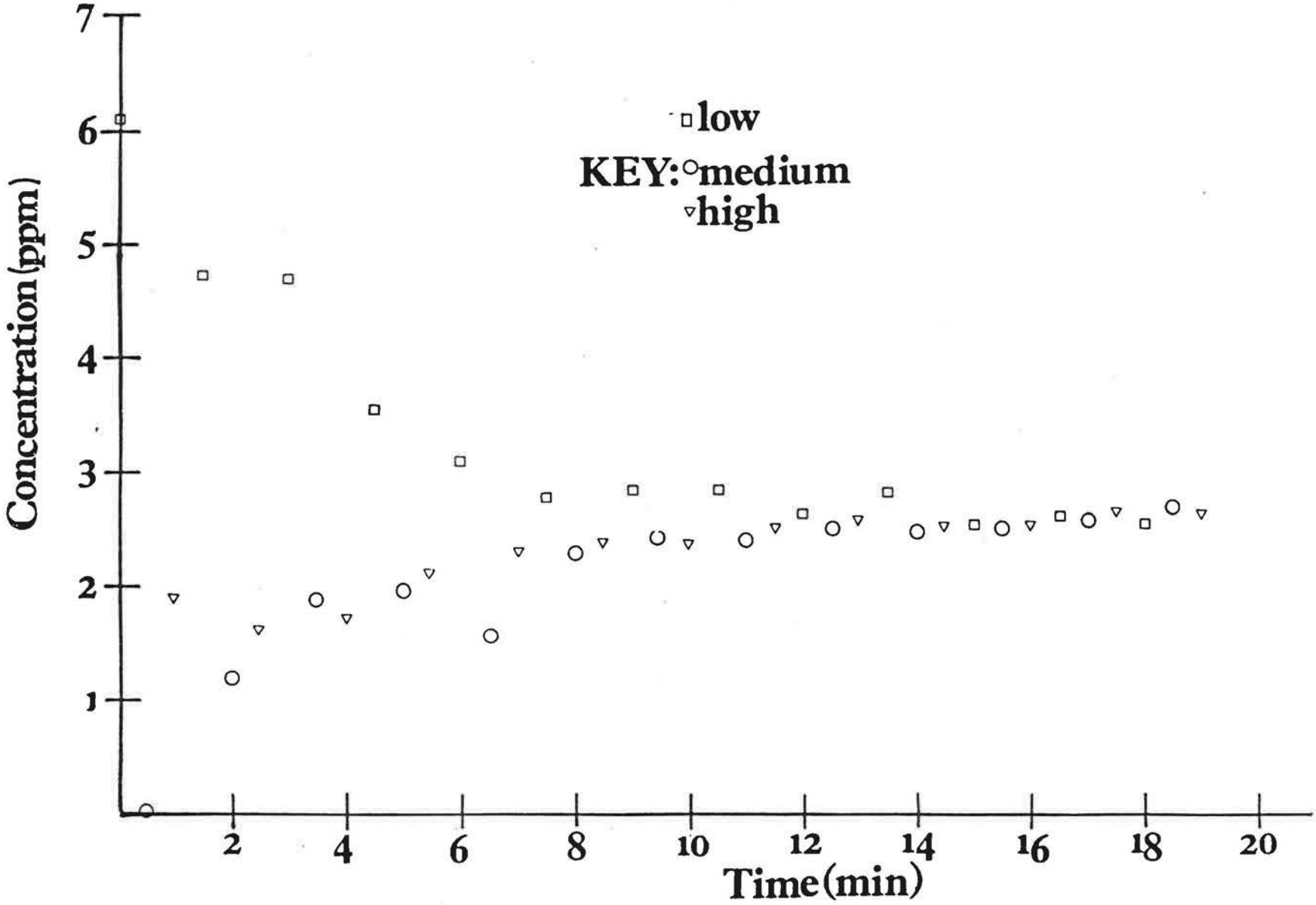

FIGURE 32 TRACER GAS DECAY(NO MECHANICAL MIXING FANS)

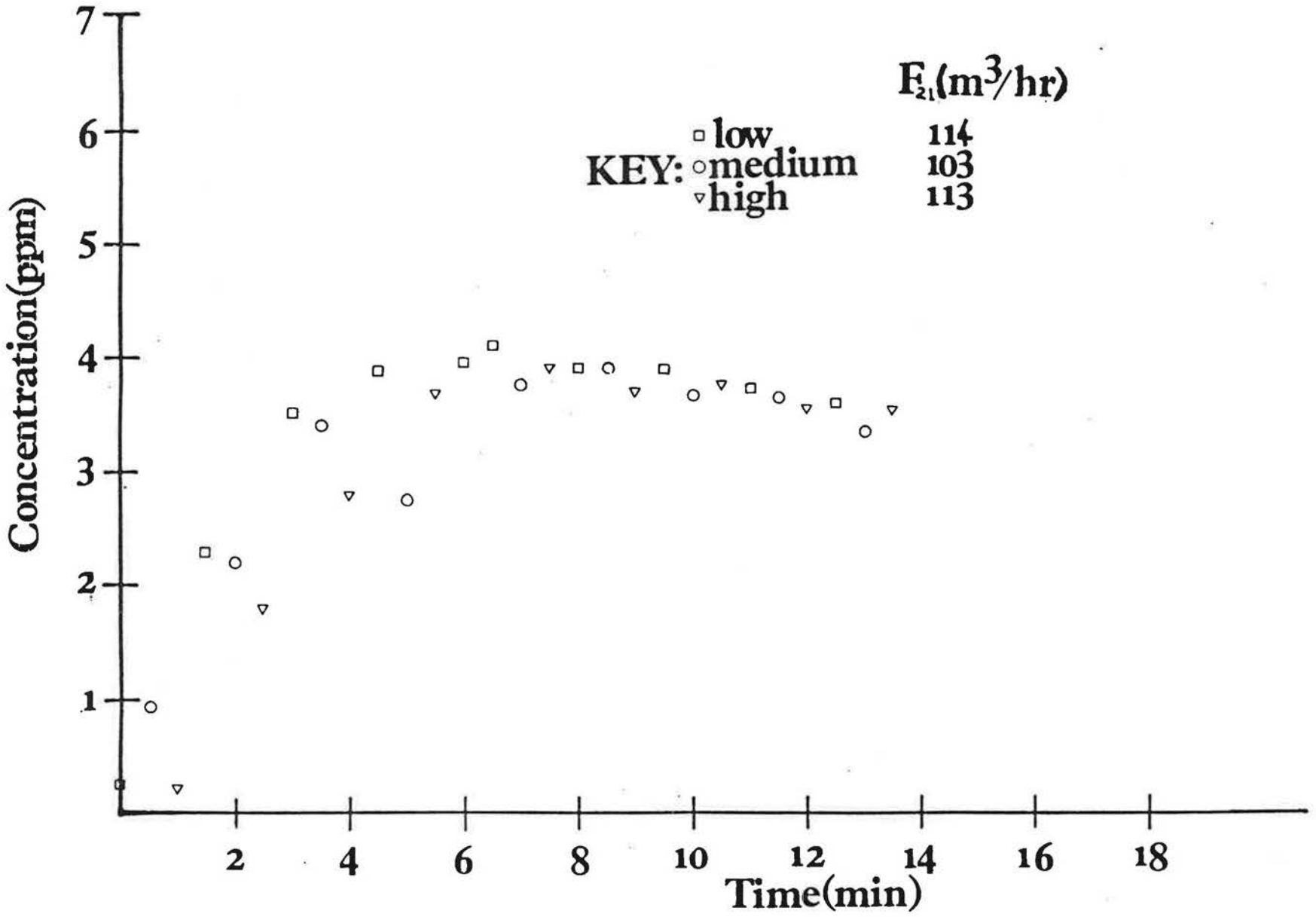

FIGURE 33 GROWTH OF FREON 12 CONCENTRATION IN CHAMBER 1 (1-WAY AIRFLOW)

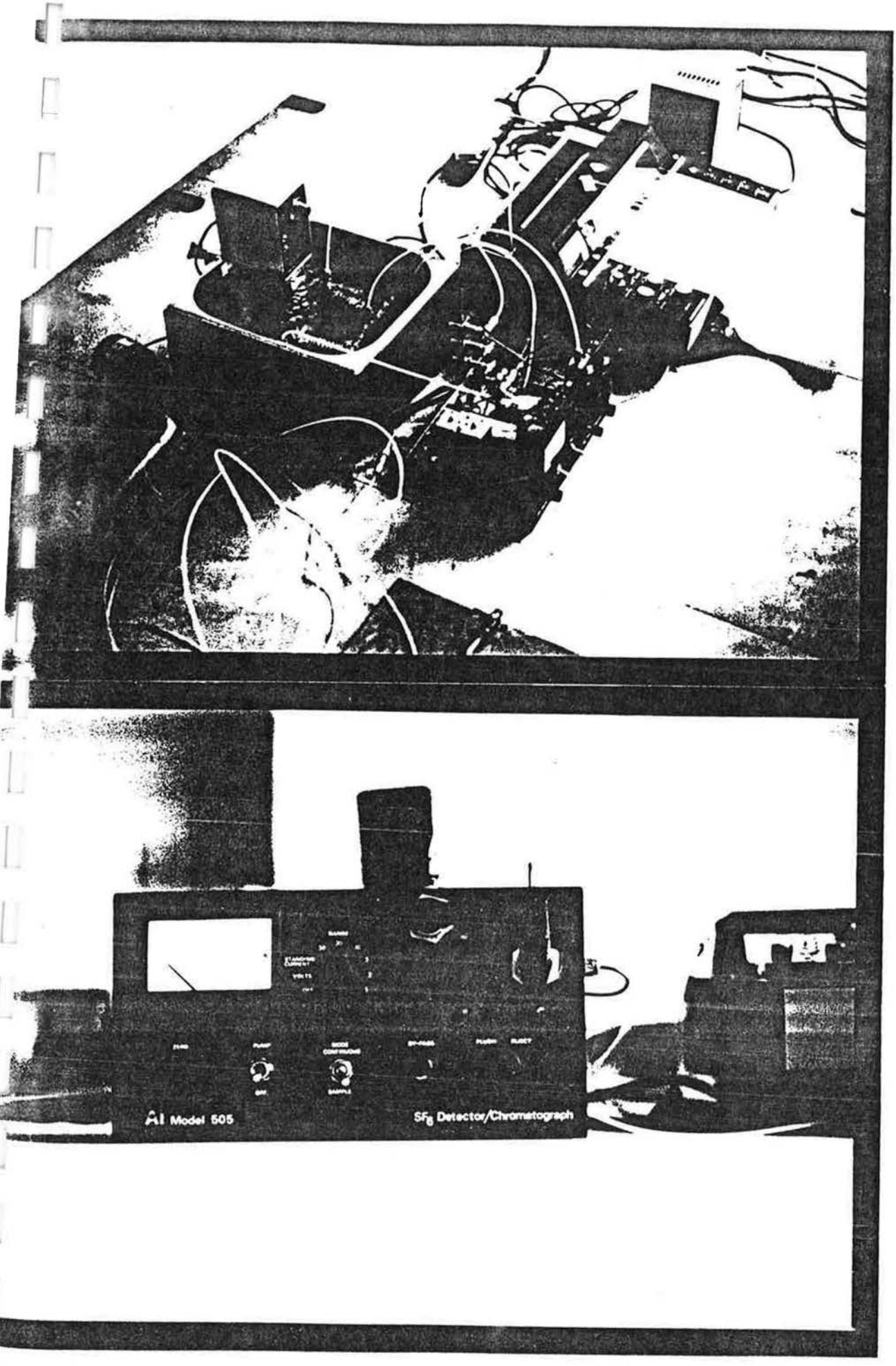

URE 34 PHOTOGRAPHS OF MEASURING TECHNIQUE

Chapter 7: EXPERIMENTAL RESULTS AND APPLICATIONS

7.1) General

The results given in this chapter are intended to show the versatility of the rapid sampling multiple-tracer gas technique.

The experimental applications presented were all obtained in terraced council dwellings in the North West, all dwellings being built in the past five years. The data obtained are divided into four types of air movement test using single and multiple tracer gas measurements.

(i) Single-cell measurements of roofspace ventilation rates.
(ii) Two-cell measurements of whole house to roofspace air movements.
(iii) Two-cell measurements of two directional air movements between the ground floor and first floor of a house.
(iv) Three-cell measurements of air movements between three spaces in a house.

7.2) Single-cell measurements of roof ventilation rates

The provision of roof ventilators to provide adequate roof ventilation is becoming increasingly important for the prevention of roof condensation in insulated, low energy dwellings. Adequate roof ventilation implies good air movement with no pockets of still air and sufficient roof air volume changes to prevent moisture build-up in roof timbers or undertiling materials.

The building regulations (England and Wales) require roofspaces above insultated ceilings to be cross ventilated by use of permanent openings having a minimum open area of 0.3% roof plan area or in accordance with BS.5250 [34]. To achieve the minimum open area, combinations of soffit and ridge ventilators are used. There is little available information on the effects of using different combinations of roof ventilators.

Tables (7.1) to (7.4) inclusive show the variations in roof ventilation rate for different roof ventilators. The ventilators considered are soffit slot, soffit plus ridge tile and ridge tile only (soffit sealed).

Comparison between different ventilators is achieved by sealing all roof vents, the response of the roofspace to fortuitous air infiltration (via cracks around rooftiles and gaps in sarking felt) with prevailing wind conditions then being determined.

Figure (35) shows graphically the response of a roofspace to different types of roof ventilator. The figure shows that soffit ventilators provide between 0.5-9 air changes per hour for wind speeds up to 5m/sec, soffit vents being generally independant of wind direction. Winds less than 2m/sec normal to soffit achieving a 20% large ventilation rate than parallel ones. Soffit plus ridge vents provide roof ventilation rates between 1 - 9.5 air changes per hour approximately for wind speeds up to 5m/sec. The increasing uncertainty in roof ventilation rates implies that soffit plus

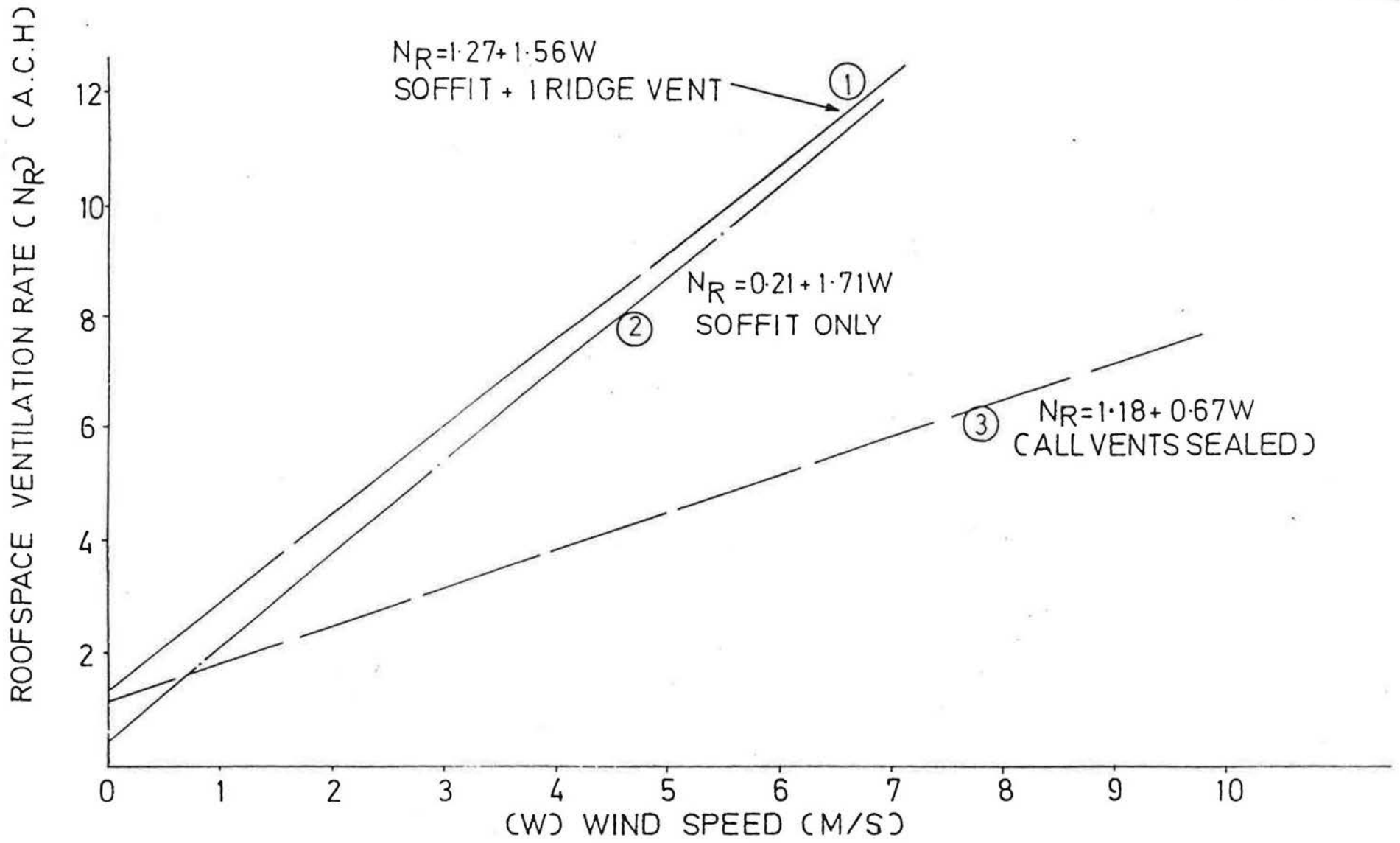

FIGURE 35 ROOFSPACE VENTILATION – SOFFIT AND RIDGE VENTS

ridge vent combinations are susceptable to changes in wind direction for wind speeds less than 3m/sec, normal winds producing the higher ventilation rates. This observation is confirmed by examining the response of a single ridge vent to changes in wind direction (figure 36), when wind speeds of less than 1 m/s occur the roof ventilation rate tends to its "background" all sealed level. Site observations show that with ridge tiles a strong dependance on prevailing wind direction occurs, winds blowing normal to the ridge achieve the highest ventilation rates.

7.3) Two-cells: house to roofspace air movement

The effects of roof ventilators and prevailing weather conditions on house to roof space air movements are very important. The application of loft insulation reduces heat transfer to the roofspace resulting in colderroof temperatures; it does not effect the amount of water vapour transferred by diffusion and air movements across the ceiling. In winter conditions, higher house air temperatures than outside plus the moisture generated will create vapour pressure differences house to roofspace. Water vapour diffusion contributes 7%-18% of water vapour input to a roofspace.

Air movement via cracks and holes around roof hatches and service pipes are the major culprits; air movement contributes 82%-93% of the total moisture vapour input into a roofspace (see ref [16]).

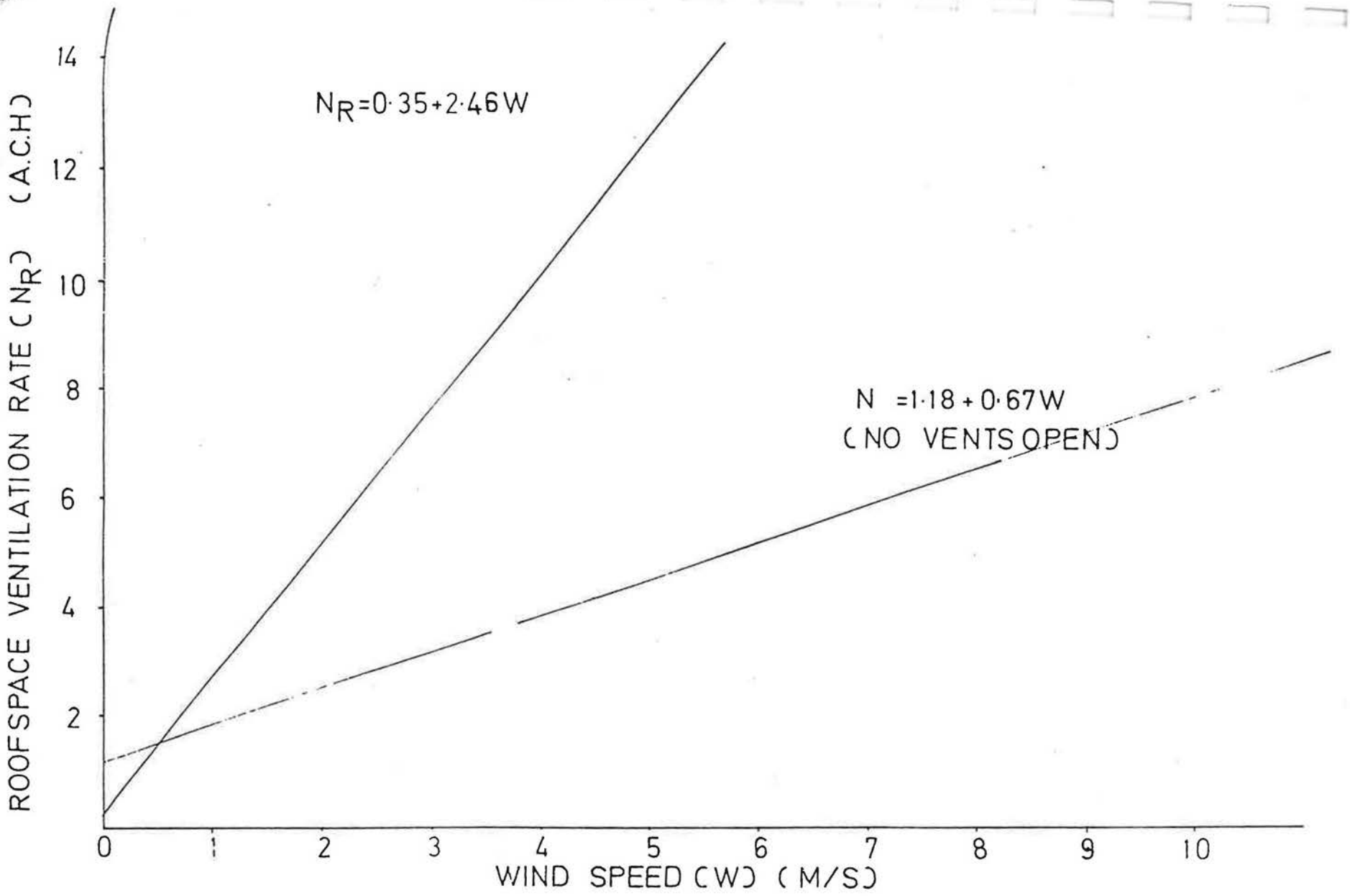

FIGURE 36 ROOFSPACE VENTILATION - 1 RIDGE VENT

The influence of types of roof ventilators on the proportion of exfiltrating house air leaving via the roofspace is shown in figure(37). Examination of this figure shows that with all vents sealed (FH-R/FH-0) lies between 0.2-0.3 for wind speeds upto 5m/sec.

The influence of soffit vents show that (FH-R/FH-O) lies between 0.1-0.45 for wind speeds up to 5m/sec. Similarly for a soffit plus ridge ventilator combination (FH-R/FH-O) lies between 0.12-0.57 for wind speeds up to 5m/sec.

Generally figure (37) implies that soffit/ridge ventilator combinations may induce up to 25% more exfiltrating house air to leave via the roofspace than occurs using soffit vents only.

The size of air movements, house to roofspace, for the different combinations of roof ventilator are shown in figure (38). If no roof vents are open, 25 m^3/hr of house air escapes via the roofspace and is generally constant for wind speeds up to 5 m/sec.

If a single ridge vent only is open, the amount of house air leaving via the roofspace lies between 35-60 m^3/hr for wind speeds up to 5m/sec.

The use of a high level ridge vent with no openings at soffit level contravenes BS 5250 [34] and is used for experimental purposes only.

The influence of soffit ventilators on house to roofspace air movements shows the resulting airflows are between 15-65m^3/hr for wind speeds up to 5m/sec.

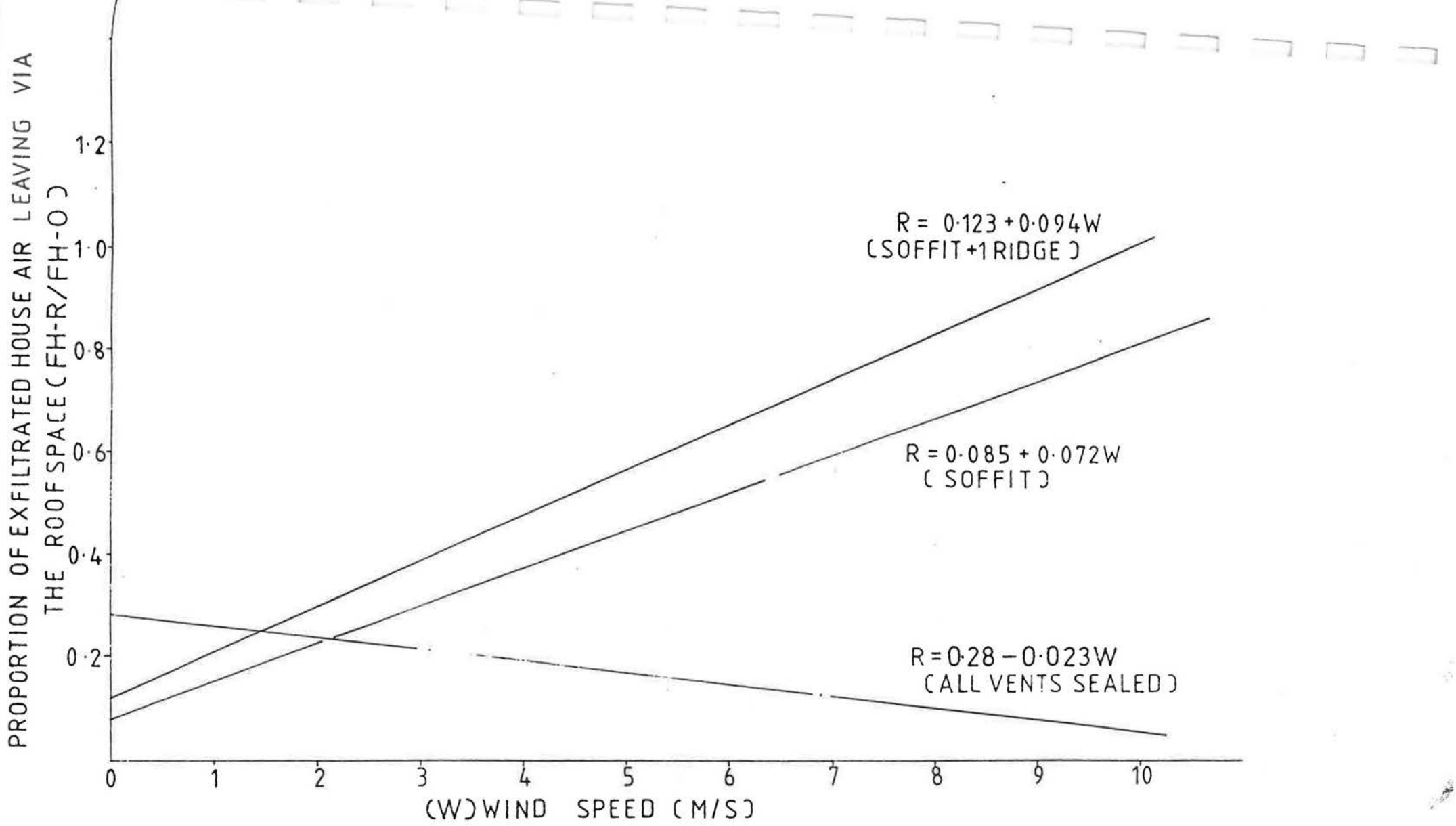

FIGURE 37 HOUSE TO ROOF AIRFLOW – EFFECT OF DIFFERENT ROOF VENTILATORS

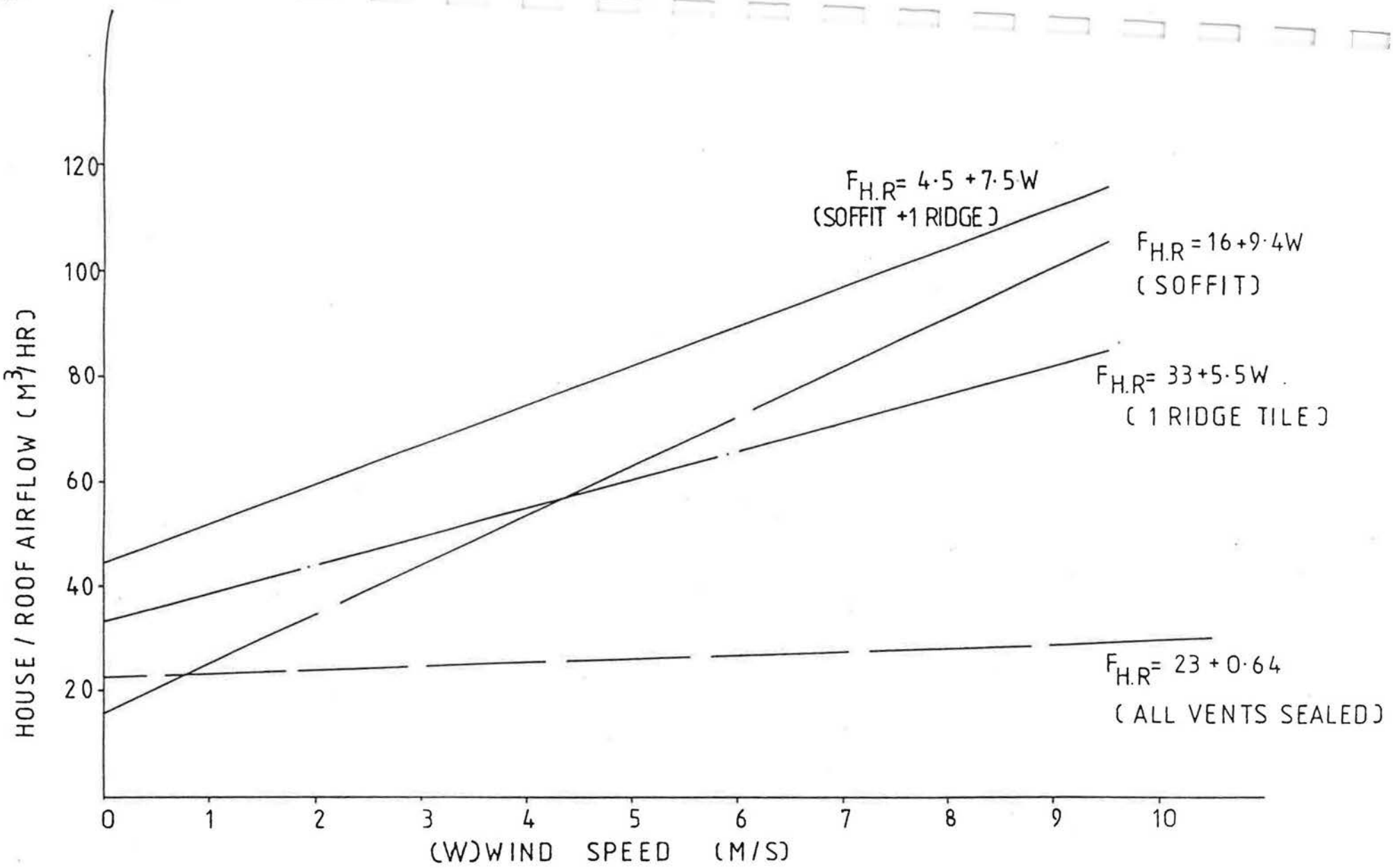

FIGURE 38 HOUSE TO ROOF AIRFLOW USING DIFFERENT ROOF VENTILATORS

Combining soffit vents and a ridge vent produces house to roofspace airflows between 45-80 m^3/hr for wind speeds up to 5m/sec.

For the house tests, the data collected suggests that soffit/ ridge ventilator combinations may induce approximately 25% more house to roofspace air movement than soffit vents only.

Further, at low wind speeds ($<$ 1m/sec), the soffit plus single ridge vent provides a roof ventilation rate of 2.9 air changes per hour compared with the roof ventilation rate of 2.2 air changes per hour provided by soffit vents alone.

Generally the data collected shows soffit plus ridge ventilater combinations to be very susceptible to prevailing wind direction.

7.4) Two cell : two directional air movements

This section shows the results of dividing a house into two distinct cells, cell (10) is the ground floor of a dwelling and cell (2) the first floor. Two Freon tracer gases are used typically Freon

12 is released in Cell (1) and Freon 114 in cell (2). Mixing of air and tracer gas has been carried out with all connecting doors open and with all doors closed, mixing of air/tracer gases is good in both cases. The twenty site tests summarized in table (7.9) shows that two directional airflows of about equal size exist between the ground floor and first floor of a dwelling.

The size of these airflows is equivalent to approximately 1 house volume change per hour (150-250 m^3/hr).

If warm moist air is generated in a kitchen, the subsequent distribution of the moisture laden air throughout the rest of the house may give rise to condensation of water vapour on a cold surface.

Cold surfaces may be found where cupboards are fitted near external walls, in unheated bedrooms (windows, wall, ceilings) and in roof-spaces where in extreme cases the condensing water vapour gives rise to staining and mould growth of ceilings and failure of the roof structural timber.

Generally, the vertical temperature gradient found in housing would suggest one directional air movement between ground floor and first floor. The two directional air movements found are in all probability caused by a variety of factors, turbulent air motions arising from randomly distributed structural crackage causing infiltration and exfiltration of air, the effects of windows (crackage

and purpose provided openings), the geometry of the stairwell which provides a large opening connecting the two floors, along with the effect of a cold external wall joining part of the stairwell enclosure.

Two directional flows between floors are strongly influenced by extract fans; a kitchen extract fan will effectively reduce a ground floor to first floor airflow by approximately 80%. A similar influence is exerted by a bathroom extract fan. It should be noted that closing of the kitchen door or bathroom door when the fan is running completely removes any influence the fan is having on two directional air movements. Similar difficulties are observed if the incident wind direction is directly onto the face of an extract fan discharge louvre.

The twenty measurements given in table (7.9) are given to show the usefulness of the multiple tracer technique in determining the possible influences of a number of variables, long term data collection will enable airflow modelling and validation to progress.

A specimen two directional result with theoretical curve shapes and the site data points collected, is shown in figure (39).

7.5) Three cell measurements

The fourteen test summarized in table (7.10) show the effects of releasing three tracer gases in three different rooms of a dwelling

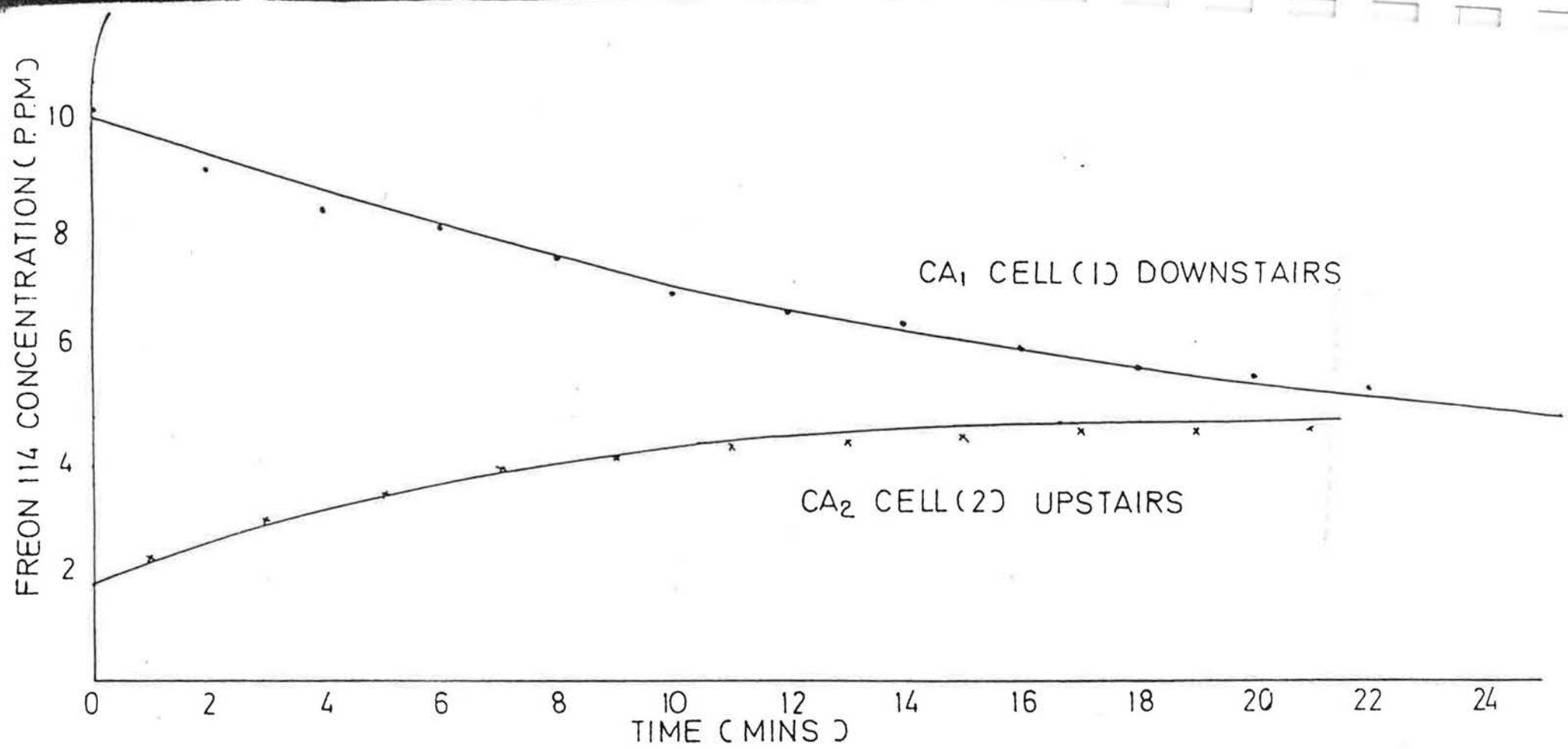

FIGURE 39a FREON 114 RELEASED DOWNSTAIRS

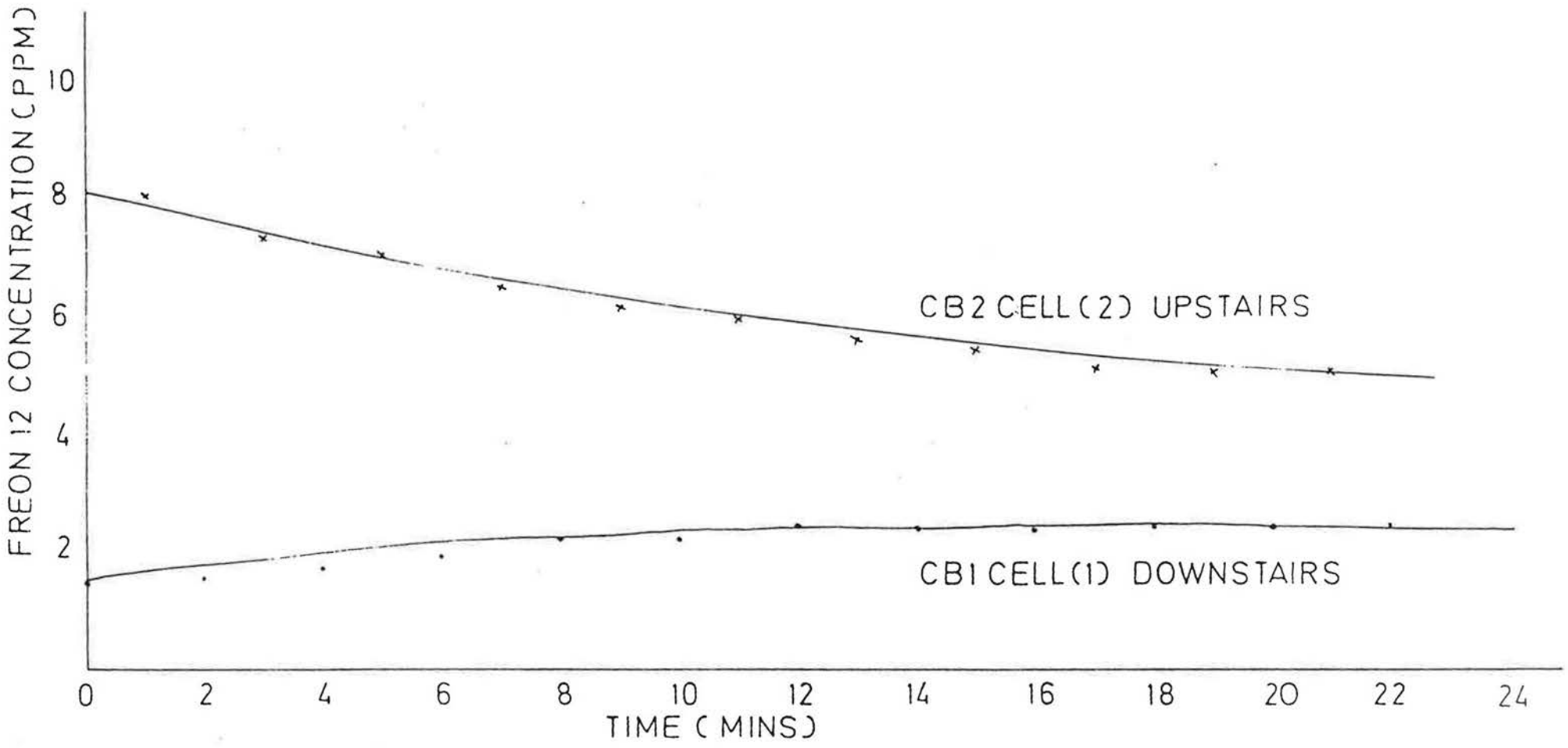

FIGURE 39b FREON 12 RELEASED UPSTAIRS

Tests (1) to (6) are the result of releasing Freon 114 in the ground floor of a house, releasing Freon 12 in the first floor and B.C.F. in the roofspace, see Figure (40). For the house studied ground floor to first floor air movements were approximately 110-220 m^3/hr, Air movements from first floor to ground floor lie in the range 160-306m^3/hr, with a one directional airflow between house and roofspace of 28-40 m^3/hr. Switching a kitchen extract fan on reduces ground floor to first floor airflows by approximately 85%, the size of the one directional airflows between house and roofspace is also reduced by approximatley 50%. The effectiveness of the kitchen extract fan on dwelling internal air movements is highly dependent on the kitchen door being open and the location of the extract fan discharing to atmosphere relative to incident wind conditions.

Tests (7) to (10) are the result of releasing Freon 12 in the kitchen of a house, Freon 114 in a bedroom immediately above the kitchen, the surrounding spaces being occupied with B.C.F. The relative locations of the spaces tested are shown in figure (41), the size of inter-cell airflows connecting the kitchen to the rest of the house are strongly influenced by relative door positions. When the kitchen door is closed the connection airflows lie between 0-15 m^3/hr, with the kitchen door open two directional airflow occurs and the flows are approximately 15-23 m^3/hr inflow into kitchen and 30-45 m^3/hr outflow from kitchen to its surroundings. The small connecting flows between kitchen and the bedroom immediately above show that crackage in the kitchen ceiling can cause moisture laden air to enter the bedroom.

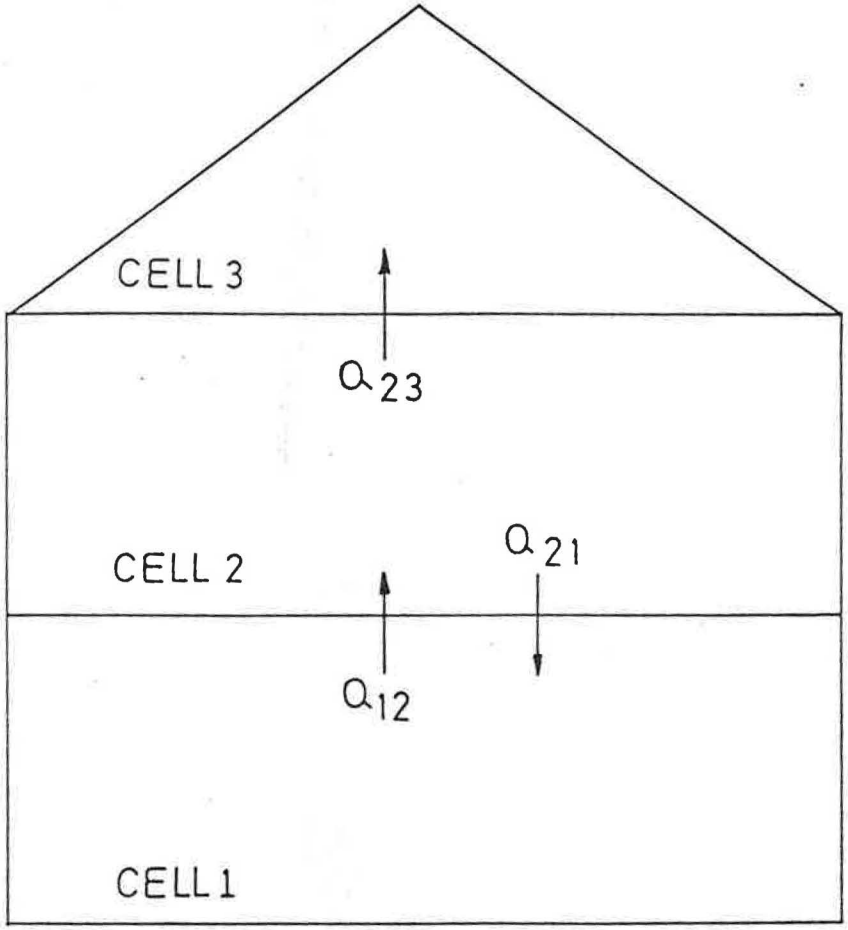

FIGURE 40 AIRFLOWS - DOWNSTAIRS, UPSTAIRS, ROOFSPACE

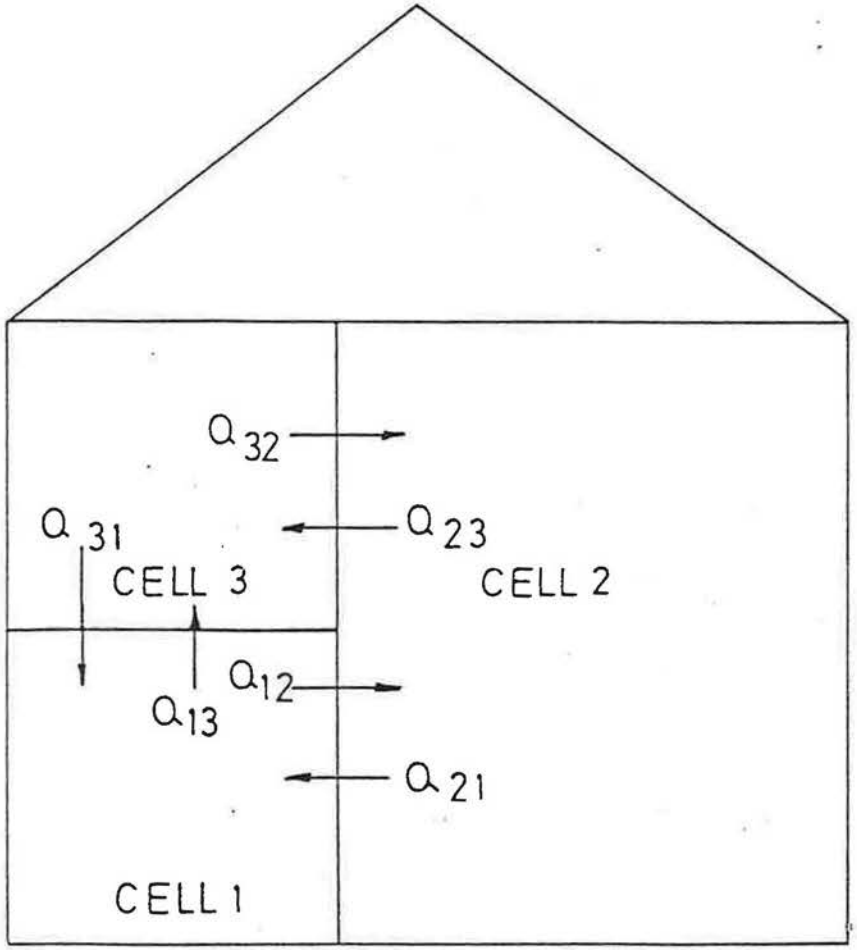

CELL 1 : KITCHEN
CELL 2 : SURROUNDINGS
CELL 3 : BEDROOM

FIGURE 41 AIRFLOWS - KITCHEN, BEDROOM, SURROUNDINGS

Tests (11) to (14) show the effects of releasing Freon 12 in a bedroom Freon 114 in the bathroom and BCF in the remaining spaces. The relative locations of the spaces tested are shown in figure (42), Once again the interspace airflows are strongly influenced by relative door and window openings. Tests (11) and (12) show this quite clearly, if the bathroom window and door are open then a large air movement (100-125 m^3/hr) from the surroundings into the bathroom occurs with no air movement from the bathroom into the house. When the bathroom window is shut and the door open , a two directional airflow exists between the bathroom and the rest of the house. This two directional air movement is approximately 25-38 m^3/hr moving from surroundings into bathroom and 15-25 m^3/hr moving from the bathroom into the house.

The preceeding discussion is intended to show the usefulness and general flexibility of multiple tracer gas measurements. The data presented here is taken from air movement measurements in four terraced houses and can therefore only be taken as indicative of air movements which may generally exist in terraced housing.

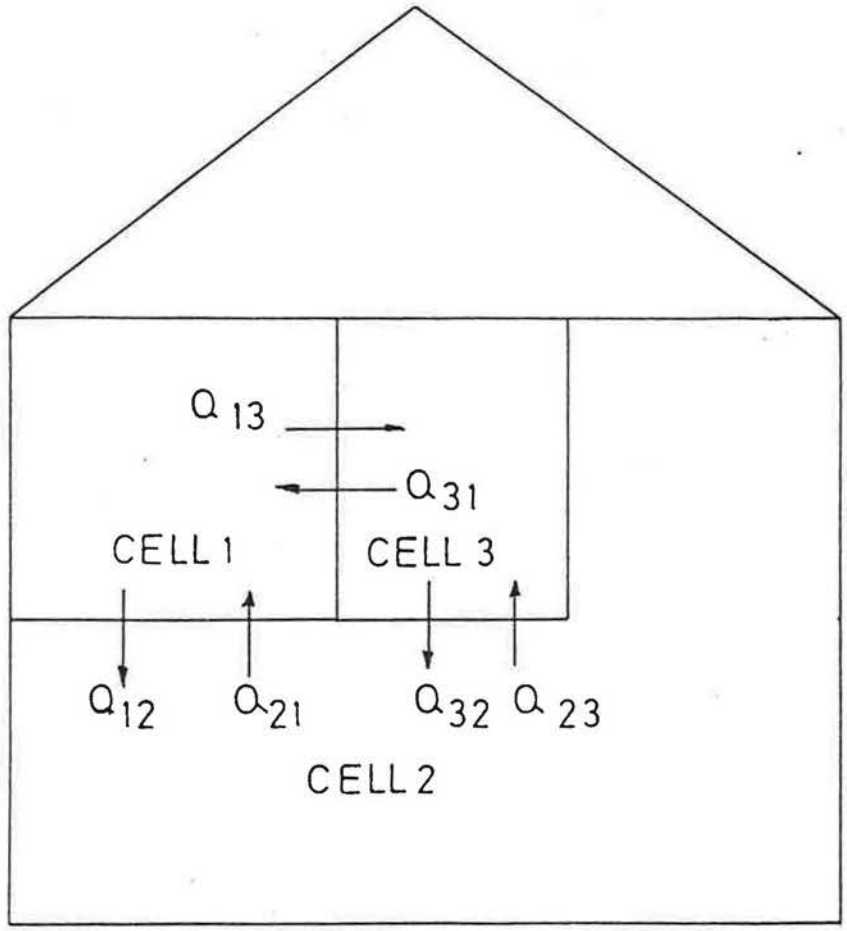

CELL 1 : BEDROOM
CELL 2 : SURROUNDINGS
CELL 3: BATHROOM

FIGURE 42 AIRFLOWS - BEDROOM, SURROUNDINGS, BATHROOM

Test No	Type of Test	Temp(In) db	°C wb	Temp(Out) db	°C wb	Roof Ventilation Rate (ACH)	Wind Speed m/s	Wind Direction	Comments
1	ROOF VENTILATION	17	12	12.5	9.5	2.7 ± .33	1.5	SOUTH EAST	ROOF VENTS SEALED
2	" "	"	"	"	"	2.7 ± .28	3	SOUTH	"
3	HOUSE/ROOF AIR FLOW	"	"	"	"	2.83± .41	1.5	"	"
4	" "	"	"	"	"	2.43± .18	2.5	SOUTH EAST	"
5	ROOF VENTILATION	16	"	"	10	2.47± .26	2	SOUTH WEST	"
6	" "	"	"	"	"	1.56± .19	1	SOUTH WEST	"
7	HOUSE/ROOF AIR FLOW	"	"	"	"	1.65± .27	1	SOUTH	"
8	ROOF VENTILATION	"	"	"	"	0.45± .08	STILL	-	"
9	" "	15	"	14	12	1.31± .11	1	EAST	"
10	HOUSE/ROOF AIR FLOW	"	"	"	"	4 ± .2	3.5	NORTH EAST	"
11	ROOF VENTILATION	"	"	"	"	2.7 ± .33	2	EAST	"
12	" "	14.5	11	11	9	4.75± .4	3.5	NORTH	"
13	" "	"	"	"	"	5.28± .27	5.5	"	"
14	HOUSE/ROOF AIR FLOW	"	"	"	"	4.5 ± .19	5	NORTH WEST	"
15	ROOF VENTILATION	"	"	"	"	2.5 ± .25	4	" "	"
16	" "	"	"	"	"	2.2 ± .22	4	" "	"
17	HOUSE/ROOF AIRFLOW	13.7	10	9.5	8	2.4 ± .31	1	NORTH EAST	"
18	ROOF VENTILATION	"	"	"	"	1.24± .1	0.5	" "	"
19	" "	"	"	"	"	2.61± .18	2.5	" "	"
20	ROOF VENTILATION	"	"	"	"	2.32± .2	1.75	" "	"

TABLE (7.1) Roof Ventilation (All roof Ventilators sealed)

Test No	Type of Test	Temp (In) db °C	Temp (In) wb	Temp (out) db °C	Temp (out) wb	Roof Ventilation Rate (ACH)	Wind Speed (m/s)	Wind Direction	Comments
21	ROOF VENTILATION	18	14.5	10	8	5.87 ± .48	5	NORTH	ROOF VENTS SEALED
22	" "	"	"	"	"	3.44 ± .22	2.5	"	"
23	HOUSE/ROOF AIR FLOW	"	"	"	"	2.4 ± .2	1.5	"	"
24	" " " "	"	"	"	"	2.39 ± .11	2	"	"
25	ROOF VENTILATION	16.5	13	11	10	2.28 ± .15	1	EAST	"
26	HOUSE/ROOF AIR FLOW	"	"	"	"	1.21 ± .1	1	"	"
27	ROOF VENTILATION	"	"	"	"	1.27 ± .11	1.5	"	"
28	HOUSE/ROOF AIR FLOW	"	"	"	"	1.23 ± .2	1	"	"
29	ROOF VENTILATION	20	15	"	9	2.0 ± .19	.5	NORTH	"
30	HOUSE/ROOF AIR FLOW	"	"	"	"	2.0 ± .11	.5	NORTH	"
31	ROOF VENTILATION	"	"	"	"	3.7 ± .29	2.0	"	"
32	" "	16	13	15	13	7.8 ± .61	10	"	"
33	HOUSE/ROOF AIR FLOW	"	"	"	"	4.88 ± .4	6	"	"
34	ROOF VENTILATION	"	"	"	"	2.05 ± .31	4.5	NORTH EAST	"
35	HOUSE/ROOF AIR FLOW	"	"	"	"	3.05 ± .11	6	" "	"
36	ROOF VENTILATION	"	"	"	"	3.18 ± .32	3	" "	"
37	" "	15	"	10	8	4.88 ± .49	3	" "	"
38	HOUSE/ROOF AIR FLOW	"	"	"	"	2.67 ± .21	2.5	" "	"
39	ROOF VENTILATION	"	"	"	"	1.8 ± .09	2	" "	"

TABLE (7.1) (Contd)

Test No	Type of Test	Temp (In) db °C	Temp (In) wb	Temp (Out) db °C	Temp (Out) wb	Roof Ventilation Rate (ACH)	Wind Speed (m/s)	Wind Direction	Comment
40	ROOF VENTILATION	15	13	10	8	2.32 ± .31	3	NORTH EAST	ROOF VENTS SEALED
41	HOUSE/ROOF AIR FLOW	"	10	11	9	3.83 ± .33	3.5	NORTH	"
42	ROOF VENTILATION	"	"	"	"	7 ± .95	5	"	"
43	HOUSE/ROOF AIR FLOW	"	"	"	"	3.87 ± .41	3.5	"	"
44	ROOF VENTILATION	"	"	"	"	5.5 ± .68	4.5	"	"

TABLE (7.1) (Contd)

Test No	Type of Test	Temp (In) db °C	Temp (In) wb	Temp (Out) db °C	Temp (Out) wb	Roof Ventilation Rate (ACH)	Wind Speed (m/s)	Wind Direction	mer
45	ROOF VENTILATION	-	-	-	-	9.75 ± 1.51	3.4	NORTH	1 Ridge Tile Open.(Soff sealed).
46	" "	-	-	-	-	10.7 ± 2.21	3.4	"	"
47	" "	-	-	-	-	13.2 ± 3	4.6	"	"
48	" "	-	-	-	-	13.8 ± 2.9	4.6	"	"
49	" "	15	10.5	6.5	5	2.9 ± .35	3	NORTH EAST	"
50	" "	"	"	"	"	6.6 ± .47	3.5	"	"
51	" "	10	6	5	4	2.7 ± .11	0.25	NORTH WEST	"
52	HOUSE/ROOF AIR FLOW	"	"	"	"	1.6 ± .2	0.1	"	"
53	ROOF VENTILATION	"	"	"	"	0.9 ± .11	0.1	"	"
54	HOUSE/ROOF AIR FLOW	10.5	7	4	3	1.5 ± .25	0.25	NORTH	"
55	ROOF VENTILATION	"	"	"	"	2.9 ± .25	0.75	"	"
56	HOUSE/ROOF AIR FLOW	"	"	"	"	1.6 ± .16	0.5	"	"
57	" " " "	13	8	5	4	3 ± .22	0.5	"	"
58	ROOF VENTILATION	15	"	"	"	10.5 ± 2	4	"	"
59	HOUSE/ROOF AIR FLOW	10	"	3	3	1.4 ± .11	0.25	"	"
60	ROOF VENTILATION	"	"	"	"	2.2 ± .13	0.5	"	"
61	HOUSE/ROOF AIR FLOW	"	"	"	"	2 ± .22	0.5	"	"
62	ROOF VENTILATION	"	"	"	"	2.1 ± .32	0.75	"	"

Roof Ventilation (1 Ridge Tile Open) TABLE (7.2)

Test No	Type of Test	Temp (In) db °C wb	Temp (Out) db °C wb	Roof Ventilation Rate (ACH)	Wind Speed (m/s)	Wind Direction	Comment
63	ROOF VENTILATION	13 8	6 5.5	26 ± 5	6.1	NORTH WEST	1 Ridge Tile Open (Soff sealed)
64	" "	" "	" "	12.4 ± 2.9	6.1	"	"
65	HOUSE/ROOF AIR FLOW	" "	" "	11.7 ± 3.1	5	"	"
66	ROOF VENTILATION	" "	" "	9.6 ± 2	3.2	"	"
67	HOUSE/ROOF AIR FLOW	" 9	5 4.5	3.6 ± .8	0.7	"	"
68	ROOF VENTILATION	" "	" "	4.5 ± .4	1.3	NORTH	"
69	" "	" "	" "	3 ± .11	1.3	/	"
70	HOUSE/ROOF AIR FLOW	" "	" "	4.4 ± .44	1.7	"	"
71	ROOF VENTILATION	" "	" "	3.7 ± .19	1.9	"	"
72	HOUSE/ROOF AIR FLOW	" "	" "	4.2 ± .3	1.9	"	"
73	" "	14 "	4 3.5	0.9 ± .1	0.1	NORTH EAST	"
74	ROOF VENTILATION	" "	" "	1.4 ± .21	0.25	EAST	"
75	HOUSE/ROOF AIR FLOW	" "	" "	3.2 ± .31	1.1	"	"
76	ROOF VENTILATION	" "	" "	2.2 ± .19	1.6	"	"
77	HOUSE/ROOF AIR FLOW	" "	" "	4.1 ± .3	2.3	"	"
78	ROOF VENTILATION	" "	" "	3 ± .19	2.0	"	"
79	HOUSE/ROOF AIR FLOW	10 6	5 4	1 ± .05	0.25	SOUTH EAST	"
80	ROOF VENTILATION	" "	" "	1.2 ± .11	0.25	"	"

TABLE (7.2) (Contd)

Test No	Type of Test	Temp (In) db °C	Temp (In) wb	Temp (Out) db °C	Temp (Out) wb	Roof Ventilation Rate (ACH)	Wind Speed (m/s)	Wind Direction	Comment
81	HOUSE/ROOF AIR FLOW	10	6	5	4	0.8 ± .08	0.2	SOUTH EAST	1 Ridge Tile Open.(Soff sealed)
82	ROOF VENTILATION	"	"	"	"	1.4 ± .1	0.25	"	"
83	HOUSE/ROOF AIR FLOW	"	"	"	"	1.3 ± .14	0.25	"	"
84	HOUSE/ROOF AIR FLOW	12	8	4	3	8.2 ± 1	2.7	NORTH	"
85	ROOF VENTILATION	"	"	"	"	9 ± 2	4	"	"
86	HOUSE/ROOF AIR FLOW	"	"	"	"	7 ± .65	4	"	"
87	ROOF VENTILATION	"	"	"	"	9.2 ± 1.1	4.6	"	"
88	HOUSE/ROOF AIR FLOW	"	"	"	"	5 ± .5	3.4	"	"
89	ROOF VENTILATION	"	"	"	"	5.6 ± .65	2.9	"	"
90	ROOF VENTILATION	13	7	2	0	9.6 ± .39	5	NORTH WEST	"
91	" "	"	"	"	"	11.6 ± 2	7	" "	"
92	" "	"	"	"	"	11.6 ± 4	7	"	"
93	" "	"	"	"	"	12.2 ± 3.1	7.5	"	"
94	" "	"	"	"	"	13.7 ± 1.3	6	"	"
95	" "	"	"	"	"	12 ± 2.5	7	"	"
96	ROOF VENTILATION	20	13	2.5	"	5.1 ± .5	2.5	NORTH	"
97	HOUSE/ROOF AIR FLOW	"	"	"	"	4.2 ± .31	2	"	"
98	ROOF VENTILATION	"	"	"	"	5.2 ± .19	2	NORTH WEST	"

TABLE 7.2 (Contd)

Test No	Type of Test	Temp (In) db °C	Temp (In) wb	Temp (Out) db °C	Temp (Out) wb	Roof Ventilation Rate (ACH)	Wind Speed (m/s)	Wind Direction	Comment
100	HOUSE/ROOF AIR FLOW	20	13	2.5	0	3.7 ± .11	3	WEST	1 Ridge Tile Open (Soff (sealed)
101	ROOF VENTILATION	"	"	"	"	5 ± .28	3.75	"	"
102	HOUSE/ROOF AIR FLOW	"	"	"	"	4.1 ± .11	3	"	"
103	ROOF VENTILATION	16	12	7	6	4 ± .35	2.75	NORTH WEST	"
104	ROOF VENTILIATION	"	"	"	"	5.6 ± .25	3.5	"	"
105	HOUSE/ROOF AIR FLOW	"	"	"	"	4.9 ± 1	4	WEST	"
106	ROOF VENTILATION	"	"	"	"	2.7 ± .65	1.5	NORTH	"
107	HOUSE/ROOF AIR FLOW	"	"	"	"	4.5 ± .19	2.5	WEST	"
108	ROOF VENTILATION	"	"	"	"	4.9 ± .11	2.5	NORTH	"
109	HOUSE /ROOF AIR FLOW	"	"	"	"	5.7 ± .18	3	"	"

TABLE (7.2) (Contd)

Test No	Type of Test	Temp (In) db °C	Temp (In) wb	Temp (Out) db °C	Temp (Out) wb	Roof Ventilation Rate (ACH)	Wind Speed (m/s)	Wind Direction	Comment
110	ROOF VENTILATION	20	16	10	8	2.9 ± .11	2.5	EAST	Soffit + 1 Ridge Tile O
111	" "	"	"	"	"	2.1 ± .09	1.25	SOUTH EAST	"
112	" "	"	"	"	"	4.8 ± .38	0.5	NORTH EAST	"
113	HOUSE/ROOF AIR FLOW	"	"	"	"	5.4 ± .5	4	SOUTH EAST	"
114	" "	"	"	"	"	6.6 ± .56	4.5	SOUTH EAST	"
115	ROOF VENTILATION	"	"	"	"	10 ± 3	5	"	"
116	HOUSE/ROOF AIR FLOW	"	"	"	"	7.8 ± .95	4.5	EAST	"
117	" "	22	15	11	10	4.8 ± .29	4	NORTH EAST	"
118	ROOF VENTILATION	"	"	"	"	7.9 ± 1	5	NORTH	"
119	" "	"	"	"	"	6.4 ± 1	4	EAST	"
120	HOUSE/ROOF AIR FLOW	"	"	"	"	5.1 ± .58	3.5	"	"
121	ROOF VENTILATION	"	"	"	"	6.4 ± .33	5	"	"
122	HOUSE/ROOF AIR FLOW	"	"	"	"	4.8 ± .71	3	"	"
123	ROOF VENTILATION	"	13	7	4	9.9 ± 2	7	SOUTH	"
124	HOUSE/ROOF AIR FLOW	"	"	"	"	11 ± 1.5	8	"	"
125	ROOF VENTILATION	"	"	"	"	22.5 ± 5	8	EAST	"
126	HOUSE/ROOF AIR FLOW	"	"	"	"	7.6 ± 2.5	5	SOUTH EAST	"
127	ROOF VENTILATION	"	"	"	"	11 ± 1.8	6	SOUTH	"

Roof Ventilation (Soffit + 1 Ridge Tile) TABLE (7.3)

Test No	Type of Test	Temp (In) db °C	wb	Temp (Out) db °C	wb	Roof Ventilation Rate (ACH)	Wind Speed (m/s)	Wind Direction	Comment
128	ROOF VENTILATION	22	13	7	4	15.1 ± 1.85	7.5	SOUTH EAST	Soffit + 1 Ridge Tile Op
129	HOUSE/ROOF AIR FLOW	"	"	"	"	12 ± 1.1	0	"	"
130	ROOF VENTILATION	"	"	"	"	15.7 ± 1.58	10	"	"
131	HOUSE/ROOF AIR FLOW	"	"	"	"	10.3 ± 2	7.5	"	"
132	ROOF VENTILATION	"	"	"	"	16.1 ± 5	7.5	"	"
133	" "	"	15	"	5.5	8.9 ± .61	4	NORTH	"
134	" "	"	"	"	"	10.2 ± 1	5	"	"
135	" "	"	"	"	"	9.2 ± 1	5	"	"
136	HOUSE/ROOF AIR FLOW	"	"	"	"	8.5 ± .95	4.5	"	"
137	ROOF VENTILATION	"	"	"	"	9.6 ± 2	5	"	"
138	" "	"	"	"	"	9.1 ± 1.8	4.75	"	"
139	" "	"	"	"	"	8.8 ± 1	4.5	"	"
140	" "	"	"	"	"	6.2 ± .5	3.5	"	"
141	" "	"	"	"	"	5.7 ± .38	3	"	"
142	" "	19	12	"	6	10.8 ± .59	6	EAST	"
143	" "	"	"	"	"	7 ± .78	3.75	"	"
144	HOUSE/ROOF AIR FLOW	"	"	"	"	4.6 ± .11	3	NORTH EAST	"
145	ROOF VENTILATION	"	"	"	"	12.8 ± 1	6.5	EAST	"

TABLE (7.3) (Contd)

Test No	Type of Test	Temp (In) db °C	Temp (In) wb	Temp (Out) db °C	Temp (Out) wb	Roof Ventilation Rate (ACH)	Wind Speed (m/s)	Wind Direction	Comment
146	HOUSE/ROOF AIR FLOW	19	12	7	4	6.1 ± 1.9	5	EAST	Soffit + 1 Ridge Tile O
147	ROOF VENTILATION	"	"	"	"	13.1 ± 1.95	6.5	"	"
148	HOUSE/ROOF AIR FLOW	"	"	"	"	7.8 ± .37	5	SOUTH EAST	"
149	ROOF VENTILATION	"	"	"	6	6.4 ± .62	4.5	EAST	Soffit + 1 Ridge Tile O
150	" "	22	15	8	"	3.7 ± .31	.5	NORTH EAST	"
151	" "	"	"	"	"	6.2 ± .33	4	"	"
152	HOUSE/ROOF AIR FLOW	"	"	"	"	6.1 ± .3	3.75	"	"
153	ROOF VENTILATION	"	"	"	"	9.75 ± 2.5	3.5	NORTH	"
154	" "	"	"	"	"	12.6 ± 2.6	5	"	"
155	" "	"	"	"	"	6.4 ± 1	2.5	"	"
156	HOUSE/ROOF AIR FLOW	"	"	"	"	6.5 ± .55	4	NORTH EAST	"
157	ROOF VENTILATION	"	"	"	"	10 ± 1	4.5	NORTH	"
158	HOUSE/ROOF AIR FLOW	"	"	"	"	9.8 ± 2.2	4	"	"
159	ROOF VENTILATION	"	"	"	"	6.9 ± 1.6	3	"	"
160	" "	"	"	"	"	7.40 ± 1	5	SOUTH EAST	"

TABLE 7.3 (Contd)(

Test No	Type of Test	Temp (In) db °C	wb	Temp (Out) db °C	wb	Roof Ventilation Rate (ACH)	Wind Speed (m/s)	Wind Direction	Comment
161	ROOF VENTILATION	22	15	8	6	8.2 ± 1.1	5	EAST	Soffit Vents only
162	" "	"	13	11	7	9.8 ± .55	6	"	"
163	" "	"	"	"	"	10.4 ± .5	5	"	"
164	" "	"	"	"	"	9.8 ± 1.7	5.5	SOUTH EAST	"
165	" "	"	"	"	"	10.3 ± 1.91	5	"	"
166	" "	"	"	"	"	11.2 ± 1.1	5	NORTH EAST	"
167	" "	"	"	"	"	6.2 ± .31	3.5	NORTH	"
168	" "	"	"	"	"	5.9 ± .77	2.5	"	"
169	" "	"	"	"	"	7.6 ± .49	3.5	"	"
170	" "	"	"	"	"	8.6 ± .52	4.5	"	"
171	" "	"	"	"	"	10.4 ± 2.1	5	"	"
172	" "	"	"	"	"	5.4 ± 1	3	"	"
173	" "	"	"	"	"	7.6 ± 1.1	4	"	"
174	" "	"	"	"	"	7.2 ± .9	4	"	"
175	HOUSE/ROOF AIR FLOW	"	"	"	"	8 ± .33	5	EAST	"
176	" "	"	"	"	"	6.8 ± .39	4.5	"	"
177	ROOF VENTILATION	20	12	9	6	4.8 ± .48	3	"	"

Roof Ventilation (Soffit Vents only TABLE (7.4)

Test No	Type of Test	Temp (In) db °C	wb	Temp (Out) db °C	wb	Roof Ventilation Rate (ACH)	Wind Speed (m/s)	Wind Direction	Comment
178	HOUSE/ROOF AIR FLOW	20	12	9	6	4.1 ± .28	2.5	EAST	Soffit Vents only
179	ROOF VENTILATION	"	"	"	"	7.2 ± .4	4	"	"
180	" "	"	"	"	"	11.5 ± 2.6	5	"	"
181	ROOF VENTILATION	"	"	"	"	5.9 ± .33	3.75	"	"
182	HOUSE/ROOF AIR FLOW	"	"	"	"	3 ± .11	2	NORTH EAST	"
183	ROOF VENTILATION	"	"	"	"	1.4 ± .08	1	"	"
184	" "	22	15	10	8	8.7 ± .44	4	SOUTH EAST	"
185	" "	"	"	"	"	6 ± .25	3.5	"	"
186	" "	"	"	"	"	7.8 ± 1	3.75	"	"
187	HOUSE/ROOF AIR FLOW	"	"	"	"	7 ± .66	4	"	"
188	" "	"	"	"	"	6.7 ± .46	3.5	"	"
189	" "	"	"	"	"	6.4 ± .33	3.5	"	"
190	ROOF VENTILATION	"	14	9	"	1.9 ± .11	2	EAST	"
191	HOUSE/ROOF AIR FLOW	"	"	"	"	3.9 ± .28	2.75	"	"
192	ROOF VENTILATION	"	"	"	"	4.6 ± .44	3	"	"
193	HOUSE/ROOF AIR FLOW	"	"	"	"	5.1 ± .44	2.75	"	"
194	ROOF VENTILATION	"	"	"	"	6.7 ± .29	2.5	NORTH EAST	"
195	" "	"	"	"	"	7.3 ± .62	3	NORTH EAST	"

TABLE (7.4) (Contd)

Test No	Type of Test	Temp (In) db °C	Temp (In) wb	Temp (Out) db °C	Temp (Out) wb	Roof Ventilation Rate (ACH)	Wind Speed (m/s)	Wind Direction	Comment
196	HOUSE/ROOF AIR FLOW	22	14	9	8	7.5 ± .66	5	EAST	Soffit Vents Only
197	" "	"	"	"	"	4.4 ± .11	3	"	"
198	ROOF VENTILATION	"	"	"	"	4.4 ± .19	2.5	WEST	"
199	" "	"	"	"	"	4.2 ± .25	3	"	"
200	HOUSE/ROOF AIR FLOW	"	"	"	"	6.2 ± .6	5	SOUTH WEST	"
201	" ""	"	"	"	5	4.2 ± .27	3.5	"	"
202	" "	"	"	"	"	6 ± .48	5	"	"
203	ROOF VENTILATION	"	"	"	"	4.1 ± .33	4	"	"
204	HOUSE/ROOF AIR FLOW	"	"	"	"	4.9 ± .31	5	"	"
205	ROOF VENTILATION	21	13	6	5	7.6 ± 1	4	"	"
206	HOUSE/ROOF AIR FLOW	"	"	"	"	6 ± .5	3.75	SOUTH EAST	"
207	ROOF VENTILATION	"	"	"	"	5.2 ± .42	3.5	"	"
208	HOUSE/ROOF AIR FLOW	"	"	"	"	6.1 ± .49	3	"	"
209	" "	"	"	"	"	5.1 ± .58	2.5	"	"
210	ROOF VENTILATION	"	"	"	"	9.6 ± .67	4	"	"
211	" "	"	"	"	"	9.6 ± 1.1	4	"	"

TABLE 7.4 (Contd)

Test No	Temp(In) db °C	wb	Temp(Out) db °C	wb	Whole House Ventilation Rate (ACH)	Roof Ventilation Rate (ACH)	House to Roof Air Flow(m^3/hr)	Ratio $\frac{F_{H-R}}{F_{H-O}}$	Wind Speed (m/s)	Wind Direction	Comments
3	17	12	12.5	9.5	0.4 ± .05	2.83 ± .41	28 ± 3.5	.35	1.5	SOUTH	All window vents shut
4	"	"	"	"	0.4 ± .03	2.43 ± .18	27 ± 3	.34	2.5	"	"
7	16	"	"	10	0.35 ± .1	1.65 ± .27	25 ± 2	.36	1	"	"
10	15	"	14	12	0.4 ± .05	4 ± .2	28 ± 4	.35	3.5	N/EAST	All window vents open
14	14.5	11	11	9	0.85 ± .11	4.5 ± .19	15 ± 1	.09	5	N/WEST	"
17	13.5	10	9.5	8	0.4 ± .06	2.4 ± .31	31 ± 2.5	.39	1	N/EAST	"
23	18	14.5	10	8	0.8 ± .1	2.4 ± .2	22 ± 2	.14	1.5	NORTH	"
24	"	"	"	"	0.75 ± .09	2.39 ± .11	19 ± 1	.13	2	"	"
26	16.5	13	11	10	0.4 ± .05	1.21 ± .1	21 ± 2	.26	1	EAST	"
28	"	"	"	"	0.35 ± .04	1.23 ± .2	17 ± 1	.24	1	"	"
30	20	15	"	9	0.5 ± .05	2 ± .11	19 ± 1	.19	0.5	NORTH	"
33	16	13	15	13	1.1 ± .15	4.88 ± .4	26 ± 4	.12	6	"	"
35	"	"	"	"	0.7 ± .12	3.05 ± .11	28 ± 5	.2	6	N/EAST	"
38	15	"	10	8	0.85 ± .17	2.67 ± .21	25 ± 2.5	.15	3.4	"	"
41	"	10	11	9	1.0 ± .15	3.83 ± .33	30 ± 1.5	.15	3.5	NORTH	"
43	"	"	"	"	0.7 ± .1	3.87 ± .41	35 ± 3	.25	3.5	"	"

House/Roof Air Flows (All roof ventilators sealed) TABLE (7.5)

Test No	Temp(In) db °C	wb	Temp(Out) db °C	wb	Whole House Ventilation Rate (ACH)	Roof Ventilation Rate (ACH)	House to Roof Air Flow (m^3/hr)	Ratio $\frac{F_{H-R}}{F_{H-O}}$	Wind Speed (m/s)	Wind Direction	Comments
52	10	6	5	4	0.4 ± .06	1.6 ± .2	27 ± 2	.34	0.1	N/WEST	All window vents shut
54	10.5	7	4	3	0.5 ± .07	1.45 ± .25	24 ± 1.5	.24	0.25	NORTH	All window vents open
56	10.5	7	4	3	0.55 ± .09	1.6 ± .16	40 ± 5	.36	0.5	"	Window vents open downstairs, shut upstairs
57	5	4	13	8	0.5 ± .1	3 ± .22	42 ± 6	.42	0.5	"	"
59	3	3	10	8	0.4 ± .03	1.4 ± .11	11 ± .5	.14	0.25	"	"
61	4	3	10	8	0.65 ± .06	2.0 ± .22	37 ± 1.5	.28	0.5	"	All window vents open
65	6	5.5	13	8	1.15 ± .11	11.7 ± 3.1	91 ± 9	.36	5	N/WEST	"
67	5	4.5	13	9	0.65 ± .1	3.6 ± .8	48 ± 5	.37	0.7	NORTH	"
70	5	4.5	13	9	0.75 ± .09	4.4 ± .44	45 ± 5	.3	1.7	"	"
72	5	4.5	13	9	0.78 ± .05	4.2 ± .3	41 ± 4	.26	1.9	"	"
73	4	3.5	14	9	0.68 ± .05	0.9 ± .1	23 ± 1.5	.17	0.1	N/EAST	"
75	4	3.5	14	9	0.7 ± .05	3.2 ± .31	40 ± 3.5	.286	1.1	EAST	"
77	4	3.5	14	9	0.8 ± .09	4.1 ± .3	48 ± 5.5	.3	2.3	"	"
79	5	4	10	6	0.7 ± .1	1 ± .05	12 ± 1	.09	0.25	S/EAST	"
81	5	4	10	6	0.4 ± .1	0.8 ± .08	16 ± 0.5	.2	0.2	"	"
83	5	4	10	6	0.5 ± .05	1.3 ± .14	25 ± 1.5	.25	0.25	"	"
84	4	3	12	8	1 ± .11	8.2 ± 1	75 ± 9.5	.375	2.7	NORTH	"
86	4	3	12	8	1.2 ± .18	7 ± .65	70 ± 7	.29	4	"	"

House/Roof Air Flows (1 No. Ridge Tile Open) TABLE (7.6)

Test No	Temp(In) db °C	Temp(In) wb	Temp(Out) db °C	Temp(Out) wb	Whole House Ventilation Rate (ACH)	Roof Ventilation Rate (ACH)	House to Roof Air Flow(m^3/hr)	Ratio $\frac{F_{H-R}}{F_{H-0}}$	Wind Speed (m/s)	Wind Direction	Comments
88	4	3	12	8	$0.9 \pm .07$	$5 \pm .5$	46 ± 3	.26	3.4	NORTH	All window vents open
97	20	13	2.5	0	$0.64 \pm .08$	$4.2 \pm .31$	63 ± 6.5	.49	2	"	"
100	"	"	"	"	$0.7 \pm .11$	$3.7 \pm .11$	57 ± 6	.41	3	WEST	"
102	"	"	"	"	$0.75 \pm .07$	$4.1 \pm .11$	52 ± 6	.35	3	"	"
105	16	12	7	6	$0.6 \pm .1$	4.9 ± 1	49 ± 2.5	.41	4	"	"
107	"	"	"	"	$0.61 \pm .12$	$4.5 \pm .19$	41 ± 3.5	.34	2.5	"	"
109	"	"	"	"	$0.75 \pm .08$	$5.7 \pm .18$	55 ± 3	.37	3	NORTH	"

TABLE (7.6) (Contd)

Test No	Temp(In) db °C	wb	Temp(Out) db °C	wb	Whole House Ventilation Rate (ACH)	Roof Ventilation Rate (ACH)	House to Roof Air Flow(m^3/hr)	Ratio $\frac{F_{H-R}}{F_{H-0}}$	Wind Speed (m/s)	Wind Direction	Comments
113	20	16	10	8	0.85 ± .1	5.4 ± .5	50 ± 5	.29	4	S/EAST	Window vents open
114	"	"	"	"	0.83 ± .05	6.6 ± .56	61 ± 6	.37	4.5	"	"
116	"	"	"	"	0.8 ± .11	7.8 ± .95	62 ± 8.5	.39	4.5	EAST	"
117	22	15	11	10	0.8 ± .08	4.8 ± .29	63 ± 7	.39	4	N/EAST	"
120	"	"	"	"	0.73 ± .08	5.1 ± .58	60 ± 6.5	.41	3.5	EAST	"
122	"	"	"	"	0.92 ± .12	4.8 ± .71	64 ± 3.5	.35	3	"	"
124	"	13	7	4	0.9 ± .1	11 ± 1.5	89 ± 10	.49	4	SOUTH	"
126	"	"	"	"	0.75 ± .21	7.6 ± 2.5	105 ± 11	.7	5	S/EAST	"
129	"	"	"	"	0.85 ± .19	12 ± 1.1	124 ± 15	.73	7	S/EAST	"
131	"	"	"	"	0.9 ± .11	10.3 ± 2	112 ± 11	.62	7.5	"	"
136	"	15	"	5.5	1 ± .2	8.5 ± .95	126 ± 13	.63	4.5	NORTH	"
144	19	12	"	6	0.75 ± .08	4.6 ± .11	63 ± 8	.42	3	N/EAST	"
146	"	"	"	"	1 ± .1	6.1 ± 1.9	95 ± 12	.48	5	EAST	"
148	"	"	"	"	0.87 ± .1	7.8 ± .37	127 ± 20	.73	5	S/EAST	"
152	22	15	8	"	0.75 ± .11	6.1 ± .3	95 ± 9.5	.63	3.75	N/EAST	"
156	"	"	"	"	0.67 ± .05	6.5 ± .55	98 ± 11	.73	4	"	"
158	"	"	"	"	0.85 ± .09	9.8 ± 2.2	107 ± 10.5	.63	4	NORTH	"

House/Roof Air Flow (Soffit + 1 No. Ridge Tile Open) TABLE (7.7)

Test No	Temp(In) db °C	wb	Temp(Out) db °C	wb	Whole House Ventilation Rate (ACH)	Roof Ventilation Rate (ACH)	House to Roof Air Flow(m^3/hr)	Ratio $\frac{F_{H-R}}{F_{H-O}}$	Wind Speed (m/s)	Wind Direction	Comments
175	22	13	11	7	0.6 ± .1	8 ± .33	85 ± 6.5	.71	5	EAST	Window vents opens
176	"	"	"	"	0.7 ± .05	6.8 ± .39	76 ± 6.5	.54	4.5	"	"
178	20	12	9	6	0.9 ± .05	4.1 ± .28	53 ± 8	.29	2.5	"	"
182	"	"	"	"	0.7 ± .11	3 ± .11	25 ± 1.5	.18	2	N/EAST	"
187	22	15	10	8	0.95 ± .15	7 ± .66	82 ± 4.5	.43	4	S/EAST	"
188	"	"	"	"	0.75 ± .12	6.7 ± .46	50 ± 5	.33	3.5	"	"
189	"	"	"	"	0.75 ± .19	6.4 ± .33	52 ± 3.5	.35	3.5	"	"
191	"	14	9	"	0.82 ± .06	3.9 ± .28	37 ± 3.5	.225	2.75	EAST	"
193	"	"	"	"	0.9 ± .1	5.1 ± .44	43 ± 2	.24	2.75	"	"
196	"	"	"	"	0.7 ± .11	7.5 ± .66	68 ± 9	.485	4.5	"	"
197	"	"	"	"	0.5 ± .1	4.4 ± .11	26 ± 3.5	.26	3	"	"
200	"	"	"	5	1 ± .25	6.2 ± .6	63 ± 6.5	.315	5	S/WEST	"
201	"	"	"	"	0.55 ± .05	4.2 ± .27	41 ± 4.5	.37	3.5	"	"
202	"	"	"	"	0.65 ± .05	6 ± .48	39 ± 4	.3	5	"	"
204	"	"	"	"	0.72 ± .07	4.9 ± .31	35 ± 1.5	.243	5	"	"
206	21	13	6	"	0.75 ± .11	6 ± .5	52 ± 5.5	.35	3.75	S/EAST	"
208	"	"	"	"	0.7 ± .09	6.1 ± .49	49 ± 5	.35	3	"	"
209	"	"	"	"	0.8 ± .15	5.1 ± .58	43 ± 3.5	.27	2.5	"	"

House/Roof Air Flows (Soffits Open) TABLE (78)

Test No	Temp(up) db °C	wb	Temp(Dn) db °C	wb	Temp(Out) db °C	wb	Downstairs Vent Rate (ACH)	Upstairs Vent Rate (ACH)	Airflow Downstairs to Upstairs (m^3/hr)	Airflow Upstairs to Downstairs (m^3/hr)	Wind Speed m/s	Wind Direction	Comments
1	22	15	22	15	10	7	0.54 ± 0.09	$0.25 \pm .05$	155 ± 18	160 ± 16	1	NW	All window vents shut
2	22.5	14.5	22	15	8	6	$0.7 \pm .1$	$0.2 \pm .05$	176 ± 25	135 ± 18	3.5	"	"
3	18	13	17	12	14	10	$1.25 \pm .15$	$0.55 \pm .1$	85 ± 20	40 ± 6	5	N	Window vents open house unheated.
4	"	"	"	"	"	"	$1.40 \pm .14$	$0.8 \pm .09$	40 ± 10	27 ± 5	4	NE	"
5	22	16	23	17	6	4	$0.30 \pm .06$	$0.28 \pm .05$	138 ± 15	126 ± 15	2	N	Window vent shuts
6	"	"	"	"	"	"	$0.47 \pm .08$	$0.20 \pm .07$	186 ± 19	232 ± 35	0.5	N	"
7	22	16	22	16	5	4	$0.70 \pm .08$	$0.22 \pm .08$	141 ± 20	100 ± 10	4	NE	"
8	"	"	"	"	"	"	0.75 ± 0.07	$0.21 \pm .03$	128 ± 13	220 ± 22	3	N	Window vents open Kitchen fan on.
9	"	"	"	"	"	"	$0.53 \pm .1$	$0.18 \pm .05$	165 ± 19	130 ± 8	2.5	NE	All window vents shut
10	18	15	18	15	10	8.5	$1.0 \pm .15$	$0.65 \pm .1$	130 ± 10	160 ± 9	3	S	Window Vents Open
11	19	16	21	18	11	10	$2.4 \pm .1$	$0.75 \pm .15$	30 ± 5	100 ± 5	5	W	Kitchen fan on
12	21	17	22	17	11	9	$2.1 \pm .15$	$1.4 \pm .2$	10 ± 8	80 ± 8	4	W	Window vents open. kitc fan on.
13	"	"	"	"	"	"	$1.7 \pm .09$	$0.6 \pm .06$	30 ± 3	90 ± 13	5	W	Window Vents shut.Fan c
14	"	"	"	"	"	"	$1.7 \pm .11$	$0.8 \pm .1$	10 ± 5	65 ± 5	5	W	"

Two Cell Airflows

TABLE (7.9)

Test No	Temp(dn) db °C	wb	Temp(Up) db °C	wb	Temp(Out) db °C	wb	Downstairs Vent Rate (ACH)	Upstairs Vent Rate (ACH)	Airflow Downstairs to Upstairs (m^3/hr)	Airflow Upstairs to Downstairs (m^3/hr)	Wind Speed m/s	Wind Direction	Comments
15	18	14	17	15	11	10	0.9 ± .11	0.5 ± .05	158 ± 20	185 ± 18	5	S.WEST	All window vents open
16	19	15	21	17	12	10	2.0 ± .15	1.05 ± .1	10 ± 10	100 ± 15	2	WEST	All vents open. Kitchen fan on.
17	21	17	21.5	16.5	10.5	8	1.36 ± .1	1.0 ± .09	50 ± 8	140 ± 15	5	WEST	"
18	20	17	21	16	10.5	8	1.5 ± .2	0.5 ± .1	230 ± 35	240 ± 40	6	WEST	All vents open
19	21	16	22	17	9	7.5	1.25 ± .2	0.5 ± .03	165 ± 10	145 ± 18	3	SOUTH	"
20	18	15.5	18	15.5	10	8.5	2.3 ± .15	1.10 ± .15	25 ± 16	130 ± 13	5	SOUTH	All vents open. Kitchen fan on.

TABLE (7.9) (Contd)

Test No.	Ventilation e (A	Ventilation I (AC	Ventilation Ra ACH	(m^3)	m^3 hr	m^3/h	(m^3)	(m^3 hr)	m^3/h			
1	0.8 ± .1	0.5 ± .03	5 ± .65	120± 18	160± 21	0	0	35± 4	0	2.5	N.WEST	Windows shut. All doors open
2	1.6 ± .18	0.67± .01	4.8± .28	10 ± 10	170± 27	0	0	18 ±6	0	3.5	S.WEST	Kitchen Fan on " " "
3	1.8 ± .09	0.85± .09	2.9 ± .15	15± 5	115 ± 12	0	0	15 ± 1	0	1	NORTH	"
4	0.9 ± .04	0.35 ±.02	3.6 ± .16	310±42	220 ± 25	0	0	42 ± 6	0	2	SOUTH	Kitchen Fan off
5	2.2± .18	0.75 ±.1	5.2 ± .45	175±25	221 ± 10	0	0	30 ±10	0	7.5	EAST	" " " Kitchen wir open
6	0.62±.07	0.86± .1	8.8 ± 1.5	220±21	306 ± 40	0	0	45±15	0	8	"	All windows shut Kitchen fan on
				The above data should be studied in conjunction with figure (40)								
7	1.8± .25	1.1± .11	2.6 ± .35	30±10	23±13	15 ±15	3± 8	100±15	0	1.5	EAST	All doors & windows open.
8	1.5±.15	1.3±.22	2 ± .2	45±8	15± 3	8 ± 10	12±2	85±21	0	3.5	"	"
9	0.8±.05	0.85±.1	1.1±.15	15±10	0	12± 3	5±2	28±8	10±1	4.5	WEST	All doors & Windows shut
10	1 ± .03	0.6 ±.04	0.75±.09	50±2	35± 4	29 ± 8	10±5	32± 4	32±8	3	S.WEST	" " "
				The above data should be studied with figure (41)								
11	1.9±.15	0.8± .03	3.6±.15	24±2	23±3	2±4	0	125±15	0	1	S.WEST	Cell(3)Door& Window open only.
12	1.5± .1	1.2±.09	3 ± .3	35± 5	25±3	12± 12	20±2	100±25	10±5	2.5	WEST	" "
13	2± .15	0.8± .1	1.5±.07	15± 2	0	35±5	25±5	25± 8	15±6	4	S.WEST	All doors shut.Wind shut
14	1.9±.25	1.1± .11	1.6±.1	28±3	10±2	12±8	2± 10	38± 10	25±5	5.5	WEST	Cell(3) Door open
				The above data should be studied with figure (42)								

TABLE (7.10) THREE CELL AIRFLOWS

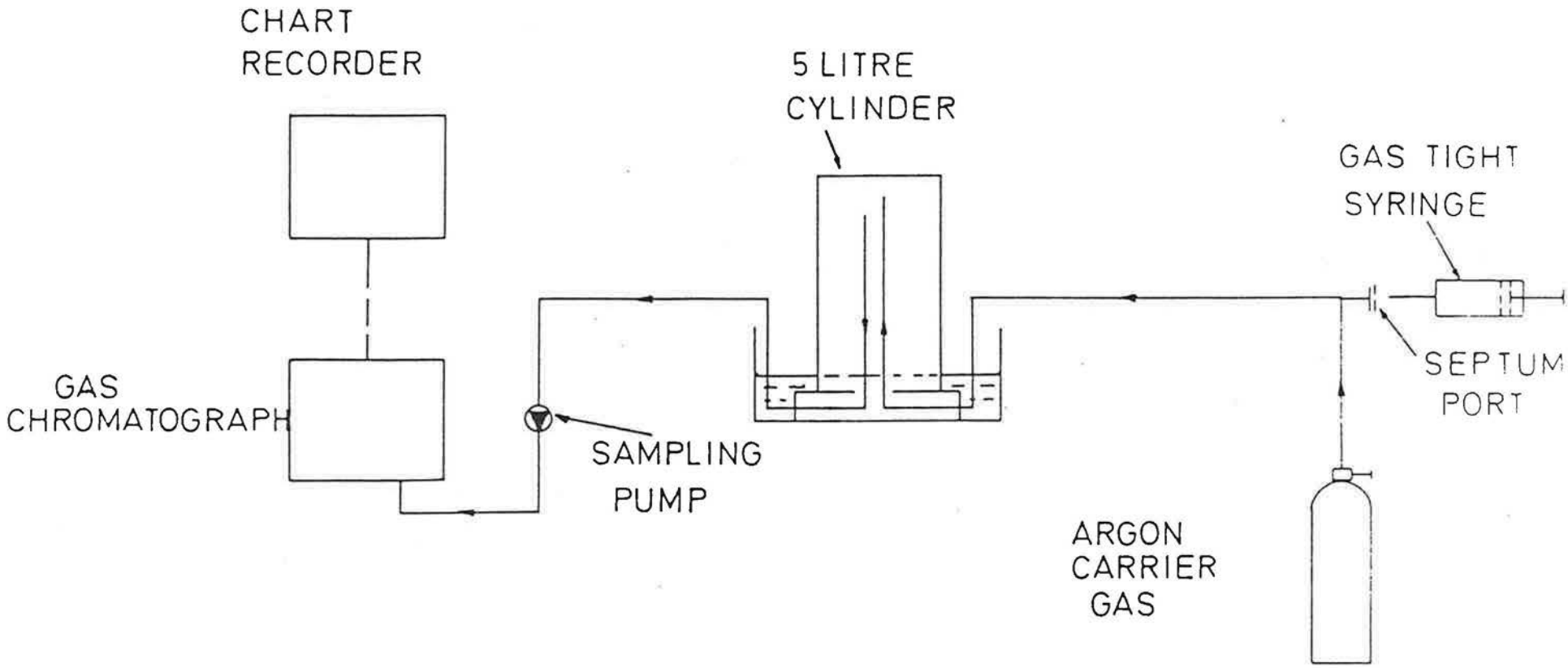

FIGURE 29 SCHEMATIC LAYOUT OF DETECTOR CALIBRATION SYSTEM

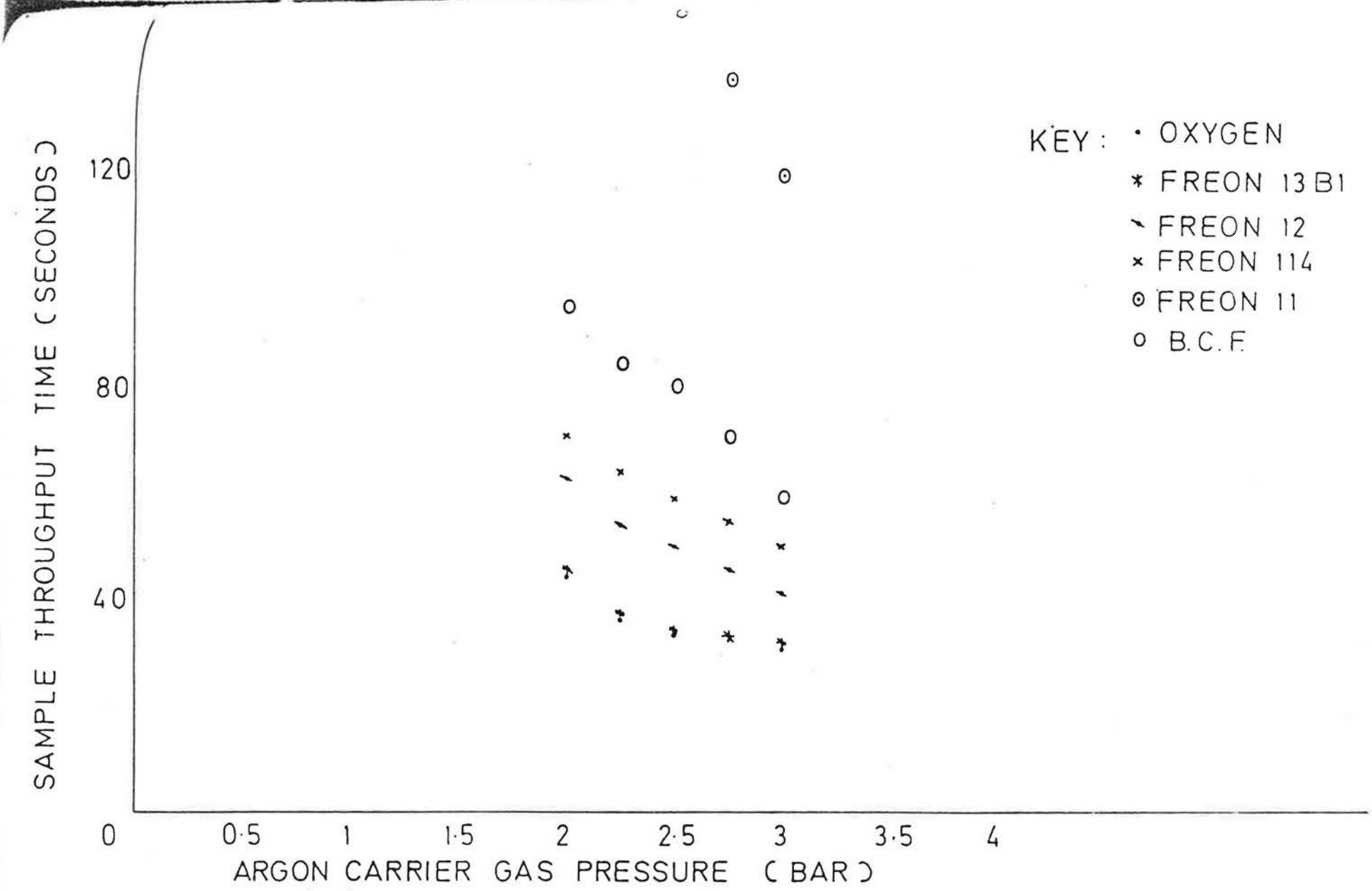

FIGURE 26 EFFECT OF CARRIER GAS PRESSURE ON TRACER THROUGHPUT TIME (SQUALANE COLUMN AT 30 °C)

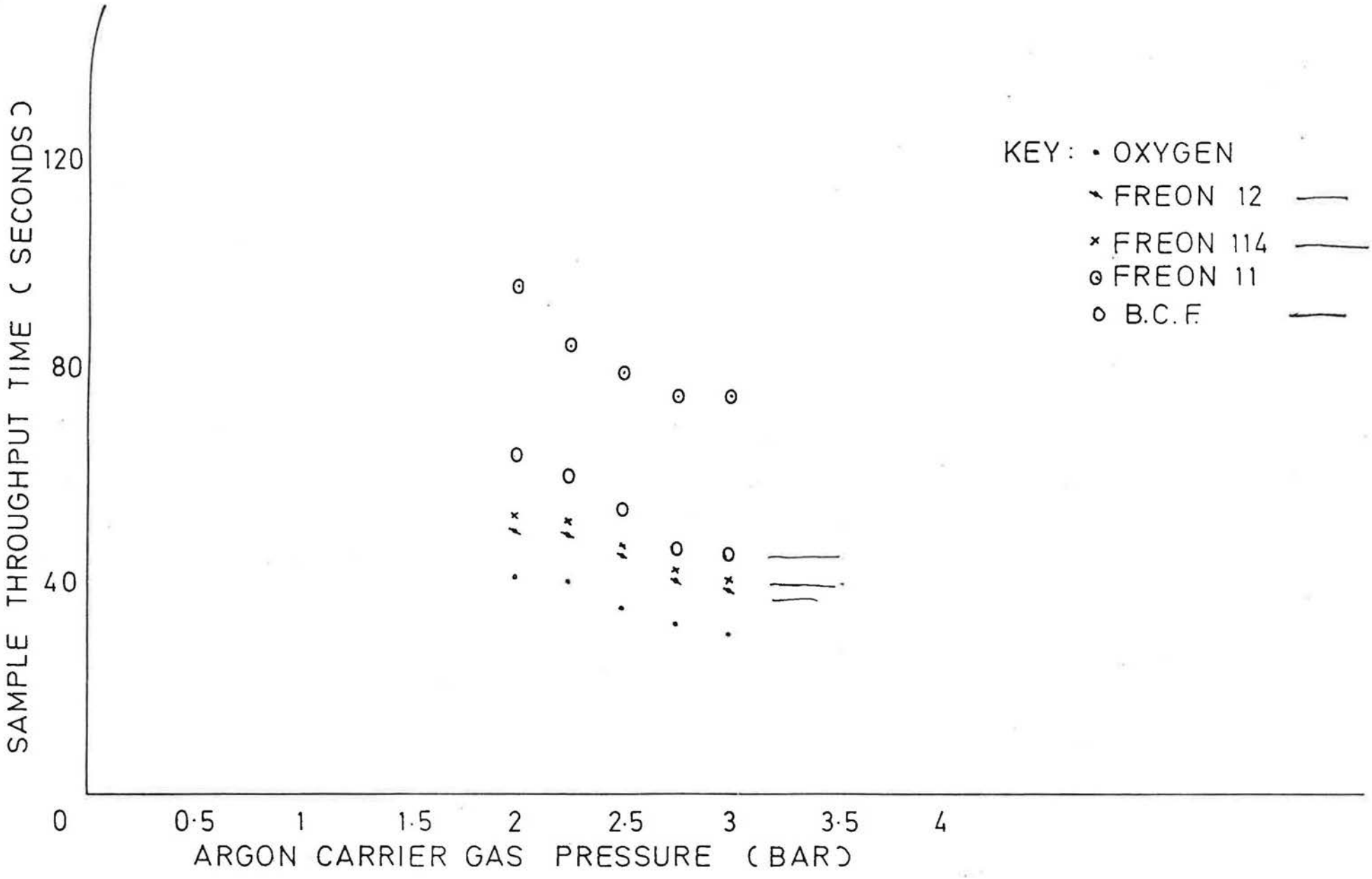

FIGURE 27 EFFECT OF CARRIER GAS PRESSURE ON TRACER THROUGHPUT TIME
(SQUALANE COLUMN AT 60°C)

CHAPTER 8: CONCLUSIONS, DEVELOPMENTS AND FURTHER WORK

Conclusions from application of manual apparatus.

This study describes the theory, analysis and instrumentation required for the simultaneous measurement of three Freon tracer gases in air.

Multiple tracer gas techniques avoid the extended test times associated with single tracer gas measurements and the inherant assumption of reproducable air movements during this period.

Improvements to the instrumentation developed by I'Anson et al [26] reduced test times from approximately 60 minutes to 15 minutes for three space airflow measurements. Consequently the larger number of data points available in a given time interval help to minimise the effects of random measurement errors on individual data points.

The method of data analysis adopted, unlike existing numerical methods, uses all of the tracer gas concentration data points to calculate inter-space airflows. The main disadvantage is that the simplified theoretical equations used to calculate inter-space airflows ignore the effects of recirculation of tracer gas between connected spaces. The simplified theoretical equations are therefore approximate, the degree of approximation being a function of time from injection of tracer gas and size of connecting airflows. The inter-space airflows calculated from these equations are then used in the exact theoretical equations which include the effects of recirculation of tracer gas between connected spaces. The resulting tracer gas concentration, time histories can then be compared with the data points obtained from site measurements of tracer gas concentrations.

A further disadvantage common to all tracer gas measurements, is the problem of mixing air and tracer gas. The theoretical equations rely on being able to take a sample of air from each space which gives the concentration of each tracer gas contained in it. If the tracer gases are of higher concentrations in some regions than others, then it is not only possible to measure an unrepresentative concentration but also the theory itself becomes unreliable since it is based on these concentrations being constant. The solution to this problem is to mix the air in each space continuously with mixing fans and to take samples through a manifold with inlets at different positions in the space. A sampling manifold is already in use, but if the air was continuously mixed the airflows and air change rates themselves would be changed. The only method of measuring airflows using tracer gases without altering them is a decay method and this disadvantage must be bourne in mind. However, it should be stated that for the air movement tests carried out in this study poor mixing of air and tracer gases has not been a problem.

If a significant mixing problem does occur, the effect will be seen when comparison is made between concentration measurements and theoretical tracer gas concentrations which assume uniform mixing.

Development of apparatus

To improve the ease of data collection, the manual equipment described in this study is currently being automated. Using an Apple IIe microcomputer enables collection of the electron capture detector signal, outputed via a multiple channel analogue/digital convertor to the comp-

utor. Automatic sampling of air/tracer gas mixtures and space selection is achieved using multiple port valves driven by reversible 12 Volt D.C. motors.

8.3) Further applications of technique

Extensive application of this multiple tracer gas technique in dwellings would greatly improve our understanding of air movements between connected spaces, induced by wind and temperature difference effects. The influences of building geometry, local terrain effects and occupancy could also be considered.

Other applications for this technique include:

(i) Assessing cross-infection risk between adjacent hospital ward units.

(ii) Simulating the spread of contaminants to enable the performance characteristics of process extraction systems to be established.

(iii) As a method of measuring ventilation and air movements in large single spaces like warehouses.

8.4) Major future development of the technique

The existing technique measures simultaneously three tracer gas concentrations, there is a definite requirement for a further three tracer gases. A system capable of measuring six tracer gas concentrations simultaneously would enable the entire air movement pattern in a terraced or semi-detached house to be quantified. This would enable a detailed examination of condensation risk by airborne moisture,

being carried into unheated bedrooms or into roof spaces. The technique would be available for use as a method of validating multiple space air movement models proposed for dwellings.

REFERENCES

1. Building Research Establishment. Heat loss from dwellings. B.R.E. Digest 190, June, 1976

2. DEWSBURY, J. A survey of research into some aspects of air infiltration. MSc. Dissertation U.M.I.S.T 1981.

3. LAGUS, P.L. Characterization of building infiltration by the tracer dilution method. Energy 2, P.461-464, 1977.

4. ETHERIDGE, D.W. Crack flow equations and scale effects. Building and Environment 12, P. 181-189, 1977.

5. GRIMSRUD, D.T. et al. Air leakage, surface pressures and infiltration rates in houses. 2ND. C.I.B. Symposium on Energy Conservation in the Built Environment, Copenhagen 1979.

6. ETHERIDGE, D.W. and ALEXANDER, D.K. The British Gas multi-cell model for calculating infiltration. ASHRAE Transactions, 86, Pt. II, 1980.

7. BILLSBORROW, R.E. and FRICKS, F.R. Model varifications of analogue infiltration predictions. Building Science, 10, 1975.

8. GUSTEN, J. Full-scale wind pressure measurements on low-rise buildings. Wind Pressure Workshop, Brussels, March, 1984.

9. LEE, B.E. A method for assessment of wind induced natural ventilation forces acting on low rise building arrays. BSERT, 1, 1980.

10. DICK, J.B. Experimental studies of natural ventilation of houses. Journal of I.H.V.E, 17, P. 420, 1949.

11. DICK, J.B. and THOMAS, D.A. Ventilation research in occupied houses. Journal of I.H.V.E. 19, 1951.

12. GRIMSRUD, D.T. Infiltration, pressurization correlation using detailed measurements on a Californian house. ASHRAE Transactions, 85, PTI, 1979.

13. Building Research Establishment. Principles of natural ventilations B.R.E. Digest 210. 1978.

14. Building Research Establishment. The assessment of wind loads. B.R.E. Digest 119, 1970.

15. DUTT, G.S. Condensation in attics: are vapour barriers really the answer? Energy and Buildings, 2, p. 251-258, 1979.

16. Building Research Establishment. Condensation in insulated domestic roofs. B.R.E. Digest 270, 1983

17. DICK, J.B. Measurement of ventilation using tracer gas techniques Heating, Piping and Air Conditioning, 22(5), p. 131-137, May 1950.

18. SANDERS, C.H. Air movements in houses: A new approach. Building Research and Practice, 10(3), May, 1982

19. PRIOR, J., LITTLER, J and ADLARD, M. Development of a multi-tracer gas techique for observing air movement in buildings. Air Infiltration Review, 4 (3), May, 1983

20. PERERA, M, WALKER, R.R. and OGLESBY, O.D. Ventilation rates and intercell airflow rates in a naturally ventilated office building. 4th AIC Conference on Air Infiltration Reduction in Existing Buildings, Switzerland, September, 1983.

21. I'ANSON, S.J, IRWIN, C. and HOWARTH, A.T. Airflow measurements using three tracer gases. Building and Environment, 17(4), p. 245 - 252, 1982.

22. HITCHIN,E.R and WILSON, G.B. A review of experimental techniques for the investigation of natural ventilation in buildings. Building Science, 2, p. 59 - 82, 1967.

23. SHERMAN, M. et al. Air infiltration measurement techniques. 1st Air Infiltration Conference on Air Infiltration Instrumentation and Measuring Techniques, Windsor, England, 1980.

24. SINDEN, F.W. Multi-chamber theory of air infiltration. Building and Environment, 13, p. 21-28, 1978.

571

25. PERERA, M. Review of techniques for measuring ventilation rates in multi-celled buildings. E.C. Contractor's Meeting on Natural Ventilation, Brussels, September, 1982.

26. I'ANSON, S.J. The development of a multiple tracer decay method for measuring air-flows in houses. MSc. Thesis U.M.I.S.T. 1982.

27. PENMAN, J.M. and RASHID, A.A.M. An experimental determination of ventilation rates in occupied rooms using atmospheric carbon dioxide. Building and Environment, 15, p.45-47, 1980.

28. HONMA, H. Method for measuring airflows in buildings. Building Research Establishment Library Translation No. 1940, 1972.

29. HILDEBRAND, F.B. Introduction to Numerical Analysis, 2nd Edn, McGraw-Hill, New York, 1974.

30. SALTZMAN, B.E. et al. Halogenated compounds as gaseous meteorological tracers. Analytical chemistry, 38(6), P. 753-758, 1966.

31. FOORD, N and LIDWELL, O.M. A method for studying air movements in complex occupied buildings such as hospitals: Halocarbons as gas tracers using gas chromatography. Building Services Engineer, 41, 1973.

32. CLEMONS, C.A. and ALTSHULLER, A.P. Responses of electron-capture detector to halogenated substances. Analytical Chemistry, 38(1), p. 133-136, 1966.

33. IRWIN, C., EDWARDS, R.E. and HOWARTH, A.T. An improved multiple tracer gas technique for the calculation of air movement in buildings. Air Infiltration Review, 5(2), February, 1984

34. BRITISH STANDARDS INSTITUTION. Code of basic data for the design of buildings: The control of condensation in dwellings. BS. 5250, 1975.

APPENDIX (A)

APPENDIX (A)

METHOD 1 : CALCULATING TWO DIRECTIONAL, TWO CELL AIRFLOWS USING A WORKED EXAMPLE.

General

When measurements are made of tracer gas concentrations in air, uncertainties in the measured values of concentration occur. These uncertainties are caused by imperfect mixing of air and tracer gas, lack of repeatability in the measuring equipment and other faults in the measurement method.

In the measurement of airflows such errors are seen as the spread of concentration points about the plotted curve giving the best fit. The magnitude of such errors will vary between different measurement methods, for the following discussion we shall state that such errors are of the order $\pm$ 5%.

To simulate the effects of measurement errors on the calculation of airflows using Perera's analysis, equations (3.4.4) - (3.4.7) are solved for known airflows and initial tracer gas concentrations. Figures (3) and (4) show the time histories of tracer gas (A) released in Cell (1) and tracer gas (B) released in Cell (2). The effects of imposing a random measurement error of $\pm$ 5% on each data point is also shown; by solving the resulting curve shapes using Perera's analysis method for the "unknown" airflows (S1, S2, Q12, and Q21), we can quantify the resulting errors on our calculated values of intercell airflows and air change rates.

n2) Calculating Concentration gradients

Concentration gradients are estimated by drawing a best-fit curve over a limited number of data points (Perera suggests a 5 minute period). A tangent is drawn to this curve and the concentration gradient estimated.

Considering tracer gas (A), from figure (A1) the concentration gradients $\frac{dC_{A1}}{dt}$ and $\frac{dC_{A2}}{dt}$ are estimated as

$$\frac{dC_{A1}}{dt} = \frac{\Delta C_{A1}}{\Delta t} = \frac{(6.95 - 8.5)}{(0.166-0.083)} = -18.7$$

$$\frac{dC_{A2}}{dt} = \frac{\Delta C_{A2}}{\Delta t} = \frac{(4.2 - 3.95)}{(0.166-0.083)} = 3$$

between time t = 0.083 hours (5 minutes), t = 0.166 hours (10 minutes)

Similarly for tracer gas (B), from figure (A2) the concentration gradients $\frac{dC_{B1}}{dt}$ and $\frac{dC_{B2}}{dt}$ are:

$$\frac{dC_{B1}}{dt} = \frac{(3 - 2.80)}{(0.166-0.083)} = 2.4$$

$$\frac{dC_{B2}}{dt} = \frac{(6.2 - 6.65)}{(0.166-0.083} = -5.4$$

The concentration gradients calculated are estimates of concentration gradients at time = 0.125 hours, therefore the absolute values of tracer gas concentration are required at this time. Figures (A1) and (A2) give :

C_{A1} = 7.65 ppm , C_{A2} = 4.1 ppm

C_{B1} = 3 ppm , C_{B2} = 6.4 ppm.

A.3) Calculating S_1, S_2, Q_{12}, and Q_{21}

The tracer gas equations (3.4.4.) - (3.4.7) are now solved for the "unknown" airflows S_1, S_2, Q_{12} and Q_{21}.

For cell (1)

$$V_1 \frac{dC_{A1}}{dt} = Q_{21}C_{A2} - S_1C_{A1} \quad (A.3.1)$$

$$V_1\frac{dC_{B1}}{dt} = Q_{21}C_{B2} - S_1C_{B1} \quad (A.3.2)$$

For cell (2)

$$V_2\frac{dC_{A2}}{dt} = Q_{12}C_{A1} - S_2C_{A2} \quad (A.3.3)$$

$$V_2\frac{dC_{B2}}{dt} = Q_{12}C_{B1} - S_2C_{B2} \quad (A.3.4.)$$

Solving equations (A.3.1) - (A.3.2) for Q_{21} and S_1 we obtain

$$-(100 \times 18.7) = 4.1\ Q_{21} - 7.65\ S_1 \qquad (A.3.5)$$

$$(100 \times 2.4) = 6.4\ Q_{21} - 3\ S_1 \qquad (A.3.6)$$

Re-arranging equation (A.3.5) for S_1:

$$S_1 = 0.536\ Q_{21} + 244.44 \qquad (A.3.7)$$

Similarly re-arranging equation (A.3.6) for Q_{21} we obtain:

$$Q_{21} = 0.469\ S_1 + 37.5 \qquad (A.3.8)$$

Solving equations (A.3.7) and (A.3.8) for S_1 and Q_{21} by the Gauss Seidel iterative technique.

$S_1 = 352\ m^3/hr$

$Q_{21} = 203\ m^3/hr$

Equations (A.3.3.) and (A.3.4) are solved in an identical manner, substituting for $\frac{dC_{A2}}{dt}$, $\frac{dC_{B2}}{dt}$, C_{A1}, C_{A2}, C_{B1} and C_{B2} we obtain

$$100\ (3) = 7.65\ Q_{12} - 4.1\ S_2 \qquad (A.3.9)$$

$$100\ (-5.4) = 3\ Q_{12} - 6.4\ S_2 \qquad (A.3.10)$$

Equations (A.3.9) and (A.3.10) are re-arranged for S_2 and Q_{12} and solved using the Gauss-Seidal iterative technique.

$S_2 = 138\ m^3/hr$

$Q_{12} = 113\ m^3/hr$

A.4) Errors in calculated airflows

Comparison between the "real" and calculated airflows S_1, S_2, Q_{12} and Q_{21} show the following errors:

$$\frac{\Delta S_1}{S_1} = \frac{|S_{1(R)} - S_{1(C)}|}{S_{1\,(R)}} \times 100 \qquad (A.4.1)$$

$$= \frac{|275 - 352|}{275} \times 100$$

$$\frac{\Delta S_1}{S_1} = 28\%$$

where $S_{1(R)}$ is the known value of S_1

" $S_{1\,(C)}$ is the calculated value of S_1 found from Perera's analysis.

Similarly

$$\frac{\Delta S_2}{S_2} = \frac{|200 - 134|}{200} = 31\%$$

$$\frac{\Delta Q_{12}}{Q_{12}} = \frac{|200 - 113|}{200} = 43.5\%$$

$$\frac{\Delta Q_{21}}{Q_{21}} = \frac{|200 - 203|}{200} = 1.5\%$$

Such errors occur primarily because of the method of estimating the concentration gradients.

The most probable size of error in the concentration gradient can be found from:

$$\Delta\left(\frac{dC}{dt}\right) = \left((\Delta C^2_{(t2)} + \Delta C^2_{(t1)})^{\frac{1}{2}} / (t_2 - t_1)\right) \qquad (A.4.1)$$

where $\Delta\left(\frac{dc}{dt}\right)$ is the absolute standard error in the concentration gradient.

$\Delta C_{(t1)}$ is the absolute standard error in tracer concentration at time (t1)

$\Delta C_{(t2)}$ is the absolute standard error in tracer concentration at time (t2).

Using equation (A.4.1) the most probable errors in the four concentration gradients can be estimated.

For $\frac{dC_{A1}}{dt}$ equation (A.4.1) becomes:

$$\frac{dC_{A1}}{dt} = [((0.33)^2 + (0.075)^2)^{\frac{1}{2}} / 0.083]$$

$$\frac{dC_{A1}}{dt} = \pm 4.1$$

Similarly $\frac{dC_{A2}}{dt} = \pm 1.95$

$$\frac{dC_{B1}}{dt} = \pm 1.83$$

$$\frac{dC_{B2}}{dt} = \pm 3.56$$

The effects of such large uncertainties in calculated values of tracer concentration gradients are the large errors in calculated airflows S_1, S_2, Q_{12} and Q_{21}.

To test the goodness-of-fit between tracer gas concentration data and airflows calculated from such data, equations (A.3.1) - (A.3.4) are solved using these calculated airflows and the intial tracer gas concentrations. The resulting time histories of tracer gas concentrations can then be compared with "site" concentration data points.

Figures (A3) and (A4) show the effects of a random $\pm$ 5% error on concentration data, the poor estimates of inter-cell airflows result in large discrepancies between "site" data points and the theoretical curve shapes derived from such data.

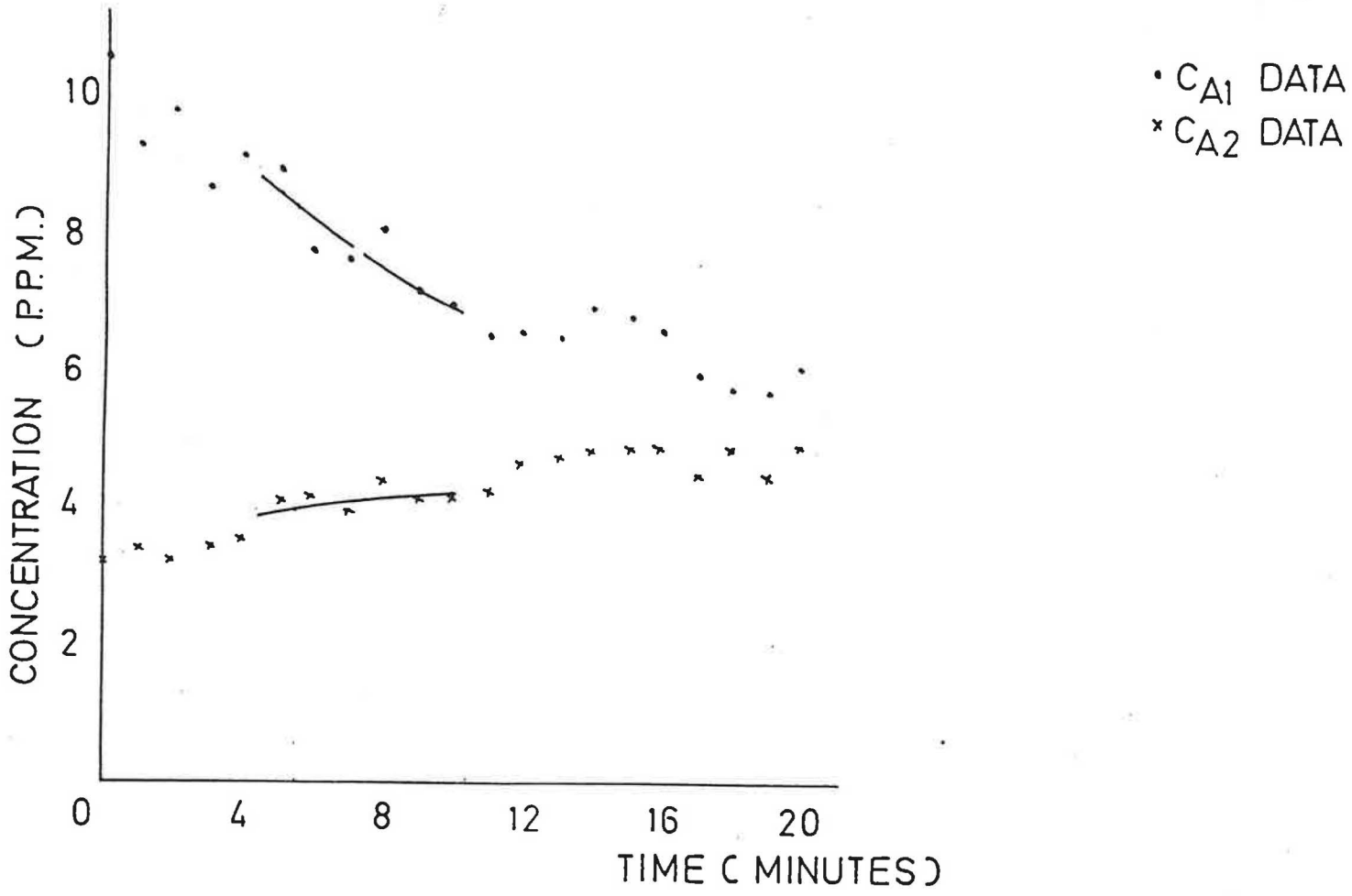

FIGURE A1 ESTIMATING CONCENTRATION GRADIENTS (C_A)

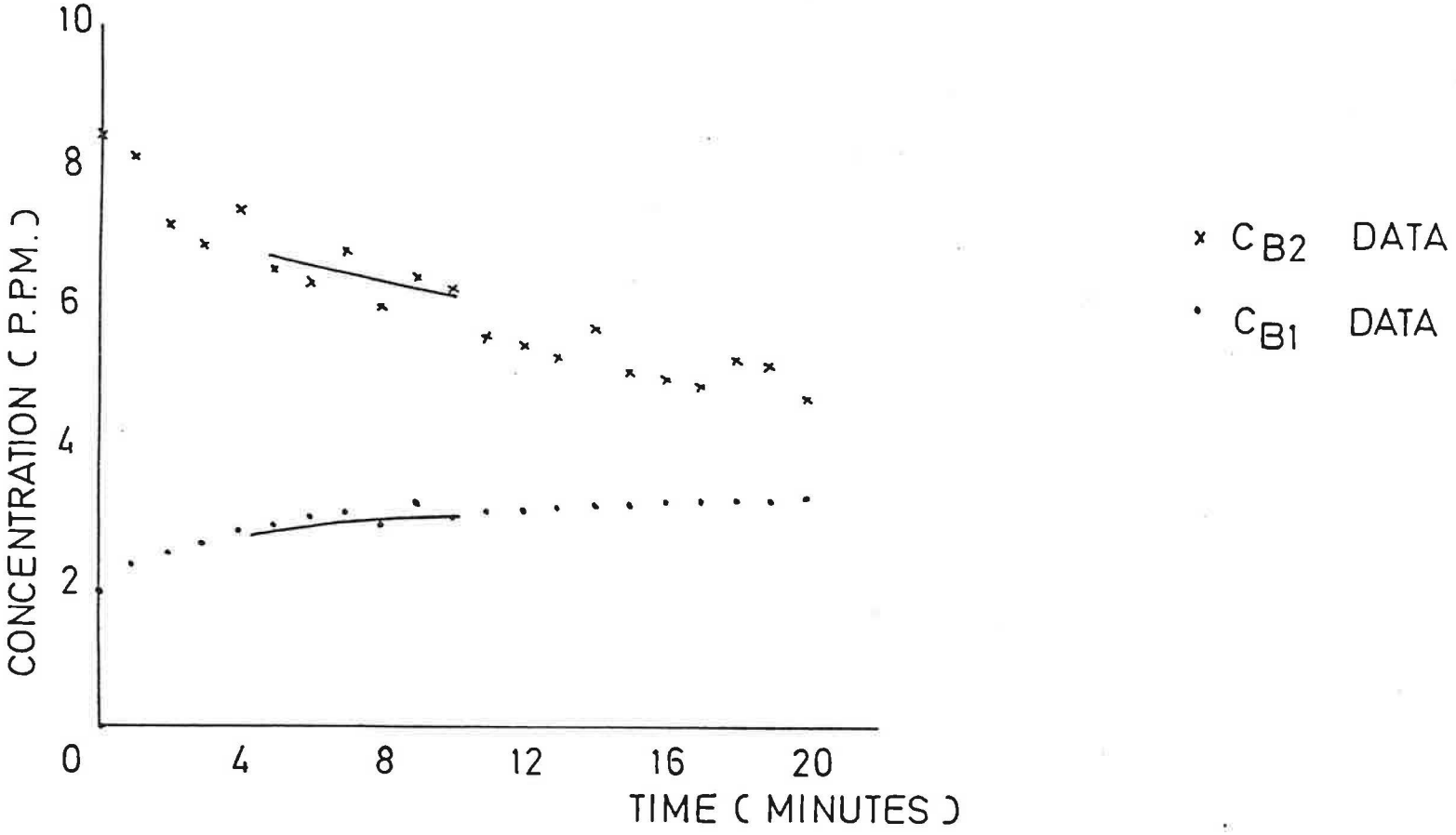

FIGURE A2 ESTIMATING CONCENTRATION GRADIENTS (C_B)

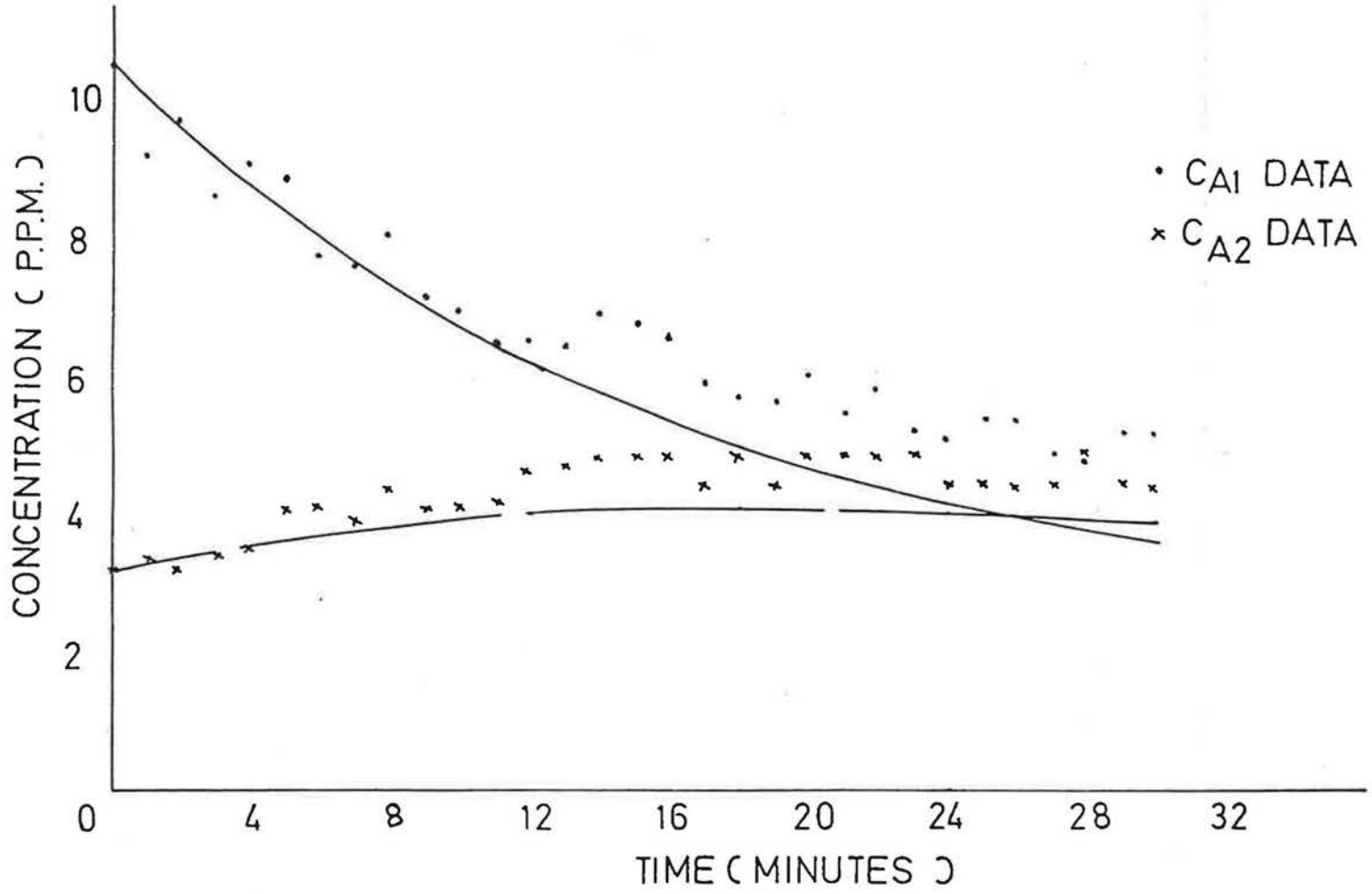

FIGURE A3 "GOODNESS-OF-FIT" FOR CA(t) USING PERERA ANALYSIS

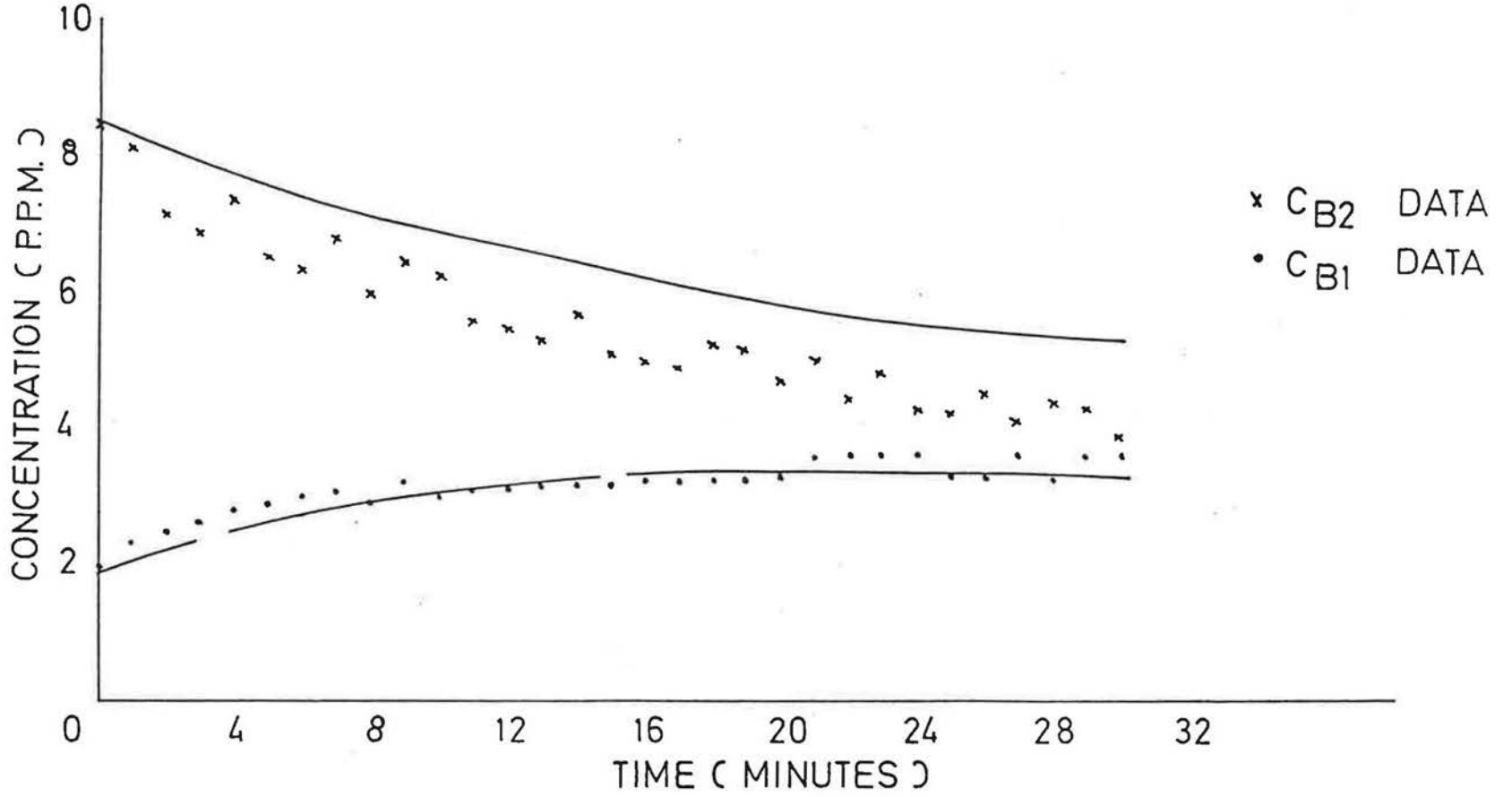

FIGURE A4 "GOODNESS-OF-FIT" FOR CB(t) USING PERERA ANALYSIS

APPENDIX (B)

APPENDIX (B)

METHOD 2 : CALCULATING TWO CELL, TWO DIRECTIONAL AIRFLOWS USING A WORKED EXAMPLE

B1) General

To simulate the effects of measurement errors on the calculation of inter-cell airflows using Penman's analysis equation (3.5.1), the conservation of mass of tracer gas equation, is solved for known airflows and initial tracer gas concentrations.

Figures (3) and (4) show the time histories of tracer gas (A) released in Cell (1) and tracer gas (B) released in Cell (2). The effects of imposing a random measurement error of $\pm$ 5% on each data point is also shown; by solving the resulting curve shapes using Penman's method of analysis for the "unknown" airflows (Q_{21}, Q_{12}, Q_{01},Q_{02}) we can quantify the resulting errors on our calculated values of inter-cell airflows and air change rates.

B2) Calculating Q_{21}, Q_{12}, Q_{01}, Q_{02}.

The time histories of tracer gas concentration, for the two cell case, are described by equations (3.5.3) - (3.5.6):

For Cell (1)

$$V_1[C_{A1(t2)} - C_{A1(t1)}] = [-\int_{t1}^{t2} C_{A1}\,dt]\ Q_{01} + [\int_{t1}^{t2} (C_{A2} - C_{A1})\,dt]\ Q_{21} \qquad (B.2.1)$$

$$V_1[C_{B1(t2)} - C_{B1(t1)}] = [-\int_{t1}^{t2} C_{B1}\,dt]\ Q_{O1} + [\int_{t1}^{t2} (C_{B2} - C_{B1})\,dt]\ Q_{21} \qquad (B.2.2.)$$

For Cell (2)

$$V_2[C_{A2(t2)} - C_{A2(t1)}] = [-\int_{t1}^{t2} C_{A2}\,dt]\ Q_{O2} + [\int_{t1}^{t2} (C_{A1} - C_{A2})\,dt]\ Q_{12} \qquad (B.2.3)$$

$$V_2[C_{B2(t2)} - C_{B2(t1)}] = [-\int_{t1}^{t2} C_{B2}\,dt]\ Q_{O2} + [\int_{t1}^{t2} (C_{B1} - C_{B2})\,dt]\ Q_{12} \qquad (B.2.4)$$

The tracer gas concentration, time points given in figures (3) and (4) are divided into several time periods.

(tj = 1, 2...K); Considering equation (B.2.1) and assuming that K=4 then equation (B.2.1) is solved using a "least square" approximation as suggested by Hildebrand [29].

Expressing equation (B.2.1) in generalized form:

$$V_1\ \delta C_k = -\ a_k Q_{O1} + b_k Q_{21} \qquad (B.2.5)$$

where δC_k is $= C_{A1(t2)} - C_{A1(t1)}$

$$a_k = \int_{t1}^{t2} C_{A1}\,dt$$

$$b_k = \int_{t1}^{t2} (C_{A2} - C_{A1})\,dt$$

1st Normal equation is:

$$V_1 \sum_{k=1}^{k=4} \delta C_k = -Q_{O1} \sum_{k=1}^{k=4} a_k + Q_{21} \sum_{k=1}^{k=4} b_k \qquad (B.2.6)$$

2nd normal equation is:

$$V_1 \sum_{k=1}^{k=4} \delta C_k b_k = -Q_{01} \sum_{k=1}^{k=4} a_k b_k + Q_{21} \sum_{k=1}^{K=4} b_k^2 \qquad \text{(B.2.7)}$$

With reference to figure (3), $C_{A(t)}$ concentration data gives values of a_k and b_k using numercial integration:

for k = 1 ,time (t1) = 0.083 hrs, (t2) = 0.116 hrs, δC_k = - 1.32

k = 2 , " (t1) = 0.133 hrs, (t2) = 0.166 hrs, δC_k = - 1.16

k = 3 , " (t1) = 0.166 hrs, (t2)= 0.2 hrs, δC_k = -0.35

k = 4 , " (t1) = 0.2 hrs, (t2)= 0.233 hrs, δC_k = -0.35

Simpsons rule yields the following values for a_k and b_k

k = 1, a_k = 0.52, b_k = - 0.25

k = 2, a_k = 0.48, b_k = - 0.21

k = 3, a_k = 0.48, b_k = - 0.20

k = 4, a_k = 0.43, b_k = - 0.12

Substituting into equation (B.2.6) for a_k, b_k, δC_k the first normal equation becomes:

$$- 318 = -1.91\ Q_{01} - 0.78 Q_{21} \qquad \text{(B.2.8)}$$

Similarly the 2nd normal equation (B.2.7) becomes:

$$- 68.2 = -0.37\ Q_{01} - 0.16\ Q_{21} \qquad \text{(B.2.9)}$$

Re-arranging equation (B.2.8) for Q_{01}:

$$Q_{01} = 166.5 - 0.41\ Q_{21} \qquad \text{(B.2.10)}$$

Similarly, re-arranging equation (B.2.9) for Q_{21} we obtain:

$$Q_{21} = 426.2 - 2.31\ Q_{01} \qquad \text{(B.2.11)}$$

Solving equations (B.2.10) and (B.2.11) by numerical iteration

$$Q_{01} = 28\ m^3/hr$$

$$Q_{21} = 362\ m^3/hr.$$

The calculated values of Q_{01}, and Q_{21} are based on tracer gas (A) concentration data in Cell (1), a second set of calculated values of Q_{01} and Q_{21} are available by using tracer gas (B) Concentration data.

Using tracer gas (B) data, the normal equations become:

$$50 = -0.81\ Q_{01} + 0.76\ Q_{21} \qquad \text{(B.2.12)}$$

$$10.1 = -0.15\ Q_{01} + 0.15\ Q_{21} \qquad \text{(B.2.13)}$$

Numerical iteration gives the following values:

$$Q_{01} = 110\ m^3/hr$$

$$Q_{21} = 177\ m^3/hr$$

The two remaining airflows Q_{O2} and Q_{12} are calculated in an identical manner using the tracer gas concentration data in Cell (2), when using tracer gas (A) data :

$Q_{O2} = 45\ m^3/hr$

$Q_{12} = 62\ m^3/hr$

and using tracer gas (B) data :

$Q_{O2} = 58\ m^3/hr$

$Q_{12} = 100\ m^3/hr$

B3) Errors in Calculated airflows

Comparison between "real" and "calculated" airflows Q_{O1}, Q_{O2}, Q_{12} and Q_{21} show the following errors:

$$\frac{\Delta Q_{O1}}{Q_{O1}} = \frac{|Q_{O_1(R)} - Q_{O1(C)}|}{Q_{O1(R)}} \times 100 \qquad (B.3.1)$$

From Cell (1), tracer gas (A) data gives

$$\frac{\Delta Q_{O1}}{Q_{O1}} = \frac{|75 - 28|}{75} \times 100 = 63\%$$

$$\frac{\Delta Q_{21}}{Q_{21}} = \frac{|200-362|}{200} \times 100 = 81\%$$

Tracer gas (B) data gives :

$$\frac{\Delta Q_{O1}}{Q_{O1}} = \frac{|75 - 110|}{75} \times 100 = 47\%$$

$$\frac{\Delta Q_{21}}{Q_{21}} = \frac{|200 - 177|}{200} \times 100 = 11.5\%$$

For Cell (2), tracer gas (A) data gives:

$$\frac{\Delta Q_{O2}}{Q_{O2}} = \frac{|50 - 45|}{50} \times 100 = 10\%$$

$$\frac{\Delta Q_{12}}{Q_{12}} = \frac{|200 - 62|}{200} \times 100 = 69\%$$

Tracer gas (B) data gives:

$$\frac{\Delta Q_{O2}}{Q_{O2}} = \frac{|50 - 58|}{50} \times 100 = 16\%$$

$$\frac{\Delta Q_{12}}{Q_{12}} = \frac{|200 - 100|}{200} \times 100 = 50\%$$

Such errors occur because of the method used to estimate the concentration difference term

$$\delta C_k = [C_{Al(t2)} - C_{Al(t1)}]$$

If the two concentration data points have a random error, then the most probable size of absolute error in the concentration difference term can be found from:

$$\Delta C_k = [\Delta C^2_{(t2)} + \Delta C^2_{(t1)}]^{\frac{1}{2}} \qquad (B.3.2)$$

where ΔC_k is the absolute standard error in the concentration difference over time period (K), (K = 1,2....K)

$\Delta C_{(t1)}$, $\Delta C_{(t2)}$ is the absolute standard error in tracer concentration at times $_{(t1)}$ and $_{(t2)}$ respectively.

Considering tracer gas (A), cell (1), for K = 1 equation (B.3.2) becomes:

$$\Delta C_{A1} = [0.44^2 + 0.38^2]^{\frac{1}{2}}$$

$$\Delta C_{A1} = \pm 0.58$$

The calculated concentration difference from site data is $\delta C_{A1} = 1.32$, therefore a random $\pm$ 5% error on the data may lead to approximately a 44% uncertainty in the concentration difference term. The same problems occur in all δC_k terms that are based on only two site data points of tracer gas concentrations. Hopefully, the larger the number of pairs of points (K) used, the more the effects of random errors on site data will be minimised.

Figures (B1) and (B2) show the effects of a random $\pm$ 5% error on concentration data, the poor estimates of inter-cell airflows result in large discrepancies between "site" data points and the theoretical curve shapes derived from such data.

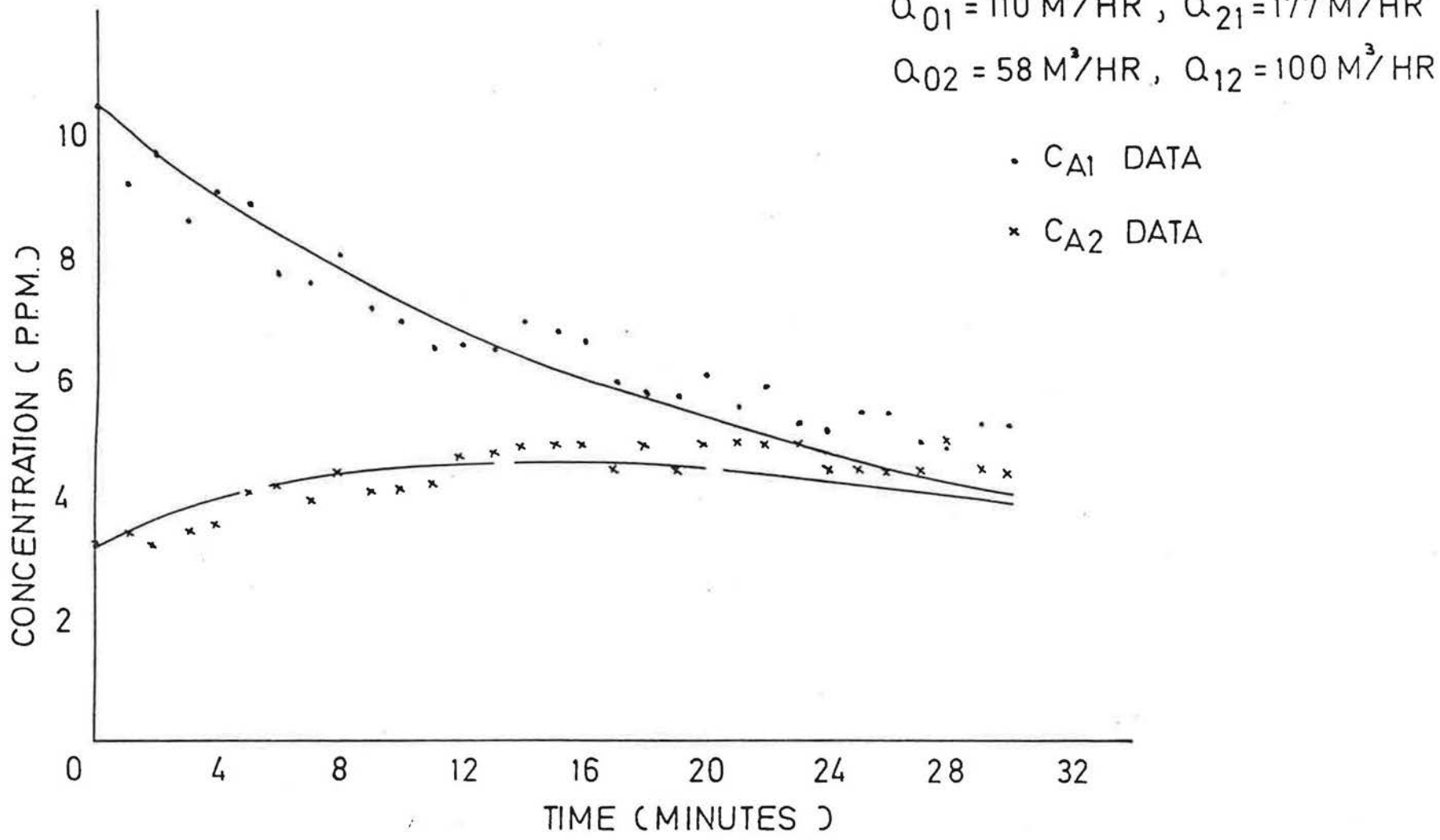

FIGURE B1 "GOODNESS-OF-FIT" FOR CA(t) USING PENMAN ANALYSIS

$Q_{01} = 110\ M^3/HR$, $Q_{21} = 177\ M^3/HR$

$Q_{02} = 58\ M^3/HR$, $Q_{12} = 100\ M/HR$

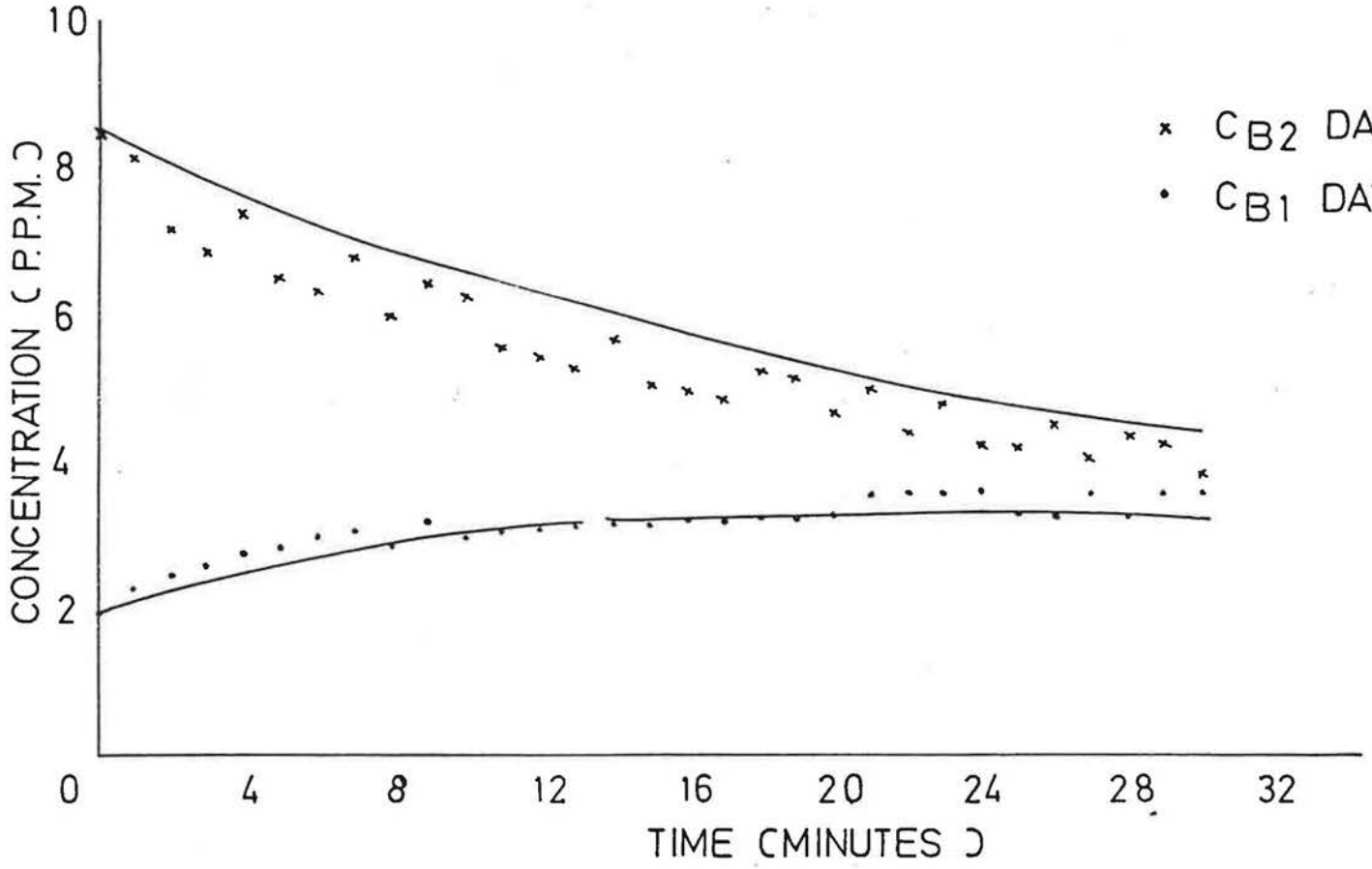

FIGURE B2 "GOODNESS-OF-FIT" FOR $C_B(t)$ USING PENMAN ANALYSIS

APPENDIX (C)

APPENDIX (C)

METHOD 3: CALCULATING TWO DIRECTIONAL, TWO CELL AIRFLOWS USING A WORKED EXAMPLE.

(C.1) General

To simulate the effects of measurment errors on the calculation of inter-cell airflows, equations (3.6.2) - (3.6.5) are solved for known airflows and initial tracer gas concentrations.

Figures (3) and (4) show the time histories of tracer gas (A) concentration released in Cell (1) and tracer gas (B) released in Cell (2). The effects of imposing a random measurement error of $\pm$ 5% on each data point is also shown. The resulting curve shapes can be solved for the "unknown" airflows using I'Ansons method and the resulting errors in the calculated values of inter-cell airflows quantified.

(C.2) Calculation of coefficients(Y) and (Z)

The time histories of tracer gas concentrations are described by equations (3.6.17) - (3.6.20).

For tracer gas (A)

$$C_{A1(t)} = A \exp(Yt) + B \exp(Zt) \qquad (C.2.1)$$

$$C_{A2(t)} = C \exp(Yt) + D \exp(Zt) \qquad (C.2.2)$$

The coefficients A,B,C,D,Y and Z are defined in Chapter (3), Section (3.11).

To calculate the coefficients (Y) and (Z) equation (C.2.1) can be rewritten as

$$C_{Al(t)} = A\ U_1^{\,t} + B\ U_2^{\,t} \qquad (C.2.3)$$

where $U_1 = \exp Y$, $U_2 = \exp Z$.

The coefficients U_1 and U_2 are found as the roots of algebraic equation

$$U^2 - \alpha_1 U - \alpha_2 = 0 \qquad (C.2.4)$$

α_1 and α_2 are calculated from observed values of tracer gas concentration. Using a least square method suggested by Hildebrand [29], α_1 and α_2 are found as follows:

$$\alpha_1 \sum_{K=1}^{K-2} C_{(k)} + \alpha_2 \sum_{K=0}^{K-3} C_{(k)} = \sum_{K=2}^{K-1} C_{(k)} \qquad (C.2.5)$$

$$\alpha_1 \sum_{K=1}^{K-1} C_{(k)} \cdot C_{(k-1)} + \alpha_2 \sum_{K=0}^{K-3} C_{(k)}^2 = \sum_{K=2}^{K-1} C_{(k)} \cdot C_{(K-2)} \qquad (C.2.6)$$

U_1 and U_2 are then found as the roots of equation (C.2.4). C_{Al} data therefore enables an estimate of the coefficients.

(Y) and (Z). The preceding method of estimating (Y) and (Z) can be repeated for a second estimate of these coefficients using C_{A2} data.

With reference to figure (3), using $C_{A1(t)}$ concentration data between time $_{(t)}$ = 0.083 hours and $_{(t)}$ = 0.166 hours to estimate α_1 and α_2, equations (C.1.5) and (C.1.6) become

$$22.72\alpha_1 + 23.37\alpha_2 = 22.11 \qquad \text{(C.2.7)}$$

$$176.72\alpha_1 + 182.2\alpha_2 = 172.15 \qquad \text{(C.2.8)}$$

solving for α_1, α_2 we obtain

$$\alpha_1 = 0.543, \quad \alpha_2 = 0.418$$

Substituting these values into equation (C.2.4)

$$U^2 - 0.543U - 0.418 = 0 \qquad \text{(C.2.9)}$$

Solving U_1 and U_2

$$U_1 = \frac{0.543 + (0.543)^2 - (4 \times 0.418)}{2} \qquad \text{(C.2.10)}$$

U_1 has complex roots

Similarly

$$U_2 = \frac{0.543 - (0.543)^2 - (4 \times 0.418)}{2} \qquad \text{(C.2.11)}$$

and U_2 has complex roots.

If C_{A2} data is used to calculate the coeffcients (Y) and (Z) the roots of equation (C.2.4) U_1 and U_2 are also complex.

Therefore using I'Ansons method this "site" data would be regarded as unsuitable for analysis. The same difficulties occur if the concentration data found using tracer (B) were used. It is apparent that the method of analysis adopted by I'Anson is extremely sensitive to measurement errors on observed data.

To illustrate this point, let us repeat the process of calculating α_1 and α_2 for C_{A1} concentration data which are exact but have been rounded to one decimal place (the solid line figure (3))

Equations (C.2.5) and (C.2.6) become:

$$23.8\alpha_1 + 24.5\alpha_2 = 23.1 \qquad \text{(C.2.12)}$$

$$194.5\alpha_1 + 200.2\alpha_2 = 188.75 \qquad \text{(C.2.13)}$$

solving for α_1 and α_2

$\alpha_1 = 2.45$ $\alpha_2 = -1.43$

Substituting these values into equation (C.2.4)

$$U^2 - 2.45U + 1.43 = 0 \qquad \text{(C.2.14)}$$

The roots U_1, U_2 of equation (C.2.14) are

$U_1 = 1.49$, $U_2 = 0.96$

The values U_1 and U_2 for C_{A1} tracer gas concentration data correct to three decimal places are

$U_1 = 0.98$, $U_2 = 0.91$

This implies that round off errors on the observed data causes an error of 5% - 50% in the calculated coeffcients U_1, U_2 for the worked example given.

Bearing in mind that the calculated coefficients U_1 and U_2 are in turn used to calculate coefficients A,B,C and D it is apparent that the effects of observation errors will impose large errors on the calculated airflows and all ventilation rates. As has been shown here if random measurement errors are of the order $\pm$ 5% the roots of the quadratic equation (C.2.4) are found to be complex.

APPENDIX (D)

APPENDIX (D)

CALCULATING 2 CELL AIRFLOWS USING A WORKED EXAMPLE

D1) General

To simulate the effects of measurement errors on the calculation of inter-cell airflows using the analysis method shown in chapter (4), the conservation of mass of tracer gas equation (4.2.1) is solved for known airflows and initial tracer gas concentrations.

Figures (10) and (11) show the time histories of tracer gas (A) released in Cell (1) and tracer gas (B) released in Cell (2). The effects of imposing a random measurement error of $\pm$ 5% on each data point is also shown, by solving the resulting curve shapes for the "unknown" airflows (N_1, N_2, Q_{12}, Q_{21}) we can quantify the resulting errors on the calculated values of inter-cell airflows and air change rates.

D2) Calculating N_1, Q_{21}, N_2, Q_{12}

The unknown airflows and cell air change rates are found from equations (4.3.16) - (4.3.19):

$$N_1 = \frac{1}{A} - \frac{\tilde{C}_{A1}}{CO_{A1}A} + \frac{Q_{21}CO_{A2}}{V_1 CO_{A1} A} \frac{(e^{-N_2' t} - e^{-N_1' t})}{(N_1' - N_2')} \qquad (D2.1)$$

$$Q_{21} = \frac{[\tilde{C}_{B1} + CO_{B1}(N_1 A - 1)][V_1(N_1' - N_2')]}{CO_{B2}[\exp(-N_2' t) - \exp(-N_1' t)]} \qquad (D2.2)$$

$$N_2 = \frac{1}{D} - \frac{\tilde{C}_{B2}}{CO_{B2} D} + \frac{Q_{12} CO_{B1}}{V_2 CO_{B2} D} \frac{(\exp(-N_1' t) - \exp(-N_2' t))}{(N_2' - N_1')} \qquad (D2.3)$$

$$Q_{12} = \frac{[\tilde{C}_{A2} + CO_{A2}(DN_2 - 1)][V_2(N_2' - N_1')]}{CO_{A1}[\exp(-N_1' t) - \exp(-N_2' t)]} \qquad (D2.4)$$

The first order estimates of Cell (1) and Cell (2) air change rates N_1' and N_2', are found from a least squares fit of $C_{A1(t)}$ data (figure (10)) and $C_{B2(t)}$ data (figure (11)). Taking the first six data points in each case and using the computer program (G1) given in appendix (G), the first order estimates of cell air change rates are:

N_1' = 1.71 air changes/hour

N_2' = 2.77 air changes/hour

Reference to figure (D1) shows the result of the least squares fit of Ln $C_{(t)}$ data plotted against time.

The remaining unknowns in equations (D.2.1) - (D.2.4) are $\tilde{C}_{A1}$, $\tilde{C}_{B1}$, $\tilde{C}_{A2}$, $\tilde{C}_{B2}$, A and D.

The mean concentrations of tracer gas $\tilde{C}_{A1}$, $\tilde{C}_{B1}$, $\tilde{C}_{A2}$ and $\tilde{C}_{B2}$. are found by numerical integration of <u>all</u> data points.

Considering CA_1, Using Simpson's rule:

$$\int_{t=0}^{t=t} C_{Al(t)}\,dt = \frac{h}{3}\left[C_{Al(o)} + 4C_{Al(1)} + C_{Al(2)} + 4C_{Al(3)} + \ldots.C_{Al(t)}\right] \qquad (D2.5)$$

$$\text{and } \tilde{C}_{Al} = \frac{\int_{t=0}^{t=t} C_{Al(t)}\,dt}{{}_{o}\Delta t_{t}} \qquad (D2.6)$$

Taking each $C_{Al(t)}$ data point between t = 0 and t =0.25 hours

$\tilde{C}_{Al(t)}$ = 7.65 ppm, where (t)= 0.125 hours

Similarly $\tilde{C}_{A2(0.125)}$ = 4.1 ppm

$\tilde{C}_{B1(0.125)}$ = 3ppm , $\tilde{C}_{B2(0.125)}$ = 6.4 ppm

The remaining unknowns A and D are Maclaurin series expansions for N_1' and N_2' found from :

$$A = -t + \frac{N_1' t^2}{2!} - \frac{N_1'^2 t^3}{3!} + \frac{N_1'^3 t^4}{4!} - \frac{N_1'^4 t^5}{5!} \quad X\ (-1) \qquad (D2.7)$$

$$D = -t + \frac{N_2' t^2}{2!} - \frac{N_2'^2 t^3}{3!} + \frac{N_2'^3 t^4}{4!} - \frac{N_2'^4 t^5}{5!} \quad X\ (-1) \qquad (D2.8)$$

where time (t) = 0.125 hrs

$$A = \left(-0.125 + \frac{1.71 \times 0.125^2}{2!} - \frac{1.71^2 \times 0.125^3}{3!} + \frac{1.71^3 \times 0.125^4}{4!} - \frac{1.71^4 \times 0.125^5}{5!}\right) \times (-1$$

A = 0.113

Similarly D = 0.105

Substituting into equation (D2.1), N_1 becomes:

$$N_1 = \frac{1}{0.113} - \frac{7.65}{0.113 \times 10} + \frac{Q_{21}\ 3.15}{100 \times 10 \times 0.113} \qquad \frac{0.707 - 0.8075}{1.71 - 2.77}$$

$$N_1 = 2.07 + 0.0026\ Q_{21} \qquad \text{(D2.9)}$$

Similarly equation (D2.2) becomes for Q_{21}

$$Q_{21} = 142 + 28\ N_1 \qquad \text{(D2.10)}$$

Iterating equations (D2.9) and (D2.10) gives

N_1 = 2.63 Air changes/hour, Q_{21} = 215 m^3/hour

Solving equations (D2.3) and (D2.4) for N_2, Q_{12}

$$N_2 = \frac{1}{0.105} - \frac{6.4}{8.27 \times 0.105} + \frac{Q_{12}\ 1.9}{100 \times 8.27 \times 0.105} \qquad \frac{0.8075 - 0.707}{2.77 - 1.71}$$

$$N_2 = 2.15 + 0.002\ Q_{12} \qquad \text{(D2.11)}$$

And for Q_{12}

$$Q_{12} = 101.1 + 35.2\ N_2 \qquad \text{(D2.12)}$$

Iterating equations (D2.11) and (D2.12) gives

N_2 = 2.54 Air changes/hour, Q_{12} = 190 m^3/hour

The computer program (G2) given in Appendix (G), calculates values for the four unknown airflows (N_1, N_2, Q_{12} and Q_{21}).

D3) Error estimates in N_1, N_2, Q_{12}, Q_{21}.

Considering the absolute standard error in the calculated value of N_1, Chapter (4), section (4.4), equation (4.4.2) gives us:

$$(\Delta N_1)^2 = \left|\frac{\partial N_1}{\partial N_1'}\Delta N_1'\right|^2 + \left|\frac{\partial N_1}{\partial N_2'}\Delta N_2'\right|^2 + \left|\frac{\partial N_1}{\partial CO_{A1}}\Delta CO_{A1}\right|^2 + \left|\frac{\partial N_1}{\partial CO_{A2}}\Delta CO_{A2}\right|^2 +$$

$$\left|\frac{\partial N_1}{\partial \tilde{C}_{A1}}\Delta \tilde{C}_{A1}\right|^2 + \left|\frac{\partial N_1}{\partial V_1}\Delta V_1\right|^2 + \left|\frac{\partial N_1}{\partial Q_{21}}\Delta Q_{21}\right|^2 + \left|\frac{\partial N_1}{\partial A}\Delta A\right|^2 \qquad (D3.1)$$

The partial derivates can be evaluated from equations (4.4.3) - (4.4.10); considering the first partial derivative $\frac{\partial N_1}{\partial N_1'}$

from equation (4.4.3) :

$$\frac{\partial N_1}{\partial N_1'} = \frac{(CO_{A1}AV_1)(N_1'-N_2')(Q_{21}CO_{A2}te^{-N_1't}) - (Q_{21}CO_{A2}(e^{-N_2't} - e^{-N_1't})CO_{A1}AV_1)}{[CO_{A1}AV_1(N_1' - N_2')]^2} \qquad (D3.2)$$

$$\frac{\partial N_1}{\partial N_1'} = \frac{(10\times0.113\times100)(1.71-2.77)(215\times3.15\times0.125\times0.8075)}{[10\times0.113\times100(1.71-2.77)]^2} -$$

$$\frac{(215\times3.15(0.7073-0.8075)\times10\times0.113\times100)}{[10\times0.113\times100(1.71-2.77)]^2}$$

$$\frac{\partial N_1}{\partial N_1'} = -\frac{8265.4}{14619.23} + \frac{7668.23}{14619.23}$$

$$\frac{\partial N_1}{\partial N_1'} = 0.04$$

Similar calculations give values for the remaining partial derivatives in equation (D3.1), therefore the absolute standard error in N_1 is calculated from:

$$\Delta N_1^2 = |0.04\Delta N_1'|^2 + |0.04\Delta N_2'|^2 + |0.125\,\Delta CO_{A1}|^2 + |0.152\,\Delta CO_{A2}|^2 +$$

$$|0.8\,\Delta\tilde{C}_{A1}|^2 + |0.005\,\Delta V_1|^2 + |0.0024\,\Delta Q_{21}|^2 + |21.43\Delta A|^2 \qquad \text{(D3.3)}$$

where $N_1 = |2.75 - 2.63| = 0.12$

$N_2 = |2.5 - 2.54| = 0.04$

$CO_{A1} = |10 - 10| = 0$

$CO_{A2} = |3 - 3.15| = 0.15$

$C_{A1} = |7.83 - 7.65| = 0.18$

$V_1 = |100 - 100| = 0$

$Q_{21} = |200 - 215| = 15$

$A = |0.1057 - 0.113| = 0.007$

Substituting for these values into equation (D3.3) gives the absolute standard error in N_1 of:

$\Delta N_1 = \pm 0.21$ air changes/hour

Therefore $N_1 = 2.63 \pm 0.21$ Air changes/hour

Similar calculations enable estimates of the absolute errors for N_2, Q_{21} and Q_{12} using equations (4.4.12) - (4.4.40) given in section (4.4), Chapter (4).

APPENDIX (E)

APPENDIX (E)

CALCULATING 3 CELL AIRFLOWS USING A WORKED EXAMPLE

E1) General

To simulate the effects of measurement errors on the calculation of inter-cell airflows using the analysis method shown in Chapter (5) the conservation of mass of tracer gas equation (5.2.1) is solved for known airflows and initial tracer gas concentrations.

Figures (16), (17) and (18) show the time histories of tracer gas (A) released in Cell (1), gas (B) released in Cell (2) and gas (C) released in Cell (3) respectively. The effects of imposing a random measurement error of $\pm$ 5% on each data point is also shown; by solving the resulting curve shapes for the "unknown" airflows (N_1, N_2, N_3, Q_{12}, Q_{13}, Q_{23}, Q_{32}, Q_{21}, Q_{31}), the resulting errors on the calculated values of inter-cell airflows may be estimated.

E2) Calculating N_1, Q_{21} and Q_{31}

The unknown airflows and cell air change rates are found from equations (5.3.10) -(5.3.18); considering Cell (1) only

$$N_1 = \frac{1}{A} - \frac{\tilde{C}_{A1}}{CO_{A1}A} + \frac{Q_{21}\ CO_{A2}}{V_1 CO_{A1}A}\ \frac{(e^{-N_2't} - e^{-N_1't})}{(N_1' - N_2')} + \frac{Q_{31}\ CO_{A3}}{V_1 CO_{A1}A}\ \frac{(e^{-N_3't} - e^{-N_1't})}{(N_1' - N_3')} \qquad (E2.1)$$

$$Q_{21} = \frac{\left(\tilde{C}_{B1} + CO_{B1}(N_1 A - 1) - \frac{Q_{31} CO_{B3}}{V_1}\left(\frac{e^{-N_3' t} - e^{-N_1' t}}{(N_1' - N_3')}\right)\right) V_1 (N_1' - N_2')}{CO_{B2}[\exp(-N_2' t) - \exp(-N_1' t)]} \quad \text{(E2.2)}$$

$$Q_{31} = \frac{\left(\tilde{C}_{C1} + CO_{C1}(N_1 A - 1) - \frac{Q_{21} CO_{C2}}{V_1}\left(\frac{e^{-N_2' t} - e^{-N_1' t}}{(N_1' - N_2')}\right)\right) V_1 (N_1' - N_3')}{CO_{C3}\,(\exp(-N_3' t) - \exp(-N_1' t))} \quad \text{(E2.3)}$$

The first order estimates of Cell (1), Cell (2) and Cell (3) air change rates N_1', N_2' and N_3' are calculated from a least square fit of $C_{A1(t)}$ data (figure 16), $C_{B2(t)}$ data (figure 17) and $C_{C3(t)}$ data (figure 18)

Taking the first six data points and using the computer program (G1) in appendix (G), the first order estimates of cell air change rates are:

N_1' = 3 air changes/hour

N_2' = 1.2 air changes/hour

N_3' = 1.8 air changes/hour

Of the remaining unknowns in equation (E2.1)-(E2.3), the mean concentrations of tracer gas $\tilde{C}_{A1}$, $\tilde{C}_{B1}$, $\tilde{C}_{C1}$ are found by numerical integration of <u>all</u> data points.

Considering $\tilde{C}_{A1}$, using Simpson's rule:

$$\int_{t=0}^{t=t} C_{A1(t)}\,dt = \frac{h}{3}\left(C_{A1(o)} + 4C_{A1(1)} + C_{A1(2)} + 4\,C_{A1(3)} + \ldots\ldots C_{A1(t)}\right) \quad \text{(E2.4)}$$

and $$\tilde{C}_{A1} = \frac{\int_{t=0}^{t=t} C_{A1(t)}\,dt}{\Delta t} \quad \text{(E2.5)}$$

$0\ t$

Considering the time interval t = 0, t =0.2 hours from Simpson's rule $\tilde{C}_{A1(t)}$ = 9.45 ppm, where t = 0.1 hours.

Similarly $\tilde{C}_{B1(0.1)}$ = 1.84 ppm, $\tilde{C}_{C1(0.1)}$ = 3.87 ppm.

The remaining mean concentrations are found in an identical manner using numerical integration and have the following values:

$\tilde{C}_{A2(0.1)}$ = 4.18 ppm, $\tilde{C}_{B2(0.1)}$ = 8.61 ppm, $\tilde{C}_{C2(0.1)}$ = 2.03 ppm

$\tilde{C}_{A3(0.1)}$ = 1.94 ppm, $\tilde{C}_{B3(0.1)}$ = 3.53ppm, $\tilde{C}_{C3(0.1)}$ = 9.49 ppm.

With reference to figures (16) (17) and (18) the initial tracer gas concentrations at time zero are as follows:

CO_{A1} = 12.6 ppm, CO_{B1} = 0.95 ppm, CO_{C1} = 4.2 ppm.

CO_{A2} = 3.8 ppm, CO_{B2} = 10.45 ppm, CO_{C2} = 1.57 ppm

CO_{A3} = 1.05 ppm, CO_{B3} = 3.15 ppm, CO_{C3} = 11.55 ppm.

The remaining unknown A, is found using a Maclaurin expansion for N_1 and is found from:

$$A = -t + \frac{N_1' t^2}{2!} - \frac{N_1'^2 t^3}{3!} + \frac{N_1'^3 t^4}{4!} - \frac{N_1'^4 t^5}{5!} \quad X\ (-1) \qquad (E2.6)$$

where time (t) = 0.1 hours

$$A = -0.1 + \frac{(3x.1)^2}{2!} - \frac{3^2 x.1^3)}{3!} + \frac{(3^3 x.1^4)}{4!} - \frac{(3^4 x.1^5)}{5!} \times (-1)$$

A = 0.086

$$= \frac{1}{0.086} - \frac{9.45}{12.6 \times 0.086} + \frac{Q_{21} 3.8}{100 \times 12.6 \times .086} \frac{0.887-0.741}{3-1.2} + \frac{Q_{31} 1.05}{100 \times 12.6 \times .086} \frac{0.835-0.741}{3-1.8}$$

$$N_1 = 2.9 + 0.0028Q_{21} + 0.00076Q_{31} \qquad \text{(E2.7)}$$

Similarly equation (E2.2) becomes:

$$Q_{21} = \frac{1.84 + 0.95(0.086N_1 - 1) - \frac{Q_{31} 3.15}{100} \frac{0.094}{1.2} \times 100 \ (3-1.2)}{10.45 \ [0.887 - 0.741]}$$

$$Q_{21} = 9.63 \ N_1 + 105 - 0.29 \ Q_{31} \qquad \text{(E2.8)}$$

And equation (E2.3) becomes:

$$Q_{31} = \frac{3.87 + 4.2(0.086N_1 - 1) - \frac{Q_{21} 1.57}{100} \frac{0.146}{1.8} \times 100 \ (3-1.8)}{11.55 \ [0.835 - 0.741]}$$

$$Q_{31} = 39.7N_1 - 36.3 - 0.14Q_{21} \qquad \text{(E2.9)}$$

Iterating equations (E2.7) - (E2.9) gives:

N_1 = 3.25 Air changes/hour

Q_{21} = 113 m^3/hour

Q_{31} = 77 m^3/hour

The unknown airflows and airchange rates in cell (2) and cell (3) are found by solving equation (5.3.13) - (5.3.18).in a similar manner.

The computer program (G3) given in appendix (G) solves, by numerical iteration, all the nine unknown airflows and air change rates for the 3 cell case.

The remaining airflows are:

N_2 = 2.07 Air changes/hour

Q_{12} = 106 m^3/hour

Q_{32} = 42 m^3/hour

N_3 = 2.34 Air changes/hour

Q_{13} = 75 m^3/hour

Q_{23} = 111 m^3/hour.

E3) Estimating errors in calculated airflows using "real" data.

Considering the absolute standard error in the calculated value of N_1, the major sources of error are described by equation (5.6.1), Chapter (5) which gives:

$$(\Delta N_1^2) = \left|\frac{\partial N_1}{\partial CO_{A1}} \Delta CO_{A1}\right|^2 + \left|\frac{\partial N_1}{\partial CO_{A2}} \Delta CO_{A2}\right|^2 + \left|\frac{\partial N_1}{\partial CO_{A3}} \Delta CO_{A3}\right|^2 + \left|\frac{\partial N_1}{\partial \tilde{C}_{A1}} \Delta \tilde{C}_{A1}\right|^2 + \left|\frac{\partial N_1}{\partial A} \Delta A\right|^2 \quad \text{(E3.1)}$$

The major sources of errors in N_1 which can be estimated are caused by uncertainties in:

CO_{A1}, CO_{A2}, CO_{A3}, $\tilde{C}_{A1}$ and A.

The partial derivatives of equation (E2.1) are calculated from equations (5.4.6) - (5.4.10), section (5.4), Chapter (5).

Equation (5.4.6) for $\frac{\partial N_1}{\partial CO_{A1}}$ is:

$$\frac{\partial N_1}{\partial CO_{A1}} = \frac{\tilde{C}_{A1}}{CO_{A1}^2 A} - \frac{Q_{21} CO_{A2}}{CO_{A1}^2 A V_1} \frac{e^{-N_2' t} - e^{-N_1' t}}{(N_1' - N_2')} - \frac{Q_{31} CO_{A3}}{V_1 CO_{A1}^2 A} \frac{e^{-N_3' t} - e^{-N_1' t}}{(N_1' - N_3')} \qquad (E3.2)$$

$$= \frac{9.45}{12.6^2 \times .086} - \frac{113 \times 3.8}{12.6^2 \times 0.86 \times 100} \frac{0.813 - 0.722}{1.18} - \frac{77 \times 1.05}{100 \times 12.6^2 \times .086} \frac{.791 - .722}{0.91}$$

$$\frac{\partial N_1}{\partial CO_{A1}} = 0.66$$

Equation (5.4.7) for $\frac{\partial N_1}{\partial CO_{A2}}$ is

$$\frac{\partial N_1}{\partial CO_{A2}} = \frac{Q_{21}}{CO_{A1} V_1 A} \frac{(e^{-N_2' t} - e^{-N_1' t})}{(N_1' - N_2')} \qquad (E3.3)$$

$$\frac{\partial N_1}{\partial CO_{A2}} = \frac{113}{12.6 \times 100 \times .086} \frac{0.813 - 0.722}{1.18}$$

$$\frac{\partial N_1}{\partial C_{A2}} = 0.08$$

Equation (5.4.8) for $\frac{\partial N_1}{\partial CO_{A3}}$ is:

$$\frac{\partial N_1}{\partial CO_{A3}} = \frac{Q_{31}}{CO_{A1} V_1 A} \frac{(e^{-N_3' t} - e^{-N_1' t})}{(N_1' - N_3')} \qquad \text{(E3.4)}$$

$$\frac{\partial N_1}{\partial CO_{A3}} = \frac{77}{(12.6 \times 100 \times .086)} \frac{(0.791 - 0.722)}{0.91}$$

$$\frac{\partial N_1}{\partial CO_{A3}} = 0.054$$

Equation (5.4.9) for $\frac{\partial N_1}{\partial \tilde{C}_{A1}}$ is:

$$\frac{\partial N_1}{\partial \tilde{C}_{A1}} = - \frac{1}{CO_{A1} A} \qquad \text{(E3.5)}$$

$$\frac{\partial N_1}{\partial \tilde{C}_{A1}} = - \frac{1}{12.6 \times 0.086}$$

$$\frac{\partial N_1}{\partial \tilde{C}_{A1}} = - 0.92$$

Equation (5.4.10) for $\frac{\partial N_1}{\partial A}$ is :

$$\frac{\partial N_1}{\partial A} = -\frac{1}{A^2} + \frac{\tilde{C_{A1}}}{CO_{A1}A^2} - \frac{Q_{21}CO_{A2}}{V_1CO_{A1}A^2}\frac{(e^{-N_2't} - e^{-N_1't})}{(N_1' - N_2')} - \frac{Q_{31}CO_{A3}}{V_1CO_{A1}A^2}\frac{(e^{-N_3't} - e^{-N_1't})}{(N_1' - N_3')}$$

(E3.6)

$$\frac{\partial N_1}{\partial A} = -\frac{1}{.086} + \frac{9.45}{12.6x.086^2} - \frac{113 \times 3.8}{100x12.6x.086^2}\,0.077 - \frac{77 \times 1.05}{100x12.6x.086^2}\,0.076$$

$$\frac{\partial N_1}{\partial A} = -38$$

Substituting these values into equation (E3.1):

$$(\Delta N_1)^2 = |0.66\Delta CO_{A1}|^2 + |0.08\,\Delta CO_{A2}|^2 + |0.054\Delta CO_{A3}|^2 + |0.92\Delta \tilde{C_{A1}}|^2 + |38\Delta A|^2$$

The uncertainties in CO_{A1}, CO_{A2} and CO_{A3} are estimated using equation (5.6.4):

$$\Delta CO_{A1} = \frac{\sum_{1}^{P} |C_{A1(s)} - C_{A1(c)}|}{P} \qquad \text{(E3.7)}$$

where P is the number of data points, and $C_{A1(s)}$ is a measured concentration of C_{A1} at time (t).

$C_{A1(c)}$ is the calculated value of C_{A1} concentration at time (t).

See Figure (E1)

Using the data given in figure (16) and equation (E3.7), the uncertainties in CO_{A1}, CO_{A2} and CO_{A3} are :

CO_{A1} = 0.41 ppm

CO_{A2} = 0.19 ppm

CO_{A3} = 0.08 ppm

Similarly the uncertainties in $\tilde{C}_{A1(t)}$ are found from equation (5.6.5):

$$\Delta \tilde{C}_{A1(t)} = | \tilde{C}_{A1(t)(s)} - C_{A1(t)(c)} | \qquad \text{(E3.8)}$$

where $\tilde{C}_{A1(t)(s)}$ is calculated from numerical integration

$C_{A1(t)(c)}$ is calculated from fundamental tracer equation using calculated airflows derived from site data. (see Figure 19)

From figure (19), $CA_{1(t)(c)}$ = 9.55 ppm, $CA_{1(t)(s)}$ = 9.45 ppm

$\Delta \tilde{C}_{A1(t)}$ = 0.10 p.p.m.

The uncertainty in A, the Maclaurin expansion is found from equation (5.6.6):

$$\Delta A = \left| A - \frac{(1 - e^{-N_1 t})}{N_1} \right| \qquad \text{(E3.9)}$$

$$\Delta A = \left| 0.086 - \frac{(1 - e^{-(3.25 \times 0.1)})}{3.25} \right|$$

ΔA = 0.00062

Equation (E3.1) becomes:

$$(\Delta N_1)^2 = |0.66 \times 0.41|^2 + |0.08 \times 0.19|^2 + |0.054 \times 0.08|^2 + |0.92 \times 0.1|^2 + |38 \times 0.00062|^2$$

$$\Delta N_1 = \pm \ 0.28 \text{ Air Changes/hour}$$

The errors in the remaining airflows can be calculated in a similar manner using the error equations given in Chapter (5), Section (5.4).

APPENDIX (F) PUBLISHED PAPERS

ENERGY EFFICIENT DOMESTIC VENTILATION SYSTEMS FOR ACHIEVING ACCEPTABLE INDOOR AIR QUALITY

3rd AIC Conference, September 20-23 1982, London, UK

PAPER

VENTILATION AND INTERNAL AIR MOVEMENTS FOR SUMMER AND WINTER CONDITIONS

A T HOWARTH, P J BURBERRY, C IRWIN AND S J I'ANSON

Department of Building, University of Manchester Institute of Science and Technology, PO Box 88, Sackville Street, Manchester, M60 1QD, U.K.

SYNOPSIS

Present standards of ventilation have been established for many years. Until very recently, except in air conditioned buildings, the form, fenestration and workmanship in buildings were not dissimilar to those of 60 or 70 years ago when bathing habits were much more restrained and the air in dwellings had to be able to cope with a variety of unflued gas appliances. There was no pressing need, however, to modify standards. Recently the thermal problems of building design have concentrated attention upon the need for more precisely controlled ventilation. The motivation arises from changes in patterns of occupancy, types of heating installation, changes in fenestration, changes in the thermal mass of buildings and from external noise levels. There are two major aspects. One is providing adequate levels of ventilation to assist in controlling peak summer time temperatures and the other is the need to reduce ventilation rates to a minimum to conserve energy. This paper distinguishes the problems of designing natural ventilation systems for summer and winter conditions and discusses in detail the objectives, methods and some field studies directed towards the solution of winter ventilation problems.

Experimental work has been conducted in a 'low energy' house equipped with adjustable slot ventilators in the window frames. Both tracer gas decay methods and pressurisation tests indicate similar increases of air flow when the ventilators were opened.

1. INTRODUCTION

The relative importance of ventilation in terms of energy conservation has increased very rapidly in recent years. Restrictions on window area and stringent requirements for insulation standards in walls, roofs and floors mean that, in modern dwellings, ventilation is a dominant element in heat loss. At first thought it is very surprising that no legislation exists in the U.K. to control ventilation rates. The situation is, however , similar in most other developed countries. The explanation lies in the difficulty of designing to achieve a given ventilation standard and also of testing to see whether particular standards have been achieved. The conventional methods of assessing ventilation rates using tracer gases are elaborate and time consuming; they require highly skilled operators and the results are subject to weather influences making it difficult to produce results which would be sufficiently definitive for legal purposes. Pressurisation techniques provide a relatively simple comparison of airtightness of buildings, but there is no well established technique of using the results of pressurisation tests to predict the natural ventilation rates of the building in use.

2. SUMMER AND WINTER VENTILATION

Opening lights in windows have served the purposes of ventilation for many years and it may be questioned why they cannot continue to do so. In this context it is important to distinguish between the requirements of summer time ventilation and the problems of minimum ventilation rates in winter. In non air conditioned buildings opening lights in windows serve fairly effectively to control the high rates of ventilation appropriate to summer conditions. Disturbance of papers and curtains can represent an annoyance but generally speaking the degree of controllability afforded by relatively large opening lights works well.

It does not work well in winter conditions and particularly so in circumstances where security demands that, while occupants are absent, windows should be secured. In winter time even a very narrow opening of a large opening light gives relatively high rates of ventilation and is likely to result in draughts being experienced because of the usual location of opening lights. Prolonged closure of the windows did not however represent a serious problem in the past. Habitable rooms were required to have either a flue or a special ventilator to fresh air. Quite apart from these provisions, the general level of airtightness of both the construction and the windows themselves tended to be low so that a significant rate of ventilation would take place even when the opening lights themselves were shut. Window manufacturers have, for some time, been concerned to improve the effectiveness of sealing of their windows and this, coupled with the abolition of the requirement for ventilation of habitable rooms and the powerful motivation in both new and existing buildings to reduce ventilation rates to save energy, results in potentially very low ventilation rates in the winter in many dwellings. It is therefore becoming apparent that opening windows, whilst meeting the requirements for summer ventilation do not provide a solution to the problem of winter ventilation. The situation is a particularly critical one since, to be effective, ventilation rates have to be controlled within narrow limits. From the point of view of energy conservation the ventilation rate in the heating season should be reduced to a minimum, but from the point of view of condensation risk it is vital that an adequate flow of air is maintained. Thus, although reducing ventilation is an extremely cost effective way of reducing heat loss, it is clearly very important that effective ways of control should be developed to prevent the disastrous consequences which can arise from over-enthusiastic but injudicious attempts at reducing ventilation.

3. CONTROLLED VENTILATION

Quite apart from the great differences in the living habits of occupants individual dwellings vary very greatly in their airtightness. Siting, microclimatic factors, orientation and fenestration all play significant parts in addition to the effects

of choice of materials and standards of workmanship. In a series of measurements of ventilation rates in dwellings built in the ten years prior to 1925, Warren[1] found variations between 0.45 and 1.25 air changes per hour with windows closed. The trend is clearly towards lower rates of natural ventilation (see section 3.2).

It is not possible to predict in advance what ventilation rates will be encountered in dwellings and it is difficult to do so, except by actual tests, in existing buildings. Unless a careful window opening regime is maintained, ventilation rates in the lower range are likely, giving rise to higher than normal moisture concentrations in the internal air and consequently to increase the risk of condensation.

One approach to this problem might be the careful study of materials and workmanship to determine which design features and standards of workmanship could be used to give desired standards by means of infiltration through the fabric. If possible this would certainly be a highly cost effective way of dealing with the problem. In practice, however, there seems no practical possibility that the necessary factors could be sufficiently closely specified or controlled and the only quick practicable method of testing, the pressurisation technique, will give a good measure of airtightness but there is no direct correlation between this and the mechanism of ventilation.

3.1 Full Mechanical Ventilation

A realistic approach to the problem, which has already been adopted in some countries, is to make the whole of the basic construction, including doors and windows, as airtight as possible and then to provide specific controllable features for winter ventilation.

Clearly the most predictable way to control low levels of ventilation is by mechanical means. In some countries where energy conservation is very important this method is being adopted. It is said that 95% of new Swedish dwellings are built to be as tightly sealed as possible and equipped with mechanical extract systems extracting through kitchens and bathrooms giving an overall ventilation rate of one half air change per hour. Although this may be a very effective solution in Sweden there are several reasons which prevent it being readily adopted as a solution in this country. Although temperatures in this country occasionally do drop to extremely low levels by any standard, such occasions are comparatively short lived and do not occur every year. A more consistent level of cold in Sweden means that window opening in kitchens and bathrooms is not a feasible ventilation measure in winter and the building regulations require the provision of quite expensive means of permanent natural ventilation. Thus there is a more acute situation recognised by occupants and the cost of the natural ventilation provisions can be set against a

large part of the cost of the mechanical ventilation system which requires much simpler exit provisions through the building fabric. To ensure that the controlled low rate of ventilation is maintained the background infiltration is minimised by very high standards of workmanship in sealing the building and also, if condensation with low rates of ventilation is to be avoided, in ensuring that no cold bridges will cause trouble. In addition the amount of moisture basically present in the atmosphere at very low temperatures is much less than that at higher temperatures. In terms of condensation risk, therefore, the low temperatures represent an advantage.

In the U.K. climate where typical winter temperatures hover just above freezing and the relative humidities are extremely high it is by no means certain that the ventilation rates used successfully in Sweden would be adequate. The additional expense of full mechanical ventilation in the U.K. would be considerable, designers could be less certain that they would function efficiently, the noise levels would give rise to complaint and, on the experience associated with mechanical systems installed to overcome aircraft noise it is very likely that the fans would not be adequately maintained or repaired when necessary. In this country one must, therefore, look to the possibilities of providing natural means of controllable ventilation, perhaps operating in conjunction with simple extract fans.

3.2 Natural Ventilation

The first prerequisite is to separate the winter ventilation function from the opening lights. A system of controllable ventilators separate from but perhaps included in the window opening is an obvious possibility. One factor which does appear to be quite clear is that there should be a manually operated adjustment, the position of which can be observed by the users so that repeatable settings can be made to meet differing conditions.

In a range of weather conditions the whole house ventilation rate with internal doors open was measured using the tracer gas decay method. Fig. 1 shows the results, plotted against wind speed. The internal-external temperature difference varied between $5^{o}C$ and $9^{o}C$. Inevitably there is scatter but there is a clear indication that the use of the ventilator openings is likely to produce a higher rate of ventilation, especially at higher wind speeds. The superimposed lines are obtained by linear regression analyses of the results with closed and open vents respectively. The distance between the lines suggests that the ventilation rate may be expected to increase by 16 - 27% when all the ventilators are opened.

During the course of a broad investigation of ventilation rates and internal air movements in a range of dwellings results have emerged which indicate the effects of built in hit and miss slot ventilators and of extract fans. The houses so equipped are

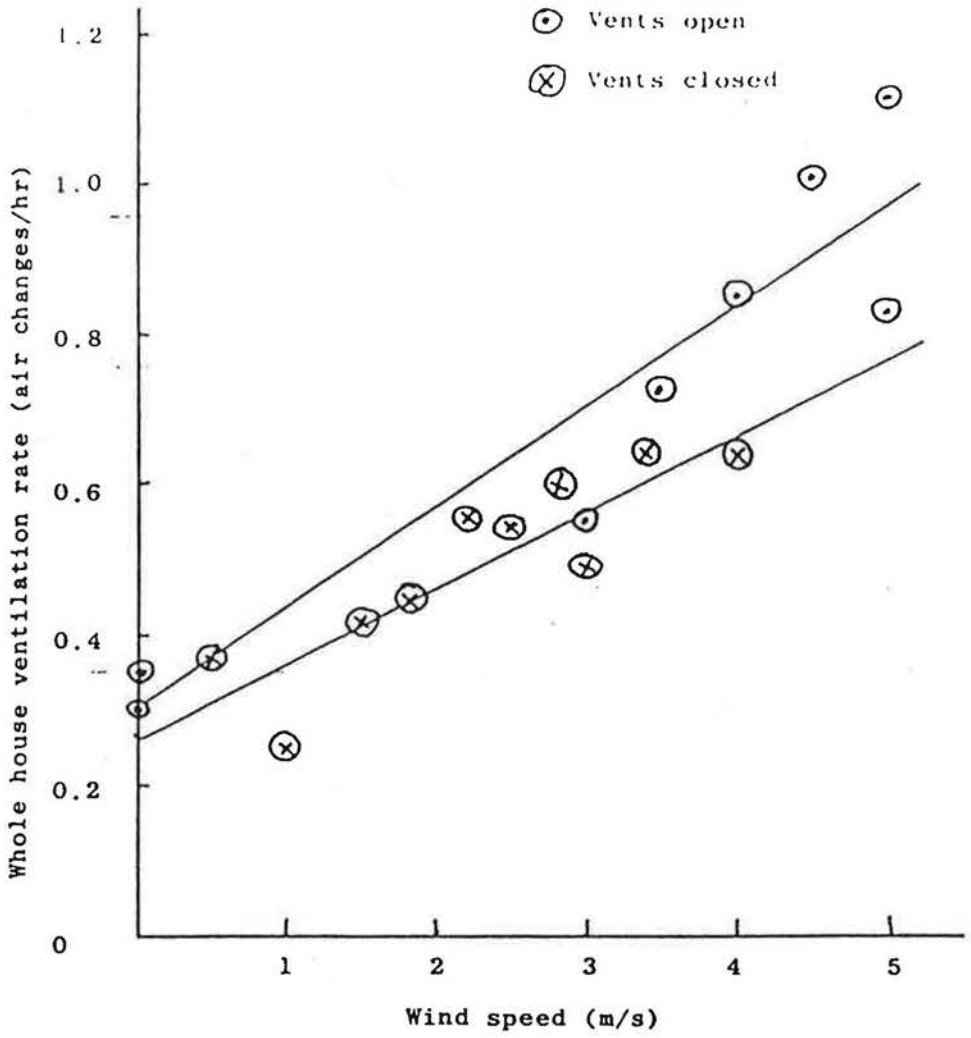

FIG. 1. Comparison of ventilation rates with ventilators open and closed.

newly constructed with double glazing and storm porches. Each window frame incorporates a slot ventilator most of which may be closed or opened to produce an open area of 7000mm^2. The ventilator in the kitchen is permanently open. The dwelling tested was end-terraced with a volume of 200 m^3.

The ventilation rates were measured by a tracer gas decay method which employs multiple tracer gases so that the internal air exchanges between major zones can be assessed. In addition, a pressurisation test was performed at 50 Pa.

The results show the effectiveness of the simple slots employed in one particular dwelling. It is clear that they do provide an increased rate of ventilation without the disadvantage of the relatively large opening lights.

Many devices of this type are on the market at present, some of which have a flap arrangement intended to give fixed ventilation rates irrespective of pressure differences across the unit. There is an important need to evaluate the performance of these units, both when installed and over a period of time.

A possible method of testing such devices when installed is the use of the pressurisation technique.

During the investigations described, the average of pressurisation and depressurisation tests at 50 Pa produced a throughput of 0.675 m^3/s with the slot ventilators closed and 0.785 m^3/s with the ventilators open - an increase of 16%. Some measure of correlation between the pressurisation results and the ventilation measurements is evident; both techniques giving a similar assessment of the effect of the ventilation openings.

It should be noted from Fig. 1 that low levels of ventilation rate are to be found in still atmospheric conditions with values as low as 0.25 - 0.30 air changes per hour.

3.3 Simple Extract Fans

The houses tested were equipped with simple extract fans discharging through the wall near to the cooking appliance. In a series of decay tests, the whole house ventilation rate varied between 1.1 and 1.9 air changes per hour with the fan on and the window vents closed. The combined effect of the fan and the open window vents was to produce higher ventilation rates of between 1.6 and 3.0 air changes per hour. An important effect of the fan is to produce a different flow pattern throughout the house. Fig. 2 demonstrates the changes of direction and flow rates. Strong evidence is also indicating that flow into roof spaces and cavities is considerably reduced when an extract fan is running in the house. Thus the primary effect is to remove moist air from the zone in which water vapour is generated but the secondary effect is to reduce the flow from the ground floor to the first floor thus minimising convection of warm moist air into remote rooms with low occupancy and a likely minimum of heating.

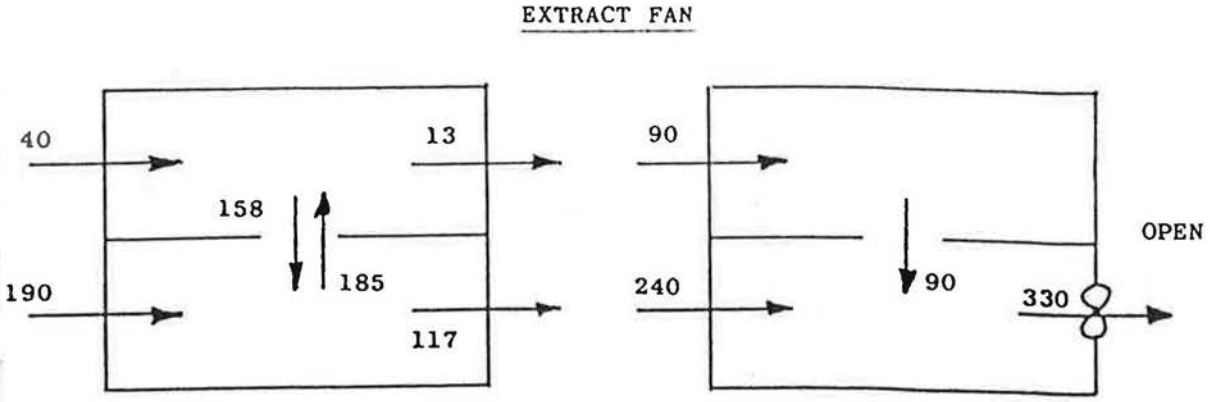

FIG. 2. Whole house air flows with open ventilators and the effect of kitchen extract fan. (Flows in m^3/hr).

4. CONCLUSIONS

1. There is a clear and conflicting distinction between the requirements for summer ventilation and for winter ventilation.

2. Built in controllable ventilation slots can provide a level of ventilation compatible with winter requirements.

3. The appropriate sizing of ventilators (and hence the extent of the increased ventilation which they provide) is not known; further research which correlates the winter ventilation requirement with ventilation size is necessary.

4. Kitchen extract fans are highly effective means of keeping moisture generated in cooking out of the main part of the house and its roof space. Reversals of stair well flows have been clearly observed.

5. REFERENCES

1. WARREN, P.R.
"Factors influencing air change in houses"
University of Aston Conference, Sept. 1975.

Building and Environment, Vol. 17, No. 4, pp. 245–252, 1982
Printed in Great Britain

0360-1323/82/040245-08$03.00/0

Air Flow Measurement Using Three Tracer Gases

S. J. I'ANSON*
C. IRWIN*
A. T. HOWARTH*

A technique is described for measuring air flows between internal zones of houses. The theory is given for measuring one- and two-directional flows and the equipment used for practical measurements is described. The tracer gases used are Freon 12, Freon 114 and BCF. Their concentrations are measured using a gas chromatograph. Specimen results of one- and two-directional air flows between a house and its roof are included. The possible applications of the method in houses are discussed.

1. INTRODUCTION

DURING the present energy crisis it has become clear that a great deal of energy and money can be saved by the increased use of insulation. This reduces the amount of heat conducted through the fabric of the building, but does nothing to limit the heat loss due to the infiltration of cold air and the exfiltration of warm air. In fact, heat loss due to these ventilation effects can account for 30–40% of the fuel bill in well-insulated houses. Many authors, including Dick [1], Etheridge and Nevrala [2] and Kronvall [3], have written about the measurement of ventilation rates, air leakage rate and energy savings through the sealing of structures.

The way in which air flows between internal spaces of houses has received much less attention. Marsh [4], the BRE [5] and Dutt [6] have drawn attention to the occurrence of condensation in cold zones of the house (like the roof, where there is loft insulation) due to warm, humid air (from, for example, the kitchen) entering these zones from the rest of the house. Since, in cold, still conditions, 30% of the air leaving a house can be through the roof [7], and 10 kg of water vapour a day may be released in a normal household [5], it is clearly necessary to learn more about the internal air flows. Another useful application of a detailed knowledge of room-to-room air movement is in sizing first floor radiators for low-energy houses, where the overheating of bedrooms, due to convective heat gains from downstairs, is common.

In the past, work on air flows between internal spaces has been done by Sinden [8], Foord and Lidwell [9, 10], Dick [11] and Sanders [7]. Sinden evolves the necessary analysis for the interpretation of room-to-room air flow measurements by a continuous flow tracer gas method. Foord and Lidwell investigated the spread of airborne infection in hospitals. They used a continuously released tracer gas in one room to represent the release of bacteria and measured the resulting concentrations in other rooms. In their work, Foord and Lidwell used a sophisticated multiple tracer system with fixed piping, carrying samples to a central instrument room from the spaces of interest. Since this work was done in a fully air conditioned hospital with mechanically induced ventilation rates in excess of six air changes per hour throughout, the air flows being measured were constant and repeatable, allowing measurements to be accurately achieved over long periods. In naturally ventilated buildings each weather change alters the flows being measured, making this technique less appropriate than Dick's, which used a tracer decay method to measure flows between rooms. He used substantially the same technique and analysis as the present work, but using only one tracer gas and with no allowance for recirculation effects. Sanders continued Dick's work to measure house to roof air flows using nitrous oxide as a tracer gas.

The present technique for measuring air flows is a combination of the theoretical work of Dick with the multiple tracer gas analysis technique evolved by Foord and Lidwell. This method of measuring air flows between spaces is equally valid for one-directional air flows (for example, from a house to the roof [7]) or for two-directional flows (for example, the air flows in both directions between two rooms on the same floor of a house with the doors open). The theory required for both types of measurement is included in Section 2.

2. THEORY

Kronvall [3] and Jones [12] present a detailed review of the use and derivation of the decay equation for single-volume ventilation calculations.

In the following analysis non-zero number subscripts refer to a particular room or internal space. The zero subscript indicates the value of the variable at zero time. Letter subscripts refer to a particular

*Department of Building, UMIST, Manchester M60 1QD, U.K.

tracer gas. For example, C_{0A1} is the initial concentration of tracer gas A in room 1.

Figure 1 shows two zones of a building, both ventilated to the outside and with air flowing between the rooms in both directions. A practical example of two such zones is the upstairs and downstairs of a two-storey house. Q is the amount of air flowing out of the zone to outside in m^3/s and F is the air flow rate between the two zones, in m^3/s, in the direction indicated by the subscripts. If a tracer gas A is released, for example, in zone 1 and allowed to mix with the air, some of it will be carried to zone 2 where it will also mix with the air and some will be returned to zone 1. Let us define $t = 0(s)$ as the time when initial mixing is complete and the concentrations in the two zones are C_{0A1} and C_{0A2} respectively, in ppm.

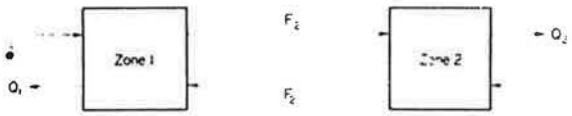

Fig. 1. Air flow between two zones of a house.

The rate at which tracer A is entering zone 1 is given by

$$F_{21}C_{A2}$$

and the rate at which it is leaving, by

$$F_{12}C_{A1} + Q_1C_{A1},$$

so the rate of decrease of volume of tracer A in zone 1 at time t is given by

$$-V_1\left(\frac{dC_{A1}}{dt}\right) = C_{A1}(F_{12} + Q_1) - F_{21}C_{A2}. \quad (1)$$

Similarly, the rate of decrease of volume of tracer A in zone 2 is given by

$$-V_2\left(\frac{dC_{A2}}{dt}\right) = C_{A2}(F_{21} + Q_2) - F_{12}C_{A1}. \quad (2)$$

By rearranging (1) and (2), equations for C_{A1} and C_{A2} can be obtained:

$$C_{A1} = \frac{N_2V_2}{F_{12}}C_{A2} + \frac{V_2}{F_{12}}\frac{dC_{A2}}{dt} \quad (3)$$

$$C_{A2} = \frac{N_1V_1}{F_{21}}C_{A1} + \frac{V_1}{F_{21}}\frac{dC_{A1}}{dt}, \quad (4)$$

where N_1 and N_2 are the air change rates of zones 1 and 2 in air changes per second and are given by

$$N_1V_1 = F_{12} + Q_1 \text{ and } N_2V_2 = F_{21} + Q_2. \quad (5)$$

By substituting for C_{A2} from equation (4) into equation (3), and for C_{A1} from equation (3) into equation (4), two second-order differential equations can be obtained:

$$\frac{V_1V_2}{F_{12}}\frac{d^2C_{A2}}{dt^2} + \frac{V_1V_2}{F_{12}}(N_1 + N_2)\frac{dC_{A2}}{dt} + \left(N_1N_2\frac{V_1V_2}{F_{12}} - F_{21}\right)C_{A2} = 0 \quad (6)$$

$$\frac{V_1V_2}{F_{21}}\frac{d^2C_{A1}}{dt^2} + \frac{V_1V_2}{F_{21}}(N_1 + N_2)\frac{dC_{A1}}{dt} + \left(\frac{N_2V_2N_1V_1}{F_{21}} - F_{12}\right)C_{A1} = 0, \quad (7)$$

which are both linear homogeneous equations with constant coefficients. For all practical cases, these can be solved in the normal way by application of an auxiliary equation to give:

$$C_{A2} = \left[\frac{F_{12}C_{0A1}}{V_2} - (N_2 + Z)C_{0A2}}{Y - Z}\right]\exp Yt + \left[\frac{(Y + N_2)C_{0A2} - \frac{F_{12}C_{0A1}}{V_2}}{Y - Z}\right]\exp Zt \quad (8)$$

$$C_{A1} = \left[\frac{F_{21}C_{0A2}}{V_1} - (N_1 + Z)C_{0A1}}{Y - Z}\right]\exp Yt + \left[\frac{(Y + N_1)C_{0A1} - \frac{F_{21}C_{0A2}}{V_1}}{Y - Z}\right]\exp Zt, \quad (9)$$

where

$$Y = \frac{-N_1 - N_2 + \sqrt{\left((N_1 + N_2)^2 - 4\left(N_1N_2 - \frac{F_{12}F_{21}}{V_1V_2}\right)\right)}}{2} \quad (10)$$

and

$$Z = \frac{-N_1 - N_2 - \sqrt{\left((N_1 + N_2)^2 - 4\left(N_1N_2 - \frac{F_{12}F_{21}}{V_1V_2}\right)\right)}}{2} \quad (11)$$

If the concentration of tracer gas A is monitored in zones 1 and 2, then C_{A2}, C_{A1}, t, V_1 and V_2 are known. This leaves N_1, N_2, F_{12}, F_{21}, C_{0A1} and C_{0A2} as unknowns. If a least squares fit of the experimental points for C_{A2} and t to equation (8) and C_{A1} and t to equation (9) is carried out, these values can be calculated (see Appendix 1).

If only one-directional flows are present, the processing of results can be simplified to the extent where it is unnecessary to use a computer. This is a common situation in houses and occurs, for example, in the flow of air between a house and its roof [7].

Let $F_{21} = 0$ and equations (8) and (9) become

$$C_{A2} = C_{0A2}\exp(-N_2t) + \frac{F_{12}C_{0A1}}{V_2(N_1 - N_2)}[\exp(-N_2t) - \exp(-N_1t)] \quad (12)$$

$$C_{A1} = C_{0A1} \exp(-N_1 t). \quad (13)$$

Figure 2 shows the approximate shapes of equations (12) and (13). In this simpler case C_{0A1} and N_1 are first found by drawing the usual straight line graph for equation (13). C_{0A1} is taken from the graph C_{A2} against t, and V_2 is measured directly. This leaves N_2 and F_{12} as unknowns. A second tracer gas B is released in zone 2 at the same time as tracer A is released in zone 1, and since zone 2 is ventilated only to the outside,

$$C_{B2} = C_{0B2} \exp(-N_2 t). \quad (14)$$

N_2 can be calculated from the usual straight line graph, leaving F_{12} as the only unknown. F_{12} is now varied until the theoretical curve of equation (12) fits the experimental curve of C_{A2} against time. The value of F_{12} when the best fit is obtained is the true value.

A more complicated situation which frequently occurs is where there is one-directional air flow to a third zone from one of two zones involved in a two-directional flow (Fig. 3). Clearly the normal one-directional equations do not apply since the decay in the source room is not purely exponential but involves recirculation. To calculate the required curve

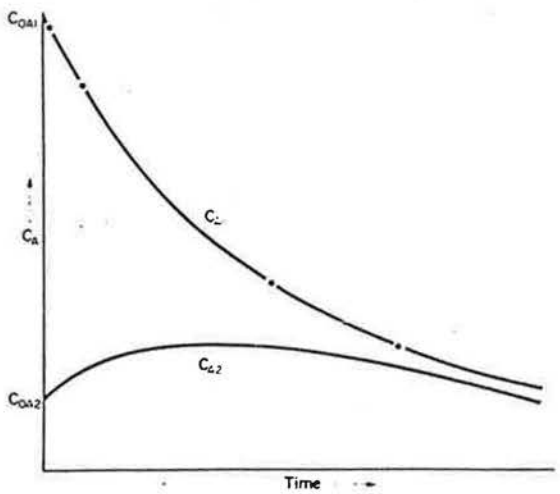

Fig. 2. Concentration against time curve shapes for a one-directional air flow.

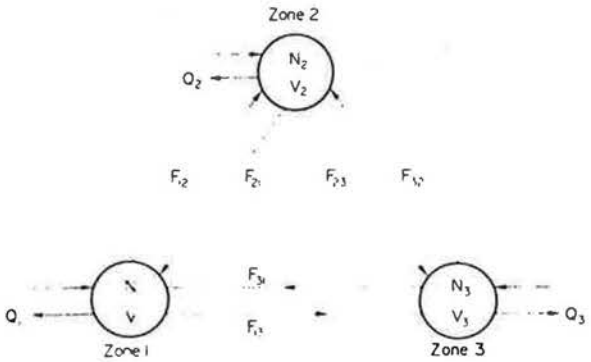

Fig. 3. Air flow between three zones of a house.

shape a separate integration must be performed. If the flow is from, say, room 2, where equation (8) describes the behaviour of tracer gas A released there, then since F_{13}, F_{31} and F_{23} are zero,

$$C_{A3} = A \exp Yt + B \exp Zt, \quad (15)$$

where

$$A = \frac{\frac{F_{12}C_{0A1}}{V_2} - (N_2 + Z)C_{0A2}}{Y - Z}$$

and

$$B = \frac{(Y + N_2)C_{0A2} - \left(\frac{F_{12}C_{0A1}}{V_2}\right)}{Y - Z}$$

and C_{A3} is given by

$$\frac{dC_{A3}}{dt} + N_3 C_{A3} = \frac{F_{23}C_{A2}}{V_3},$$

which can be solved to give

$$C_{A3} = C_{0A3} \exp(-N_3 t) + \frac{F_{23}A}{V_3(Y + N_3)}[\exp Yt - \exp(-N_3 t)] + \frac{F_{23}B}{V_3(Z + N_3)}[\exp Zt - \exp(-N_3 t)]. \quad (16)$$

F_{23} can now be calculated in the same way as for the simple one-directional case above, assuming A, B, Y and Z have already been calculated from the two-directional flow calculation and N_3 has been found by releasing a third tracer gas, as in the simple one-directional case (equation 14).

3. METHOD

The technique has been employed using three tracer gases released simultaneously in each of three internal zones of a house. The concentrations are measured using a portable gas chromatograph. The three tracer gases used are Freon 12 (dichlorodifluoromethane), Freon 114 (dichlorotetrafluoroethane) and BCF (bromochlorodifluoromethane). These can all be conveniently detected using an Analytical Instruments Ltd. Model 505 SF_6 leak detector fitted with a squalane column of length 2.4 m. Figure 4 illustrates the sampling system. Although only small quantities are used, giving parts per billion concentrations, it has, however, been decided to look for replacements for Freon 12 and Freon 114 due to the possibility of their destroying stratospheric ozone [13].

By means of three separate sampling tubes, the air from the three rooms can be sampled in turn. It is pumped into the instrument by the internal diaphragm pump, where a known volume of the mixture is abstracted with a sampling valve. This sample is then

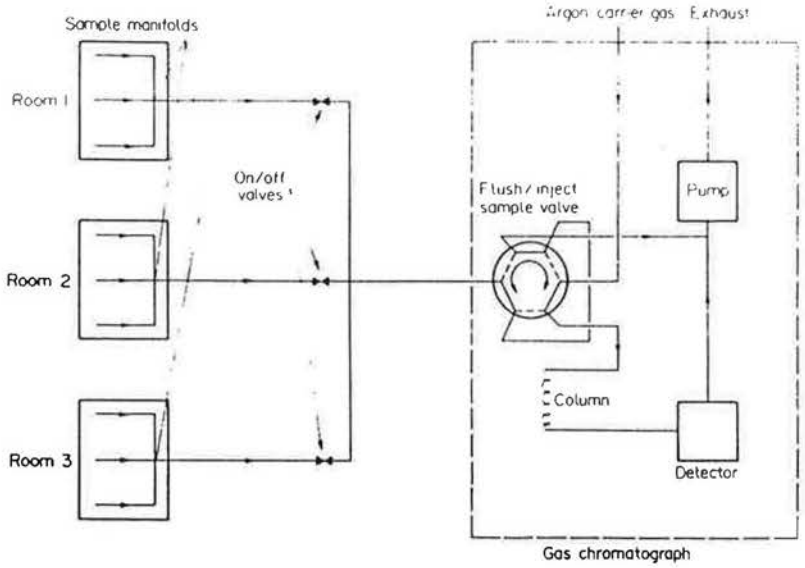

Fig. 4. Sampling system.

carried through the chromatographic column by the argon carrier gas, where it is separated into its component gases. Thus each gas arrives at a different time at the electron capture detector, which gives an electrical output proportional to the amount of each gas present. Figure 5 shows a typical chart recorder trace of the detector output. The sensitivity of the instrument to each gas is different, so that it must be separately calibrated for all three. This is not necessary to calculate the results, since only relative concentrations of each tracer gas are required, but to predict the quantitity of gas to be injected. Although all the gases of interest emerge within one minute, there are several gases contained in trace amounts in the atmosphere which take about two minutes to pass through the column. This is the limiting factor for the sampling time, so that a maximum of twenty samples per hour can be analysed.

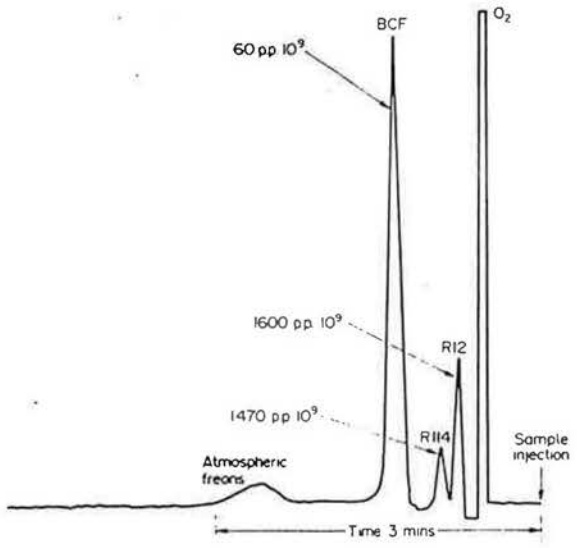

Fig. 5. Typical chart recorder trace of chromatograph output.

In order to allow for the effect of stratification of tracer gas and non-isothermal air flows, each of the three sampling tubes is terminated with a three-way manifold so that air is taken from three different levels in each zone. This is not an ideal solution, but it is thought that little of the total error is from this source (see Appendix 2).

When a test is to be performed the three tracer gases are released in the three spaces under consideration, where they are mixed for several minutes with oscillating desk fans. Sufficient samples are then taken from the three rooms for the curve shapes required to be defined. This normally takes about ninety minutes, which gives a total of thirty samples or approximately ten per zone. The zones are not always sampled in strict rotation because, very often, one room is of more interest at a particular stage of the test. For example, if one of the zones under test is the roof-space, which may have a ventilation rate in excess of ten air changes per hour (ACH), then if this is not sampled frequently at the start of the test, insufficient points will be available to determine the ventilation rate. When all the samples have been taken, the concentrations of each tracer gas for each room are plotted against time. The ventilation rate of each room and the flows between the rooms can then be calculated as explained in Section 2. If, for example, the three zones are the downstairs, upstairs and roof-space of a house (zones 1, 2 and 3, say), in which tracer gases A, B and C respectively are released, then firstly N_1, N_2, F_{12} and F_{21} can be calculated as described in Section 2 for the two-directional flow case (equations 8 and 9). N_3 can be calculated using the usual straight line method (see equation 14) since the flow into the roof from the other zones is one-directional. F_{23} can then be calculated using an equation of the form of equation (16) in the manner

described in Section 2, since this is the only remaining unknown.

4. SPECIMEN RESULTS

Two results are presented here of the flow of air between a house and its roof-space, and the two-directional flow between the upstairs and downstairs of a house.

One-direction result

As expected, there was no flow of air from the roof-space to the house, and the single-direction method of Section 2 could be used. Only two zones were being investigated so only two tracer gases were required and their behaviour could be described by equations (12), (13) and (14). Tracer A in this case is Freon 114, tracer B is BCF, zone 1 is the house and zone 2 is the roof-space.

The house was a new middle-terraced three-bedroom house, with draught-stripped doors and windows and insulated walls and roof. The ventilation of the roof-space was provided by a continuous gap of approximately 10 mm width behind the fascia board. The volume of the house was 200 m^3 and that of the roof was 40 m^3.

Figures 6 and 7 show the normal semi-logarithmic plots of tracer gas concentration with time for Freon 114 in the house and BCF in the roof respectively. The ventilation rates obtained were 0.5 ACH for the house and 4.3 ACH for the roof space. Figure 8 shows the variation of Freon 114 with time both in the house and roof-space. The theoretical curve for a flow rate of 28 m^3/h from the house to the roof is shown superimposed on the experimental points for the concentration of Freon 114 in the roof-space.

Two-direction result

For the two-directional case the general equations (8) and (9) describe the behaviour of each gas released. In this case, Freon 114 (say, gas A) was released downstairs and Freon 12 (gas B) upstairs, and the house was similar to that described for the one-direction result.

Figure 9 shows the experimental points for Freon 114 both upstairs and downstairs, and Fig. 10 shows the same for Freon 12. The least squares method gave a result of:

$$N_1 = 2.2 \text{ ACH}, \quad N_2 = 1.5 \text{ ACH}$$

$$F_{12} = 120 \text{ m}^3/\text{h}, \quad F_{21} = 160 \text{ m}^3/\text{h},$$

which are used to plot the theoretical curves shown in

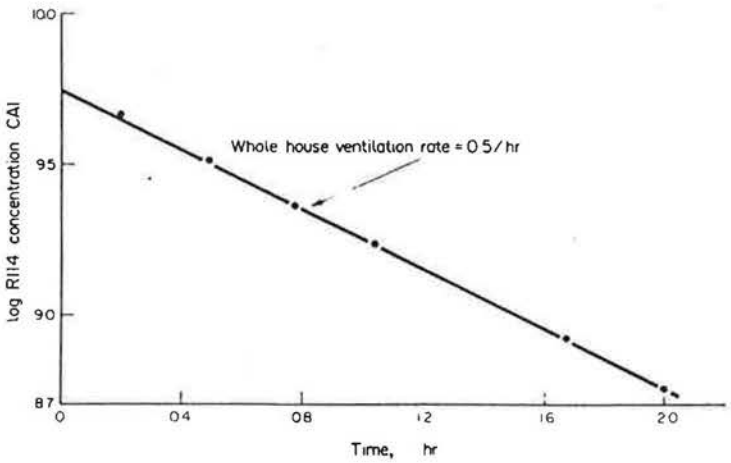

Fig. 6. (Example 1) Log concentration against time for Freon 114 in the house.

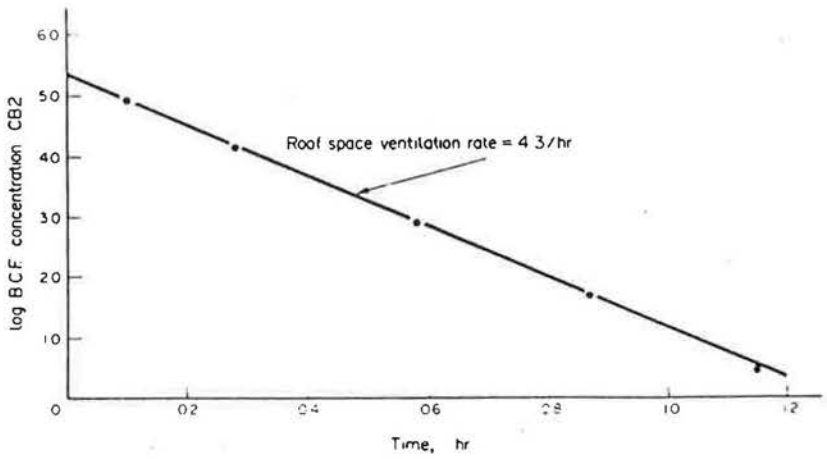

Fig. 7. (Example 1) Log concentration against time for BCF in the roof-space.

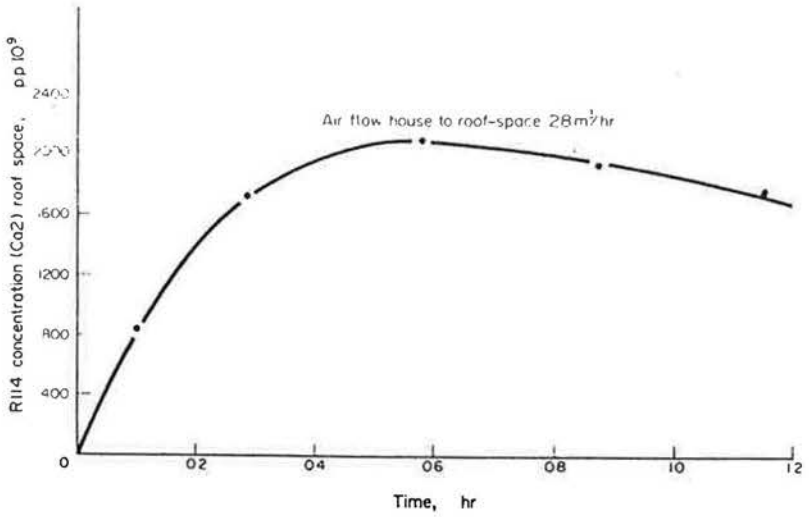

Fig. 8. (Example 1) Concentration against time for Freon 114 in the roof-space.

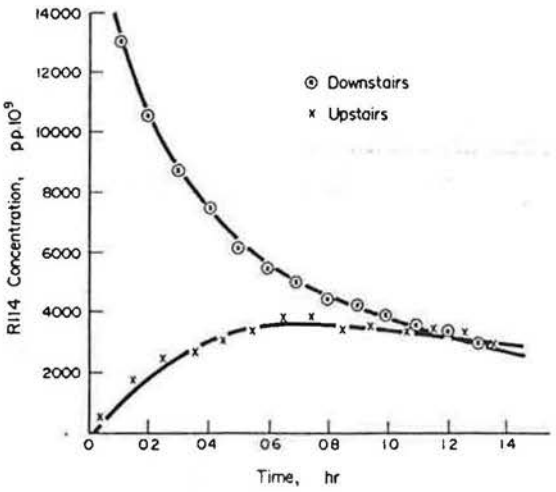

Fig. 9. (Example 2) Concentrations of Freon 114 against time, upstairs and downstairs.

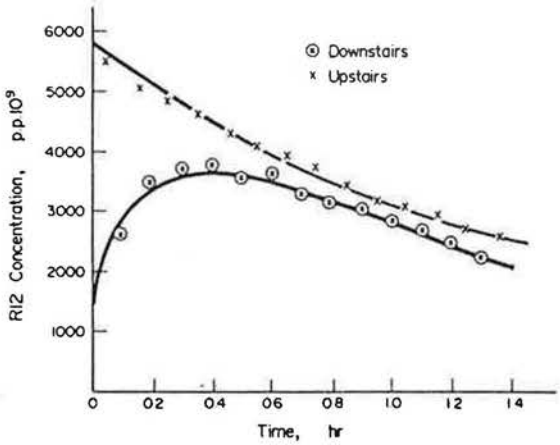

Fig. 10 (Example 2) Concentrations of Freon 12 against time, upstairs and downstairs.

Figs. 9 and 10, where zone 1 is downstairs and zone 2 is upstairs. The actual ventilation rates rather than air change rates are:

fresh air supply to downstairs = 82 m^3/h
fresh air supply to upstairs = 44 m^3/h.

5. CONCLUSIONS

The multiple tracer gas technique for measuring air flows between internal zones of houses which has been described enables measurements of the interconnecting air flows between up to three rooms and their respective ventilation rates to be completed in about two hours by one person. It has been shown how flow rates can be calculated manually where only single-direction air flows exist. In the two-directional case, the flows and ventilation rates can easily be worked out with the aid of a computer to do the otherwise tedious least squares curve-fitting procedures.

Many useful measurements are possible using this technique. For example, the calculation of the possibility of condensation in a roof-space due to warm humid air from the kitchen and bathroom being carried there is made possible. Where the three zones are the downstairs, upstairs and roof-space of a house, the relative strengths of stack effect and wind effect can be observed under different weather conditions since all the ventilation rates and the upward and downward flows of air through the house can be measured in one two-hour test.

It is believed that this is a strong new technique for the building services researcher because it is simple to use, quick and gives a large quantity of information.

Acknowledgements—The authors are grateful to the Building Research Establishment and the Science Research Council, whose financial support has made possible this work.

REFERENCES

1. J. B. Dick, Experimental studies of natural ventilation of houses. *J. I.H.V.E.* 17, 420 (1949).
2. D. W. Etheridge and D. J. Nevrala, Air infiltration and out thermal environment. *Bldg. Serv. envir. Engr.* 1, 10–13 (1979).
3. J. Kronvall, Airtightness—measurement and measurement methods. Swedish Council for Building Research No. D8: 1980.
4. P. Marsh, *Thermal Insulation and Condensation*. Construction Press, Hornby (1979).
5. BRE Digest 180, Condensation in roofs. (1975).
6. G. S. Dutt, Condensation in attics: are vapour barriers really the answer? *Energy Bldg.* 2, 251–258 (1979).
7. C. Saunders, Air movement in houses: a new approach. *Bldg. Res. Pract.* 10, 160–175 (1982).
8. F. W. Sinden, Multi-chamber theory of air infiltration. *Bldg. Envir.* 13, 21–28 (1978).
9. N. Foord and O. M. Lidwell, A method for studying air movement in complex occupied buildings such as hospitals; halocarbons as gas tracer using gas chromatography. *Bldg. Serv. Engr.* 41, 53–100 (1973).
10. N. Foord and O. M. Lidwell, Airborne infection in a fully air conditioned hospital: I. Air transfer between rooms. *J. Hyg.* 75, 15–30 (1975).
11. J. B. Dick, Measurement of ventilation using tracer gases. *Heat. Pip. Air Condit.* 22, 131–137 (1950).
12. W. P. Jones, *Air Conditioning Engineering, Chapter* 17. *Ventilation and a Decay Equation*. Edward Arnold, Port Melbourne (1973).
13. J. Knight, Fluorocarbons. *C.I.B.S. J.* 33 (March 1981).
14. T. Grimsrud, M. H. Sherman, J. E. Janssen, A. N. Pearman, D. T. Harrje, An intercomparison of tracer gases used for air infiltration measurements. *A.S.H.R.A.E. Trans.* 1, 258 (1980).
15. F. B. Hildebrand, *Introduction to Numerical Analysis*, 2nd Edn. McGraw-Hill, New York (1974).

APPENDIX 1

Prony method of exponential approximation

The Prony method is a technique for fitting experimental points to a theoretical curve made up of the sum of several exponential terms. For a full description of the method see Hildebrand [15].

When a tracer gas (A) is released in a two-zone situation involving recirculation, the concentrations in the two zones are given by

$$C_{A1} = A \exp Yt + B \exp Zt$$

and

$$C_{A2} = C \exp Yt + D \exp Zt,$$

as derived in Section 2. These must, firstly, be rewritten as:

$$C_{A1} = A\mu_1^t + B\mu_2^t \tag{17}$$

$$C_{A2} = C\mu_1^t + D\mu_2^t, \tag{18}$$

where $\mu_1 = \exp Y$, $\mu_2 = \exp Z$.

It is necessary, when using this method, that the N experimental points are equally spaced and that the variables are changed such that $t = 0, 1, 2, \ldots, N-1$.

From equation (17),

$$\begin{aligned} A + B &= C_{A1}(0) \\ A\mu_1 + B\mu_2 &= C_{A1}(1) \\ A\mu_1^2 + B\mu_2^2 &= C_{A1}(2), \\ &\vdots \\ A\mu_1^{N-1} + B\mu_2^{N-1} &= C_{A1}(N-1). \end{aligned} \tag{19}$$

If the constants μ_1 and μ_2 are known, then this set would comprise N linear equations in the two unknowns A and B. For $N > 2$ these could be solved using a least squares method for A and B.

However, if the μs are unknown, then they must be calculated, which is difficult because the equations are non-linear in the μs.

Let μ_1 and μ_2 be the roots of the algebraic equations

$$\mu^2 - \alpha_1\mu - \alpha = 0 \tag{20}$$

so that the l.h.s. is identified with the product $(\mu - \mu_1)(\mu - \mu_2)$. In order to determine α_1 and α_2 we multiply the first equation in (19) by α_2, the second by α_1 and the third by -1, and add the results. Using equation (20) the result becomes

$$C_{A1}(2) - \alpha_1 C_{A1}(1) - \alpha_2 C_{A1}(0) = 0.$$

A set of $N-3$ additional equations of similar type is obtained in the same way by starting instead successively with the second, third, ... $(N-2)$th equations. In this way it is found that (19) and (20) imply $N-2$ linear equations

$$\begin{aligned} C_{A1}(1)\alpha_1 + C_{A1}(0)\alpha_2 &= C_{A1}(2) \\ C_{A1}(2)\alpha_1 + C_{A1}(1)\alpha_2 &= C_{A1}(3), \\ &\vdots \\ C_{A1}(N-2)\alpha_1 + C_{A2}(N-3)\alpha_2 &= C_{A1}(N-1). \end{aligned} \tag{21}$$

This set can be solved exactly if $N = 4$, or, as is more usual, approximately by the method of least squares as explained in Hildebrand. Using this method two equations are obtained from (21):

$$\alpha_1 \sum_{a=1}^{N-2} C_{A1}(a) + \alpha_2 \sum_{a=0}^{N-1} C_{A1}(b) = \sum_{d=2}^{N-1} C_{A1}(d)$$

$$\alpha_1 \sum_{a=1}^{N-1} C_{A1}(a)C_{A1}(a-1) + \alpha_2 \sum_{b=0}^{N-3} (C_{A1}(b))^2 = \sum_{d=2}^{N-1} C_{A1}(d)C_{A1}(d-2).$$

α_1 and α_1 have thus been determined, and μ_1 and μ_2 are found as roots of equation (20).

Thus from the values of C_{A1} and time, A, B, Y and Z can be calculated and from C_{A2} against time C, D, Y and Z can be calculated. From these values the air flows and ventilation rates can be found:

$$N_1 = \frac{ADY - BCZ}{BC - AD}$$

$$N_2 = \frac{BCY - ADZ}{AD - BC}$$

$$F_{12} = \frac{V_2}{C_{0A1}}[CY + DZ + C_{0A2}N_2]$$

$$F_{21} = \frac{V_1}{C_{0A2}}[AY + BZ + C_{0A1}N_1].$$

If a second tracer gas had been released, a second set of values for these parameters could also be found.

One-directional case

The method used to fit the concentration points to the theoretical curves given by equations (12) and (16) is given below.

Both equations (12) and (16) are of the form

$$C_A = A(t)F + B(t).$$

Using a least squares technique, given in full in Ref. [7], the flow rate may be calculated from

$$F = \frac{\Sigma(C_A(t)A(t) - \Sigma(A(t)B(t))}{\Sigma(At))^2}.$$

APPENDIX 2

Errors

There are three main sources of error in the measurement of flow rates by this technique: (1) systematic errors of measurement; (2) random errors of measurement; and (3) weather dependence.

(1) *Systematic errors.* The systematic errors of measurement are caused by lack of repeatability in the equipment and by faults in the measurement method. Instrument repeatability should only introduce a large error over a long period as the standing current begins to change with time. To avoid this our tests are kept short and these errors are thought to contribute ±3%.

The faults in the measurement method are mainly due to the difference of the densities of the tracer gases and air, and imperfect mixing of the tracer gases with the house air. Grimsrud *et al.* [14] estimate different tracer gases used to measure the ventilation of the same volume simultaneously give results varying by up to 10%.

Therefore the systematic contribution to the total error is estimated at about 13%.

(2) *Random errors.* These are the errors of measurement which occur in any measurement due to the addition of many smaller errors which combine to give an error which appears to be random. If many measurements are made of the same quantity, these errors appear as a symmetrical distribution about the mean value. In the measurement of air flows random errors are seen as the spread of points about the plotted curve giving the best fit. The magnitude of the random errors is best estimated for each measurement statistically, but for the present purposes it is sufficient to allow ±5% to be added to the systematic errors.

(3) *Weather dependence.* The weather dependence error is not an error in the measurement of the flows but a variation of the flows themselves during the test. It is impossible to put a figure to this, since air flows between rooms can be reversed by quite small weather variations. What this means is that there is little point in trying to measure air flows too accurately in naturally ventilated houses since, ten minutes after a measurement has been completed, the flow rate may have changed significantly.

Overall, then, it is thought that to state an error of ±18% for each flow rate measured is reasonable and that this is of sufficient accuracy for the results to be very useful in characterising the behaviour of air in a house.

An Improved Multiple Tracer Gas Technique for the Calculation of Air Movement in Buildings

C. Irwin and R.E. Edwards
Department of Building, UMIST, Manchester, UK
A.T. Howarth
Department of Building, Sheffield City Polytechnic, UK

Introduction

This paper describes a series of tests carried out in two interconnected environmental chambers, to determine the accuracy of airflows calculated from tracer gas measurements using a new rapid sampling system.

Sampling System

The schematic layout of the tracer gas sampling system is shown in Figure 1. Using two chromatographic separation columns in parallel and a portable gas chromatograph (Analytical Instruments Ltd., Model 505), it was possible to measure the concentration of Freon 12 (dichlorodifluoromethane) and Freon 114 (1,2 dichlorotetrofluoromethane) in air. The two 4-port valves were switched sequentially such that the column not in use was continuously flushed with argon. For the two tracer gases tested, a sampling interval of 30 seconds was used. This system was capable of measuring three tracer gases simultaneously, the third tracer gas being BCF (bromochlorodifluoromethane); this would extend the sampling interval to 45 seconds.

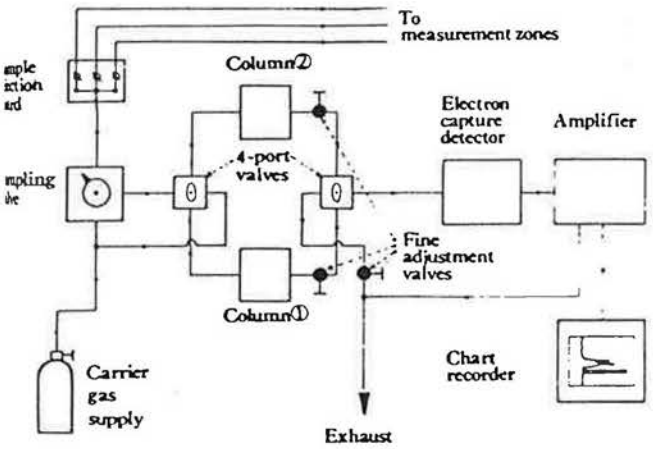

Figure 1. Sampling system

Test Procedure

The two environmental chambers used were 30m³ in volume, each having a separate ducted supply and extract ventilation system. Air/tracer gas in both chambers was sampled at three levels, i.e. floor level, 1.5 m high and 2.4 m high (50 mm below ceiling).

Air movement between the two chambers took place through two 100 mm diameter holes in the partition wall, one 100 mm above floor level and the second 1 m above floor level. The supply air flow rate to both chambers was set to provide a steady airflow through the low level opening from chamber 2 to chamber 1. A ducted low speed fan on the other opening induced air movement from chamber 1 to chamber 2. Air velocites in the supply ductwork were measured using a pitot tube and inclined-tube manometer. The air velocities through both openings in the partition wall were measured using a hot wire anemometer. The tracer gases were injected manually and mixed using desk fans.

Test Results and Analysis

Initially, a single chamber ventilation rate measurement was taken to observe any significant differences between measured gas concentration for the two columns used (Test 1). Figure 2 shows the exponential decay of tracer gas concentration.

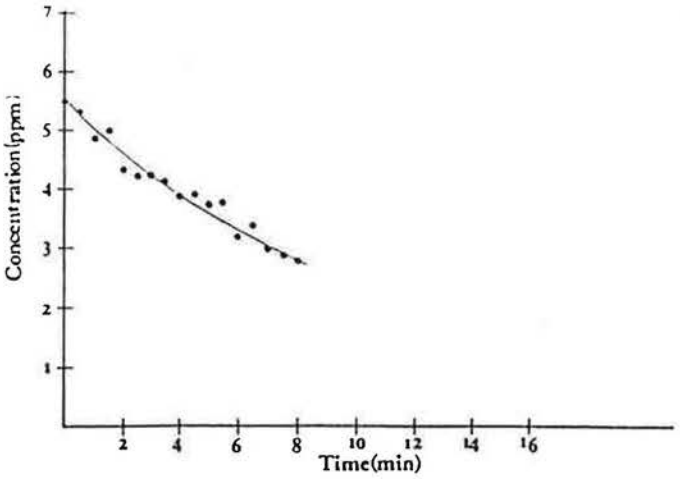

Figure 2. Tracer gas concentration decay in single space

The time taken for Freon 12 to mix with air in a single chamber without the aid of mechanical mixing (Test 2) is shown in Figure 3. A pulse of tracer gas was released at floor level and allowed to disperse. The tracer gas concentration tended to equilibrium after approximately 10 minutes

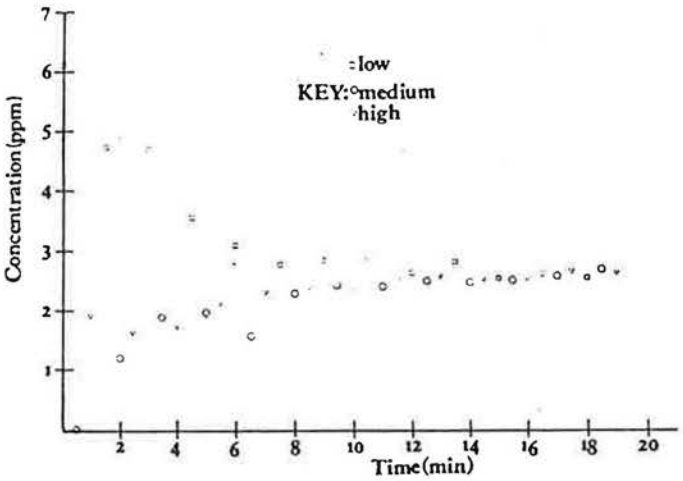

Figure 3. Tracer gas (R12) concentration in chamber 1 – no mixing.

A one-directional airflow was induced from chamber 2 to 1 by switching off the supply air system to chamber 1 (Test 3). Freon 12 was released in chamber 2, mixed, and the growth

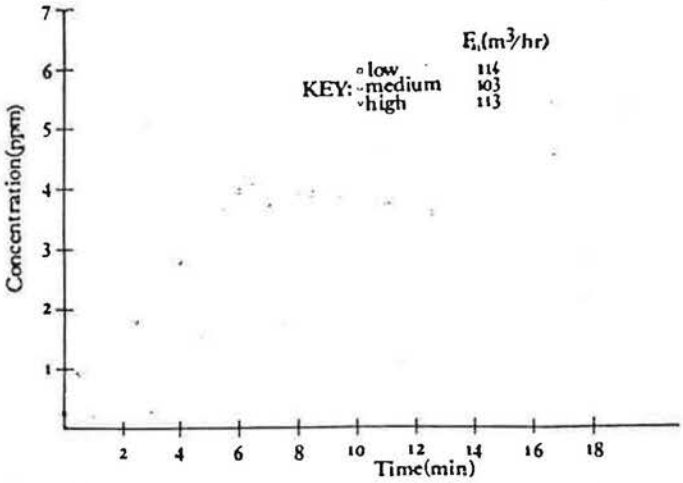

Figure 4. Growth of tracer gas (R12) concentration in chamber 1

tracer concentration monitored at the three different levels chamber 1. Figure 4 shows the three growth curves tained; the three estimates of air movement suggest non-uniform mixing errors of approximately ±7%.

ble 1 summarises the air movement data obtained in osequent tests using two tracer gases. Tests 4 to 5 are the result of a one-directional airflow from chamber 2 to chamber 1. The errors found between calculated and easured airflows were 2.3% and 5.5% respectively. Supply inputs measured using a pitot tube and those calculated rom tracer gas measurement show reasonable agreement; the error lies between 5% and 10%.

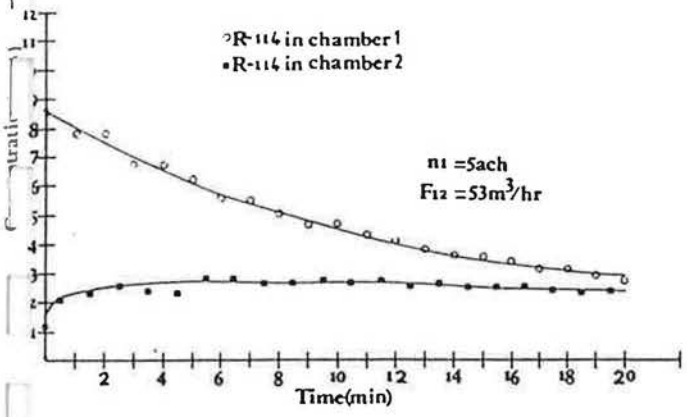

Figure 5. Concentration of tracer gas (R114) in both chambers with a two-directional airflow

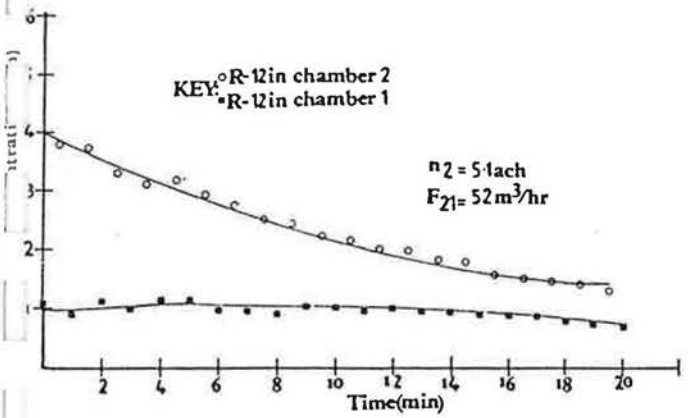

Figure 6. Concentration of tracer gas (R12) in both chambers with a two-directional airflow

ble 1. Summary of Results

Tests 6 to 8 inclusive were with two-directional air movement between the chambers. Figure 5 and 6 show the tracer gas concentration time points obtained during Test 6. The error found between calculated and measured airflows lies between 0% and 8%. Supply air inputs to both chambers measured directly and from tracer measurements again show reasonable agreement, with an error of between 4% and 10%.

Discussion

The magnitude of the two-directional airflows was calculated using a one-directional approximation to give 'first order' estimates.[1]

Where two-directional air movement exists between two connected spaces, recirculation of tracer gas will occur. Consequently the shape of the tracer decay curve in the source room will not be a simple exponential function. The error associated with ignoring recirculation of tracer gas is a complex function of time, air change rate and intercell air movement.[2]

Generally the slope of the tracer decay curve in the source room for time from 0–10 minutes closely approximates to a single exponential function. After this period, the fact that the decay curves represent the sum of two exponential functions becomes increasingly significant.

Provided a sufficient number of concentration and time points are available i.e. at least ten, then a good estimate of the source room air change rate is obtained using the 'first order' estimations. The growths of tracer concentration in the receiving rooms are less strongly dependent on time, so that sufficiently accurate estimations of air flow can be obtained using this method over a period of up to 30 minutes.

References

1. S.J. l'Anson, C. Irwin and A.T. Howarth
   Air flow measurement using three tracer gases.
   Building and Environment, Vol. 17, No. 4, pps245–252, 1982.
2. C. Irwin, R.E. Edwards and A.T. Howarth
   The measurement of airflows using a rapid response multiple tracer gas technique
   To be published

This research, sponsored by UK Science and Engineering and Research Council (SERC), is based in the Department of Building, UMIST, under the joint supervision of Professor P.J. Burberry and Dr A.T. Howarth.

The authors thank Mr Alan Taylor-Firth of the Department of Building, Sheffield City Polytechnic for his kind cooperation in making available the double environmental chamber.

Test No.	Calc. Supply Rate (1) m³/hr	Calc. Supply Rate (2) m³/hr	Measured Supply Rate (1) m³/hr	Measured Supply Rate (2) m³/hr	Calc. Airflow (1)–(2) m³/hr	Calc. Airflow (2)–(1) m³/hr	Measured Airflow (2)–(1) m³/hr	Measured Airflow (2)–(1) m³/hr	% Error Measured (1)–(2) Calc.	% Error Measured (2)–(1) Calc.
1		See Figure 2								
2		See Figure 3								
3		See Figure 4								
4	110	116	105	127	–	43	–	44	–	2.3
5	50	180	55	170	–	127	–	134	–	5.5
6	98	100	90	110	53	52	52	54	2.0	3.9
7	111	119	120	108	31	49	31	47	0	4.1
8	57	53	60	55	51	26	53	24	3.9	7.6

The measurement of airflows using a rapid response tracer gas technique

C. Irwin, B.Sc., R.E. Edwards, B.Sc., M.Sc., and

A. T. Howarth, M.Phil, Ph.D.

Messrs Irwin and Edwards are currently working at the Department of Building, University of Manchester Institute of Science and Technology (UMIST). Dr Howarth is currently Principal Lecturer at the Department of Building, Sheffield City Polytechnic.

LIST OF SYMBOLS

In this paper, the following system of notation is used:

N_X	ventilation rate in cell x (air changes per hour)
Q_X	amount of air flowing from cell x to outside ($m^3\ hr^{-1}$)
F_{XY}	air flow from cell x to cell y ($m^3\ hr^{-1}$)
C_{A_x}	concentration of tracer gas A in cell x (ppm)
C_{OA_x}	concentration of tracer gas A in cell x at time = 0 (ppm)
t	time (hr)

SUMMARY

The multiple tracer gas technique of I'Anson et al. has been improved, in order to increase the rate at which samples can be taken. Using parallel gas chromatographic separation columns, in conjunction with an electron capture detector, it is now possible to take an air/tracer gas sample once every 30 seconds in the case of a 2-zone ventilation and air movement test. Rapid sampling enables a new, simplified analysis of the air movement between two connected zones to be employed. This analysis derives ventilation rates and intercell airflows simultaneously. A speciment set of results for 2 cell ventilation/air movement is given.

1. Introduction

a) Single cell model

The measurement of ventilation rates and internal airflows by tracer gas techniques, as originally proposed by Dick[2] has been developed and extended by several workers, for example Sinden[3], Sherman[4], Perera[5] and I'Anson et al.[1] for the determination of multi-cell air movements. This paper is concerned with the development and refinement of the work of I'Anson et al. in terms of data collection and analysis.

The analysis of single volume tracer gas decay (assuming good mixing) is simple and well established. Briefly, if a pulse of tracer gas is released in a cell of volume V_1, then the rate of decay of tracer concentration with time is described by the equation

$$C_{(t)} = C_0 \, e^{-N_1 t} \qquad (1)$$

where $C_{(t)}$ is the tracer concentration at time t;

C_0 is the concentration at t = o;

and N_1 is the air change rate per unit time.

In practice, the air change rate, N, is determined from a least squares fit of $\ell n\ C_{(t)}$ against time.

b) Two cell model

The equations describing variations of tracer gas concentration in two connected cells, using two different tracer gases A and B, are far more complex than for the single cell, single tracer case. Figure 1 shows the airflow paths for the two cell case. I'Anson et al.[1] have shown that the concentration of tracer gas A released in room 1, C_{A_1}, at time t is given by

$$C_{A_1} = \left[\frac{\frac{F_{21}\ C_{OA_2}}{V_1} - (N_1 + Z)\ C_{OA_1}}{Y-Z} \right] \exp Yt + \left[\frac{(Y + N_1)\ C_{OA_1} - \frac{F_{21}\ C_{OA_2}}{V_1}}{Y-Z} \right] \exp Zt \qquad (2)$$

The concentration of tracer gas A in room 2 at time t, C_{A_2}, is given by

$$C_{A_2} = \left[\frac{\frac{F_{12} C_{OA_1}}{V_2} - (N_2 + Z) C_{OA_2}}{Y-Z} \right] \exp Yt \qquad (3)$$

$$+ \left[\frac{(Y + N_2) C_{OA_2} - \frac{F_{12} C_{OA_1}}{V_2}}{Y-Z} \right] \exp Zt$$

where

$$Y = \frac{-N_1 - N_2 + \sqrt{\left((N_1 + N_2)^2 - 4 \left(N_1 N_2 - \frac{F_{12} F_{21}}{V_1 V_2}\right) \right)}}{2} \qquad (4)$$

and

$$Z = \frac{-N_1 - N_2 - \sqrt{\left((N_1 + N_2)^2 - 4 \left(N_1 N_2 - \frac{F_{12} F_{21}}{V_1 V_2}\right) \right)}}{2} \qquad (5)$$

If the concentration of tracer gas A is monitored in cells 1 and 2, then C_{A_1}, C_{A_2}, C_{OA_2}, V_1, V_2 and t are known, leaving N_1, N_2, F_{21}, F_{12} and Y and Z as unknowns: these are obtained using an exponential approximation known as the Prony analysis, as suggested by Hildebrand[6]. Equations (2) and (3) are rewritten as

$$C_{A_1} = A \mu_1^t + B \mu_2^t \qquad (6)$$

and $$C_{A_2} = C \mu_1^t + D \mu_2^t \qquad (7)$$

The values of the coefficients Y and Z in equation (3) should be real and negative. However, extraneous variables (such as changes in wind speed and wind direction during a test) can cause deviations from the expected tracer gas concentration decay and growth curves. This can result in the values of Y and Z being calculated as positive or complex, and the data set in question would have to be discarded as physically meaningless. Hildebrand discusses this occurrence, and states quite simply that this is an inherent weakness of this particular analytical technique. Where site measurements are concerned, it is clearly undesirable to be in a position where a significant proportion of the data acquired has to be rejected because of the inability of the mathematical analysis technique to deal with short term irregularities in concentration/time data. The next section re-examines the equations of conservation of tracer gas, and considers an alternative method of data analysis.

2. Alternative method for the analysis of two-directional airflows between two connected spaces

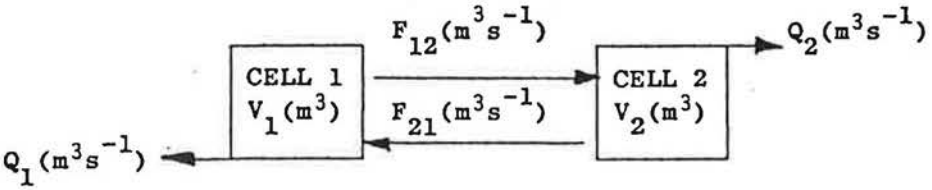

If tracer gas A is released in cell 1 and allowed to mix with the air, some of it will be carried to cell 2, where it will also mix with the air, after which some may be returned to cell 1. Let us define t = o (seconds) as the time when initial mixing is complete: the concentrations of tracer gas A in cells 1 and 2 are given by C_{OA_1} and C_{OA_2} respectively. Now the rate at

which tracer gas A is entering cell 1 is given by $F_{21} C_{A_2}$ and the rate at which it is leaving by $F_{12} C_{A_1} + Q_1 C_{A_1}$: hence, the rate of decrease of volume of tracer gas A in cell 1 at time t is given by

$$-V_1 \frac{d C_{A_1}}{dt} = C_{A_1} (F_{12} + Q_1) - F_{21} C_{A_2} \tag{8}$$

Similarly, the rate of decrease of volume of tracer A in cell 2 is given by

$$-V_2 \frac{d C_{A_2}}{dt} = C_{A_2} (F_{21} + Q_2) - F_{12} C_{A_1} \tag{9}$$

Since

$$N_1 = \frac{F_{12} + Q_1}{V_1} \quad \text{and} \quad N_2 = \frac{F_{21} + Q_2}{V_2}$$

equations (8) and (9) become:

$$\frac{d C_{A_1}}{dt} + N_1 C_{A_1} = \frac{F_{21}}{V_1} C_{A_2} \tag{10}$$

and

$$\frac{d C_{A_2}}{dt} + N_2 C_{A_2} = \frac{F_{12}}{V_2} C_{A_1} \tag{11}$$

Using $e^{N_1 t}$ as the integrating factor for equation (10);

$$C_{A_1} e^{N_1 t} = \int \frac{F_{21} C_{A_2}}{V_1} e^{N_1 t} \, dt + A \tag{12}$$

and using $e^{N_2 t}$ as the integrating factor for equation (11);

$$C_{A_2} e^{N_2 t} = \int \frac{F_{12} C_{A_1}}{V_2} e^{N_2 t} dt + A \qquad (13)$$

For equation 12 to be solved, the variation with time of C_{A_2} must be known or approximated. If it is assumed that, initially, no recirculation of tracer gas A occurs (i.e. $F_{21} = o$) then, from Dick's equations[2], C_{A_2} is given by

$$C_{A_2} = C_{OA_2} e^{-N_2 t} + \frac{F_{12} C_{OA_1}}{V_2(N_2-N_1)} \left[e^{-N_1 t} - e^{-N_2 t} \right] \qquad (14)$$

Substituting for C_{A_2} in (12) and solving:

$$C_{A_1} = C_{OA_1} e^{-N_1 t} + \frac{F_{21} C_{OA_2}}{V_1(N_1-N_2)} \left[e^{-N_2 t} - e^{-N_1 t} \right]$$

$$+ \frac{F_{21} F_{12} C_{OA_1}}{V_1 V_2 (N_2-1)} \left[te^{-N_1 t} + \frac{(e^{-N_2 t} - e^{-N_1 t})}{N_2 - N_1} \right] \qquad (15)$$

Similarly, equation (13) can be solved by substitution for C_{A_1} to give

$$C_{A_2} = C_{OA_2} e^{-N_2 t} + \frac{F_{12} C_{OA_1}}{V_2(N_2-N_1)} \left[e^{-N_1 t} - e^{-N_2 t} \right]$$

$$+ \frac{F_{12} F_{21} C_{OA_2}}{V_1 V_2 (N_1-N_2)} \left[te^{-N_2 t} + \frac{(e^{-N_2 t} - e^{-N_1 t})}{N_2 - N_1} \right]$$

$$+ \frac{F_{21} F_{12}^2 C_{OA_1}}{V_1 V_2^2 (N_2-N_1)} \left[\frac{2e^{-N_2 t} - 2e^{-N_1 t}}{(N_2 - N_1)^2} + \frac{(te^{-N_2 t} + te^{-N_1 t})}{(N_2 - N_1)} \right] \qquad (16)$$

The same derivation can also be applied to a second tracer gas (B) released at the same time in cell 2. Figures 2 and 3 show the shape of equations (15) and (16). Comparison is made with the predicted curve shapes of

I'Anson et al[1]: the effects of recirculation are also shown.

If the concentrations of tracer gas A are monitored in cells 1 and 2, then C_{A_1}, C_{A_2} t, V_1 and V_2 are known, leaving N_1, N_2. F_{12}, F_{21}, C_{OA_1} and C_{OA_2} as unknowns. By using a curve fitting technique on sets of experimental values of C_{A_1}, C_{A_2} amd t, these unknowns can be calculated. (See Appendix 1).

3. Experimental

a) Limitations of the existing technique

The existing technique, as used by I'Anson et al.[1] uses an AI 505 portable gas chromatograph, fitted with a 3 m long, 6 mm diameter 10% squalane separation column, used in conjunction with an electron capture detector. This piece of equipment has a sampling interval, for the two cell case, of 1 minute. In order to reduce errors in the values of airflows derived by the new simplified analysis, sufficient data points must be acquired within 15 minutes of the start of the test, that is, before recirculation terms become significant. On the basis of 10 data points per cell per test, a sampling interval of 45 seconds or less is required. Clearly, some improvement in the rate of sampling of the existing gas chromatograph was needed. Two ways of improving the sampling interval, whilst still retaining the same type of basic unit, were considered.

The first option was to duplicate the existing equipment and to sample alternatively with each. This was rejected for three reasons: first, the effective reduction in portability caused by having to use twice as much equipment; secondly, the expense involved; and thirdly, but for an experimental viewpoint most importantly, the uncertainty of obtain ing two AI 505 gas chromatographs with identical output characteristics.

For example, variations in the quality of the electron capture detector amplifier board fitted in the AI 505 have been observed, with differences in output of up to 40%.

The option selected was to use two gas chromatographic separation columns of identical packing and length attached in parallel to one gas chromatograph unit. Sampling valves would be arranged so that samples passing through each column would be passed alternately to the electron capture detector. A faster sampling rate is achieved by virtue of the fact that the "dead time" associated with waiting for a sample to pass through a single column is eliminated. Such an arrangement has two very attractive advantages: first, the portability of the original apparatus would be hardly changed; and secondly, the cost of such a system is considerably less than duplicating the AI 505 unit (£200 in valves and columns against £2000 for a new unit). The major technical difficulty envisaged was ensuring that the two separation columns behaved in an identical manner, though, as events transpired, this was not as big a problem as originally feared.

b) Design of the new system

For 2 zone work, it is sufficient to be able to detect 2 Freons on a gas chromatograph, in this case Freon 12 and Freon 114. Previous experience with single column operation has shown that the best compromise between throughput time and peak resolution is given by a column packing of 10% squalane on a CNAW support, with a column length of 3 m and diameter 6 mm.

It is essential that the columns are both kept under a trickle of gas during operation. If the gas stream to either column were to be interrupted during operation, then gas starvation and retention of atmospheric

contaminants would take place, with resulting deleterious effects on system stability. Therefore, the sampling valve system to be used had to provide for carrier gas trickle over the column not directly connected to the electron capture detector. Such a flow pattern could have been achieved using an arrangement of simple 2-way valves. However, for ease of operation, two four port zero dead volume valves, as manufactured by Whitey Valves Inc., were chosen. By a single 90^{o} turning action, two inputs can be directed via either of two outlets (Fig 4).

A schematic diagram of the new system is shown in Figure 5. The position of valve 1 determines the column to which the gas sample is diverted: the sampling valve used is the one originally supplied with the AI 505 model. The needle valves located after the separation columns are used to equalise the pressures in both legs of the system, ECD output being sensitive to operating pressure. The position of valve 2 determines whether the gas stream from a separation column is sent to the electron capture detector or else to exhaust. Preliminary tests showed that the resistance of the ECD was significantly higher than that of the exhaust section of the system: this affects baseline stability when columns are switched over. To overcome this, a needle valve is situated in the exhaust line, enabling its resistance to be matched to that of the ECD.

The pattern of valve switching which would be used during a ventilation test in which a 30 second sampling interval was employed is summarised in Table 1.

TABLE 1

Time (secs)	Action	Position of Valve 1	Position of Valve 2	System Status
0-3	Inject sample	a	b	Sample directed to column 1
12	Switch 1	b	b	Sample going through column 1: column 2 on line ready for next sample
23	Switch 2	b	a	ECD on line to column 1. ready to receive sample
30-33	Inject sample	b	a	First sample shows as ECD output: second sample column 2
42	Switch 1	a	a	First sample still being output: second sample going through column 2: column 1 on line ready for next sample
52	Switch 2	a	b	First sample finished with: ECD on line ready to receive second sample
60-63	Inject Sample	a	b	Second sample shows as ECD output: third sample directed to column 1

c) Problems encountered during commissioning

After initial difficulties involving pressure imbalances within the system had been resolved, the single most potentially serious problem would be variations in response between the two separation columns. With this in mind, it was decided to adopt the following three conditions as standard operating procedure in an attempt to minimise potential difficulties:

i) Columns to be bought from the same manufacturer, and to be packed during the same production run from the same batch of packing material.

ii) Both columns to be baked in parallel in an oven at 100°C for 12 hours, with the purging gas to be drawn from the same cylinder.

iii) When not in use, both columns to be kept under a blanket of argon in parallel, with the purging gas to be drawn from the same cylinder.

With these conditions imposed, laboratory tests showed that against a background tracer gas concentration of 40% of full scale deflection, the maximum difference in response between any pair of columns used was not greater than 2.5%. Whilst this was a reasonable starting point, it was clearly highly desirable to reduce any potential systematic error to the absolute minimum.

Attention was then turned to the effect of column operating temperature. At room temperature, small fluctuations in temperature can have significant effects on the performance of a column, both in terms of sample throughput time for a given carrier gas pressure and more importantly, baseline stability. If such fluctuations and variations could be eliminated, then it was conceivable that column performances would become more closely matched.

To investigate this possibility, a small thermostatically controlled water bath/stirrer unit was purchased, with intention of holding both columns at a constant operating temperature, $\pm$ 0.1°C. Clearly, the holding temperature had to be above the likely range of ambient temperatures which

could be encountered; to this end, the water bath thermostat was set at a nominal 30°C (86°F). At this temperature, against a background tracer gas concentration of 40% of full scale deflection, the maximum difference in response between any pair of columns used was not greater than 0.5%; furthermore, the higher operating temperature effectively eliminated baseline drift problems previously encountered with the system at ambient temperature operating conditions.

4. Results and Discussion

The specimen result presented here shows the flow of air between the upstairs and downstairs of a dwelling. Freon 114 was released downstairs, and Freon 12 upstairs. Figure 6 shows the decay of Freon 114 downstairs and its growth upstairs; Figure 7 shows the decay of Freon 12 upstairs and its growth downstairs. The analysis of this data, using the curve fitting technique described in Appendix 1 gives the following values of ventilation and airflow rates:

$N_1 = 2.5$ ach $\qquad N_2 = 2.1$ ach

$F_{21} = 230\ m^3\ hr^{-1} \qquad F_{12} = 125\ m^3\ hr^{-1}$

The uncertainty in these values is of the order of $\pm$ 10%, based on a series of validation tests carried out in two interconnected environmental chambers[7].

The simplified analytical solution enables estimates of air change rates and intercell airflows to be calculated directly from site measurements of the variations of tracer gas concentrations with time. The new method can cope more readily with random measurement errors than the Prony method used previously[1]. The rapid sampling system shortens the length

of tests, and hence minimises the effects of extraneous variables (e.g. wind speed and direction) which could otherwise cause significant variations in site data.

5. Conclusions

The new improved tracer gas analysis system, used in conjunction with the simplified mathematical analysis for the airflow between two interconnected zones,is a useful tool for measuring airflows and ventilation rates in a short time period, enabling errors due to the effects of extraneous variables on site data to be minimised. Currently, the technique and analysis are being extended to the cases of three and four interconnected cells.

The usefulness of this technique with regard to ventilation and air movement measurements in large single cells (i.e. industrial premises) is currently being evaluated.

The system is also being fully automated, both in terms of valve control and data acquisition. An Apple IIe microcomputer, in conjunction with analogue to digital and digital to analogue conversion modules, is being used to fulfil both functions. A suite of data analysis and data manipulation programs is also being developed; again this will be used on the Apple IIe.

APPENDIX 1 - Analysis of two cell airflows N_1, N_2, F_{12} and F_{21}

The technique discussed here assumes the effects of recirculation of tracer gas between connected cells is time dependent, the contribution of recirculated tracer gas being small for time (t) < 20 minutes. Consequently equations(15) and (16) for $C_{(t)}$ can be simplified too:

Considering Cell 1

Gas A

$$C_{A_1} = C_{OA_1} (1 - A N_1) + \frac{F_{21} C_{OA_2}}{V_1(N_1'-N_2')} \left[\exp(-N_2't) - \exp(-N_1't)\right] \quad (1)$$

Gas B

$$C_{B_1} = C_{OB_1} (1 - A N_1) + \frac{F_{21} C_{OB_2}}{V_1(N_1'-N_2')} \left[\exp(-N_2't) - \exp(-N_1't)\right] \quad (2)$$

Considering Cell 2

Gas A

$$C_{A_2} = C_{OA_2} (1 - B N_2) + \frac{F_{12} C_{OA_1}}{V_2(N_2'-N_1')} \left[\exp(-N_1't) - \exp(-N_2't)\right] \quad (3)$$

Gas B

$$C_{B_2} = C_{OB_2} (1 - B N_2) + \frac{F_{12} C_{OB_1}}{V_2(N_2'-N_1')} \left[\exp(-N_1't) - \exp(-N_2't)\right] \quad (4)$$

where

$$\widetilde{C}_{(t)} = \left(\int_{t=o}^{t=t} C_{(t)} \, dt \right) \Big/ {}_{t_o}^{\Delta t}$$

the integral is evaluated using numerical integration of site $C_{(t)}$ data points.

$(1 - A\ N_1)$ is a Maclaurin series expansion of $\exp(-N_1 t)$

$$A = -t + \frac{N_1'^2 t^2}{2'} - \frac{N_1'^2 t^3}{3'} + \frac{N_1'^3 t^4}{4'} - \frac{N_1'^4 t^5}{5!}$$

$(1 - B\ N_2)$ is a Maclaurin series expansion of $\exp(-N_2 t)$

$$B = -t + \frac{N_2'^2 t^2}{2!} - \frac{N_2'^2 t^3}{3!} + \frac{N_2'^3 t^4}{4'} - \frac{N_2'^4 t^5}{5!}$$

N_1', N_2' are "first-order" estimates of N_1 and N_2, found from taking $\ell n\ C_{(t)}$, times (t) for C_{A_1} and C_{B_2} data points.

Equations (1) and (2) can be solved using numerical iteration for N_1, F_{21} this gives

$$N_1 = \frac{1}{A} - \frac{\tilde{C}_{A_1}}{C_{0A_1} A} + \frac{F_{21}\ C_{0A_2}}{C_{0A_1}\ A\ V_1\ (N_1' - N_2')} \left[\exp(-N_2' t) - \exp(-N_1' t)\right] \qquad (5)$$

$$F_{21} = \frac{V_1\ (N_1' - N_2')}{C_{0B_2}} \left[\exp(-N_2' t) - \exp(-N_1' t)\right] \left[\tilde{C}_{B_1} - C_{0B_1}\ (1 - A\ N_1)\right] \qquad (6)$$

Similarly equations (3) and (4) give

$$N_2 = \frac{1}{B} - \frac{\tilde{C}_{B_2}}{C_{0B_2} B} + \frac{F_{12}\ C_{0B_1}}{V_2 (N_2' - N_1') C_{0B_2} B} \left[\exp(-N_1' t) - \exp(-N_2' t)\right] \qquad (7)$$

$$F_{12} = \frac{V_2\ (N_2' - N_1')}{C_{0A_1}} \left[\exp(-N_1' t) - \exp(-N_2' t)\right] \left[\tilde{C}_{A_2} - C_{0A_2}\ (1 - B\ N_2)\right] \qquad (8)$$

The iteration generally converges in less than ten steps.

The calculated values of N_1, N_2, F_{12} and F_{21} can be used in equations (15) and (16) to enable comparison between theoretical curve shapes and the site data points.

ACKNOWLEDGEMENTS

The authors wish to acknowledge the financial support of the Science and Engineering Research Council.

REFERENCES

(1) S I'Anson, C Irwin and A T Howarth:

Air flow measurement using three tracer gases.

Building and Environment, Vol 17, No. 4, pp.245-252, 1982.

(2) J B Dick:

Experimental studies of natural ventilation of houses.

Journal of IHVE, 17, p.420, (1949).

(3) F W Sinden:

Multi-chamber theory of air infiltration.

Building and Environment, 13, p.21-28, (1978).

(4) M H Sherman, D T Grimsrud, P E Condon and B V Smith:

Air infiltration measurement techniques.

First Symposium of the Air Infiltration Centre: "Instrumentation and Measuring Techniques", Windsor, England, (October 1980).

(5) M D A E S Perera:

Review of techniques for measuring ventilation rates in multi-celled buildings.

Proceedings of the EEC Contractors Meeting on Natural Ventilation, Brussels, (September 1982).

(6) F B Hildebrand:

Introduction to Numerical Analysis.

Chapter 9, pp.458-462, McGraw-Hill Inc., 1982.

(7) C Irwin, R E Edwards and A T Howarth:

An improved multiple tracer gas technique for calculating air movement in buildings.

Air Infiltration Review, Vol. 5, No. 2, 1984.

APPENDIX (G) COMPUTER PROGRAMS

```
G1

OY.

REM SINGLE VOLUME VENTILATION RATE CALC
PRINT "TYPE IN NO. OF POINTS"
INPUT L
DIM C(L),T(L)
PRINT"TYPE IN C,T(MINS)(K=2)?";Z
FOR I=1TOL
INPUT C(I),T(I)
NEXT I
LET P=0
LET Q=0
LETW=0
LETX=0
LETZ=0
FOR J=1 TO L
LET P=P+LOG(C(J))*T(J)
LET Q=Q+LOG(C(J))
LET W=W+T(J)
LET X=X+(T(J))12
LETZ=Z+(LOG(C(J)))12
NEXT J
REM P,Q,W,X,Z ARE SUMS OF XY,Y,X,X12,Y12
LET A=(W*Q-L*P)/(L*X-W12)
LET B=(Q*X-P*W)/(L*X-W12)
LET Y=0
FOR K=1 TO L
LET Y=Y+(LOG(C(K))+A*T(K)-B)12
NEXT K
REM Y IS SUM OF (Y(OBS)-Y(L.S.))12
LET S=Y/(L-1)
PRINT"N="A*60"ACH & C0="EXP(B)
PRINT
PRINT"CORRELATION COEFF.="(L*P-W*Q)/SQR((L*X-W12)*(L*Z-Q12))
PRINT
PRINT"L.S. ERROR IN N="SQR(L*S/(L*X-W12))*60
PRINT
PRINT"L.S ERROR IN C0="(SQR(S*X/(L*X-W12)))*EXP(B)
END
Y.
```

```
G2
REM THIS PROGRAM CALCULATES
REM N1,N2,N3 & F12 F13 F21
REM F11 F31 F32
REM
REM THIS PROGRAM CALCS
REM N1,N2,F12,F21
REM USING IRWIN EQN'S
Z=0:X=0:Q=0:A1=0:B2=0
OPEN1,4,"
INPUT"HOW MANY ZONES(MAX=2)?";Z
INPUT"WHICH ZONE ?";X
PRINT#1,"ZONE="X
INPUT"COA1=";C1:INPUT"COA2=";C2
INPUT"COB1=";C3:INPUT"COB2=";C4
INPUT"N1=";N1:INPUT"N2=";N2
INPUT"V1=";V1:INPUT"V2=";V2
INPUT"WHAT TIME INTERVAL BETWEEN     POINTS (MINS)";Q
Y=Q/60:V3=";V3
INPUT"HOW MANY POINTS?";W:BETWEEN POINTS(MINS)";
INPUT"T ZERO CA1&CB1 ?";A1
INPUT"T ZERO CA2&CB2 ?";B2
FOR I=1TOW
E1=EXP(-N1*A1):E2=EXP(-N2*A1)
X1=EXP(-N1*B2):X2=EXP(-N2*B2)
J1=E2-E1:J2=X1-X2
J3=J1+J3:J4=J2+J4
S1=-A1+((N1*A1↑2)/2)-((N1*A1↑3)/6)+((N1*A1↑4)/24)-((N1*A1↑5)/120)
S2=  -B2+((N2*B2↑2)/2)-((N2*B2↑3)/6)+((N2*B2↑4)/24)-((N2*B2↑5)/120)
S3=S3+S1:S4=S4+S2:A1=A1+Y:B2=B2+Y
NEXT I
INPUT"SUM OF CA1(T)POINTS";R1
INPUT"SUM OF CB1(T)POINTS";R2
INPUT"SUM OF CA2(T)POINTS";R3
INPUT"SUM OF CB2(T)POINTS";R4
H1=C1*W:H2=C2*W:H3=C3*W:H4=C4*W
H5=C2/(V1*(N1-N2)):H6=C4/(V1*(N1-N2))
H7=C1/(V2*(N2-N1)):H8=C3/(V2*(N2-N1))
REM THIS GIVES VALUES OF F21&N1
INPUT"CHOOSE A VALUE FOR F21";AF2
FOR I=1TO 10
A6=-1*C1*S3:A7=-1*C3*S3
RV1=((H1-R1)/A6)+(H5*J3/A6)*AF2
AF2=((R2-H3)/(J3*H6))+(A7/(J3*H6))*RV1
PRINT"N1="RV1;"F21="AF2
NEXT I
PRINT#1,"N1="RV1,"F21="AF2
REM THIS CALCS N2&F12
INPUT"CHOOSE A VALUE FOR F12";AF1
A8=-1*C4*S4:A9=-1*C2*S4
FOR I=1TO10
RV2=((H4-R4)/A8)-(H8*J4/A8)*AF1
AF1=((R3-H2)/(J4*H7))+(A9/(J4*H7))*RV2
PRINT"N2="RV2,"F12="AF1
NEXT I
PRINT#1,"N2="RV2,"F12="AF1
CLOSE 1,4
END
```

```
REM THIS PROGRAM CALCULATES
REM N1,N2,N3 & F12,F13,F21
REM F23,F31,F32
OPEN1,4
Z=0:X=0:Q=0:A1=0:B2=0:D1=0
INPUT"HOW MANY ZONES(M=3)";Z
INPUT"WHICH ZONE";X
PRINT#1,"ZONE="X
INPUT"C0A1=";C1:INPUT"C0A2=";C2
INPUT"C0A3=";C5
INPUT"C0B1=";C3:INPUT"C0B2=";C4
INPUT"C0B3=";C6
INPUT"C0C1=";C7:INPUT"C0C2=";C8
INPUT"C0C3=";C9
INPUT"N1=";N1:INPUT"N2=";N2
INPUT"N3=";N3
INPUT"V1=";V1:INPUT"V2=";V2
INPUT"V3=";V3
INPUT"WHAT TIME INTERVAL BETWEEN POINTS(MINS)";Q
Y=Q/60
INPUT"HOW MANY POINTS";W
INPUT"T ZERO CA1,CB1&CC1";A1
INPUT"T ZERO CA2,CB2&CC2";B2
INPUT"T ZERO CA3,CB3&CC3";D1
FOR I=1TOW
E1=EXP(-N1*A1):E2=EXP(-N2*A1)
E3=EXP(-N3*A1)
X1=EXP(-N1*B2):X2=EXP(-N2*B2)
X3=EXP(-N3*B2)
Z1=EXP(-N1*D1):Z2=EXP(-N2*D1)
Z3=EXP(-N3*D1)
J1=E2-E1:J2=X1-X2:J5=Z1-Z3
J6=E3-E1:J7=X3-X2:J8=Z2-Z3
J3=J1+J3:J4=J2+J4:G1=J5+G1
G2=J6+G2:G3=J7+G3:G4=G4+J8
S1=-A1+((N1*A1↑2)/2)-((N1*A1↑3)/6)+((N1*A1↑4)/24)-((N1*A1↑5)/120)
S2=-B2+((N2*B2↑2)/2)-((N2*B2↑3)/6)+((N2*B2↑4)/24)-((N2*B2↑5)/120)
S5=-D1+((N3*D1↑2)/2)-((N3*D1↑3)/6)+((N3*D1↑4)/24)-((N3*D1↑5)/120)
S3=S1+S3:S4=S4+S2:S6=S6+S5:
A1=A1+Y:B2=B2+Y:D1=D1+Y
NEXTI
INPUT"SUM OF CA1(T)POINTS";R1
INPUT"SUM OF CB1(T)POINTS";R2
INPUT"SUM OF CC1(T)POINTS";R5
INPUT"SUM OF CA2(T)POINTS";R3
INPUT"SUM OF CB2(T)POINTS";R4
INPUT"SUM OF CC2(T)POINTS";R6
INPUT"SUM OF CA3(T)POINTS";R7
INPUT"SUM OF CB3(T)POINTS";R8
INPUT"SUM OF CC3(T)POINTS";R9
H1=C1*W:H2=C2*W:H3=C3*W:H4=C4*W
L1=C5*W:L2=C6*W:L3=C7*W:L4=C8*W
L5=C9*W
H5=C2/(V1*(N1-N2)):H6=C1/(V2*(N2-N1))
H7=C1/(V3*(N3-N1)):H8=C5/(V1*(N1-N3))
M1=C5/(V2*(N2-N3)):M2=C2/(V3*(N3-N2))
M3=C4/(V1*(N1-N2)):M4=C3/(V2*(N2-N1))
M5=C3/(V3*(N3-N1)):M6=C6/(V1*(N1-N3))
M7=C6/(V2*(N2-N3)):M8=C4/(V3*(N3-N2))
P1=C8/(V1*(N1-N2)):P2=C7/(V2*(N2-N1))
P3=C7/(V3*(N3-N1)):P4=C9/(V1*(N1-N3))
```